The mechanism of activation of the death-inducing mitochondrial protein BCL-2/E1B 19kDa interacting protein (BNIP3)

by

Christine Vande Velde

A thesis submitted to the Faculty of Graduate Studies of the University of Manitoba
in partial fulfillment of the requirements for the degree of

Doctor of Philosophy

Department of Biochemistry and Medical Genetics
University of Manitoba, Winnipeg, Manitoba

THE UNIVERSITY OF MANITOBA

FACULTY OF GRADUATE STUDIES

*****

COPYRIGHT PERMISSION PAGE

The Mechanism of Activation of the Death-Inducing Mitochondrial Protein BCL-2/E1B 19kDa Interacting Protein (BNIP3)

BY

Christine Vande Velde

A Thesis/Practicum submitted to the Faculty of Graduate Studies of The University of Manitoba in partial fulfillment of the requirements of the degree

of

Doctor of Philosophy

Abstract

Many apoptotic signaling pathways are directed to mitochondria, where they initiate the release of apoptogenic proteins and open the proposed mitochondrial permeability transition (PT) pore that ultimately results in the activation of the caspase proteases responsible for cell disassembly. BNIP3 is a member of the BCL-2 family that is expressed in mitochondria and induces cell death without a functional BH3 domain. Previous work has demonstrated that endogenous BNIP3 is loosely associated with mitochondrial membranes in normal tissue but when overexpressed, fully integrates into the mitochondrial outer membrane via its TM domain to induce cell death. Surprisingly, BNIP3-mediated cell death is independent of Apaf-1, caspase activation, cytochrome *c* release, and nuclear translocation of apoptosis inducing factor. However, cells transfected with BNIP3 exhibit early plasma membrane permeability, mitochondrial damage, extensive cytoplasmic vacuolation, and mitochondrial autophagy, yielding a morphotype that is typical of necrosis. These changes were accompanied by rapid and profound mitochondrial dysfunction characterized by sustained opening of the mitochondrial PT pore, proton electrochemical gradient ($\Delta\psi m$) suppression, and increased reactive oxygen species production. The PT pore inhibitors cyclosporin A and bongkrekic acid blocked mitochondrial deregulation and cell death. We propose that human *bnip3* is a gene that mediates a necrosis-like cell death through early PT pore opening and mitochondrial dysfunction.

Acknowledgements

I would like to acknowledge the three people in my life who have helped me achieve my goal. I am grateful to my supervisor and mentor, Dr. Arnold H. Greenberg, for sharing his wisdom with me, for the many opportunities he provided me, and for teaching me how to think about science and "ask the right questions". I sincerely thank my fellow lab mate, Dr. Jeannick Cizeau, for putting up with me everyday, for his friendship, for talking science with me, for "motivating" me, and for teaching me how to do science. I am privileged to have worked alongside such a scientist and I am appreciative of the many contributions he made to my project. I am also grateful to my mother, Karen Vande Velde, for her unwavering patience and guidance, for worrying with me, celebrating with me, for listening to me, for loving me – and, at times, for motivating me. Thank you for not giving up on me, for believing in me, and for helping me to achieve my goals. You have been an undying source of strength in my life and I thank you.

I would also like to acknowledge the members of my extended advisory committee, including Drs. Sabine Mai, Barbra Triggs-Raine, Klaus Wrogemann, Spencer Gibson, and James Davie, for their support and thoughtful inspection of my thesis. I would also like to thank Dr. Leigh Murphy for the many reference letters she has written on my behalf.

I would also like to thank the members of the Greenberg lab, both past and present, especially Judie Alimonti, Tracy Brown, Angela Kemp, for their contributions to this project. As well, thank you to all the staff and students of Manitoba Institute of Cell Biology and the Department of Biochemistry and Medical Genetics, for their friendship, advice, and tolerance of me. In addition, thank you to the future Dr. Jeanna Strutinsky, MD, for her beautiful personality and gorgeous smile. Her friendship made the lab a happy place when it definitely wasn't. And finally, thank you to Sunita Pandey, for always being a great friend and letting me miss her birthdays!

"If I have seen farther, it is by standing on the shoulders of giants."
Sir Isaac Newton

dedicated to my mentors:

my mother Karen Vande Velde & Dr. Arnold H. Greenberg

Table of contents

List of Figures

List of Tables

List of Abbreviations

α-MEM	alpha-minimal essential medium
A	alanine
Ac	acetyl
ADP	adenosine diphosphate
AIF	apoptosis inducing-factor
AM	acetoxymethyl
ATP	adenosine triphosphate
BA	bongkrekic acid
BH	BCL-2 homology
BNIP3	Bcl-2/nineteen kiloDalton interacting protein-3
BSA	bovine serum albumin
C	cysteine
$CaCl_2$	calcium chloride
$CaPO_4$	calcium phosphate
CARD	caspase recruitment domain
ceBNIP3	*C. elegans* BNIP3
ClCCP	carbonyl cyanide m-chlorophenylhydrazone
cm	centimeter
$CoCl_2$	cobalt chloride
CsA	cyclosporin A
CTL	cytotoxic T lymphocyte
Cy3	cyanine fluorochrome
D	aspartate
DD	death domain
DED	death effector domain
$DiOC_6$	3,3'-dihexyloxacarbocyanine iodide
DISC	death-inducing signaling complex
DMEM	Dulbecco's Modified Eagle Medium
DMF	*N,N*-dimethylformamide
DNase	deoxyribonuclease
DTT	dithiothreitol
E	glutamate
ECL	enhance chemiluminescence
EDTA	ethylenediaminetetraacetic acid
ER	endoplasmic reticulum
FBS	fetal bovine serum
FITC	fluorescein isothiocyanate
fmk	fluoromethylketone
g	gravity
G	glycine
H_2O_2	hydrogen peroxide
HA	hemagglutinin
HBSS	Hank's Buffered Saline Solution
HE	dihydroethidium

HeBS	Hepes-buffered saline
HCl	hydrochloric acid
HRP	horseradish persoxidase
HSP60	heat shock protein 60
IgG	Immunoglobulin G
JC-1	5,5',6,6'-tetrachloro-1,1',3,3'-tetraethylbenzimidazolylcarbocyanine iodide
$K_3Fe(CN)_6$	potassium hexacyanoferrate (III)
$K_4Fe(CN)_6 \bullet 3H_2$	potassium hexacyanoferrate (II)
kb	kilobase
KCl	potassium chloride
kDa	kiloDalton
L	leucine
M	molar
MDa	megaDalton
MEFs	mouse embryonic fibroblasts
$MgSO_4$	magnesium sulfate
ml	milliliter
mM	millimolar
mRNA	messenger ribonucleic acid
Na_2HPO_4	sodium hydrogen phosphate
NaCl	sodium chloride
NaOH	sodium hydroxide
NIX	BNIP3-like protein-X
NK	natural killer
nm	nanometer
nM	nanomolar
NMR	nuclear magnetic resonance
NP-40	Nonidet P-40
P	proline
PAGE	polyacrylamide gel electrophoresis
PARP	poly(ADP-ribose) polymerase
PBS	phosphate-buffered saline
PCD	programmed cell death
PI	propidium iodide
PMSF	phenylmethylsulfonyl fluoride
pNA	p-nitroalanine
PT	permeability transition
ROS	reactive oxygen species
PAGE	polyacrylamide gel electrophoresis
PCD	programmed cell death
PS	phosphatidylserine
Q	glutamine
R	arginine
RFU	relative fluorescence unit
S	serine
SDS	sodium dodecyl sulfate

SE	standard error
T	threonine
TAE	Tris-acetate buffer
TE	Tris-EDTA buffer
TES	N-tris[hydroxymethyl]methyl-2-amino ethane sulfonic acid
TM	transmembrane
Tris	Tris (hydroxymethyl) aminomethane
TUNEL	terminal deoxynucleotidyl transferase-mediate dUTP nick end labeling
Tween-20	Polyoxyethylenesorbitan
UV	ultraviolet
V	valine
v/v	volume/volume
W	tryptophan
w/v	weight/volume
X-gal	5-bromo-4-chloro-3-indolyl-β-D-galactopyranoside
z	benzyloxycarbonyl
$Å^2$	square Angstroms
$\Delta\psi m$	mitochondrial transmembrane potential
μg	microgram
μl	microliter
μm	micron
μM	micromolar

1.0 Introduction

1.1 Cell death

Recently, a significant number of studies have placed an emphasis on the role of cell death in both normal cellular homeostasis and the generation of pathological conditions. The primary focus in this area has been on apoptosis, which is a genetically encoded, highly conserved mechanism for clearing damaged, unnecessary, or harmful cells from a multicellular organism (Vaux and Korsmeyer, 1999). Apoptosis is essential to morphogenesis, development, pathogenic defense, and cellular homeostasis. Specific examples of apoptosis include the removal of cells comprising interdigital webs in mammals, loss of the tail in the tadpole, and establishment of sexual dimorphism via Mullerian duct regression during normal mammalian male development (referenced in Minn *et al.*, 1998). Apoptosis also plays a major role in the development of the immune system, including removal of T-lymphocytes, which express inappropriate or autoreactive antigens on their surface, and B-lymphocytes following an immune response (Vaux *et al.*, 1994). In addition, virally-infected cells can be recognized by natural killer (NK) cells and cytotoxic T-lympocytes (CTL) which kill the target cell via release of death granules (Shi *et al.*, 1992; Shi *et al.*, 1996). And of course, cells are continuously produced in a multicellular organism necessitating the removal of aged and/or damaged cells from the total population. In each of these contexts, apoptosis is believed to rely on a cell's interpretation of the overall balance between survival and death signals, both intrinsic and extrinsic (Raff, 1992). Examples of these signals include growth factor withdrawal, ligation of death receptors, viral infection, hypoxia, anoikis, treatment with cytotoxic or

genotoxic agents, inappropriate oncogene activation or tumour suppressor gene inactivation (Minn *et al.*, 1998).

Deregulation of this essential process likely results in several pathological conditions. Insufficient cell death contributes to a variety of diseases, including autoimmunity disorders such as systemic lupus erythematosus, tumorigenesis, and some viral infections (Thompson, 1995; Adams and Cory, 1998). Likewise, excessive cell death is the cause of a number of neurodegenerative diseases, including Alzheimer's and Parkinson's diseases. As well, infection by human immunodeficiency virus (HIV) accelerates cell death of lymphocytes and progression to Acquired Immunodeficiency Syndrome (AIDS) (Thompson, 1995; Adams and Cory, 1998).

Kerr *et al.* (1972) coined the term apoptosis, taken from the ancient Greek, meaning "falling off" of leaves or petals, to describe cell death bearing a distinct morphology and is also referred to as type I physiological cell death (Figure 1). Apoptotic cell death is an active process typically characterized by chromatin condensation, DNA fragmentation, loss of cell volume, and plasma membrane blebbing (Minn *et al.*, 1998). During the programmed death of the cell, the integrity of the plasma membrane is maintained at all times so as to contain the toxic contents of the apoptotic cell, and thereby avoid an inflammatory response. Furthermore, loss of phospholipid asymmetry such that phosphatidylserine, which is normally confined to the inner leaflet of the plasma membrane, is now presented on the outer surface, likely serves as a signal to neighboring cells and/or phagocytes to remove the dying cell via phagocytosis (reveiwed in Minn *et al.*, 1998; Schlegel and Williamson, 2001). Furthermore, a novel receptor has been identified that specifically recognizes phosphatidylserine and is

ubiquitously expressed is critically required for efficient removal of all types of apoptotic cells (Fadok *et al.*, 2000). Biochemical features of apoptosis include activation of a family of cysteine aspartyl proteases (caspases), release of cytochrome *c* from the mitochondria, opening of the permeability transition (PT) pore, suppression of mitochondrial transmembrane potential ($\Delta\psi m$), increased reactive oxygen species (ROS) production, and maintenance of intracellular ATP levels following $\Delta\psi m$ loss (Kroemer *et al.*, 1998). The precise order of the mitochondrial dysfunction events in apoptosis is controversial and not clearly delineated as yet (Kroemer *et al.*, 1998; Zamzami *et al.*, 1998; Denecker *et al.*, 2001). However, caspase activation is an ATP-dependent process that leads to the ordered disassembly of the cell and activation of deoxyribonucleases (DNases) that are necessary for packaging the DNA and cytosol into apoptotic bodies (Minn *et al.*, 1998; Denecker *et al.*, 2001).

At the other end of the spectrum of cell death is necrosis. Necrosis is regarded as an unregulated, passive response to toxicants or physical injury (McConkey, 1998). It is characterized by extensive cytoplasmic vacuolation, mitochondrial swelling, and early plasma membrane permeability without major nuclear damage (Table 1) (Kerr *et al.*, 1972; Tsujimoto, 1997; Kitanaka and Kuchino, 1999). Biochemical determinants of necrotic cell death are less well defined but are believed to be focused on the mitochondria with rapid suppression of $\Delta\psi m$ and increased ROS production, as well as ATP depletion (McConkey, 1998; Kitanaka and Kuchino, 1999). Biochemical studies designed to determine the pathway leading to necrosis are often complicated by the fact that some events/mediators are common to both apoptosis and necrosis (McConkey, 1998). Furthermore, both apoptotic and necrotic cell death can occur simultaneously in

cells exposed to the same death signal (Leist *et al.*, 1997). The intensity of the insult and the timing of the response will dictate which path is taken (McConkey, 1998). Apoptosis requires ATP, while necrosis does not. Therefore, the balance between these two modes of cell death is believed to be governed by the level of intracellular ATP. When ATP has breached a critical intracellular concentration, the mode of cell death preferentially switches from apoptosis to necrosis (McConkey, 1998). In addition, mitochondrial disruption, in the form of PT pore opening, $\Delta\psi m$ suppression and oxidative stress, is involved in both modes of cell death. However, rapid ROS production, $\Delta\psi m$ suppression, and PT pore opening are characteristic features of necrosis while these events occur later in apoptotic cell death more as a consequence of apoptosis (ie. after cytochrome *c* and dATP/ATP release) (McConkey, 1998). Another example of this overlap is intracellular Ca^{++} homeostasis. Sustained low to moderate cytosolic Ca^{++} increases (200-400 nM) are common in apoptosis. In contrast, large scale Ca^{++} influx (>1 μM) is characteristic of necrosis which results in mitochondrial Ca^{++} overload, thereby propagating mitochondrial disruption (McConkey, 1998). To date, the only event that continues to be specific to necrosis is ATP depletion (Nicotera and Leist, 1997; McConkey, 1998). Necrotic cell death is characterized by greater than 70% ATP depletion (McConkey, 1998). In contrast, ATP is required for caspase activation and subsequent nuclear condensation and DNA fragmentation which defines apoptosis (Leist *et al.*, 1997; Eguchi *et al.*, 1999).

An alternate way to remove a cell is via self-digestion, referred to as autophagy or type II physiological cell death (Kitanaka and Kuchino, 1999). Autophagy is defined as the bulk degradation of cellular proteins and/or organelles and is neither an apoptotic nor

a necrotic pathway (Zakeri *et al.*, 1995; Bursch, 2001). Studies in yeast have identified fourteen autophagy genes which are expressed during starvation and cell differentiation (Mizushima *et al.*, 1998). Recently, the first mammalian gene, *beclin1*, was identified and determined to be under-expressed in breast carcinomas, suggesting that deregulation of autophagy can result in tumorigenesis (Aita *et al.*, 1999; Liang *et al.*, 1999). In mammalian cells, autophagy is characterized by substantial cytoplasmic vacuolation and late nuclear collapse and has been observed in several examples of physiological cell death (Clarke, 1990; Zakeri *et al.*, 1995; Bursch, 2001). Interestingly, opening of the PT pore (Lemasters *et al.*, 1998; Lemasters *et al.*, 1998a) can activate autophagy, however the exact pathway is still undefined. Furthermore, some apoptotic signals can also induce autophagic cell death, suggesting that these two processes are not mutually exclusive phenomena (reviewed in Bursch, 2001).

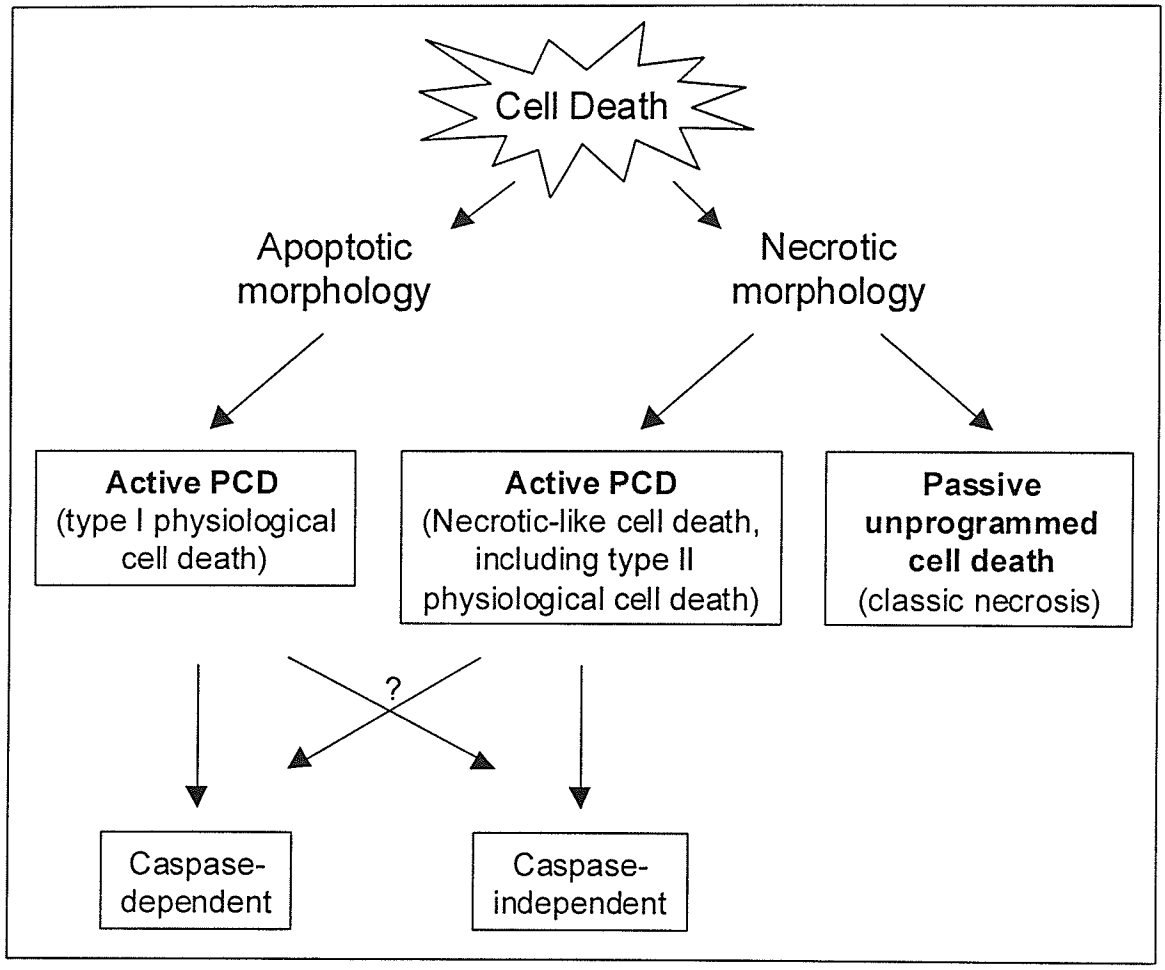

Figure 1: Morphological and functional classification of cell death. Cell death is in general divided into two groups according to the morphology, 'apoptotic' and 'necrotic'. It can be further classified into 'programmed' and 'unprogrammed' cell death according to the presence or absence of underlying regulatory mechanisms. 'Programmed' cell death (PCD) is subdivided according to its dependence on caspases in cellular disassembly. (Adapted from Kitanaka and Kuchino, 1999).

Table 1: Features of apoptosis and necrosis. (Compiled from Zakeri *et al.*, 1995; Kitanaka and Kuchino, 1999; McConkey, 1998).

Features	Apoptosis	Necrosis
Nucleus	Internucleosomal fragmentation Chromatin condensation	Late, minor DNA damage
Plasma Membrane	Intact Blebbing Phospholipid asymmetry	Early permeability
Cytoplasm	Loss of volume	Extensive vacuolation Presence of autophagosomes General organelle swelling
Mitochondria	Opening of PT[1] pore Suppression of $\Delta\psi m$[2] Production of ROS[3] Release of mitochondrial proteins	Rapid opening of PT pore Suppression of $\Delta\psi m$ Production of ROS
Energy Requirement	ATP[4]-dependent	ATP-independent
Activated Enzymes	Caspases Deoxyribonucleases	Various degradative enzymes
Environmental Response	No inflammation Phagocytosis by neighboring cells and/or macrophages	Inflammation Lysis

[1]PT, permeability transition
[2]$\Delta\psi m$, mitochondrial transmembrane potential
[3]ROS, reactive oxygen species
[4]ATP, adenosine triphosphate

1.2 The basic mechanism of apoptosis as defined in *Caenorhabditis elegans*

The nematode *C. elegans* provides an ideal and "simple" model in which to study apoptosis, also referred to as programmed cell death (PCD). Early observations discovered that during development of the hermaphrodite worm, a precise and invariant number of cells comprise the adult animal. Specifically, 1090 somatic cells are generated by a reproducible number of cell divisions (Metzstein *et al.*, 1998; Horvitz, 1999). Of these, 131 cells undergo PCD usually within one hour of the time they are formed (Sulston *et al.*, 1983; Horvitz, 1999). The pathway of cell death has been delineated through genetic, molecular and biochemical studies. Deregulation of *C. elegans* PCD, via naturally or artificially occurring mutations, results in either survival of cells that normally would die in the developing worm. Alternatively, cells that normally would survive in the developing worm may be directed to die as a consequence of a particular mutation (Horvitz, 1999).

Four main genes have been identified in screens as essential to the control of PCD in *C. elegans*: *ced-9, ced-3, ced-4* (cell death abnormal) and *egl-1* (egg laying abnormal) (Minn *et al.*, 1998; Metzstein *et al.*, 1998; Horvitz, 1999). *ced-9* is cell protective as loss of function mutations are embryonic lethal, likely due to uncontrolled cell death of cells that should normally survive (Hengartner *et al*, 1992). In contrast, gain of function mutations of *ced-9* prevent the death of all 131 cells that normally would die during development, resulting in viable but functionally compromised animals (Hengartner *et al.*, 1992; Minn *et al.*, 1998). *ced-3, ced-4,* and *egl-1* are required to induce cell death. *ced-3* and *ced-4* loss of function mutants have essentially the same phenotype as the *ced-9* gain of function mutations in that all cell death is absent (Horvitz, 1999). Recent

analysis of *egl-1* reveals that loss of function mutations abolish all PCD in the developing worm (Conradt and Horvitz, 1998). Moreover, gain of function *egl-1* mutations dominantly induce cell death in cells that would have otherwise survived (Conradt and Horvitz, 1998). Further experiments have successfully ordered these genes such that *egl-1* is an upstream negative regulator of *ced-9*, which, in turn, is a negative regulator of *ced-4*. *ced-4*, however, can induce *ced-3* activity and thus cell death (Horvitz, 1999).

The molecular basis of this linear pathway has also been determined. Initial immunoprecipitation studies identified a ternary complex of CED-9, CED-4, and CED-3 (Chinnaiyan *et al.*, 1997; Yang *et al.*, 1998). It has also been shown that CED-4 simultaneously associates with CED-3 and itself in the absence of CED-9 (Chinnaiyan *et al.*, 1997; Yang *et al.*, 1998). *In vivo*, CED-9 recruits CED-4 to intracellular membranes, likely mitochondrial (James *et al.*, 1997; Wu *et al.*, 1997; del Peso *et al.*, 1998; Chen *et al.*, 2000), possibly sequestering CED-4 from its normal function of spontaneous oligomerization in the cytosol. In this manner, CED-9 is proposed to exert its protective function. Association of EGL-1 with CED-9 successfully displaces CED-4:CED-3 complexes and negates the anti-apoptotic function of CED-9 (Conradt and Horvitz, 1998; del Peso *et al.*, 1998). Furthermore, CED-4 oligomerization mediates CED-3 activation by bringing multiple copies of CED-3 within close proximity thereby increasing the local concentration of autoproteolytic activity inherent to CED-3 (Yang *et al.*, 1998). CED-4-mediated CED-3 activation is proposed to require active ATP hydrolysis as disruption of nucleotide binding to the P-loop of CED-4 effectively abolishes CED-3 maturation (Chaudhary *et al.*, 1998). Interestingly, CED-9 binds CED-4 at the P-loop domain suggesting a means to prevent random protease activation (Chaudhary *et al.*, 1998).

Homologues of these four genes have evolved in "higher" order metazoans, albeit with increased complexity. CED-9 is homologous to the large family of BCL-2 proteins (Figure 2) (Hengartner and Horvitz, 1994). EGL-1 is analogous to a subset of pro-apoptotic BH3-only BCL-2 proteins (Conradt and Horvitz, 1998). The death effector, CED-3, is the functional equivalent of the mammalian caspase family (Yuan *et al.*, 1993). As well, mammalian Apaf-1 (Apoptotic protease activating factor-1) contains a region with significant homology to CED-4 and shows similar binding properties (Zou *et al.*, 1997). However, the mammalian apoptotic pathway also requires mitochondria, while the role of mitochondria in *C. elegans* apoptosis has not been determined. In any case, the homologous protein families demonstrate that there is a high degree of evolutionary conservation of this pathway. Furthermore, with the advent of the "Genome Era", analysis of entire genomes suggests that not all relevant proteins have been identified yet (Aravind *et al.*, 2001). There is some evidence to support this as at least three proposed functional caspases, other than CED-3, are known to exist in *C. elegans* (Shaham, 1998). In addition, sequence analysis reveals that conservation of the basic machinery of cell death extends even further "down" the evolutionary tree (Aravind *et al.*, 2001). Specifically, CED-9/BCL-2, CED-3/Caspase, and CED-4/Apaf-1 homologues have all been identified in *Danio rerio* (zebrafish) (Inohara and Nunez, 2000) and *Drosophila melanogaster* (fruit fly) (Chen and Abrams, 2000; Vernooy *et al.*, 2000).

Additional genes proposed to be involved in generation of the distinct nuclear morphology of apoptosis (*nuc-1* [encodes a DNase]) (Horvitz, 1999) and systematic engulfment and digestion of apoptotic cells (*ced-1, ced-2, ced-5, ced-6, ced-7, ced-10,* and *ced-12*) (Chung *et al.*, 2000; Hengartner, 2001) await further analysis of function.

Intriguingly, new data suggests that *C. elegans* can also undergo necrosis-like cell death via disruption of ion homeostasis (Chung *et al.*, 2000).

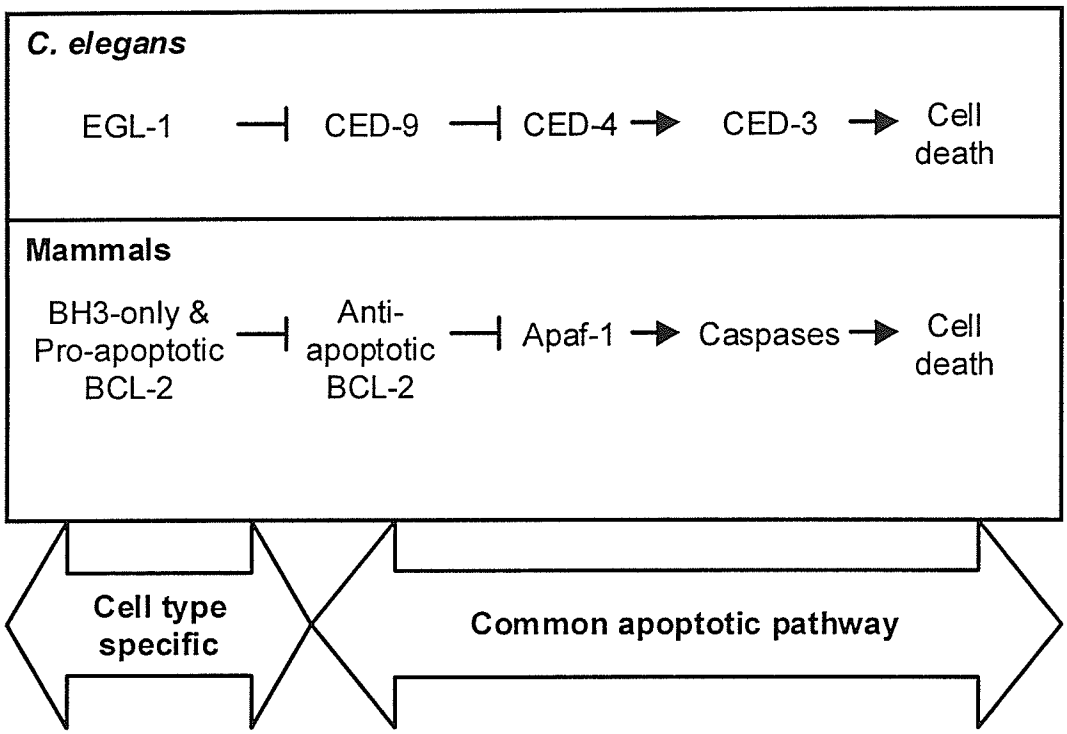

Figure 2: Evolutionary conservation of the apoptotic pathway. In *C. elegans*, EGL-1 negatively regulates CED-9 which negatively regulates CED-4 which in turn activates CED-3, yielding cell death. In mammals, corresponding protein families exist. It is postulated that the BH3-only and pro-apoptotic BCL-2 family proteins serve as cell type specific activators of apoptosis. However, subsequent steps of the apoptotic program are common to all cell types. (Adapted from Gross *et al.*, 1999).

1.3 Caspase family

In *C. elegans*, the developmental apoptotic program is efficiently executed by a single protease encoded by *ced-3* (Section 1.2; Horvitz, 1999). The finding that the protein CED-3 shared homology with mammalian interleukin-1β-converting enzyme (ICE), a cysteine protease required for maturation of the cytokine pro-interleukin-1β, marked an important milestone in delineating the mammalian apoptotic pathway as it suggested that the apoptotic pathway may be evolutionarily conserved (Yuan *et al.*, 1993). Subsequently, it was shown that overexpression of ICE in mammalian cells was sufficient to induce apoptosis, similar to overexpression of CED-3, indicating that indeed, there was a conserved apoptotic mechanism (Miura *et al.*, 1993; Cryns and Yuan, 1998). Currently, there are 14 identified mammalian proteases that share sequence similarity with CED-3 (Ranger *et al.*, 2001). This expanded family of intracellular cysteine proteases is characterized by their unique affinity for cleavage after an aspartate residue (Cohen, 1997; Cryns and Yuan, 1998; Wolf and Green, 1999). In an effort to standardize the nomenclature of these death proteases, the term 'caspase' was proposed to reflect that these are cysteine-dependent aspartate-specific proteases (Alnemri *et al.*, 1996). Furthermore, the caspases are numbered chronologically according to when they were discovered (Alnemri *et al.*, 1996). This family of proteases has been firmly implicated in the apoptotic program by targeted gene disruption studies, some of which resulted in severe developmental defects and embryonic lethality (Ranger *et al.*, 2001).

1.3.1 Structural features of caspases

There are several features shared among members of the caspase family. For example, all caspases have the conserved pentapeptide QACXG (where X is R, Q, or G) which harbors an active cysteine side chain that functions as a nucleophile during peptide bond hydrolysis (Cohen, 1997; Stennicke and Salvesen, 2000). Likewise, all caspases are maintained in a latent state as single chain zymogens until proteolytic activation is engaged by an apoptotic signal (Stennicke and Salvesen, 2000). Four distinct domains have emerged in procaspase structure: an amino-terminal prodomain, a large subunit, a small subunit, and a linker region of variable length situated between the small and large subunits and flanked by aspartate residues (Nunez *et al.*, 1998). Proteolytic activation removes the linker region first, releasing and thus permitting assembly of the large and small subunits, and subsequently removes the prodomain (Figure 3) (Nunez *et al.*, 1998; Wolf and Green, 1999).

Structural studies suggest that active members of this family share a common three-dimensional structure (Wolf and Green, 1999). Specifically, x-ray crystallography of caspase 1 revealed that the active enzyme consists of two large/small heterodimers, each containing an active site composed of residues from both the large and small subunits (Walker *et al.*, 1994; Wilson *et al.*, 1994; Wolf and Green, 1999). The active tetramer is maintained by interactions between the small subunits of each interdigitated heterodimer (Figure 3). Similar structural features have also been observed for caspases 3, 7 and 8 (Rotunda *et al.*, 1996; Mittl *et al.*, 1997; Blanchard *et al.*, 1999; Watt *et al.*, 1999; Wei *et al.*, 2000).

The amino-terminal prodomain varies in size between caspase family members and contributes to establishing two caspase subfamilies: long prodomains and short prodomains (Kumar and Colussi, 1999; Wolf and Green, 1999). In general, the activation of caspases with long prodomains is due to the presence of one of two sequence elements: the death effector domain (DED) or caspase recruitment domain (CARD) (Stennicke and Salvesen, 2000). This group includes caspases 1, 2, 4, 5, 8, 9, 10, 11, 12, 13, and 14 and *C. elegans* CED-3 (Wolf and Green, 1999). DEDs and CARDs are structurally very similar, despite a lack of sequence homology, as these motifs both contain six anti-parallel α-helices arranged in tightly packed bundles and associate via homotypic interactions (Huang *et al.*, 1996; Chou *et al.*, 1998; Eberstadt *et al.*, 1998; Wolf and Green, 1999). For example, DEDs associate primarily due to hydrophobic-hydrophobic interactions, while CARDs are hydrophilic and thus governed by complementary electrostatic interactions (Kumar and Colussi, 1999; Stennicke and Salvesen, 2000). Procaspases with short prodomains, including caspases 3, 6, and 7, are usually activated downstream of the first group (the apoptotic initiators). In addition, caspases 3, 6, and 7 mediate numerous proteolytic events that typify a dying cell, and are therefore known as apoptotic effectors or executioners (Kumar and Colussi, 1999; Wolf and Green, 1999; Stennicke and Salvesen, 2000).

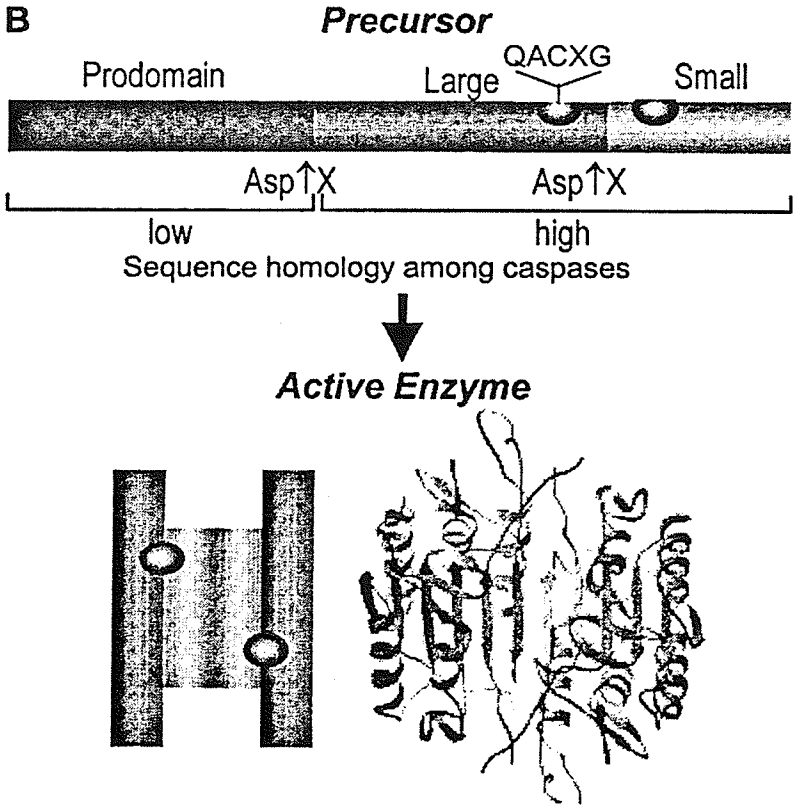

Figure 3: Schematic and three-dimensional structure of caspases. Caspases are synthesized as inactive precursors that require proteolytic cleavage at conserved aspartate residues occurring between the pro domain and the large subunit and between the large and small subunits. The amino-terminal pro domain is highly variable among caspase family members. The active caspase is a tetramer consisting of two large/small homodimers, each with an independent active site. The crystal structure of caspase 3 illustrates how the two homodimers interdigitate in the active protease. Illustrations are not to scale. (Adapted from Thornberry and Lazebnik, 1998; Ray, 2000).

1.3.2 Substrate specificity

Caspases have a unique substrate preference. Currently the only known non-caspase protease with the same affinity for aspartate residues is the mammalian serine protease granzyme B, which is also a physiological caspase activator (Shi *et al.*, 1996). All caspases require an aspartate residue at the cleavage site, referred to as position P_1 (Cryns and Yuan, 1998; Nunez *et al.*, 1998). However, substrate specificity is primarily determined by the residue four positions amino-terminal to the aspartate cleavage site, referred to as P_4. Combinatorial chemistry has identified the preferred cleavage sites for ten caspases, yielding an additional classification scheme (Cohen, 1997; Thornberry *et al.*, 1997). Based on caspase preference for amino acids in the P_4 position, there are three groups of caspases. Caspase 1-like caspases, including caspases 1, 4, and 5, prefer bulky hydrophobic residues at P_4. Their optimal cleavage site is WEXD (Cohen, 1997; Thornberry *et al.*, 1997). Based on sequence similarity, caspases 11, 12, 13, and 14 are also included in this group, however, there is currently no data available on their specificities to support this classicication (Van de Craen *et al.*, 1998; Wolf and Green, 1999). Caspase 3-like caspases prefer the small amino acid aspartate in the P_4 position. This group includes caspases 2, 3, and 7 and *C. elegans* CED-3 (Thornberry *et al.*, 1997). The third group is less discriminate in its P_4 preference. Caspases 6, 8, and 9 will accept either a leucine or valine in this position ([L/V]EXD) (Thornberry *et al.*, 1997). Due to sequence similarities between caspase 8 and 10, caspase 10 is also included in this group although its preferred cleavage site is unknown (Wolf and Green, 1999). These preferences are supported by structural studies (reviewed in Cohen, 1997). Specifically,

the residue in the P_4 position binds to a conserved site in the small subunits of the active tetramer (Nunez *et al.*, 1998). For example, caspase 1 has a large binding pocket ideally suited for binding large hydrophobic residues (Walker *et al.*, 1994; Wilson *et al.*, 1994). In contrast, caspase 3 has a very small binding pocket, suitable for binding the small side chain of aspartate (Mittl *et al.*, 1997; Wei *et al.*, 2000). Interestingly, it appears that cleavage site preference also correlates with function as the caspase 1-like group is primarily involved in cytokine processing while the other two groups are critical to apoptosis (Wolf and Green, 1999).

1.3.3 Cellular substrates

There are currently more than 100 known caspase substrates that can be broadly divided into proteins that mediate the apoptotic phenotype or those that impact cellular homeostasis. Some substrates may even contribute directly to propagation of the apoptotic signal. For example, caspases themselves have caspase recognition sites strongly suggesting autocatalytic activation (Nunez *et al.*, 1998). Furthermore, a subset of caspases contain optimal cleavage sites for a second set of caspases, thereby delineating a hierarchy of caspase activation in which initiator caspases activate effector caspases (Slee *et al.*, 1999). This activates a caspase cascade that facilitates rapid and efficient activation of the apoptotic program. In addition, the anti-apoptotic CED-9 homologues BCL-2 and BCL-X_L are inactivated and converted to pro-apoptotic proteins as a result of caspase cleavage (Cheng *et al.*, 1997; Clem *et al.*, 1998). Furthermore, the pro-apoptotic protein BID is activated by proteolytic cleavage (Li *et al.*, 1998; Luo *et al.*, 1998). In adddition, inhibitor of apoptosis proteins (IAPs) can also be cleaved by active

caspases (Deveraux *et al.*, 1999; Johnson *et al.*, 2000; Slee *et al.*, 2001; Suzuki *et al.*, 2001). Collectively, these events likely amplify or accelerate the apoptotic process (Cohen, 1997; Cryns and Yuan, 1998; Nunez *et al.*, 1998; Stroh and Schulze-Osthoff, 1998; Wolf and Green, 1999).

Cell shrinkage and nuclear damage typically characterize an apoptotic cell, therefore, cleavage of certain cellular substrates likely contributes to manifestation of this phenotype. Specifically, cytoskeletal proteins such as actin (Kayalar *et al.*, 1996; Mashima *et al.*1997) and its regulators, gelsolin (Kothakota *et al.*, 1997; Kamada *et al.*, 1998), spectrin (Wang *et al.*, 1998), and fodrin (Martin *et al.*, 1995; Cryns *et al.*, 1996; Vanags *et al.*, 1996), are all cleaved by caspases following a death signal. Proteins involved in cellular adhesion, including focal adhesion kinase (Wen *et al.*, 1997; Gervais *et al.*, 1998), Gas2 (Brancolini *et al.*, 1995), and β-catenin (Brancolini *et al.*, 1997), are also cleaved. These cleavage events are speculated to contribute to characteristic features of apoptosis such as plasma membrane blebbing, cytoplasmic condensation, and rounding up (loss of cell adhesion) (Cryns and Yuan, 1998; Stroh and Schulze-Osthoff, 1998; Wolf and Green, 1999). Likewise, changes in nuclear morphology during apoptosis may be due to cleavage of nuclear lamins, the primary structural component of the nuclear envelope, by caspase 6 (Cohen, 1997; Stroh and Schulze-Osthoff, 1998). Cleavage of lamins can trigger the collapse of the nucleus and may contribute to chromatin condensation, a hallmark of apoptosis (Lazebnik *et al.*, 1995; Orth *et al.*, 1996; Rao *et al.*, 1996; Takahashi *et al.*, 1996). However, new evidence suggests lamin cleavage is not required for chromatin condensation (Faleiro and Lazebnik, 2000). Caspase-induced

cleavage of the nuclear protein Acinus has also been reported to induce chromatin condensation during apoptosis (Sahara *et al.*, 1999).

Characteristic apoptotic DNA fragmentation occurs in two distinct stages. Specifically, chromosomal DNA is first cleaved into ~50 to ~200 kb fragments and subsequently into ~180 bp segments (Nagata, 2000). It is speculated that the initial large-scale DNA fragmentation is due to cleavage of DNA at nuclear scaffolds. This would effectively unfold the chromatin structure and possibly facilitate subsequent internucleosomal cleavage (Nagata, 2000). Apoptotic internucleosomal DNA fragmentation is mediated by DNA fragmentation factor-40/caspase-activated deoxyribonuclease (DFF40/CAD). This protein is a latent, cytosolic endonuclease that is activated following caspase activation (Liu *et al.*, 1997; Enari *et al.*, 1998; Liu *et al.*, 1998). DFF40/CAD activity is suppressed by a bound inhibitory subunit DFF45/ICAD (inhibitor of CAD). Active DFF40/CAD is released and translocated to the nucleus due to processing of DFF45/ICAD by active caspases 3 and 7 in response to an apoptotic signal (Liu *et al.*, 1997; Sakahira *et al.*, 1998; Wolf *et al.*, 1999). There is speculation that lamin cleavage may induce sufficient nuclear envelope damage to permit endonucleases such as DFF40/CAD access to the nucleus and thus facilitate DNA fragmentation (Cryns and Yuan, 1998). However, there is new evidence that suggests lamin cleavage is not a contributing factor to DNA fragmentation, but rather there is an increased permeability of nuclear pores due to activated caspase 9 (Faleiro and Lazebnik, 2000). Currently, the component(s) of the nuclear pore regulated by caspases is unknown.

There are a significant number of caspase substrates that impact various aspects of cellular homeostasis including cell cycle regulation and DNA repair mechanisms (Stroh and Schulze-Osthoff, 1998; Wolf and Green, 1999). Caspase-mediated cleavage of retinoblastoma protein (RB; Janicke *et al.*, 1996) and the mouse double minute-2 protein (MDM2; Erhardt *et al.*, 1997) may facilitate cell cycle arrest (Stroh and Schulze-Osthoff, 1998). The DNA repair protein poly(ADP-ribose) polymerase (PARP) is cleaved by caspases 3 and 7. Presumably, this cleavage event disturbs DNA repair, however this hypothesis remains to be formally tested. Regardless, PARP cleavage serves as a valuable indicator of caspase activation in experimental settings (Cohen, 1997; Stroh and Schulze-Osthoff, 1998).

There is an ever increasing list of caspase substrates that impact transcription, translation, signal transduction, and replication (reviewed in Stroh and Schulze-Osthoff, 1998). All of these substrates can be postulated to contribute to the apoptotic mechanism, either directly (structural proteins, amplifiers of apoptosis) or indirectly (disrupt cellular homeostasis; terminate survival signals) (Wolf and Green, 1999). There are even more proteins that are cleaved by caspases during apoptosis with unknown function. Intriguingly, there is accumulating data that suggests inappropriate caspase-mediated cleavage of certain substrates may contribute to the progression of neurodegenerative diseases (Stroh and Schulze-Osthoff, 1998; Wolf and Green, 1999).

Interestingly, not all caspase recognition sites are cleaved implying that there may also be structural/stereochemical requirements for cleavage. Furthermore, some cleavage events may be cell type specific either due to the expression profiles of the substrate or the caspases themselves (Stroh and Schulze-Osthoff, 1998). Finally, very few of the

more than 100 known caspase substrates have been convincingly demonstrated to truly contribute to the apoptotic process.

1.3.4 Subcellular localization

Caspases are primarily cytosolic. However, there is increasing evidence that subpopulations of various caspases exist in different cellular compartments. For example, a pool of procaspase 9 exists in the mitochondrial intermembrane space of some tissues, including non-replicating post-mitotic neurons and cardiomyocytes (Krajewski *et al.*, 1999; Susin *et al.*, 1999a; Zhivotovsky *et al.*, 1999). However, following an appropriate apoptotic signal, active caspase 9 is primarily cytosolic, suggesting that latent caspase 9 is sequestered until it is activated and unleashed on the cytosol to further the apoptotic process. It is unknown if caspase 9 becomes activated after or during cellular redistribution (Susin *et al.*, 1999a). Likewise, in response to stress on the endoplasmic reticulum (ER), ER-localized procaspase 12 is activated and redistributed to the cytosol (Nakagawa *et al.*, 2000). In some cells, procaspase 7 is cytosolic until activation, at which point it is translocated to the ER (Chandler *et al.*, 1998; Zhivotovsky *et al.*, 1999). Coincidentally, the caspase 7 substrate sterol regulatory element-binding protein-1 (SREBP-1), a resident of the ER, is cleaved following redistribution of active caspase 7 to the ER (Chandler *et al.*, 1998). This observation suggests that active caspases may redistribute throughout the cell in order to process their substrate(s). This is supported by recent work demonstrating the redistribution of active caspase 3 from the cytosol to the nucleus, presumably to target its substrate DFF45/ICAD and thus induce DNA fragmentation (Faleiro and Lazebnik, 2000). Procaspases 1, 2, 3, 8, and 9 are also

cytosolic (Zhivotovsky *et al.*, 1999). The impact of cellular compartmentalization of caspases on apoptosis is unknown but is speculated to provide an additional level of regulation that may be necessary to prevent accidental activation of the caspases. This may be particularly important to cells that have a low regenerative capacity (Krajewski *et al.*, 1999). Further work will likely identify numerous correlations between the localization of caspases and the locale of their substrates.

1.3.5 Mechanisms of caspase activation

1.3.5.1 Extrinsic (type I) pathway

Extrinsic caspase activation occurs in response to ligation of death receptors. This pathway is primarily involved in modulation and function of the immune response (Ashkenazi and Dixit, 1998). Cell surface death receptors such as Fas/CD95/Apo1, TNFR1, DR3/Apo3, DR4, and DR5/Apo2/KILLER, and DR6, are all members of the tumor necrosis factor receptor (TNFR) family (reviewed in Ashkenazi and Dixit, 1998; Baker and Reddy, 1998; Denecker *et al.*, 2001). These receptors are characterized by an intracellular carboxyl-terminal death domain (DD) that transmits an apoptotic signal upon ligation of the appropriate death ligand (Denecker *et al.*, 2001). Specifically, ligand binding triggers receptor homotrimerization. This clustering of DDs induces recruitment of adaptor proteins such as Fas-associated protein with DD (FADD) and/or TNFR-associated protein with DD (TRADD). Both TRADD and FADD are required for TNFR1 and DR3 signaling, while only FADD is required for Fas signaling (Baker and Reddy, 1998; Denecker *et al.*, 2001). TRADD interacts with the intracellular DD of TNFR1 in response to ligand binding. TRADD subsequently recruits and binds FADD

via its DD (Ashkenazi and Dixit, 1998). FADD also contains a DED motif that is required for interaction with the DED motif of procaspase 8. This DED-DED interaction effectively recruits procaspase 8 to the death-inducing signaling complex (DISC) at the cytoplasmic face of the plasma membrane (Ashkenazi and Dixit, 1998; Baker and Reddy, 1998; Denecker *et al.*, 2001). Procaspase 8 autoproteolysis is triggered due to the intrinsic proteolytic activity of procaspase 8 referred to as proximity-induced activation (Figure 4) (Salvesen and Dixit, 1999).

In response to Fas ligation, cells can die via two non-mutually exclusive types of apoptotic pathways, and thus are defined as type I and type II cells (Scaffidi *et al.*, 1998; Scaffidi *et al.*, 1999). In type I cells, there is significant and rapid activation of caspase 8 at the DISC yielding efficient and direct activation of downstream effector procaspases 3, 6, and 7 (Denecker *et al.*, 2001). In type II cells, DISC formation is less prominent and thus caspase 8 activation is considerably slower. These cells require propagation and amplification of the death signal by the mitochondria. Specifically, caspase 8 cleaves BID, a pro-apoptotic member of the BCL-2 family, to produce a truncated product (tBID) that translocates to the mitochondria and induces cytochrome *c* release (Li *et al.*, 1998; Luo *et al.*, 1998). Cytochrome *c* functions as a cofactor for procaspase 9 activation. Activated caspase 9 processes downstream effector procaspases (Denecker *et al.*, 2001). In summary, type I cells induce cell death independent of the mitochondria, the home of cytochrome *c*. In contrast, type II cells require mitochondria to induce apoptosis. In agreement with these observations are data demonstrating that BCL-2 and BCL-X_L, anti-apoptotic homologues of CED-9, can prevent cytochrome *c* release (Kluck *et al.*, 1997; Yang *et al.*, 1997), and thus effectively inhibit apoptosis in type II cells but not type I

cells (Scaffidi *et al.*, 1998). Cell type specific involvement of the death receptor and mitochondrial pathways in response to the chemotherapeutic agents doxorubicin and etoposide extends and supports the classification of type I and type II cells (Fulda *et al.*, 2001). Interestingly, a similar caspase-mediated cleavage event has been observed for the pro-apoptotic BCL-2-related protein BAD, yielding a more potent apoptotic inducer (Condorelli *et al.*, 2001).

1.3.5.2 Intrinsic (type II) pathway

Intrinsic caspase activation occurs in response to development, growth factor withdrawal, anoikis ,as well as several cytotoxic and genotoxic agents (Minn *et al.*, 1998; Denecker *et al.*, 2001). This pathway is characterized by release of cytochrome *c* from the intermitochondrial space, which functions as a co-factor for assembly of the apoptosome. The apoptosome complex consists of cytochrome *c*, dATP/ATP, procaspase 9, and the adaptor protein Apaf-1, a CED-4 homologue (described in detail in Section 1.4; Zou *et al.*, 1999). Oligomerization of Apaf-1 protein increases the local concentration of procaspase 9 and thereby triggers autocatalytic processing due to the significant intrinsic zymogen activity of procaspase 9 (Salvesen and Dixit, 1999). Subsequently, the active initiator caspase 9 proteolytically activates the effector procaspase 3 (Hu *et al.*, 1999; Zou *et al.*, 1999; Bratton *et al.*, 2001). Active caspase 3 can activate procaspases 2, 6, 8, and 10, thereby contributing to a feedback amplification loop of caspase activation which facilitates manifestation of the apoptotic phenotype (Slee *et al.*, 1999; Denecker *et al.*, 2001). Both intrinsic and extrinsic caspase activation pathways converge on the same subset of effector caspases (Figure 4).

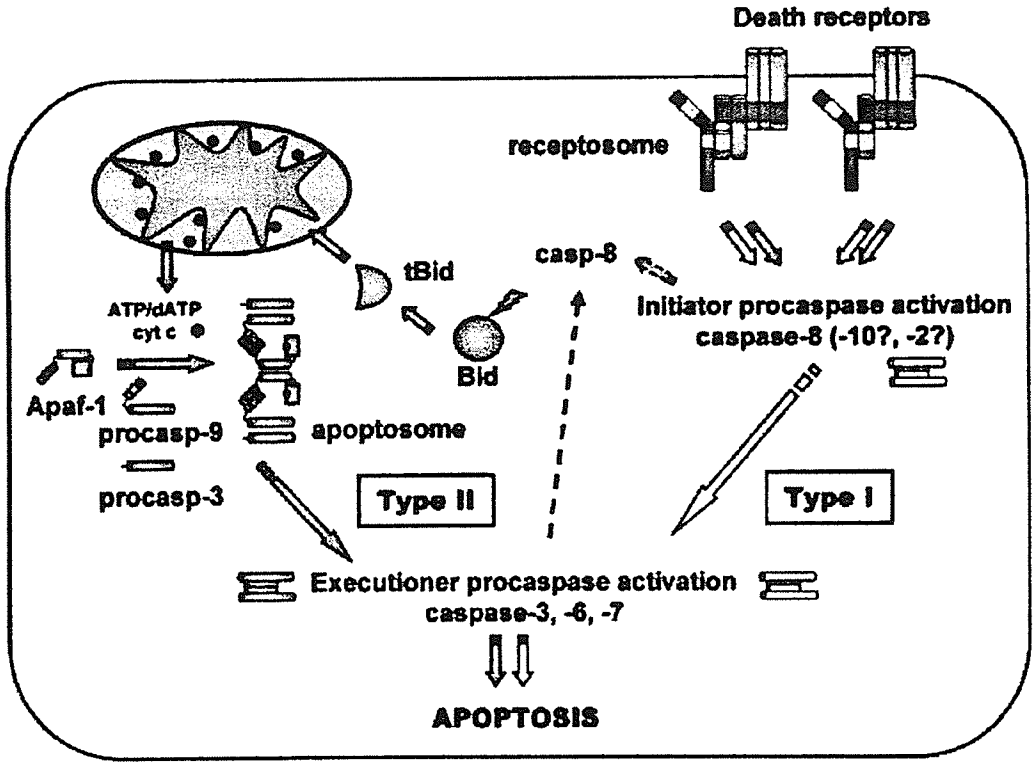

Figure 4: Extrinsic and intrinsic apoptotic signaling pathways. In extrinsic (type I) caspase activation, a large amount of active caspase-8 is generated at the receptosome complex (efficient DISC formation), which leads to direct activation of downstream procaspases. In intrinsic (type II) caspase activation, DISC formation is strongly reduced, resulting in minor procaspase 8 activation. In the latter case, propagation and amplification of the apoptotic signal by mitochondrial factors, such as cytochrome *c*, are required for activation of downstream executioner (effector) procaspases. Cytochrome *c* and ATP/dATP bind Apaf-1 and induce a conformational change, allowing oligomerization and recruitment of procaspase 9 (formation of apoptosome). Proximity-induced activation of procaspase 9 activates downstream executioner procaspases. Active effector caspases may further activate procaspase 8 in an autoamplification loop. Executioner caspases cleave substrates implicated in the morphological and biochemical features of apoptosis (Adapted from Denecker *et al.*, 2001).

1.3.6 Caspase inhibitors

As outlined in the previous sections, caspases are potent killers and are subject to various levels of regulation. There are a variety of endogenous caspase inhibitors that have evolved both in mammalian cells and viruses. There are two distinct types of caspase inhibitors: (i) those that inhibit caspase activation by competing with components of the apoptotic machinery, and (ii) those that act as pseudosubstrates and inhibit the catalytic site of caspases. In the death receptor pathway, there are a number of decoy receptors, such as DcR1/TRAIL-R3/TRID, DcR2/TRAIL-R4/TRUNDD, and DcR3 that efficiently bind ligand but lack or have a truncated intracellular signaling domain, and thus can not transmit the death signal. Therefore, these decoy receptors compete with death receptors for the activating ligand (Ashkenazi and Dixit, 1998). In addition, proteins such as FADD-like inhibiting protein (FLIP), of both viral and cellular origin, inhibit caspase activation because they share significant sequence homology to procaspase 8 but lack the essential catalytic pentapeptide (reviewed in Ashkenazi and Dixit, 1998). Specifically, this homology enables FLIP to actively compete with procaspase 8 for FADD, the critical adapter protein that mediates procaspase 8 activation. Alternatively, members of the inhibitor of apoptosis protein (IAP) family such as XIAP (X-linked IAP), c-IAP1 (cellular IAP) and c-IAP2, can bind and potently inhibit caspases 3, 7, and 9, but not caspases 1, 6, 8, or 10, or CED-3 (Deveraux *et al.*, 1997; Roy *et al.*, 1997; Deveraux *et al.*, 1998). In addition, it has recently been discovered that XIAP can inhibit the apoptosome via direct association with Apaf-1 (Bratton *et al.*, 2001). Interestingly, members of the IAP family are themselves regulated by the recently

identified XAF1 (XIAP-associated factor 1) and Smac/DIABLO (second mitochondrial activator of caspases/direct IAP binding protein with low pI) proteins (Du *et al.*, 2000; Verhagen *et al.*, 2000; Liston *et al.*, 2001). Some caspases, such as caspases 9, 3, and 2, have endogenous variants that either lack a catalytic site or other structural domain required for efficient caspase activation, and thus compete with catalytically-competent caspases for upstream activation signaling (Seol and Billiar, 1999; Droin *et al.*, 2000; Huang *et al.*, 2001).

Baculovirus p35 protein is an ideal example of a caspase pseudosubstrate. Specifically, p35 protein contains a caspase cleavage site. However, upon cleavage, the fragments generated are retained in complex with the caspase and thus function as a stoichiometric inhibitor (Bump *et al.*, 1995; Xue and Horvitz, 1995; Fisher *et al.*, 1999; Zoog *et al.*, 1999). Exogenous expression of p35 protein is a potent pan-caspase inhibitor in mammalian cells (Bump *et al.*, 1995; Xue and Horvitz, 1995). Similarly, the cowpox virus CrmA protein is also a caspase pseudosubstrate that is cleaved by caspases 1 and 8 and prevents their participation in subsequent reactions (Ray *et al.*, 1992; Zhou *et al.*, 1997). These two proteins have led to the development of synthetic peptide inhibitors that have furthered the delineation of caspase activation. The irreversible tripeptide caspase inhibitor Ac-zVAD-fmk (benzyloxycarbonyl-valine-alanine-aspartatyl methoxy fluoromethyl ketone) potently inhibits a wide range of caspases due to the lack of a specificity-directing residue in the P_4 position. Ac-zVAD-fmk is cleaved by caspases and retained in the active site via a covalent bond, thus prohibiting recycling of the enzyme (Slee *et al.*, 1996). More specific peptide inhibitors have been developed based on residue preference in the P_4 position (Section 1.3.2). Specifically, Ac-DEVD-fmk and

Ac-YVAD-fmk have been developed to selectively inhibit caspase 3-like and caspase 1-like proteases, respectively (Cohen, 1997).

1.4 Apaf-1

The significant role of CED-4 in regulating activation of CED-3 in *C. elegans* suggested that a similar molecule should exist to facilitate caspase activation in mammalian cells. This hypothesis was confirmed by the biochemical purification of Apaf-1 (apoptosis protease activating factor-1), a 130 kDa that is functionally equivalent to CED-4 (Zou *et al.*, 1997). Apaf-1 shares 22% identity and 48% similarity with CED-4, predominantly in a stretch of 320 amino acids. Interestingly, Apaf-1 also shows 21% identity and 53% similarity to CED-3 (Zou *et al.*, 1997). This region of homology is confined to the amino-terminus and is required for binding to caspases via homophilic interactions, and thus is termed the caspase recruitment domain (CARD). Other interesting structural features include a nucleotide binding domain comprised of consensus Walker A and B boxes, as well as a carboxyl-terminal WD repeat region which facilitates protein-protein interactions (Zou *et al.*, 1997).

Several studies have contributed to the molecular mechanism of Apaf-1-mediated caspase activation. In the absence of co-factors, Apaf-1 is proposed to exist in an inactive conformation such that the amino-terminal CARD domain is inaccessible due to a "folding over" of the WD repeat region (Li *et al.*, 1997). Binding of the co-factors, cytochrome *c* and dATP/ATP, both of which are released from the mitochondria, to the WD repeats and nucleotide binding domain, respectively, triggers a conformational change which exposes the CARD; thereby permitting binding of the pro domain of

procaspase 9 to the CARD of Apaf-1 (Li *et al.*, 1997). The complex consisting of Apaf-1, procaspase 9, cytochrome *c*, and dATP is referred to as the apoptosome. Association of procaspase 9 to Apaf-1 likely occurs concomitantly with Apaf-1 oligomerization, which is mediated by the CED-4 homology domain (Hu *et al.*, 1998; Srinivasula *et al.*, 1998; Zou *et al.*, 1999). Apaf-1 oligomerization brings several procaspase 9 molecules within close proximity (Zou *et al.*, 1999). Intrinsic procaspase 9 activity is sufficient for autocatalysis (Hu *et al.*, 1999; Zou *et al.*, 1999). Interestingly, there is one report that procaspase 9 can be activated without proteolytic processing (Stennicke *et al.*, 1999). Regardless, active caspase 9 activates the downstream effector caspase 3 (Hu *et al.*, 1999; Zou *et al.*, 1999). However, it is unclear whether active caspase 9 is released to seek out procaspase 3 (Zou *et al.*, 1999) or whether it is retained to process procaspase 3 that has been recruited by the WD repeats of Apaf-1 (Hu *et al.*, 1999). Recently, it has been proposed that active caspase 3 is retained in the apoptosome, while a small portion is present in the cytosol as free enzyme (Bratton *et al.*, 2001). All of these observations may be satisfied by the recent observation that Apaf-1 is proteolytically processed in response to some apoptotic stimuli (Lauber *et al.*, 2001). This cleavage event leads to the partial loss of Apaf-1's CARD and therefore may permit the release of activated caspases from the complex (Lauber *et al.*, 2001). However, Bratton *et al.* (2001) have shown that caspase 3 interacts with Apaf-1 (and the apoptosome) via interaction with XIAP (X-linked IAP), a potent member of the evolutionarily conserved IAP family of endogenous caspase inhibitors (Deveraux and Reed, 1999; Bratton *et al.*, 2001). Therefore, these authors propose a model in which active caspase 3 is retained with the apoptosome, and thus inhibited via its interaction with XIAP (Bratton *et al.*, 2001). A new mitochondrial

protein, Smac/DIABLO (second mitochondrial activator of caspases/direct IAP binding protein with low pI), provides an additional level of regulation (Du *et al.*, 2000; Verhagen *et al.*, 2000). In response to a death signal, Smac/DIABLO redistributes to the cytosol (similar to cytochrome *c*) and promotes caspase activation by antagonizing XIAP inhibition (Du *et al.*, 2000; Verhagen *et al.*, 2000) and promoting processing of procaspase 3 (Chai *et al.*, 2000). It has also been reported that Smac/DIABLO can activate procaspase 9 independently of cytochrome *c* and Apaf-1 by directly antagonizing XIAP bound to inactive (Chauhan *et al.*, 2001) or active (Ekert *et al.*, 2001) caspase 9. Furthermore, based on the identification and functional studies of a Smac/DIABLO splice variant, referred to as Smac β, an IAP-independent mechanism of Smac/DIABLO function has recently been proposed (Roberts *et al.*, 2001).

Nucleotide binding is required for caspase 9 activation, however the molecular basis for this requirement is unclear. Early reports demonstrated that both dATP or ATP bound to the nucleotide binding domain of Apaf-1, albeit at significantly different concentrations, and that nucleotide binding was a requirement for caspase activation (Zou *et al.*, 1999). Moreover, it was demonstrated that ATP hydrolysis occurred, presumably to facilitate Apaf-1 conformational change(s) and/or oligomerization by allowing cytochrome *c* to bind (Li *et al.*, 1997; Hu *et al.*, 1999; Zou *et al.*, 1999). However, recent evidence indicates that ATP hydrolysis is not required and that simple binding of the nucleotide to Apaf-1 is sufficient for apoptosome formation and function (Jiang and Wang, 2000). Interestingly, cytochrome *c* binding to Apaf-1 can occur independently of dATP, but dATP is required for subsequent caspase activation (Jiang and Wang, 2000; Purring-Koch and McLendon, 2000).

The apoptosome, comprised of Apaf-1, cytochrome *c*, dATP, and procaspase 9, exists as either a ~700 kDa or a ~ 1.4 MDa complex (Cain *et al.*, 2000). It has been proposed that the smaller 700 kDa complex is the active complex as both active caspase 9 and processed caspase 3 can be detected in cells expressing this complex (Cain *et al.*, 2000). Furthermore, cells treated with apoptotic stimuli rapidly assemble the 700 kDa complex and process caspases (Cain *et al.*, 2000). In contrast, the 1.4 MDa complex is biologically inactive, suggesting an additional level of regulation (Cain *et al.*, 2000). This is supported by recent identification of NAC, a regulator of Apaf-1 containing a CARD, which is found in association with Apaf-1 in complexes greater than 1 MDa (Chu *et al.*, 2001). However, NAC is reported to be a synergistic enhancer of Apaf-1-mediated caspase activation, not a negative regulator (Chu *et al.*, 2001). The same sequence has also been described as DEFCAP and is classified as a CED-4 homologue (Hlaing *et al.*, 2001). This group determined that DEFCAP was an apoptotic inducer and assisted in procaspase 2 activation (Hlaing *et al.*, 2001). Therefore, it still remains possible that the larger 1.4 MDa complex is maintained in an inactive state by as yet unidentified regulatory molecules, perhaps XIAP or similar proteins, as mentioned earlier (Bratton *et al.*, 2001). HSP70, which permits Apaf-1 oligomerization into large complexes but inhibits recruitment of procaspase 9 thus negatively regulating the apoptosome (Beere *et al.*, 2000; Saleh *et al.*, 2000), is an excellent candidate.

Germ line deletion of *apaf-1* in mice is lethal at embryonic day 16.5 (Cecconi *et al.*, 1998; Yoshida *et al.*, 1998). Furthermore, these animals feature severe craniofacial abnormalities, brain overgrowth, and persistence of interdigital webs (Cecconi *et al.*, 1998; Yoshida *et al.*, 1998). These studies define Apaf-1 as a critical component of PCD

and development. In addition, *in vitro* studies using cells derived from *apaf-1*$^{-/-}$ mice have significantly contributed to ordering the release of cytochrome *c* upstream of procaspase 9 activation (Cecconi *et al.*, 1998; Yoshida *et al.*, 1998). However, *apaf-1*$^{-/-}$-derived cells still remain sensitive to some apoptotic stimuli (Cecconi *et al.*, 1998; Yoshida *et al.*, 1998), suggesting that (i) *apaf-1*$^{-/-}$-derived cells can undergo apoptosis via mitochondrial-independent pathways, such as that observed in response to death receptor ligation in type I cells (Section 1.3.5.1); or (ii) alternate Apaf-1 homologues may exist. Candidates include the aforementioned NAC/DEFCAP (Chu *et al.*, 2001; Hlaing *et al.*, 2001), Nod2 (Ogura *et al.*, 2001), CARD12 (Geddes *et al.*, 2001), as well as Nod1/CARD4 (Bertin *et al.*, 1999; Inohara *et al.*, 1999). Interestingly, Nod1/CARD4 contains an amino-terminal CARD domain and a nucleotide binding domain, both of which are required for its interaction with and activation of procaspase 9 (Bertin *et al.*, 1999; Inohara *et al.*, 1999). However, this protein does not have a WD repeat region, and thus presumably functions independently of cytochrome *c* (Bertin *et al.*, 1999; Inohara *et al.*, 1999). The significance of alternate Apaf-1-like molecules is still unclear, but may suggest cell type specific mechanisms to regulate caspase activation.

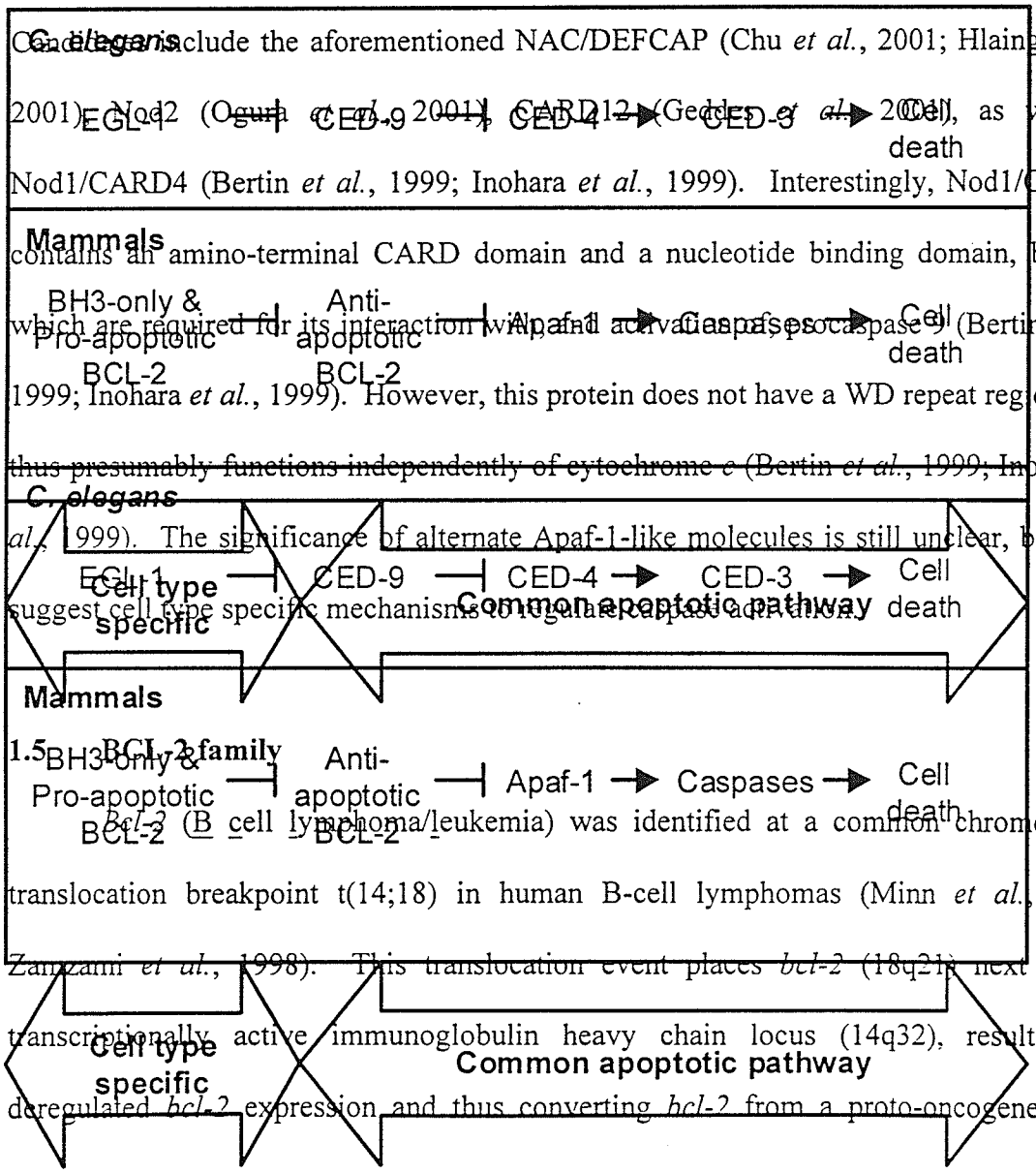

1.5 BCL-2 family

Bcl-2 (B cell lymphoma/leukemia) was identified at a common chromosomal translocation breakpoint t(14;18) in human B-cell lymphomas (Minn *et al.*, 1998; Zamzami *et al.*, 1998). This translocation event places *bcl-2* (18q21) next to the transcriptionally active immunoglobulin heavy chain locus (14q32), resulting in deregulated *bcl-2* expression and thus converting *bcl-2* from a proto-oncogene to an

oncogene (Bakhshi *et al.*, 1985; Cleary and Sklar, 1985, Cleary *et al.*, 1986). This particular translocation was identified in ~85% of human follicular lymphomas and thus classified as a proto-oncogene (Tsujimoto *et al.*, 1985). *Bcl-2* is a unique proto-oncogene in that it does not favor cell proliferation, but rather cell survival in sub-optimal growth conditions (Kelekar and Thompson, 1998). These conditions include growth factor deprivation, ultraviolet (UV) and γ-irradiation, heat shock, viral infection, and in the presence of cytotoxic lymphokines, calcium ionophores, and free radical generating agents (Schendel *et al.*, 1998). Interestingly, not only can BCL-2 inhibit apoptosis induced by the aforementioned events, but also necrosis induced by chemical hypoxia, cyanide, rotenone, antimycin A, kainic acid and tumor necrosis factor-α (TNF-α) (Gross *et al.*, 1999).

Transgenic experiments in *C. elegans*, in which BCL-2 rescued cells typically committed to cell death in both wild type and *ced-9*-deficient animals, established that BCL-2 is a functional homologue of CED-9 (Vaux *et al.*, 1992; Hengartner and Horvitz, 1994). Subsequent studies identified numerous related proteins. Currently, there are more than 20 known members of the BCL-2 family with opposing functions and varying degrees of homology in both mammalian cells and viruses (Minn *et al.*, 1998). This large family is now broadly divided into anti-apoptotic (pro-survival) and pro-apoptotic proteins. Mammalian anti-apoptotic members include BCL-2, BCL-X_L, BCL-w, MCL-1, A1, adenovirus E1B 19K, Eppstein-Barr virus BHRF-1, and *C. elegans* CED-9. The mammalian pro-apoptotic subfamily includes BAX, BAK, BCL-X_S, BOK/MTD, BAD, BIK, BID, BIM, HRK, BLK, NOXA, BCL-RAMBO and *C. elegans* EGL-1 (reviewed in Kelekar and Thompson, 1998; Minn *et al.*, 1998; Adams and Cory, 1998; Gross *et al.*,

1999; Oda *et al.*, 2000; Kataoka *et al.*, 2001). As alluded to earlier, deregulation of anti-apoptotic *bcl-2* expression is a contributing factor to the development of leukemia and lymphoma (Tsujimoto *et al.*, 1985) as well as many other types of cancer (Yang and Korsmeyer, 1996). Likewise, inactivating frameshift mutations of the pro-apoptotic *bax* gene provide a selective growth advantage to cells during the development of haemopoietic, gastric, and colorectal malignancies (Brimmell *et al.*, 1998; Ionov *et al.*, 2000). Furthermore, expression of *bax* suppresses tumorigenesis and stimulates apoptosis of tumors *in vivo* (Yin *et al.*, 1997). Therefore, study of this protein family and its role in apoptosis will contribute significantly to understanding tumorigenesis. BCL-2 family proteins are proposed to regulate cell death in a variety of ways including homo- and heterodimeric interactions, sequestering non-BCL-2 proteins, and impacting mitochondrial function (Minn *et al.*, 1998). The role of BCL-2 proteins at the mitochondria will be discussed in detail.

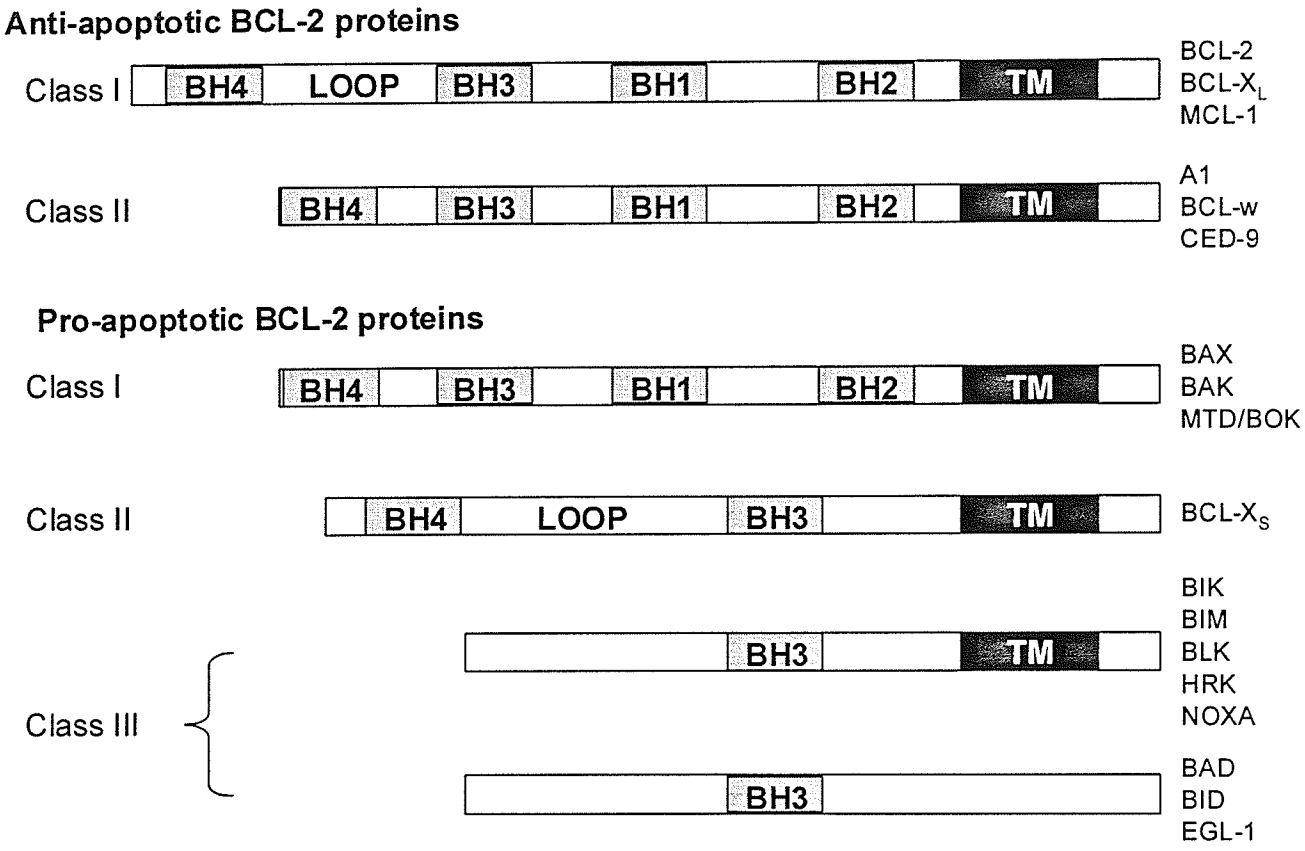

Figure 5: Classification and organization of BCL-2 family members. The general organization of the BH3 and TM domains of various BCL-2-related proteins is indicated. The family is divided into anti-apoptotic and pro-apoptotic proteins. Subgroups exist in each category, as defined by the presence or absence of the BH domains. With the exception of *C. elegans* CED-9 and EGL-1, only mammalian BCL-2-related proteins are shown. Illustrations are not to scale. (Adapted from Kelekar and Thompson, 1998).

1.5.1 Structural features of BCL-2 family proteins

The basis for establishing the BCL-2 family is four conserved regions known as the BCL-2 homology domains, BH1-4. The distribution of these domains further subdivides the BCL-2 family (Figure 5) (Adams and Cory, 1998; Kelekar and Thompson, 1998). To date, all anti-apoptotic BCL-2 proteins contain all four BH domains and a carboxyl-terminal TM domain. This set of proteins is further subdivided into class I or II proteins due to the presence or absence of a loop forming region between BH3 and BH4 domains, respectively (Kelekar and Thompson, 1998). Note that the BH4 domain is exclusive to anti-apoptotic proteins with the exception of BCL-X_S, a splice variant of BCL-X_L (Minn *et al.*, 1996). Pro-apoptotic BCL-2 proteins are divided into three classes. Class I pro-apoptotic proteins feature BH1, BH2, BH3, and TM domains and predominantly function via antagonizing anti-apoptotic proteins. Recent data suggest that these proteins can also promote cell death via heterodimerization-independent mechanisms (reviewed in Kelekar and Thompson, 1998; Minn *et al.*, 1998). Currently, BCL-X_S is the only known member of class II pro-apoptotic proteins and promotes cell death by antagonizing anti-apoptotic BCL-X_L (Minn *et al.*, 1996). Class III proteins are potent death agonists and are also referred to as "BH3-only" proteins as they share homology with BCL-2 only in this region. This region is required for heterodimerization and pro-apoptotic activity. Many BCL-2 family members also have a TM domain that dictates subcellular localization (Kelekar and Thompson, 1998; Minn *et al.*, 1998).

1.5.1.1 The BH1 and BH2 domains

The least studied of the BH domains are BH1 and BH2. The BH1 and BH2 domains are 21 and 16 residues long, respectively, and are typically separated by 30 to 40 amino acids (Minn *et al.*, 1998). Although BCL-2 proteins are often illustrated linearly, the three-dimensional association of the BH domains contributes to protein-protein interactions. This is especially evident from X-ray and NMR (nuclear magnetic resonance) studies of the antagonist BCL-X_L which demonstrate that BCL-X_L is primarily comprised of seven α-helices (Muchmore *et al.*, 1996). Specifically, the α-helices of the BH1 and BH2 domains cooperate with the α-helical BH3 domain to form a hydrophobic pocket on the surface of the protein. It is proposed that this cleft is analogous to a 'receptor' and thus facilitates interaction with pro-apoptotic proteins (Sattler *et al.*, 1997). BCL-X_S, which lacks the BH1 and BH2 domains, does not interact with any of the death agonists of the BCL-2 family indicating that these two regions are essential for heterodimerization between opposing family members (Minn *et al.*, 1996; Kelekar and Thompson, 1998). Furthermore, mutation of a conserved glycine residue (Gly^{138}) within the BH1 domain, which contributes to the hydrophobic pocket, hinders interaction with death agonists and negates the protective activity of BCL-X_L (Yin *et al.*, 1994; Sattler *et al.*, 1997; Kelekar and Thompson, 1998). The BH1 and BH2 domains are also present in pro-apoptotic family members and may be involved in mitochondrial deregulation, as described in Sections 1.5.3.3 and 1.6.

1.5.1.2 The BH3 domain

The BH3 domain is the only domain shared by all BCL-2-related proteins. Not only does it contribute to formation of the hydrophobic pocket of anti-apoptotic BCL-2 proteins (Muchmore *et al.*, 1996; Sattler *et al.*, 1997), it is the single most important domain for death agonists (Kelekar and Thompson, 1998; Minn *et al.*, 1998). So much so that an entire branch of BH3-only (class III) proteins has diverged in both mammals and the nematode *C. elegans*. The BH3 domain was initially identified as a span of 16 residues in BAK necessary for heterodimerization with anti-apoptotic BCL-2 proteins and promotion of cell death (Chittenden *et al.*, 1995; Sattler *et al.*, 1997; Kelekar and Thompson, 1998). Structural, functional, and point mutation analyses have identified eight residues that define the core of the BH3 domain (Figure 6). The crucial residues are leucine at position 1 and aspartate at position 6 of the BH3 domain core (Kelekar and Thompson, 1998). These residues are essential to heterodimerization and pro-apoptotic activity. Interestingly, these residues are also present in some BCL-2 death agonists. However, it is postulated that the presence or absence of a non-polar residue at position 4 of the BH3 core may determine anti- or pro-apoptotic activity, respectively (Kelekar and Thompson, 1998). It is likely not that simple, as sequences surrounding the BH3 domain have also been implicated in determining protein function (Sattler *et al.*, 1997).

Recently, structural studies have provided clues as to how anti- and pro-apoptotic proteins may be differentiated. As mentioned previously, X-ray and NMR examination of BCL-X_L complexed to the BH3 domain of BAK revealed that the BH3 peptide formed an amphipathic α-helix that inserted into the hydrophobic groove of BCL-X_L (Sattler *et al.*, 1997). Subsequent solving of the three-dimensional structure of the BH3-only death

agonist BID, which is surprisingly similar to BCL-X_L despite opposing function and dissimilar primary sequences outside of the BH3 domain, has provided additional insight into how the BH3 domain contributes to the regulation of cell death (Gross *et al.*, 1999). Specifically, the hydrophobic face of the BH3 domain of BID is packed against neighboring helices but it is exposed in active truncated BID (tBID) (Chou *et al.*, 1999; McDonnell *et al.*, 1999). This observation coupled with secondary structure predictions of other BCL-2-related proteins yields the emergence of two conformational subgroups based on the accessibility of the BH3 domain (Figure 6) (Gross *et al.*, 1999; McDonnell *et al.*, 1999). Specifically, anti-apoptotic or inactive pro-apoptotic proteins have their BH3 domain buried within their structure, while constitutively active pro-apoptotic proteins have an exposed BH3 domain (Gross *et al.*, 1999; McDonnell *et al.*, 1999). This model likely provides a regulatory step for modulation of BCL-2 proteins. Regardless, there are numerous biochemical studies to support the significant contribution of the BH3 domain to the heterodimerization and function of pro-apoptotic BCL-2 proteins as deletion of this region impairs pro-apoptotic activity and can disrupt protein binding (reviewed in Adams and Cory, 1998; Kelekar and Thompson, 1998; Gross *et al.*, 1999). Recently, the solution structure of full-length pro-apoptotic BAX has been solved and is remarkably similar to the structures of BCL-2, BCL-X_L, and BID (Suzuki *et al.*, 2000). Furthermore, previous studies of BCL-2 and BCL-X_L were unable to determine the impact of the carboxyl-terminal hydrophobic TM domain. However, NMR studies of full length BAX have determined that the TM domain regulates the accessibility of the BH3 domain (Suzuki *et al.*, 2000). This is supported by previous work that speculated the BH3 domain became accessible only after the integration of BAX into the outer

mitochondrial membrane via its TM domain (Section 1.5.1.4; Goping *et al.*, 1998). In addition, the same study revealed a role for the amino-terminus in regulating the accessibility of the BH3 domain of BAX (Goping *et al.*, 1998). Possible cooperative effects between the amino-terminus and the carboxyl-terminal TM domain remain to be determined.

The BH3 domain may also function as a regulatory domain that prevents the integral association of a hairpin pair of central hydrophobic α-helices (α5 and α6 of BCL-2 and BCL-X_L) with the outer mitochondrial membrane (Schendel *et al.*, 1998). Equivalent pairs of α-helices have been observed in BID and BAX (Chou *et al.*, 1999; McDonnell *et al.*, 1999; Suzuki *et al.*, 2000). This region resembles the translocation domain of bacterial toxins and have all been shown to form ion channels *in vitro* that may contribute to apoptosis via regulation of mitochondrial homeostasis (Section 1.5.3.3; Schendel *et al.*, 1998).

A

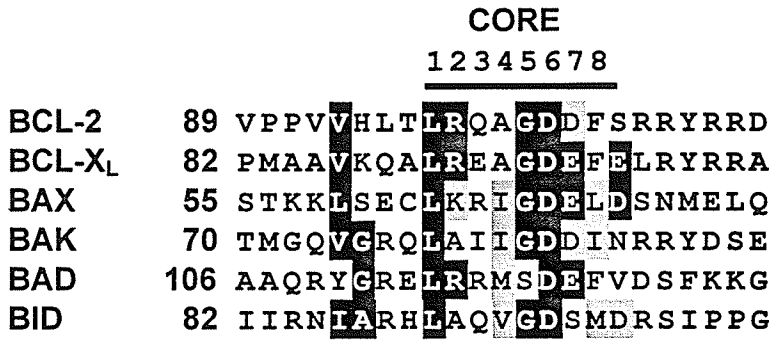

B

BH3 domain "buried"	BH3 domain "exposed"
BCL-2	cleaved BCL-2
$BCL\text{-}X_L$	cleaved $BCL\text{-}X_L$
BCL-w	
CED-9	
BID	tBID
BAX	$BCL\text{-}X_S$
BAK	BAD
MTD	NRK
	BIM
	BLK
	EGL-1

Figure 6: Sequence comparison of some BCL-2 family members and classification of BCL-2 proteins based on the availability of the BH3 domain. (A) Alignment of amino acid sequences in the BH3 domain of some BCL-2 family members. The core residues of the BH3 domain, residues 1 to 8, are indicated. Identical residues are shaded in black and similar residues are shaded in gray. (B) BCL-2 family proteins can be divided into two subgroups based on the availability of the BH3 domain. Proteins classified as BH3 domain 'buried' are predicted to be similar to the three-dimensional structure of BID and $BCL\text{-}X_L$. These proteins rely on a conformational change to induce apoptosis. Proteins classified as BH3 domain 'exposed' include truncated BCL-2-related proteins. These proteins are predicted to be constitutively active as the BH3 domain is accessible. (Adapted from McDonnell *et al.*, 1999; Kelekar and Thompson, 1998).

1.5.1.3 The BH4 domain

The amino-terminal BH4 domain is well conserved among anti-apoptotic BCL-2 proteins. The BH4 domain contributes to the anti-apoptotic activity of this protein as its deletion converts BCL-2 and BCL-X_L to pro-apoptotic proteins in some cell types (Borner *et al.*, 1994; Borner *et al.*, 1996; Hunter *et al.*, 1996; Huang *et al.*, 1998; Shimizu *et al.*, 2000a). Recently, it was shown that the BH4 domain of BCL-2 and BCL-X_L prevents mitochondrial deregulation characteristic of apoptosis (Shimizu *et al.*, 2000a). The BH4 domain facilitates interactions with itself (Hanada *et al.*, 1995) as well as non-BCL-2 proteins, such as calcineurin (Shibasaki *et al.*, 1997), Raf-1 (Wang *et al.*, 1996), p28 BAP31 (Ng *et al.*, 1997), Apaf-1 (Hu *et al.*, 1998; Newmeyer *et al.*, 2000), and *C. elegans* CED-4 (Huang *et al.*, 1998). The functional significance of these interactions with respect to the regulation of cell death is unknown.

1.5.1.4 The TM domain

The carboxyl-terminal TM domain consists of 19 hydrophobic amino acids and is present in most BCL-2 family members (Minn *et al.*, 1998; Zamzami *et al.*, 1998). This C-terminal anchoring sequence localizes proteins to the outer mitochondrial membrane and the contiguous membrane comprising the endoplasmic reticulum (ER) and nuclear envelope (Krajewski *et al.*, 1993). The prototypical anti- and pro-apoptotic proteins, BCL-2 and BAX, respectively, localize to distinct patches on the outer mitochondrial membrane, usually at the contact sites where the inner and outer membranes are in close proximity (Minn *et al.*, 1998; Zamzami *et al.*, 1998). Furthermore, it is postulated that

endogenous BAX is cytosolic or loosely associated with the mitochondria until prompted to integrate by an apoptotic signal. Regardless, deletion of the TM domain impacts on the activity of these proteins. Specifically, BCL-2 lacking its TM domain is primarily cytosolic and abolishes or diminishes its protective function. Similarly, TM-deficient BAX prevents mitochondrial localization and abolishes its pro-apoptotic function (reviewed in Zamzami *et al.*, 1998). However, targeting of BCL-2 or BAX to the mitochondria via heterologous TM domain sequences restores localization and function (Zha *et al.*, 1996a; Zhu *et al.*, 1996; Goping *et al.*, 1998). Other BCL-2 family members lacking a TM domain are primarily cytosolic, but appear to efficiently translocate and integrate into the mitochondria following an apoptotic stimulus (Kelekar and Thompson, 1998; Minn *et al.*, 1998). This has been demonstrated for BIM (Puthalakath *et al.*, 1999), BID (Li *et al.*, 1998; Luo *et al.* 1998; Gross *et al.*, 1999a), and BAD (Zha *et al.*, 1996) following various post-translational modifications.

Interestingly, localization to the mitochondria is not absolutely required for BCL-2 function. Expression of chimeric BCL-2 proteins containing TM domain sequences from ER proteins, such as actinomycin A or cytochrome b_5, are also able to inhibit apoptosis in a cell type, signal-specific manner (Zhu *et al.*, 1996; Lee *et al.*, 1999; Hacki *et al.*, 2000). Therefore, it is plausible that simply the anchoring of BCL-2 to an intracellular membrane is sufficient for cellular protection (Minn *et al.*, 1998). However, chimeric BCL-2 protein can still heterodimerize with endogenous mitochondrial BCL-2-related (and unrelated) proteins, therefore it is equally possible that chimeric BCL-2 can still influence mitochondrial function despite forced targeting to the ER (Zamzami *et al.*, 1998).

1.5.2 Post-translational modification of BCL-2 family proteins

The large number of family members suggests complex regulation perhaps designed to sense different types of cellular damage (Gross *et al.*, 1999). There is limited evidence that BCL-2-related proteins may be transcriptionally regulated in response to death stimuli (Gross *et al.*, 1999). However, there is good evidence that post-translational modifications such as, phosphorylation and proteolytic cleavage in response to various stimuli, contribute to active and inactive conformers of BCL-2 proteins (Gross *et al.*, 1999). As well, a number of BCL-2 proteins oligomerize and translocate within the cell, however it is unclear if these events are a form of post-translational modification or a consequence of modification. To complicate matters, it has also been observed that a single protein can be regulated by more than one type of modification (Zha *et al.*, 1996; Li *et al.*, 1998; Luo *et al.*, 1998; Puthalakath *et al.*, 1999).

1.5.2.1 Phosphorylation state

The activity of a signal transduction protein is often determined by its phosphorylation state. For example, in the presence of growth factors, BAD is held inactive due to phosphorylation at residues serine-136 and serine-112 (Datta *et al.*, 1997; del Peso *et al.*, 1997; Blume-Jensen *et al.*, 1998; Harada *et al.*, 1999). Serine-136 is specifically phosphorylated by AKT/PKB (protein kinase B), a serine/threonine kinase downstream of phophoinositide 3-kinase (PI3K) (Datta *et al.*, 1997; del Peso *et al.*, 1997). Protein kinase A (PKA), which is tethered to the mitochondria by A-kinase anchoring protein (AKAP), specifically targets serine-112 (Harada *et al.*, 1999).

Phosphorylated BAD is sequestered in the cytosol by a 14-3-3 protein that recognizes phosphoserine residues, thereby preventing it from acting on the mitochondria (Zha *et al.*, 1996). In the absence of growth factor, BAD is dephosphorylated and thus permitted to associate with BCL-2/BCL-X_L at the mitochondria. It is hypothesized that BAD promotes cell death by recruiting BCL-2/BCL-X_L away from other binding partners (Zha *et al.*, 1996; Gross *et al.*, 1999). Dephosphorylated BAD heterodimerizes with BCL-2 and BCL-X_L by inserting its BH3 domain into the hydrophobic clefts of BCL-2 and BCL-X_L (Gross *et al.*, 1999). It is predicted that phosphorylation renders the BH3 domain unavailable for interaction, in accordance with the model set forth by McDonnell *et al.* (1999).

The phosphorylation of BCL-2 has also been reported to impact its cytoprotective activity. Specifically, serine phosphorylation sites have been identified in the proposed loop region located between the BH4 and BH3 domains of BCL-2 and BCL-X_L (Halder *et al.*, 1995; Chang *et al.*, 1997; Ito *et al.*, 1997; Poommipanit *et al.*, 1999). These sites are proposed to negatively regulate BCL-2 function as removal of the loop region enhances apoptosis in some experimental systems (Srivastava *et al.*, 1999; Wang *et al.*, 1999). It is speculated that phosphorylation within the loop region of BCL-2 yields an altered conformation that influences its function (Gross *et al.*, 1999).

1.5.2.2 Proteolytic cleavage

Unlike phosphorylation, proteolytic cleavage is an irreversible mechanism of protein activation. BID is a cytosolic BH3-only protein that is cleaved from p22 to p15 by activated caspase 8 following ligation of death receptors (Li *et al.*, 1998; Luo *et al.*,

1998) or to p17 by granzyme B (Barry *et al.*, 2000; Sutton *et al.*, 2000; Alimonti *et al.*, 2001). This cleavage event removes amino-terminal negative regulatory sequences and permits translocation of the p15 or p17 fragment, referred to as tBID (truncated BID), to the mitochondria (Li *et al.*, 1998; Luo *et al.*, 1998). Furthermore, specific translocation of tBID to the mitochondria is due to post-translational N-myristoylation of a glycine residue exposed following proteolytic processing, suggesting yet another level of regulation (Zha *et al.*, 2000). Structural NMR studies reveal that removal of the amino-terminus exposes more than 200 $Å^2$ of previously buried hydrophobic surface. The net electrostatic charge changes from –13 for BID to –4 for tBID (McDonnell *et al.*, 1999). Interestingly, the buried surface corresponds to the hydrophobic surface of the BH3 domain that can interact with BAX (Gross *et al.*, 1999). Furthermore, there is evidence that association of tBID with BAX or BAK induces a conformational change in BAX/BAK that promotes their integration into the outer mitochondrial membrane (Desagher *et al.*, 1999; Crompton, 2000; Korsmeyer *et al.*, 2000). This event yields release of the caspase activator cytochrome *c*, however, although BAX and/or BAK are required for tBID-induced cytochrome *c* release, the molecular details of how cytochrome *c* escapes the mitochondria remain elusive (Crompton, 2000; Korsmeyer *et al.*, 2000; Wei *et al.*, 2000a; Wei *et al.*, 2001). Interesting, an analogous proteolytic cleavage event has recently been identified for BAD, also a BH3-only pro-apoptotic protein (Condorelli *et al.*, 2001). Similar to tBID, truncated BAD also translocates to the mitochondria and induces cytochrome *c* release in response to ligation of death receptors, as well as growth factor withdrawal (Condorelli *et al.*, 2001).

Anti-apoptotic BCL-2 proteins can also be cleaved by proteases. Proteolytic processing within the loop region of BCL-2 and BCL-X_L removes the amino-terminal BH4 domain and exposes the BH3 domain (Cheng *et al.*, 1997). This effectively converts BCL-2 from an anti-apoptotic protein to a pro-apoptotic protein (Cheng *et al.*, 1997). Caspases can cleave BCL-2 and BCL-X_L in response to a variety of death stimuli in a cell type dependent manner (Cheng *et al.*, 1997; Clem *et al.*, 1998; Fujita *et al.*, 1998; Fujita and Tsuruo, 1998; Grandgirard *et al.*, 1998). The cleavage fragment generated by caspase-dependent cleavage of BCL-2 anti-apoptotic proteins promotes the release of cytochrome *c* from the mitochondria (Kirsch *et al.*, 1999). This type of mechanism contributes to a feed-forward amplification loop for efficiently killing the cell following the initial activation of the caspase cascade (Kirsch *et al.*, 1999).

1.5.2.3 Oligomerization and Translocation

As mentioned previously, it is uncertain whether protein oligomerization and translocation events activate these proteins or are a consequence of other post-translational modifications. The phosphorylation-dependent relocalization of BAD and cleavage-dependent translocation of BID are but two examples of this phenomenon (Sections 1.5.2.1 and 1.5.2.2). In any case, the BCL-2 superfamily is unique in that members exhibit a high capacity for protein-protein interactions. Homo- and heterodimeric interactions between pro- and anti-apoptotic BCL-2 family proteins form the basis of the 'rheostat' model of cell death regulation (Section 1.5.3.1; Oltvai *et al.*, 1993). Recently, higher order oligomers have also been detected for some family members such as BAX and BAK *in vitro* (Antonsson *et al.*, 2000; Wei *et al.*, 2000a) and

in vivo (Antonsson *et al.*, 2001). Inactive BAX is monomeric and cytosolic while active mitochondrial BAX is cross-linkable as a homodimer (Goping *et al.*, 1998; Gross *et al.*, 1998; Conus *et al.*, 2000a). *In vitro* removal of the amino-terminus permits BAX dimerization (and thus activation), translocation and integration into the outer mitochondrial membrane (Goping *et al.*, 1998). Alteration of the amino-terminus of BAX has yet to be confirmed *in vivo*. However, it is presumed that BAX is held in an inactive conformation due to an amino-terminal regulatory sequence that buries the BH3 domain, preventing killing and dimerization (Goping *et al.*, 1998; McDonnell *et al.*, 1999). Consistent with these observations is the finding that enforced dimerization of BAX triggers translocation of BAX homodimers to the mitochondria where it exerts its pro-apoptotic activity (Gross *et al.*, 1998). Alternatively, in response to a death signal, BAX oligomerization and insertion into the mitochondrial membrane of apoptotic cells has also been observed (Antonsson *et al.*, 2001). However, NMR studies of BAX reveal that the TM domain regulates BH3 domain accessibility (Suzuki *et al.*, 2000). It remains possible that the amino-terminus and the TM domain cooperatively regulate the BH3 domain.. The accessibility of the BH3 domain of BAK is similarly regulated by the amino-terminus (Desagher *et al.*, 1999; Griffiths *et al.*, 1999). It has recently been shown that BCL-2 does not homodimerize to prevent apoptosis, but rather remains as a monomer at the mitochondria even in the presence of death stimuli (Conus *et al.*, 2000a). Furthermore, BCL-2 dimers were detected only when the BH1 and BH2 domains were removed or altered which also significantly diminished cell protective activity (Conus *et al.*, 2000a).

Sequestering proteins in different subcellular areas ensures that pathways are not activated accidentally. Likewise, the active translocation of pro-apoptotic molecules from their latent 'hiding spot' to their site of action yields an additional mode of regulation. As mentioned previously, cytosolic inactive BAX translocates (and integrates) to the outer mitochondrial membrane where it is found as a cross-linkable homodimer or oligomer, and exerts its cytotoxic activity following a death stimulus (Goping *et al.*, 1998; Gross *et al.*, 1998; Conus *et al.*, 2000a; Antonsson *et al.*, 2001). The BH3-only death agonist, BIM, normally localizes to the microtubule-associated dynein motor complex through interaction with the LC8 dynein light chain (Puthalakath *et al.*, 1999). However, in response to an apoptotic signal, BIM redistributes to the mitochondria where it interacts with and antagonizes BCL-2 (Puthalakath *et al.*, 1999).

1.5.3 Models of BCL-2 function: pro- and anti-apoptotic

As described earlier, BCL-2 family proteins are proposed to regulate cell death in a variety of ways including homo- and heterodimeric interactions, sequestering non-BCL-2 proteins, and impacting mitochondrial function (Minn *et al.*, 1998). Each model will be touched upon. However, the role of BCL-2 proteins at the mitochondria will be discussed in detail.

1.5.3.1 Rheostat model

The large number of homo- and heterodimeric interactions observed between opposing members of the BCL-2 family prompted the hypothesis that the relative ratio of pro-apoptotic proteins bound to anti-apoptotic proteins determines cell fate, at least in

part (Oltvai *et al.*, 1993). This is referred to as the rheostat model. This model is consistent with reports that certain agonists heterodimerize with a particular subset of antagonists. (However, binding pair specificity may be partially a result of tissue specific expression as revealed from knock out studies [reviewed in Minn *et al.*, 1998]). In addition, enforced homodimerization of BAX induces apoptosis (Gross *et al.*, 1998). However, mutants of BCL-X_L and BAX have been described that fail to heterodimerize through their BH3 domain but retain their cytoprotective and cytotoxic activities, respectively, indicating that BCL-2 proteins can function independently of heterodimerization (Cheng *et al.*, 1996; Simonian *et al.*, 1996; Zha and Reed, 1997; Minn *et al.*, 1999). In addition, BAX and BAK are cytotoxic to yeast, an organism known to lack endogenous BCL-2 family proteins (Ink *et al.*, 1997; Jurgensmeier *et al.*, 1997). This indicates that the simple balance of pro-apoptotic to anti-apoptotic proteins is not sufficient to control apoptosis and therefore BCL-2 proteins have the capacity to regulate cell death by alternate mechanisms.

1.5.3.2 Displacement/sequestering of Apaf-1

Based on the interaction between CED-9 with CED-4, it has also been proposed that BCL-2/BCL-X_L inhibit cell death by binding to Apaf-1, thereby preventing Apaf-1 from contributing to caspase activation (Hu *et al.*, 1998). This hypothesis is supported by early observations that BCL-X_L associated with CED-4 and this interaction was disrupted by BAX, BAK, or BIK resulting in apoptosis (Hu *et al.*, 1998). Similarly, BCL-X_L co-immunoprecipitates with Apaf-1 in mammalian cells (Hu *et al.*, 1998; Newmeyer *et al.*, 2000). In addition, expression of BCL-X_L prevents the interaction between Apaf-1 and

procaspase 9 effectively blocking caspase 9 maturation (Hu *et al.*, 1998). However, it has also been shown that although BCL-X_L associates with Apaf-1, it does not prevent procaspase 9 processing (Newmeyer *et al.*, 2000). There is increasing evidence that BCL-X_L in fact does not interact with Apaf-1 (Song *et al.*, 1998; Minn *et al.*, 1999; Moriishi *et al.*, 1999; Conus *et al.*, 2000). These studies might be rationalized with the previous observations by the recent characterization of AVEN, a novel protein that can simultaneously bind BCL-X_L and Apaf-1 (Chau *et al.*, 2000). The significance of these studies to the regulation of apoptosis remains to be determined. In addition, the role of alternate Apaf-1-like proteins, such as Nod1/CARD4, Nod2, and CARD12 (Section 1.4), cannot be dismissed as yet.

1.5.3.3 Pore formation

Structural studies reveal that the tertiary structure of BCL-2, BCL-X_L, BAX, and BID are all very similar to the translocation domain of diphtheria toxin and the pore-forming domains of colicins A and E1 despite limited sequence homology. Specifically, all of these proteins feature a hairpin pair of two central hydrophobic helices that are sandwiched between two outer layers of amphipathic α-helices (Muchmore *et al.*, 1996; Sattler *et al.*, 1997; Chou *et al.*, 1999; McDonnell *et al.*, 1999; Suzuki *et al.*, 2000). In bacteria, both diphtheria toxin and colicins kill cells by forming highly conductive voltage-gated channels that are assembled as four helix bundles that insert into the plasma membrane of target cells (London, 1992; Elkins *et al.*, 1997). The significant similarities in structures prompted the hypothesis that BCL-2 proteins may regulate cell death by forming pores in cellular membranes, specifically the mitochondrial outer

membrane (Muchmore *et al.*, 1996; Sattler *et al.*, 1997). Each residue of an α-helix contributes ~1.5 Å to its overall length and an average lipid bilayer is ~30 Å across its hydrophobic internal surface (Montal and Mueller, 1972; reviewed in Schendel *et al.*, 1998). Therefore, approximately 20 consecutive hydrophobic residues are required to span a lipid bilayer (Schendel *et al.*, 1998). Intriguingly, the two central helices of BCL-X_L (α5,α6) are each sufficiently long enough to span a cellular membrane once. Therefore, since each BCL-X_L monomer contributes two helices, its dimer would yield a four helix bundle and effectively form a pore (Schendel *et al.*, 1998). Intriguingly, several groups have observed that BCL-2, BCL-X_L, BAX, and BID can each form pores in liposomes or planar lipid bilayers *in vitro* (reviewed in Antonsson *et al.*, 1997; Minn *et al.*, 1997; Schlesinger *et al.*, 1997; Schendel *et al.*, 1998; Schendel *et al.*, 1999), however the assembly of a four helix bundle has not been formally demonstrated. In the case of BAX, it is predicted that oligomerization would assemble a structure comprised of more than just a four helix bundle (Antonsson *et al.*, 2001).

Pores formed by BCL-2 family members have different properties. Specifically, BCL-2 and BCL-X_L can form pores with multiple levels of conductance and show selectivity to cations (Minn *et al.*, 1997; Schendel *et al.*, 1997; Schlesinger *et al.*, 1997), while BAX pores also have multiple conductance levels but are slightly anion selective (Antonsson *et al.*, 1997; Schlesinger *et al.*, 1997). It is likely that the residues lining the mouth and length of the channel lumen determine the ionic specificity of the pore (Schendel *et al.*, 1998). It remains to be determined if increased anion transport by BAX (or its regulation by BCL-2/BCL-X_L) induces apoptosis. Furthermore, deletion of α5 and α6 from BCL-2 converts BCL-2 into a pro-apoptotic protein that presumably is unable to

form pores suggesting that other mechanisms exist (Schendel *et al.*, 1998). However, wild type BCL-2 can prevent BAX channel formation in lipid vesicles (Antonsson *et al.*, 1997). It is unknown if the observed BCL-2 inhibition is because BCL-2 prevents formation of BAX channels or because BCL-2 forms pores with opposing ion selectivity and therefore restores ionic balance.

BCL-2 and BCL-X_L do not readily form ion-conductive pores at neutral pH, but do so in low pH conditions suggesting that protonation may be required to facilitate pore formation, similar to colicin (Schendel *et al.*, 1998). In contrast, BAX ion-conductive channel formation and function are equivalent in acidic and neutral pH conditions (Schlesinger *et al.*, 1998). It has been proposed that acidic pH facilitates the association of recombinant proteins with the experimental lipid bilayers as the recombinant proteins used in all of these experiments lack the carboxyl-terminal TM domain (Schendel *et al.*, 1998). (The presence of the TM domain reduces protein solubility and impairs purification of recombinant protein.) Therefore, the function of the TM domain may be to bring these molecules in contact with lipid membranes (Schlesinger *et al.*, 1997).

As mentioned, the structural studies revealed that helices α5 and α6 are hidden within the interior of BCL-2-related proteins. Therefore, a conformational change is likely required for pore formation. It is possible that these helices are exposed and inserted into the membrane in response to binding of the BH3 domain at the hydrophobic pocket (Schendel *et al.*, 1998). Recently, the tertiary structure of full length BAX demonstrated that the BH3 domain is protected by the hydrophobic TM domain (Suzuki *et al.*, 2000). However, integration of the TM domain into the outer mitochondrial membrane induced a conformation change that exposed the BH3 domain (Suzuki *et al.*,

2000). Therefore, this conformational change and/or subsequent protein-protein interactions through the BH3 domain may permit and/or facilitate insertion of α5 and α6 into the mitochondrial membrane (Schendel *et al.*, 1998). The latter hypothesis is favorable as BH3-mediated homo- and heterodimerization of BCL-2-related proteins have been observed (Section 1.5.1.2). It is noteworthy, however, that the significance of BCL-2 proteins as ion channels in apoptosis is unclear, as these structures have only recently been confirmed *in vivo* (Antonsson *et al.*, 2001).

1.6 The mitochondria and the permeability transition pore

Mitochondria are the primary energy producers of the cell and are essential to cell survival. The mitochondrion is comprised of two lipid membranes with the tightly folded cristae of the inner membrane surrounding the mitochondrial matrix. Embedded within the inner membrane are the proteins of the electron transport chain (ETC) which facilitate production of cellular energy in the form of ATP (Harris and Thompson, 2000). Normally, the inner membrane is impermeable to protons (H^+) so as to generate a proton gradient that is necessary for ATP production. The proton gradient across the inner membrane sets up an electrochemical gradient such that the matrix side of the inner membrane is negatively charged, while the side facing the intermembrane space is positively charged. This is referred to as the mitochondrial transmembrane potential ($\Delta\psi m$) (Bernardi, 1999). However, the passage of H^+ back into the matrix is possible and is a highly regulated event. The inner membrane contains many different, specific transporters including the adenine nucleotide translocator (ANT) which exchanges ADP and ATP between the mitochondrial matrix and the intermembrane space (Vieira *et al.*,

2000). The outer mitochondrial membrane surrounds the inner membrane, creating an intermembrane space, and is impermeant to the intermembrane protein, holocytochrome *c*. Movement of molecules across the outer membrane is less regulated and is primarily mediated by the voltage-dependent anion channel (VDAC, also known as porin), the most abundant protein in the outer membrane (Harris and Thompson, 2000). The increased permeability of the mitochondria is referred to as the mitochondrial permeability transition (Denecker *et al.*, 2001).

Mitochondrial membrane permeability is believed to be regulated by a large protein complex, known as the permeability transition (PT) pore, that resides at the contact sites between the inner and outer membrane (Bernardi, 1999; Crompton, 1999; Denecker *et al.*, 2001). The exact composition and arrangement of the PT pore is unknown; however, proteins of the matrix, inner and outer membranes, intermembrane space, and the cytosol have all been associated with the phenomenon of PT (Figure 7). Specifically, cyclophilin D (matrix), ANT (inner membrane), VDAC (outer membrane), and peripheral benzodiazepin receptor (PBR; intermembrane space), and hexokinase (cytsol) are the known components of the putative PT pore (Beutner *et al.*, 1998; Bernardi, 1999; Denecker *et al.*, 2001). The PT pore exists in an open and closed configuration. The open state of the PT pore permits passage of solutes of ~1500 Daltons and is promoted by high matrix Ca^{++}, inorganic phosphate, reactive oxygen species (ROS), oxidant chemicals, high matrix pH, and low $\Delta\psi m$ (Denecker *et al.*, 2001). In contrast, Mg^{++}, ADP, low matrix pH, and high $\Delta\psi m$ favor the closed conformation of the PT pore (Denecker *et al.*, 2001). Experimentally, cyclosporin A (a ligand of cyclophilin D) and bongkrekic acid (a ligand of ANT) can induce closure of the PT pore. As well,

several BCL-2-related proteins have been shown to regulate the state of PT pore (Harris and Thompson, 2000).

Prolonged PT pore opening dissipates the H^+ gradient resulting in depolarization of the mitochondria and consequently a decrease in the measured $\Delta\psi m$. In turn, this leads to uncoupling of oxidative phosphorylation, inhibition of respiration, increased ROS generation, and finally loss of ATP production (Bernardi *et al.*, 1999; Crompton, 1999; Denecker *et al.*, 2001). Increased permeability of the mitochondrial membrane also leads to hyperosmolarity of the matrix. The subsequent influx of water to restore osmotic balance results in mitochondrial matrix swelling and eventual outer membrane rupture (Gross *et al.*, 1999; Denecker *et al.*, 2001). Note that the same events which are consequences of PT pore opening (elevated ROS, decreased ATP, and intramitochondrial Ca^{++} overload) can also initiate opening of the PT pore (Kroemer *et al.*, 1998; Crompton, 1999). The sequence of these mitochondrial events, in relation to one another, remains controversial.

However, maintenance of appropriate mitochondrial permeability is a requirement for cell survival. Furthermore, free ATP/ADP exchange as well as the movement of other metabolic anions, such as creatine phosphate, between the cytosol and the matrix, is dependent on passage through the outer membrane (Harris and Thompson, 2000). The deregulation of the PT pore is an important contributor to cellular destruction (Zamzami *et al.*, 1995) and is an event in both apoptosis and necrosis (Kroemer *et al.*, 1998; Crompton, 1999; Denecker *et al.*, 2001). The fact that apoptosis and necrosis can be triggered by the same events leads to the hypothesis that the type of cell death to which the mitochondria contributes may be dependent on the timing of the deregulation.

Specifically, in apoptosis PT pore opening is primarily considered to be an amplification step that is secondary to initial caspase activation, while it is an early event in necrotic cell death (Kroemer *et al.*, 1998; Crompton, 1999).

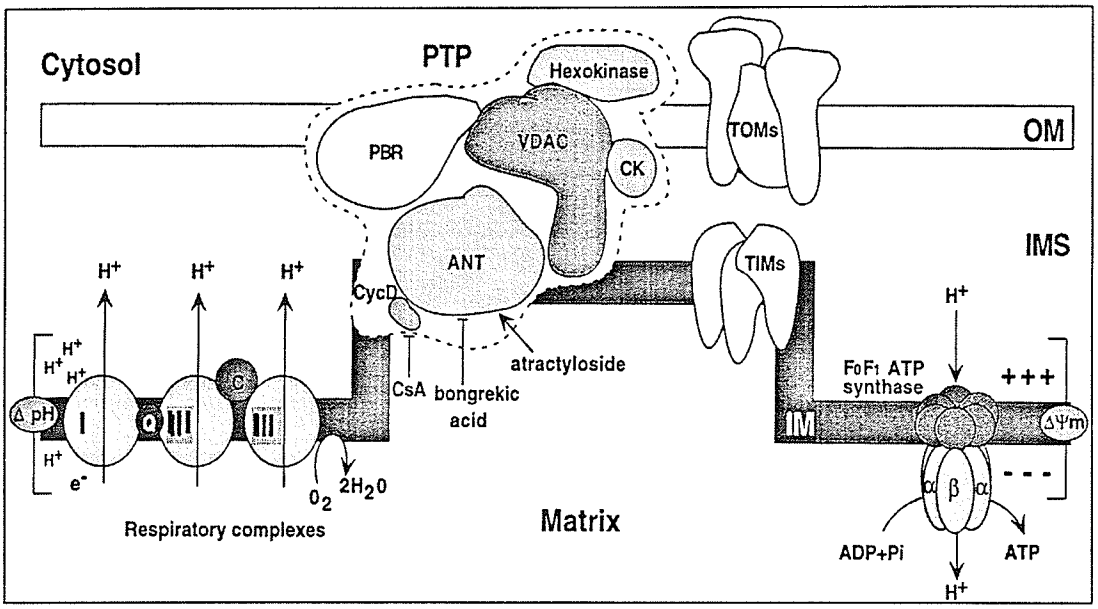

Figure 7: A schematic representation of the respiratory complexes, the F_0F_1-ATPase, and the PT pore complex in the mitochondrial inner membrane (IM) and outer membrane (OM). The localization and function (if known) of the different proteins are depicted. The $\Delta\psi m$ is principally achieved by a H^+ gradient generated by electron transport (ΔpH). This H^+ gradient is used by the F_0F_1-ATPase to synthesize ATP. The PT pore is proposed to be composed or influenced by clustered components of the inner and outer mitochondrial membrane, including hexokinase, creatine kinase (CK), voltage-dependent anion channel (VDAC), adenine nucleotide translocator (ANT), the peripheral benzodiazepine receptor (PBR), and the mitochondrial matrix protein cyclophilin D (CycD). Different agents that induce or inhibit PT pore opening are shown. (Adapted from Gross *et al.*, 1999).

1.6.1 Mitochondrial dysfunction in apoptosis

PT pore opening, $\Delta\psi m$ suppression, and ROS production are all observed in apoptosis. However, the role of these events in the apoptotic program is controversial (Kroemer *et al.*, 1998; Bernardi, 1999). Furthermore, a large part of the controversy arises from the timing of these events in relation to cytochrome *c* release. There is a substantial amount of data in the literature that suggests the primary contribution of mitochondria to apoptosis is the release of apoptogenic proteins that facilitate caspase activation and/or facilitate the ordered disassembly of the cell. There are several soluble apoptogenic proteins localized to the mitochondrial intermembrane space that are released in response to an appropriate death signal. The major ones include cytochrome *c*, procaspases 2, 3, and 9 (Susin *et al.*, 1999a; discussed in Section 1.3.4), the nuclease apoptosis-inducing factor (AIF) (Susin *et al.*, 1999), and the newly identified IAP antagonist Smac/DIABLO (Du *et al.*, 2000; Verhagen *et al.*, 2000; Section 1.4). As well, there are 75 other proteins released from the mitochondria that have been identified via mass spectrometry with unknown function in apoptosis (Patterson *et al.*, 2000). However, the release of cytochrome *c*, which promotes caspase activation, is largely believed to be the most important form of mitochondrial deregulation in apoptosis.

1.6.1.1 Cytochrome *c* release

Apocytochrome *c* is synthesized in the cytosol and imported into the mitochondrial intermembrane space where it is converted to holocytochrome *c* via attachment of a haem group by haem lyase (Reed, 1997b). In healthy cells,

holocytochrome *c* shuttles electrons between complexes III and IV of the electron transport chain, and thus is essential to ATP production (Lehninger *et al.*, 1993). However, the redistribution of holocytochrome *c* to the cytosol is highly apoptogenic as cytochrome *c* is a co-factor, along with dATP/ATP, for Apaf-1-mediated caspase activation and thus is a critical component of the apoptotic program (Section 1.4; Reed, 1997b). The mechanism of how cytochrome *c* escapes the mitochondria is unknown, however three primary models exist. The three proposed models for cytochrome *c* release are: (i) mitochondrial swelling and subsequent outer membrane rupture in response to PT pore opening or metabolic changes (Vander Heiden *et al.*, 1997; Vander Heiden *et al.*, 1999a); (ii) regulated cytochrome *c* exit from the mitochondria through the PT pore (Shimizu *et al.*, 1999); and (iii) an undefined cytochrome *c*-specific channel in the mitochondrial outer membrane (Kluck *et al.*, 1999).

As mentioned previously, increased permeability of the mitochondrial membrane can lead to hyperosmolarity of the matrix and subsequent matrix swelling and expansion of the tightly folded inner membrane. Due to the larger surface area of the numerous cristae of the inner membrane compared to the outer membrane, non-specific rupture of the outer membrane eventually occurs (Gross *et al.*, 1999; Harris and Thompson, 2000; Denecker *et al.*, 2001). Ultimately, this would release all intermitochondrial proteins into the cytosol, including cytochrome *c*. In the context of the cell, increased mitochondrial permeability can be due to changes in the state of the PT pore or changes in downstream metabolites (that may also regulate the PT pore) (Harris and Thompson, 2000).

Mitochondria are a repository for a variety of essential metabolites and ions that regulate the PT pore. In addition, pro-apoptotic proteins such as BAX and BAK can

induce PT pore opening and $\Delta\psi m$ suppression (Pastorino *et al.*, 1998; Pastorino *et al.*, 1999; Shimizu and Tsujimoto, 2000). Prolonged opening of the PT pore has been correlated with membrane depolarization, while short "flickers" do not affect cell viability (Pastorino *et al.*, 1999; Petronilli *et al.*, 2001). It has also been shown that only prolonged PT pore opening leads to cytochrome *c* release possibly due to increased matrix volume which makes more cytochrome *c* available for release (Pastorino *et al.*, 1999; Petronilli *et al.*, 2001). This speculation is rooted in electron micrographs that shown that 85-90% cytochrome *c* is localized to pleiomorphic intercristal spaces that communicate with the intermembrane space by narrow tubular "channels" (Frey and Mannella, 2000). Therefore, matrix/intercristal volume changes caused by the PT pore would increase the amount of cytochrome *c* available for release (Petronilli *et al.*, 2001). Interestingly, although cytochrome *c* release would be speculated to disturb ATP production, and thus favor necrosis, there are two major observations that appear to rationalize this supposed contradiction. First, as alluded to earlier, mitochondria appear to contain two populations of cytochrome *c*. Specifically, 85-90% of the total mitochondrial cytochrome *c* is localized to "compartments" formed by the tightly folded cristae which form bottleneck-type "entrances" that limits the movement of cytochrome *c* within the intermembrane space (Frey and Mannella, 2000). Thus, only 10-15% of the cytochrome *c* contained within a single mitochondrion, which is likely sufficient for caspase activation, is actually available to be released (Frey and Mannella, 2000). The remaining intermitochondrial cytochrome *c* is likely more than sufficient to maintain the appropriate amount of ATP production that is required for apoptosis (Eguchi *et al.*, 1999). Alternatively, it has been observed that there are two subsets of mitochondria

within an apoptotic cell, functional and non-functional (D'Herde *et al.*, 2000). Specifically, it was determined that cells cultured without required growth factors exhibited two distinct populations of respiring, cytochrome *c*-containing and non-respiring cytochrome *c*-deficient mitochondria. Therefore, this study suggested that a subset of mitochondria release enough cytochrome *c* to activate the caspase pathway, while a second subset of mitochondria maintain a functional ETC to facilitate energy requiring steps in the apoptotic program (D'Herde *et al.*, 2000).

Matrix swelling has been observed in response to growth factor withdrawal and treatment with the kinase inhibitor, straurosporine, and was prevented by the anti-apoptotic protein BCL-X_L (Vander Heiden *et al.*, 1997). Furthermore, it was subsequently established that BCL-X_L regulates mitochondrial volume by facilitating mitochondrial ATP/ADP exchange (Vander Heiden *et al.*, 1999a). Alternatively, ion channels formed by pro-apoptotic BCL-2 homologues may also disrupt mitochondrial physiology and thereby contribute to matrix swelling and non-specific release of cytochrome *c* (Schendel *et al.*, 1998).

The previous model of cytochrome *c* release predicts massive disruption of the organelle, either directly or indirectly. However, there is recent evidence that shows some cell types can recover from cytochrome *c* release (Hakem *et al.*, 1998; Yoshida *et al.*, 1998; Martinou *et al.*, 1999). Furthermore, cytochrome *c* release from isolated mitochondria has been shown to be independent of outer membrane rupture (Doran and Halestrap, 2000). It follows then, that in order for cells to recover and survive, mitochondrial function must be maintained or at least restored. Therefore, the mechanism of cytochrome *c* release must be specific and gentle enough to permit cells to

recover from cytochrome *c* efflux, provided that downstream apoptotic events are sufficiently blocked (Von Ahsen *et al.*, 2000). It is possible that the PT pore itself or an alternate specific transporter/channel acts as a conduit for cytochrome *c* to escape from the mitochondria. The PT pore as a conduit model is largely favored by early data that showed PT pore opening preceded caspase-mediated apoptotic events, and thus cytochrome *c* release, and was blocked by BCL-2/BCL-X_L (Zamzami *et al.*, 1995; Castedo *et al.*, 1996; Marchetti *et al.*, 1996; Zamzami *et al.*, 1996). However, the open PT pore is only permeable to molecules up to 1.5 kDa, far from the predicted molecular mass of cytochrome *c* of 15-16 kDa. There is also substantial evidence that indicates cytochrome *c* release can occur independently of $\Delta\psi m$ suppression, which is often used as an indirect albeit not always accurate, indicator of PT pore opening (Kluck *et al.*, 1997; Yang *et al.*, 1997; reviewed in Bernardi *et al.*, 1999). However, there is recent evidence to indicate that BCL-2 related proteins interact with components of the PT pore. For example, pro-apoptotic BAX directly interacts with ANT (Marzo *et al.*, 1998) and VDAC (Narita *et al.*, 1998) and in both cases facilitates cytochrome *c* release. There is intriguing new data that suggests BAX and VDAC together form a pore larger than that made by BAX or VDAC alone, and that this large BAX-VDAC pore is permeable to cytochrome *c* (Shimizu *et al.*, 2000b). Furthermore, it has been shown that BCL-2/BCL-X_L closes the VDAC channel and prevents cell death, perhaps by recruiting BAX away from VDAC (Shimizu *et al.*, 2000a).

Since BCL-2 proteins are present at the mitochondrial surface, perhaps they form the proposed cytochrome *c*-specific pore. The pro-apoptotic proteins BID and BAX have been reported to induce a limited permeabilization of the mitochondrial outer membrane

to facilitate cytochrome *c* release (Kluck *et al.*, 1999). Furthermore, active p15 BID triggers BAK and/or BAX activation via the BH3 domain, inducing multimerization of BAK or BAX molecules, thereby facilitating cytochrome *c* release (Crompton, 2000; Korsmeyer *et al.*, 2000). This is supported by studies demonstrating an increase in the proportion of BAX dimers and oligomers in response to death signals (Antonsson *et al.*, 2000). In addition, BAX oligomerization and channel formation have been shown to be required for cytochrome *c* release from liposomes and from isolated mitochondria (Antonsson *et al.*, 2000). Even more intriguing is the recent finding that BAX is present as an oligomeric complex in the mitochondrial membranes of apoptotic cells (Antonsson *et al.*, 2001). Probably the strongest support for this model is the recent finding that germline deletion of BAX and BAK prevents cytochrome *c* release in response to a variety of death signals, and thus are absolute requirements for cytochrome *c* release (Wei *et al.*, 2001). In addition, electron microscopy and tomography of isolated mitochondria incubated with recombinant BID and BAX do not reveal any lesions in the outer mitochondrial membrane and thus supports "gentle" release of cytochrome *c* rather than "abusive" rupture of the organelle (Von Ahsen *et al.*, 2000a).

There are numerous conflicting reports about the role of pro-apoptotic BCL-2 family members in cytochrome *c* release. A recent study may have found the reason for this. It was proposed that BH3-only proteins such as BID and BIK induce cytochrome *c* release independent of mitochondrial transmembrane potential and the permeability transition (PT) pore (Shimizu and Tsujimoto, 2000). In contrast, BAX and BAK, which have BH1, BH2, and BH3 domains, induce cytochrome *c* release concomitantly with PT pore opening. In addition, cytochrome *c* release induced by BAX and BAK was

dependent on efficient mitochondrial respiration while BH3-only proteins were not (Shimizu and Tsujimoto, 2000). These observations are consistent with several groups (Luo *et al.*, 1998; Priault *et al.*, 1999; Harris *et al.*, 2000; Gross *et al.*, 2000; Wei *et al.*, 2001). However, there is evidence of crosstalk between these two classes of BCL-2 proteins as BID can induce oligomerization of BAX and BAK resulting in cytochrome *c* release (Desagher *et al.*, 1999; Wei *et al.*, 2001).

1.6.1.2 AIF

AIF is a 57 kDa flavoprotein sequestered in the mitochondrial intermembrane space with strong homology to bacterial ferrodoxin and reduced nicotinamide adenine dinucleotide (NADH) oxidoreductases (Susin *et al.*, 1999). In the presence of apoptotic stimuli, such as ceramide, staurosporine, glucocorticoids, and HIV infection, AIF translocates to the nucleus and induces chromatin condensation and large-scale (≥ 50 kb) DNA fragmentation but not oligonucleosomal fragmentation (Susin *et al.*, 1999; Ferri *et al.*, 2000). It is speculated that AIF activates an unidentified latent nuclear endonuclease (Susin *et al.*, 1999). In *in vitro* experiments, AIF plus cytosol induces $\Delta\psi m$ suppression and cytochrome *c* release from isolated mitochondria (Susin *et al.*, 1999). Microinjection of AIF into live cells induces similar mitochondrial defects as well as phosphatidylserine externalization and nuclear damage (Susin *et al.*, 1999). Significantly, AIF-mediated apoptosis occurs in the presence of the broad-spectrum caspase inhibitor, Ac-zVAD-fmk, and in models deficient in Apaf-1 or caspase 9 (Joza *et al.*, 2001). Therefore, AIF-induced apoptosis can be genetically uncoupled from the Apaf-1/caspase 9 regulated apoptotic pathway and is a caspase-independent effector of apoptosis. AIF relocalization

has also been observed in necrotic cell death (Daugas *et al.*, 2000). As an oxidoreductase, AIF contains flavin adenine dinucleotide (FAD). However, this component of AIF is required for its oxidoreductase activity but not to induce apoptosis (Susin *et al.*, 1999). In this regard, AIF parallels cytochrome *c* in that it has a role in both cell survival and cell death, the latter of which is activated upon subcellular relocalization (Lorenzo *et al.*, 1999). Furthermore, AIF homologues have been identified in *C. elegans*, *Drosophila melanogaster*, *Xenopus laevis*, and *Schizosaccharomyces pombe* (Lorenzo *et al.*, 1999). Even more interesting, is the recent evidence that AIF is a critical regulator of early developmental cell death (Joza *et al.*, 2001). The signaling mechanism that induces AIF translocation remains elusive although PT pore opening has been implicated (Susin *et al.*, 1999).

1.6.2 Mitochondrial dysfunction in necrosis

With the exception of the release of cytochrome *c* and Smac/DIABLO, many of the mitochondrial events that mediate apoptosis also facilitate necrotic cell death (Kroemer *et al.*, 1998; Denecker *et al.*, 2001). One wonders, then, how the cell makes the decision of which path to take. The severity and kinetics of mitochondrial events as well as intracellular energy levels are believed to contribute to the decision (Kroemer *et al.*, 1998). Although controversial, PT pore opening and ROS production in apoptosis are generally considered to occur downstream of caspase activation (Kroemer *et al.*, 1998). In contrast, early mitochondrial dysfunction and excessive ROS production are considered to be primary causative events in necrosis (Kroemer *et al.*, 1998). In addition, ATP is required for apoptosis, but is dispensable for necrosis (Nicotera and Leist, 1997;

Tsujimoto, 1997; McConkey, 1998; Eguchi *et al.*, 1999). Interestingly, ATP levels, PT pore opening, and ROS production are all intricately related events, the order of which are highly controversial.

Although over-simplified, one mechanism of necrotic cell death hypothesizes that the bioenergetic and redox catastrophe induced by early PT pore opening "outruns" the cell's efforts to activate caspases and die by apoptosis (Hirsch *et al.*, 1997; Leist *et al.*, 1997; Kroemer *et al.*, 1998; Lemasters, 1999). This is supported by experiments in which cells treated with the apoptotic inducer staurosporine can die by necrosis if ATP production is inhibited by the addition of oligomycin, an inhibitor of the F_0F_1-ATPase (Leist *et al.*, 1997; Nicotera and Leist, 1997). Similarly, overexpression of BAX or BAK normally induces apoptosis. However, in the presence of the caspase inhibitor Ac-zVAD-fmk, although apoptosis is inhibited, as determined by lack of characteristic apoptotic nuclear damage, BAX- and BAK-expressing cells still die (Xiang *et al.*, 1996; McCarthy *et al.*, 1997). Furthermore, expression of FADD, a component of the death receptor-mediated apoptotic pathway, in caspase $8^{-/-}$ cells or in the presence of caspase inhibitors, is still sufficient to induce cell death (Kawahara *et al.*, 1998; Matsumura *et al.*, 2000). Under these conditions, FADD induces necrotic cell death (Kawahara *et al.*, 1998; Matsumura *et al.*, 2000; Denecker *et al.*, 2001). Therefore, apoptosis and necrosis also share some mediators of cell death.

It is speculated that prolonged PT pore openings disturb general mitochondrial physiology and thus induce cell death. For example, opening of the PT pore dissipates the H^+ gradient required for ATP production, thereby uncoupling oxidative phosphorylation (Gross *et al.*, 1999). This is can lead to matrix alkalinization and

cytosolic acidification, as observed in response to BAX (reviewed in Matsuyama and Reed, 2000; Matsuyama *et al.*, 2000) or the ionophore valinomycin (Furlong *et al.*, 1998). However, the role of pH as a regulator of apoptosis is debatable as transient cytosolic alkalinization due to growth factor withdrawal has also been shown to promote BAX integration into the mitochondria and subsequent cell death (Khaled *et al.*, 1999). It has also been suggested that pH changes are not causative of cell death but merely reflect metabolic alterations in the dying cell (Von Ahsen *et al.*, 2000).

ROS production is a feature of both apoptosis and necrosis. There are many cellular reactions which produce oxygen-derived free radicals (Jacobson, 1996). However, the primary intracellular site of ROS production is the mitochondria. Under normal cellular conditions, 1-2% of the oxygen reduced by mitochondria during oxidative phosphorylation can be converted to superoxide anion ($O_2^{\bullet-}$) (Boveris and Chance, 1973). Specifically, the NADH dehydrogenase (complex I) and ubisemiquinone (complex III) intermediate of the electron transport chain produce ROS as a by-product of the reactions they catalyze (Turrens, 1997). Examples of reactive oxygen-derived species include superoxide anion ($O_2^{\bullet-}$), hydroxyl radical ($^{\bullet}OH$), hydrogen peroxide (H_2O_2), nitric oxide ($NO^{\bullet}$), and peroxynitrate ($ONOO^-$). Furthermore, one species can be converted to another form via intracellular processes (Jacobson, 1996). For example, $O_2^{\bullet-}$ can be converted to H_2O_2 via superoxide dismutase. Similarly, H_2O_2 and $NO^{\bullet}$ can be converted to $^{\bullet}OH$, the most potent intracellular oxygen radical (Jacobson, 1996). The hydroxyl radical can cause lipid peroxidation, oxidation of sugars and protein thiols, DNA base damage, and strand breakage of nucleic acids (Bai *et al.*, 1999). For these reasons, cells have evolved several antioxidant systems to counteract this intracellular oxidative stress.

A balance between ROS production and levels of cellular antioxidants is required to maintain cell survival (Jacobson, 1996; Bai *et al.*, 1999). Therefore, increased ROS production or depletion of antioxidants can yield higher than acceptable levels of ROS and induce substantial cellular damage (Jacobson, 1996; Bai *et al.*, 1999).

The observation of ROS production in both apoptotic and necrotic cell death may be explained by the observation of two stages of ROS production (Tan *et al.*, 1998). Specifically, an early stage of ROS production has been observed in apoptosis where ROS levels were increased 5- to 10-fold. This early ROS production was speculated to be due to immediate depletion of the antioxidant glutathione (Tan *et al.*, 1998). However, this initial low level production of ROS may also be due to the partial release of cytochrome *c* from individual mitochondria (Frey and Manella, 2000). Alternatively, it may be due to the subset of mitochondria that have released their cytochrome *c* (D'Herde *et al.*, 2000). In both cases, ROS can be produced due to uncoupled oxidative phosphorylation. A second, later stage of ROS production is subsequently observed where ROS levels are 200- to 400-fold higher than basal levels (Tan *et al.*, 1998). This stage is presumably due to deregulation of the ETC (Tan *et al.*, 1998), as a switch from the normal 4-electron reduction of O_2 to a 1-electron reduction has been observed following cytochrome *c* release from mitochondria (Cai and Jones, 1998). Therefore, in apoptosis, this second burst of ROS production is secondary to an activated caspase pathway suggesting that ROS production may function to complement cytochrome *c*-dependent/caspase-mediated apoptosis or as a back-up system to ensure execution of a dying cell, either directly or indirectly (Cai and Jones, 1998). However, the order of cytochrome *c* release relative to ROS production is highly controversial (Cai and Jones,

1998; Dumont *et al.*, 1999; Hildeman *et al.*, 1999; von Harsdorf *et al.*, 1999). On the other hand, necrosis is characterized by ATP depletion that is presumably due to ETC deregulation (Tsujimoto, 1997; Nicotera and Leist, 1997; McConkey, 1998). Therefore, this scenario favors the rapid enhancement of ROS production in necrosis. In addition, there is new evidence that indicates ROS may play a role in directly regulating caspase activity. Specifically, caspases are cysteine proteases and therefore have a thiol residue that is susceptible to oxidation and thiol nitrosylation (Denecker *et al.*, 2001). It is not surprising then that optimal caspase activity is obtained under reducing conditions (Stennicke and Salvesen, 1997; Denecker *et al.*, 2001). This is best demonstrated by studies where in the same cellular context, low levels of ROS induce apoptosis, while excessively high ROS levels promote inactivation of caspases and death by necrosis (Hampton and Orrenius, 1997; Samali *et al.*, 1999; Denecker *et al.*, 2001). In addition, procaspase 3 can be inhibited by nitrosylation of its catalytic cysteine (reviewed in Denecker *et al.*, 2001).

PT pore opening, which is observed in both apoptotic and necrotic cell death, can also induce ROS production (Section 1.6; Takeyama *et al.*, 1993; Zoratti and Szabo, 1995; Marchetti *et al.*, 1996; Kroemer *et al.*, 1997; Hildeman *et al.*, 1999). Interestingly, the PT pore itself is subject to regulation by ROS (Kroemer *et al.*, 1998). This may be due to oxidation of a critical thiol residue of ANT, a component of the PT pore, which results in sustained opening of the PT pore (Costantini *et al.*, 2000). The controversy of whether ROS is a cause or consequence of PT pore opening has been previously considered to be dependent on the death signal (Zoratti and Szabo, 1995; Kroemer *et al.*, 1997). However, it is probably more likely that ROS and PT pore opening participate in

a feed-forward amplification loop (Kroemer *et al.*, 1998; Jabs, 1999). The decision between apoptosis and necrosis may be determined by the delicate intercommunication of these events (Denecker *et al.*, 2001). However, this hypothesis remains to be formally tested.

In *C. elegans*, *ced-9* is encoded as a part of a bi-cistronic gene that also encodes a protein similar to cytochrome b_{560} of complex II of the ETC (Hengartner and Horvitz, 1994). This intriguing observation raised the possibility that the mammalian homologue BCL-2 may function in regulation of cellular redox (Hengartner and Horvitz, 1994). This hypothesis is supported by the observations that BCL-2 can inhibit apoptosis and ROS production, and therefore functions as an antioxidant (Hockenbery *et al.*, 1993; Kane *et al.*, 1993). However, the role of BCL-2 as an antioxidant has recently been challenged. Specifically, it has been discovered that a commonly used ROS-sensitive probe, dichlorofluorescin (DCF), is oxidized by cytochrome *c* (Burkitt and Wardman, 2001). This finding has significant implications for the role of BCL-2 as an antioxidant as BCL-2 has previously been shown to inhibit cytochrome *c* release (Kluck *et al.*, 1997; Yang *et al.*, 1997). Therefore, the apparent antioxidant activity of BCL-2 measured as suppression of DCF oxidation, may actually be due to the ability of BCL-2 to prevent the release of cytochrome *c* (Cai and Jones, 1998; Burkitt and Wardman, 2001). However, BCL-2 can inhibit both cytochrome *c*- and caspase-independent cell death (Okuno *et al.*, 1998; Scaffidi *et al.*, 1998). It has also been proposed that overexpression of BCL-2 permits cells to adapt to a higher oxidative state by inducing a slightly higher level of basal H_2O_2 (Degli Esposti *et al.*, 1999). It is believed that by increasing basal H_2O_2 levels (ie. functioning as a pro-oxidant), BCL-2 enhances cellular antioxidant

mechanisms (Steinman, 1995; Degli Esposti *et al.*, 1999). However, higher ROS levels may also prevent cell death by preventing caspase activation, as discussed previously (Stennicke and Salvesen, 1997; Denecker *et al.*, 2001).

Interestingly, a mass spectroscopy approach to identify proteins released from mitochondria during cell death noted several antioxidant enzymes. It is possible that the removal of antioxidant enzymes from mitochondria, the primary site of ROS production, facilitates ROS-mediated cell death (Patterson *et al.*, 2000; Ferri and Kroemer, 2001). In addition, antioxidants were also implicated in cell death by gene microarray analysis of apoptosis-resistant cells which revealed increased expression of genes that contribute to the production of glutathione (Voehringer *et al.*, 2000). The significance of these studies to the regulation of cell death remains to be determined.

A definite marker of necrosis is ATP depletion. Mitochondria are the main producers of cellular ATP. Therefore, any disruption of electron transport and oxidative phosphorylation may result in an energetic catastrophe and ultimately compromise cell survival. Interestingly, it has recently been found that overexpression of BAX impairs oxidative phosphorylation in yeast thereby sufficiently disrupting mitochondrial respiration so as to induce ATP depletion and cell death (Harris *et al.*, 2000). Morphologically, yeast overexpressing BAX feature cytoplasmic vacuolation, disturbed mitochondrial architecture, and minor or absent nuclear damage (Harris *et al.*, 2000). As well, yeast cells that have been modified to be dependent on oxidative phosphorylation are sensitive to BAX, while respiration-incompetent cells are BAX-resistant (Gross *et al.*, 2000; Harris *et al.*, 2000). As well, it has also been reported that yeast with mutated F_0F_1-ATP synthase or deficient in ANT is resistant to BAX toxicity (Marzo *et al.*, 1998;

Matsuyama *et al.*, 1998). In addition, BCL-2 and BCL-X_L are sufficient to prevent BAX-induced cell death in yeast (Greenhalf *et al.*, 1996; Tao *et al.*, 1997; Tao *et al.*, 1998; Minn *et al.*, 1999; Gross *et al.*, 2000). These studies strongly suggest that BCL-2 family members can act on highly conserved components of the mitochondria that may directly correspond with similar molecules in mammalian cells (Gross *et al.*, 2000). Furthermore, sequence analysis of yeast has determined that there are no genes coding for analogous members of the caspase, Apaf-1, or BCL-2 families (Gross *et al.*, 2000), suggesting the existence of an alternate, likely mitochondria-dependent/mediated form of cell death.

Recently, a novel model of ATP depletion has been developed. As mentioned earlier, PARP cleavage serves as a valuable indicator of apoptotic cell death (Section 1.3.3). Since PARP is a DNA repair enzyme, it was assumed that PARP cleavage, from 116 kDa to 85 kDa, facilitated apoptosis by preventing DNA repair. However, this hypothesis has never been formerly tested and thus PARP cleavage is regarded more as a by-product, rather than a mediator, of apoptosis (Stroh and Schulze-Osthoff, 1998). Interestingly, a role for PARP in modulating cell death has recently been proposed. Excessive PARP activity leads to depletion of its substrate NAD^+. In the reactions required to synthesize new NAD^+, ATP is depleted (Ha and Snyder, 1999). Therefore, during apoptosis, the purpose of caspase-mediated PARP cleavage, and thus inactivation, may be to maintain cellular ATP supplies and thus would favor the apoptotic program (Ha and Snyder, 1999). In contrast, excessive PARP activation, perhaps in response to ROS-induced DNA damage, would favor necrosis due to PARP-mediated depletion of ATP (Ha and Snyder, 1999). The significance of this data is unclear as PARP cleavage has also been observed in necrotic cell death (Gobeil *et al.*, 2001). Specifically, a major

50 kDa cleavage fragment is generated during necrosis and is likely due to lysosomal proteases such as cathepsins B and G, that are released (Gobeil *et al.*, 2001). It is possible, however, that necrotic PARP cleavage increases PARP activity, which would still fit with the model of Gobeil *et al.* (2001). This possibility remains to be examined.

Apoptosis and necrosis are likely two extremes of a continuum of possible types of cell death whose end phenotype is dictated in part, by the availability of ATP, PT pore opening, ROS production, and kinetics of caspase activation in the dying cell (Nicotera and Leist, 1997; Formigli *et al.*, 2000). The increasing number of studies reporting "caspase-independent" cell death support this concept (Denecker *et al.*, 2001). Furthermore, it has been proposed that this continuum is a reflection of cell type-specific responses to certain stimuli (Nicotera and Leist, 1997; Kroemer *et al.*, 1998). Interestingly, BCL-2 and BCL-X_L are effective inhibitors of both apoptotic and necrotic/caspase-independent cell death (Minn *et al.*, 1998; Bai *et al.*, 1999; Okuno *et al.*, 1998; reviewed by Tsujimoto, 1997; McConkey, 1998). In both cases, BCL-2 and BCL-X_L can modulate mitochondrial homeostasis, including PT pore status, $\Delta\psi m$, ROS, and ATP production (Kluck *et al.*, 1997; Tsujimoto, 1997; Yang *et al.*, 1997; Shimizu *et al.*, 1998; Vander Heiden and Thompson, 1999; Vander Heiden *et al.*, 1999; Matsuyama *et al.*, 2000; Vander Heiden and Thompson, 2000). Finally, mitochondria are essential for cell survival and death and function to continuously monitor the overall state of the cell. Mitochondrial deregulation may be the decision point between apoptotic and necrotic cell death (Ferri and Kroemer, 2001).

1.7 BNIP3 Subfamily

The BNIP3 subfamily currently consists of the death-inducing proteins BNIP3, NIX, and the *C. elegans* orthologue ceBNIP3. BNIP3 (BCL-2/E1B Nineteen-kiloDalton interacting protein-3) was identified in a yeast two hybrid screen for potential binding partners of the adenoviral BCL-2 functional homologue, E1B 19K (Boyd *et al.*, 1994). This interaction was confirmed via coimmunoprecipitation experiments in mammalian cells. In addition, BNIP3 was demonstrated to interact with BCL-2 via the yeast two hybrid assay and coimmunoprecipitation. Interestingly, BCL-2 and E1B 19K bind to BNIP3 via regions of shared homology (Boyd *et al.*, 1994). BNIP3 was subsequently cloned from various sources and predicted to be 194 amino acids (Boyd *et al.*, 1994). Expression studies show that BNIP3 is ubiquitously expressed in mouse tissues as a 1.7 kb major transcript and 1.5 kb minor transcript. Specifically, BNIP3 mRNA is expressed in oviduct, uterus, spleen, lung, stomach, brain, heart, kidney, liver, seminal vesicle, lacrimal and submaxillary glands (Chen *et al.*, 1997). However, BNIP3 protein is found only in skin, tongue, and skeletal muscle (Vande Velde *et al.*, 2000). As well, BNIP3 protein is present in mitochondrial fractions of HeLa and 293T but not MCF-7 cell lines (Vande Velde *et al.*, 2000). The only known mammalian homologue of BNIP3 is NIX (BNIP3-like protein-X; also known as BNIP3α, BNIP3L, B5) (Matsushima *et al.*, 1998; Chen *et al.*, 1999; Imazu *et al.*, 1999; Ohi *et al.*, 1999; Yasuda *et al.*, 1999). Human NIX is 219 amino acids, shares 56% identity to human BNIP3, and has amino-terminal sequence that is distinctly different compared to the equivalent region in BNIP3 (Chen *et al.*, 1999). NIX is expressed as 3.9 kb and 1.6 kb transcripts in heart, brain, placenta, lung, liver, skeletal muscle, kidney, and pancreas (Yasuda *et al.*, 1999). BNIP3 is

evolutionarily conserved in *C. elegans*. The BNIP3 orthologue in *C. elegans*, ceBNIP3, is 221 amino acids and shares 21% identity to human BNIP3 at the amino acid level (Yasuda *et al.*, 1998a; Cizeau *et al.*, 2000). ceBNIP3 is expressed primarily in the embryonic stage and to a lesser extent in the larval stage (Cizeau *et al.*, 2000), the two main time periods of cell death in *C. elegans* (Sulston *et al.*, 1983). BNIP3 family members have four common features: (1) a PEST sequence, (2) a BH3-like domain, (3) a death-inducing carboxyl-terminal transmembrane (TM) domain, and (4) a conserved domain of 19 amino acids of unknown function (Figure 8) (Chen *et al.*, 1999; Cizeau *et al.*, 2000). The presence of a carboxyl-terminal TM domain and BH3-like domain places BNIP3 in class III of the pro-apoptotic BCL-2 proteins.

BNIP3, NIX and ceBNIP3 all have amino-terminal PEST sequences that are rich in proline (P), glutamate (E), serine (S), and threonine (T). PEST sequences are associated with proteins that are degraded via the proteasome (Rogers *et al.*, 1986). Cells transfected with BNIP3, NIX, or ceBNIP3 show decreasing amounts of protein over an extended time course. Similar results are observed with corresponding inactive/non-killing mutants lacking the TM domain, indicating that decreasing protein levels are not due to BNIP3-, NIX-, or ceBNIP3-induced cell death (Chen *et al.*, 1997; Chen *et al.*, 1999; Cizeau *et al.*, 2000). Subsequent treatment with lactacystin, a proteasome inhibitor, yields an accumulation of protein (Chen *et al.*, 1999; Cizeau *et al.*, 2000). Furthermore, degradation of NIX from the amino-terminus to an 11 kDa carboxyl-terminal fragment is prevented by the addition of lactacystin (Chen *et al.*, 1999). The significance of proteasome-mediated degradation of BNIP3 proteins is unknown.

As described earlier, the BH3 domain is an eight amino acid core sequence containing a conserved leucine and aspartate at positions 1 and 6, respectively, and forms an α-helix. These two residues are the critical component of BH3-mediated heterodimerization of BCL-2 proteins and pro-apoptotic activity (Kelekar and Thompson, 1998). Residues 110 to 118 of BNIP3 reveal limited sequence homology to other BH3-only pro-apoptotic proteins (Yasuda *et al.*, 1998; Ray *et al.*, 2000). Alignment of this region with the BH3 domain of BAK reveals that Leu^{110} and Asp^{115} of BNIP3 (and corresponding residues in NIX) are conserved (Ray *et al.*, 2000). However, secondary structure predictions of this region suggest that it is unable to form the required α-helix (Dr. A.H. Greenberg, unpublished observations). Furthermore, the predicted BH3 domain of ceBNIP3 contains two additional prolines immediately upstream of the conserved aspartate (Cizeau *et al.*, 2000), which are known helix-breakers (Branden and Tooze, 1991). It has been demonstrated via the yeast two hybrid assay that an abbreviated portion of the BH3-like domain, amino acids 110 to 115, is required for heterodimerization of BNIP3 with E1B 19K or BCL-X_L (Yasuda *et al.*, 1998). However, it has also been shown that BNIP3 lacking the BH3-like domain efficiently interacts with itself, BCL-2, BCL-X_L, and CED-9 via yeast two hybrid, coimmunoprecipitation, and an *in vitro* binding assay (Ray *et al.*, 2000). Deletion mapping studies reveal that BNIP3 requires its amino-terminus to interact with BCL-2 but not BCL-X_L. Furthermore, the TM domain was required for heterodimerization with both BCL-2 and BCL-X_L and homodimerization (Ray *et al.*, 2000). BH3-independent homo- and heterodimerization have also been observed for NIX (Imazu *et al.*, 1999; Ohi *et al.*, 1999; Yasuda *et al.*, 1999). Likewise, ceBNIP3 interacts with CED-9 and BCL-X_L via its TM domain and

independent of its BH3 domain (Cizeau *et al.*, 2000). Full length BNIP3 proteins induce cell death (Chen *et al.*, 1997; Chen *et al.*, 1999; Cizeau *et al.*, 2000). Functionally, deletion of the BH3-like domain of BNIP3 has no significant effect on cell death assessed by cellular morphology in Rat-1, MCF-7, and 10T1/2 cell lines (Ray *et al.*, 2000). However, substitution of the BH3-like domain of BNIP3 for the BH3 domain of BAX restores the killing activity of BAX in MCF-7 cells (Yasuda *et al.*, 1998). It is possible that the BH3-like domain of BNIP3 in the context of BAX is under different conformational constraints due to the additional presence of BH1, BH2, and BH4 domains of BAX (Ray *et al.*, 2000). Lack of a functional BH3 domain places BNIP3-related proteins in a unique subfamily within the larger family of pro-apoptotic BCL-2 proteins (Chen *et al.*, 1999).

BNIP3 also features a carboxyl-terminal TM domain at residues 164 to 184 that mediates homodimerization, localization, and cell death. BNIP3 homodimerization has been confirmed via two-dimensional electrophoresis of trypsin-digested fragments and the yeast two hybrid assay (Chen *et al.*, 1997). Sequence analysis of this region reveals an LXXLL motif that is proposed to be important for hydrophobic interactions (Ohi *et al.*, 1999). Uniquely, BNIP3 family homodimers are stable under reducing and alkylating conditions, as well as in the presence of 6 M urea (Chen *et al.*, 1997). The TM domain localizes BNIP3 family members to the outer mitochondrial membrane, as demonstrated by co-localization with the mitochondria-specific stain Mitotracker (Yasuda *et al.*, 1998; Ohi *et al.*, 1999) and the mitochondrial protein Heat Shock Protein-60 (HSP60) (Chen *et al.*, 1997; Chen *et al.*, 1999; Cizeau *et al.*, 2000). Removal of the TM domain yields a free cytosolic staining pattern (Chen *et al.*, 1997; Yasuda *et al.*, 1998; Chen *et al.*, 1999).

Endogenous BNIP3 is loosely associated with the outer mitochondrial membrane in muscle and MCF-7 and 293T cell lines, but is integrated via the TM domain when overexpressed (Vande Velde *et al.*, 2000). The mechanism regulating insertion into the mitochondrial membrane is unknown but is speculated to involve a conformational change and/or change in binding partners, permitting protein integration (Vande Velde *et al.*, 2000). The TM domain is also required for induction of cell death as the deletion mutant BNIP3Δ164-194 is unable to induce cell death (Chen *et al.*, 1997). Similar results have been shown for NIX and ceBNIP3 (Chen *et al.*, 1999; Cizeau *et al.*, 2000). Until recently, it was assumed that homodimerization was critical for the killing activity of BNIP3. However, there are a series of BNIP3 mutants that localize correctly to the mitochondria and kill efficiently yet do not homodimerize (Ray *et al.*, 2000) indicating that homodimerization can be separated from killing activity. Furthermore, the TM domain is believed to be critical for killing; however, TM domain swapping experiments indicate that BNIP3 can kill from mitochondrial and non-mitochondrial sites provided that the protein is anchored to an intracellular membrane (Ray *et al.*, 2000).

Overexpression of BNIP3 induces apoptosis, measured by chromatin condensation, in Rat-1 cells at approximately 12 hours post-transfection (Chen *et al.*, 1997). Cell death, as determined by cellular morphology, induced by overexpression NIX or ceBNIP3 is slightly less efficient (Chen *et al.*, 1999; Cizeau *et al.*, 2000). Cell death can only be delayed by stable overexpression of BCL-2 or BCL-X_L in Rat-1 and 10T1/2 cell lines, respectively (Chen *et al.*, 1997; Chen *et al.*, 1999; Ray *et al.*, 2000). However, high levels of BCL-X_L expression can completely suppress BNIP3-induced

cell death (Chen *et al.*, 1997; Chen *et al.*, 1999; Cizeau *et al.*, 2000). Furthermore, BCL-2/BCL-X_L inhibition is independent of the BH3 domain (Ray *et al.*, 2000).

There are conflicting reports of the role of ceBNIP3 in the context of the main apoptotic proteins of *C. elegans*, CED-3, CED-4, and CED9. ceBNIP3 is reported to bind CED-3 (Yasuda *et al.*, 1998a; Cizeau *et al.*, 2000) and may increase the processing of CED-3 (Yasuda *et al.*, 1998a). ceBNIP3 is also reported to bind CED-9 via the TM domain, independent of the BH3-like and CD domains. Similar observations have been made for the interaction of ceBNIP3 and BCL-X_L (Cizeau *et al.*, 2000). There is also some indications that co-transfection of ceBNIP3 and CED-3 yields a minimal additive effect in death-promoting activity (Yasuda *et al.*, 1998a; Cizeau *et al.*, 2000). In all cases, CED-9 is sufficient to block cell death (Yasuda *et al.*, 1998a; Cizeau *et al.*, 2000). Interestingly, ceBNIP3 can complex with CED-3, CED-9 (Yasuda *et al.*, 1998a; Cizeau *et al.*, 2000) and CED-4 (Ray *et al.*, 2000) simultaneously, forming a ternary structure (Cizeau *et al.*, 2000).

The localization of BNIP3 family members to the mitochondria and recent developments demonstrating the mitochondria as a major contributor to apoptosis raises the question of whether these proteins influence mitochondrial physiology to induce cell death. Interestingly, recombinant NIX added to isolated mitochondria induces release of cytochrome *c* and loss of transmembrane potential ($\Delta\psi m$), both of which are blocked by BCL-X_L. $\Delta\psi m$ suppression was also independent of the BH3-like domain (Imazu *et al.*, 1999). The mechanism of cell death mediated by overexpression of BNIP3 is outlined in this thesis. The study of BNIP3 family members will likely have significant consequences for pathological models of cell death.

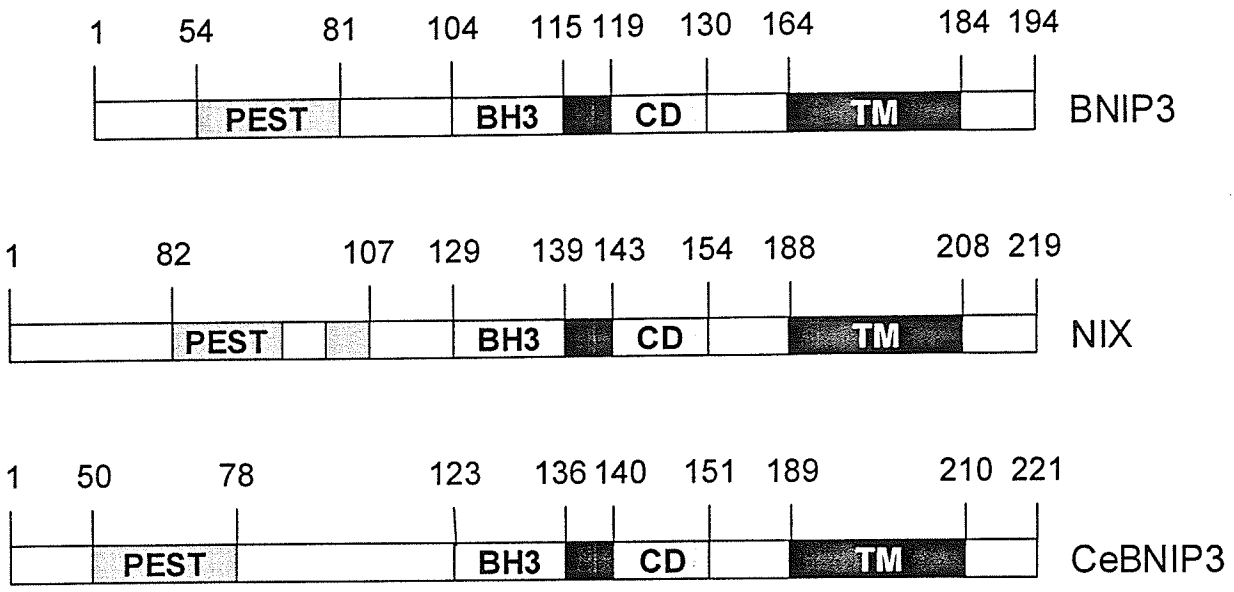

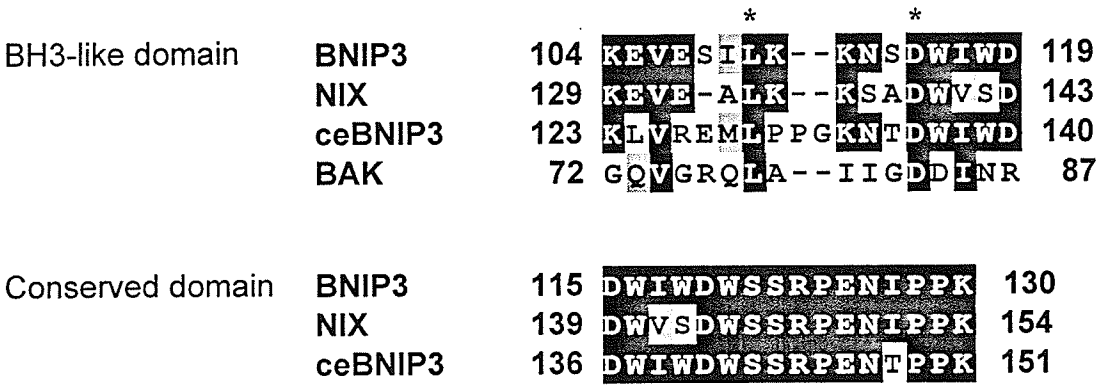

Figure 8: Schematic representation of BNIP3 family proteins. The BNIP3 family currently consists of BNIP3, NIX (also referred to as BNIP3L, BNIP3α, and B5), and the *C. elegans* orthologue ceBNIP3. Overall, human BNIP3 shares 56% and 21% with NIX and ceBNIP3, respectively. These proteins contain an amino-terminal PEST sequence, a BCL-2 homology 3 (BH3)-like domain, a conserved domain (CD), and a carboxyl-terminal transmembrane (TM) domain. Note the overlap of the BH3 and CD domains. Sequence alignments of the BH3-like and CD domains are shown. Identical and similar amino acids are shaded black and gray, respectively. Asterisks (*) indicate residues in the core of the BH3 domain with similarity to BAK. Illustrations are not drawn to scale.

2.0 Hypothesis

Overexpression of the mitochondrial, death-promoting protein BNIP3 induces cell death via the classical apoptotic pathway including caspase activation and cytochrome *c* release as it is akin to the pro-apoptotic family of BCL-2 proteins.

2.1 Specific Aims

1. To determine if BNIP3 directed to non-mitochondrial sites is able to induce cell death compared to mitochondrially-targeted BNIP3.
2. To determine the mechanism of BNIP3-induced cell death.

2.2 Significance

Deregulated cell death is a contributing factor in several pathological conditions including tumorigenesis and neurodegenerative diseases. In order to exploit programmed cell death mechanisms as potential therapeutic targets, we must first endeavor to understand their molecular basis. BNIP3 is involved in activating the cell death mechanism. Determining the role of BNIP3 in programmed cell death will contribute to the current knowledge of mammalian cellular homeostasis and the development of numerous pathological conditions.

3.0 Materials and Methods

3.1 Reagents

All chemicals were purchased from Sigma-Aldrich Chemical Co. (St. Louis, MO) unless otherwise indicated.

3.2 Cell lines

Human breast cancer MCF-7 cells and human cervical carcinoma HeLa cells were cultured in α-minimal essential medium (MEM) (Gibco-BRL, Burlington, ON) supplemented with 10% v/v fetal bovine serum (FBS) (Cansera, Rexdale, ON), 1% v/v MEM sodium pyruvate (Gibco-BRL), 1% v/v Hepes (Gibco-BRL), and 1% v/v L-glutamine (Gibco-BRL). Human embryonic kidney 293T and 293-BCL-2 epithelial cells and mouse embryonic fibroblasts (MEFs) deficient in Apaf-1, caspase 9 or caspase 3 were cultured in Dulbecco's Modified Eagle medium (DMEM) (Gibco-BRL) supplemented with 10% v/v FBS. MEFs of less than ten passages were used in experiments. MEF cell lines were developed by Dr. Raqallah Hakem (Amgen, Toronto, ON). 293-BCL-2 cells were developed by Dr. Spencer Gibson (Manitoba Institute of Biology, Winnipeg, MB).

3.3 Expression Plasmids

Construction of 3' T7-epitope tagged pcDNA3-BNIP3 and pcDNA3-BNIP3ΔTM, and 3' HA-epitope tagged pcDNA3-BNIP3 expression plasmids have been previously described (Chen *et al.*, 1997). pcDNA3-caspase-9-His_6 and pcDNA1-p35 were gifts of

Dr. Emad Alnemri (Thomas Jefferson University, Philadelphia, PA). pcDNA3-Apaf-1 and pFLAG-CMV-5a-tBID were donated by Dr. Xiaodong Wang (Howard Hughes Medical Institute, Dallas, TX) and Dr. Junying Yuan (Harvard Medical School, Boston, MA), respectively.

3.4 Antibodies

Murine monoclonal anti-T7 antibody was purchased from Novagen (Madison, WI). Murine monoclonal anti-cytochrome *c* antibodies for immunoblotting (65981A) and immunofluorescence (67971A) were purchased from BD Pharmingen (Mississauga, ON). Mouse monoclonal anti-PARP and anti-actin were purchased from Alexis Biochemicals (San Diego, CA) and ICN Biochemicals (Montreal, PQ), respectively. Mouse monoclonal anti-caspase 3 was purchased from Transduction Laboratories (Lexington, KY). Rabbit polyclonal anti-AIF was a gift of Dr. Guido Kroemer (CNRS, Paris, France). Rabbit anti-FLAG polyclonal antibody and mouse anti-HA monoclonal antibody were purchased from Zymed Laboratories Inc. (San Francisco, CA) and Boehringer Mannheim (Indianapolis, IN), respectively. Secondary antibodies, goat anti-mouse IgG-HRP, goat anti-mouse IgG-FITC, and goat anti-rabbit IgG-FITC, were all purchased from Sigma-Aldrich Chemical Co. (St. Louis, MO). Goat anti-mouse IgG-Cy3 was from Chemicon (Temecula, CA). Working dilutions of all antibodies are listed in Table 2.

Table 2: Summary of antibody dilutions used for immunoblotting and immunofluorescence detection of proteins. Antibodies were diluted in blocking buffer, as described in text.

Antibody	Working dilutions	
	Western blotting	Immunofluorescence
mouse anti-T7	1/10 000	1/1500
mouse anti-HA		1/1000
mouse anti-actin	1/10 000	
mouse anti-cytochrome *c*	1/5000	1/1000
mouse anti-caspase 3	1/3000	
mouse anti-caspase 7	1/2000	
mouse anti-caspase 9	1/7500	
mouse anti-PARP	1/5000	
mouse anti-BCL-X_L	1/2500	
rabbit anti-AIF	1/5000	1/2500
rabbit anti-FLAG	1/1000	
goat anti-mouse HRP	1/20 000	
goat anti-rabbit HRP	1/100 000	
goat anti-mouse FITC		1/1600
goat anti-rabbit FITC		1/1600
goat anti-mouse Cy3		1/2000

3.5 Transient transfection of mammalian cells

3.5.1 Calcium phosphate method

Approximately 18 hours prior to transfection, 293T cells were plated at $1x10^6$ cells per 10 cm culture dishes (Nunc, Denmark). The transfection mix was prepared as follows: 500 µl 2x HeBS (50 mM Hepes, 10 mM KCl, 12 mM dextrose, 280 mM NaCl, 1.5 mM Na_2HPO_4, pH 7.05 ± 0.05) was added drop-wise to a 15 ml conical tube containing 7.5 µg of the indicated expression plasmid(s) diluted in 438 µl double-distilled H_2O and 62 µl 2 M $CaCl_2$ under continuous aeration (Pear *et al.*, 1995). The calcium phosphate-DNA precipitate was further diluted in 6 ml DMEM + 10% v/v FBS and 25 µM chloroquinone and immediately applied to cells. The transfection mix was replaced with 10 ml DMEM+10% v/v FBS after 8 hours incubation at 37°C. The cells were further cultured for the appropriate length of time, as determined by the experiment.

3.5.2 LipofectAMINE method

Approximately 18 hours prior to transfection, cells were plated at $1x10^5$ cells per well of a 6-well plate (Nunc). In a 15 ml conical tube, various amounts of DNA (as dictated by experiment) were diluted in 100 µl OPTI-MEM I Reduced Serum Medium (Gibco-BRL). In a second 15 ml conical tube, 7 µl LipofectAMINE Reagent (Gibco-BRL) was diluted in 100 µl OPTI-MEM I. The diluted DNA was added drop-wise to the diluted LipofectAMINE Reagent. The mixture was permitted to incubate for 30 to 40 minutes at room temperature to permit formation of DNA-liposome complexes. An additional 800 µl OPTI-MEM I was added to each tube and immediately applied to cells that had been washed twice with OPTI-MEM I. The transfection mix was replaced with

fresh growth medium 5 hours after application to cells. Cells were further cultured for the appropriate length of time, as determined by the experiment.

3.6 Detection of Proteins

3.6.1 Indirect Immunofluorescence Analysis

Briefly, cells grown on coverslips were fixed with 3.7% v/v paraformaldehyde solution diluted in 1x PBS and subsequently permeabilized with two washes of 0.1% v/v NP-40 diluted in 1x PBS. Coverslips were then co-stained with appropriate primary antibodies diluted in 0.1% v/v NP-40, 10% v/v FBS in 1x PBS. Coverslips were washed three times, as before. Primary antibodies were visualized with appropriate fluorescence conjugated antibodies diluted in 0.1% v/v NP-40, 10% v/v FBS in 1x PBS. Cells were also stained with Hoechst 33342, diluted 1:2500 v/v in 0.1% v/v NP-40 diluted in 1x PBS, to determine nuclear morphology. Fluorescence was visualized and captured using a Zeiss axiophot microscope equipped with a cooled CCD camera.

3.6.2 Western Blot Analysis

Transfected and endogenous proteins were detected by sodium dodecyl sulfate (SDS) polyacrylamide gel electrophoresis (PAGE). Cells were lysed in RIPA buffer (150 mM NaCl, 50 mM Tris-HCl, pH 7.2, 0.7 μM PMSF, 1% v/v Triton X-100, 0.1% v/v SDS, 1% v/v sodium deoxycholate, 1/1000 v/v sodium azide). Aliquots of these lysates were separated by electrophoresis at 120 volts for approximately 1.5 hours through 12.5% SDS-polyacrylamide gels made according to Sambrook *et al.* (1989) in Laemmli buffer (25 mM Tris, 250 mM glycine, 0.1% w/v SDS). Following separation, gels were removed from the apparatus and incubated in transfer buffer (25 mM Tris, 190 mM

glycine, 20% v/v methanol). Proteins were transferred using a semi-dry transfer apparatus (LKB 2117 Multiphor Apparatus) in which filter paper (Munktell, Pharmacia) and nitrocellulose membrane (0.22 μm, Osmonics, Minnetonka, MN), both pre-soaked in transfer buffer, and the gels, filter paper, and membrane were assembled according to the manufacturer's instructions. Current of 37 milliamperes per 40 cm^2 gel was applied for 1 to 2 hours. Nitrocellulose membranes were incubated in blocking buffer (3% v/v BSA, 0.2% v/v Tween-20 diluted in PBS) for 1 hour at room temperature with agitation and subsequently immunoblotted with appropriate antibodies diluted in fresh blocking buffer overnight at 4°C. Membranes were washed three times in 0.2% v/v Tween-20 in PBS for 10 minutes with agitation. Appropriate secondary antibody was diluted in blocking buffer and applied to the membranes and permitted to incubate for 1 hour at room temperature with agitation. Membranes were washed as before and proteins were visualized with an enhanced chemiluminescence system (ECL) (Amersham Pharmacia Biotech, Amersham, UK).

3.7 β-Galactosidase Cell Death Assay

Cells were co-transfected with the reporter plasmid, pcDNA3-β-galactosidase plus the indicated expression plasmid(s) via the Lipofectamine method (Section 3.5.2). Twenty-seven hours post-transfection, cells were fixed with 0.2% v/v glutaraldehyde diluted in 1x PBS (phosphate buffered saline) for ten minutes and washed three times with PBS. Cells were then stained with 0.8 mg/ml 5-bromo-4-chloro-3-indolyl-β-D-galactopyranoside (X-gal) diluted in X-gal buffer (2 mM $MgSO_4$ diluted in 1x PBS, 150 mM $K_4Fe(CN)_6 \bullet 3H_2O$, 150 mM $K_3Fe(CN)_6$ mixed 8:1:1 by volume) and incubated for at

least four hours at 37°C. The percent of cell death was determined as the number of rounded, condensed, blue-staining cells in the total population of flat, blue-staining cells. This assay was used to evaluate (i) peptide caspase inhibitors, where the final amount of DNA was 0.75 μg (including 0.01 μg pcDNA3-β-gal), (ii) expression of pcDNA1-p35 as a caspase inhibitor, where the final amount of DNA was adjusted to 1.95 μg (including 0.01 μg pcDNA3-β-gal), and (iii) BNIP3-induced cell death in MEF cells, where the final amount of DNA was 1.2 μg (including 0.3 μg pcDNA3-β-gal). In all cases, the total DNA amount was adjusted with empty pcDNA3 vector (Clontech, Palo Alto, CA).

3.8 Assessment of Caspase Activation

Various doses of the broad spectrum caspase inhibitor, Ac-zVAD-fmk, or the control peptide Ac-FA-fmk (Enzyme System Products, Dublin, CA) were applied to transfected 293T cells (Section 3.5.2) six hours after transfection. Cell death was determined by the β-galactosidase assay (Section 3.7). Likewise, p35 was co-expressed with BNIP3 to assess inhibition of caspase activity.

Cleavage of endogenous caspases was detected by immunoblot analysis (Section 3.6.2). Briefly, lysates were collected from 293T cells transiently transfected via the $CaPO_4$ method (Section 3.5.1) at the indicated times. Membranes were probed with mouse monoclonal antibodies directed to caspase 3, caspase 7, caspase 9, and PARP according to Table X (Section 3.4).

Transfected 293T cells (Section 3.5.1) were also assayed for caspase cleavage via *in vitro* cleavage of the peptide, Ac-DEVD-pNA (Biomol, Plymouth Meeting, PA), according to the conditions outlined by Quignon *et al.* (1998). Two 10 cm plates of

transfected cells were required for a single reaction. Attached and detached cells were collected and washed twice in PBS and then resuspended in 1 ml PBS. An aliquot of 10 µl was used to determine cell number with a hemacytometer. An aliquot of 5 x 10^6 cells was centrifuged and resuspended in 200 µl freshly prepared NP-40 lysis buffer (10 mM Hepes/NaOH, pH 7.4, 2 mM EDTA, 1 mM DTT, 1% v/v NP-40, 1/1000 v/v PMSF, 1/1000 v/v leupeptin, 1/1000 v/v pepstatin A, 1/1000 v/v aprotinin). Cells were centrifuged at 1100 x *g* for 5 minutes. An aliquot of 120 µl was removed from the supernatant and centrifuged again at 1100 x *g*. An aliquot of 100 µl (lysate) was then removed from the supernatant and used in the assay. Protein concentration was determined using the Coomassie Plus Protein Assay kit (Pierce Chemical Co., Brockville, ON) where 300 µl reagent was applied to a well of a flat-bottomed 96 well plate (Nunc) containing 1 µl of lysate. Absorbances were measured on a spectrophotometer (Multiskan MCC/340, Titertek) at 620 nm. Using this information, all lysate samples were adjusted with NP-40 lysis buffer to contain equivalent protein concentrations. The reaction was set up in a 96 well plate where each well contained 20 µl lysate, 100 µM Ac-DEVD-pNA, 178 µl Reaction buffer (100 mM Hepes, pH 7.5, 20% v/v glycerol, 5 mM DTT, 0.5 mM EDTA). Where appropriate, samples were pre-incubated with 500 nM Ac-DEVD-fmk (Enzyme Systems Products) for 30 minutes at room temperature. Plates were incubated at 37°C for 4 hours. Data were acquired on a spectrophotometer (Multiskan MCC/340, Titertek) at 405 nm. Raw data were analyzed relative to the cleavage activity observed in untransfected cell lysates in each experiment, yielding "fold activation".

3.9 Assessment of Cytochrome c Release

Mitochondria were isolated from $CaPO_4$-transfected 293T cells (Section 3.5.1) using 70 strokes (tight pestle) in a 1 ml Dounce homogenizer (Wheaton) in 300 µl freshly prepared CFS buffer (220 mM mannitol, 68 mM sucrose, 2 mM NaCl, 2.5 mM KH_2PO_4, 0.5 mM EGTA, 2 mM $MgCl_2$, 10 mM Hepes-NaOH, pH 7.4, 5 mM pyruvate, 0.1 mM PMSF, 1 mM DTT, 1/1000 v/v aprotinin, 1/1000 v/v leupeptin, 1/1000 v/v pepstatin A) as previously described (Susin *et al.*, 2000). Mitochondria were resuspended in H buffer (300 mM sucrose, 5 mM N-tris[hydroxymethyl]methyl-2-amino ethane sulfonic acid [TES], 200 µM EGTA, pH 7.2) (Susin *et al.*, 2000). Aliquots of 5 µg protein were analyzed by electrophoresis through a SDS-15% polyacrylamide gel and immunoblotted with anti-cytochrome *c* monoclonal antibody (Section 3.6.2). Equivalent protein loading was ensured by probing the same filter with monoclonal anti-actin antibody.

Cytochrome *c* release was also determined by indirect immunofluorescence of transfected MCF-7 and 293T cells grown on coverslips (Section 3.6.1). Coverslips were co-stained with mouse anti-cytochrome *c* monoclonal antibody and an appropriate epitope antibody (rabbit anti-HA for BNIP3; rabbit anti-FLAG for tBID). Primary antibodies were visualized with Cy3-conjugated goat anti-mouse IgG and FITC-conjugated goat anti-rabbit IgG. Cytochrome *c* release was identified as the redistribution of a punctate, mitochondrial staining pattern to a diffuse, cytosolic pattern. No fewer than 200 cells were scored for each sample.

3.10 Annexin V Staining

Cells transiently transfected with $CaPO_4$ (Section 3.5.1) were collected at the indicated times and washed in cold PBS. Cells were centrifuged at 3000 x *g* for 5 min at 4°C and resuspended in 200 µl PBS. Cells were resuspended in labeling solution (1 ml [10 mM Hepes/NaOH, pH 7.4, 140 mM NaCl, 5 mM $CaCl_2$], 20 µl Annexin-V-FLUOS (Boehringer Mannheim), 20 µl propidium iodide [50 µg/ml]) and incubated at room temperature for 15 minutes. Samples were analyzed via flow cytometry (FACScalibur, Becton-Dickinson, San Jose, CA).

3.11 DNA Fragmentation Assays

3.11.1 TUNEL (Terminal Deoxynucleotidyl Transferase-mediated dUTP Nicked End Labeling) Assay

Briefly, $CaPO_4$-transfected 293T cells (Section 3.5.1) were collected on ice following 24 hours of expression. Cells were washed in PBS and resuspended to 5 x 10^5 cells/ml. Aliquots of 100 µl were permitted to adhere to poly-lysine coated slides with inscribed circles for 30 minutes at room temperature. The remaining fluid was carefully aspirated without disturbing the adhered cells. Cells were covered with 3.7% v/v paraformaldehyde solution diluted in 1x PBS and allowed to fix overnight at 4°C in a humidity chamber. Slides were then washed twice in PBS and permeabilized with 0.1% v/v Triton X-100, 0.1%v/v sodium citrate diluted in 1x PBS for two minutes on ice, and then washed twice in PBS. DNA fragmentation was detected using the *In Situ* Cell Death Detection Kit, Fluorescein (Roche Diagnostics, Mannheim, Germany), also referred to as the TUNEL assay, as per the manufacturer's recommendations. Slides were washed twice in PBS and subsequently stained with Hoechst 33342, diluted 1:2500 v/v in PBS, to

visualize the total cell population. Slides were again washed twice in PBS. FluoroGuard antifade reagent (Bio-Rad Laboratories, Hercules, CA) was applied to the cells and then covered with coverslips. Images were captured as described earlier. No fewer than 200 nuclei were scored manually for each sample.

3.11.2 Internucleosomal DNA Laddering

DNA fragmentation was also assessed via internucleosomal DNA laddering. Cells transiently transfected with $CaPO_4$ (Section 3.5.1) were collected at the indicated times and washed in cold PBS. Cells were centrifuged at 3000*g* for 5 min at 4°C and resuspended in 200 µl PBS. Genomic DNA was isolated from whole cells using the EasyDNA kit (Invitrogen, San Diego, CA) according to the manufacturer's instructions. An aliquot of 10 µg DNA was diluted in TE (10 mM Tris-HCl, pH 8.0, 1 mM EDTA) and 10% v/v loading dye (0.25% v/v bromophenol blue, 50% v/v glycerol). This aliquot was electrophoresed on a 1.5% w/v agarose gel made with TAE buffer (40 mM Tris-acetate, 1mM EDTA, pH 8.0) containing 1 µg/ml ethidium bromide run at 85 volts for one hour. DNA fragments were visualized by UV light on a transilluminator due to fluorescence of ethidium bromide intercalated with the DNA fragments.

3.12 Electron Microscopy

Transfected 293T cells (Section 3.5.1) were collected and washed twice in PBS. Cell pellets were resuspended in 500 µl fixative solution (2% v/v paraformaldehyde, 0.1% v/v gluteraldehyde diluted in 0.1 M sodium cacodylate) for 1 to 2 hour(s) at room temperature. Cells were post-fixed with 1% w/v osmium tetroxide for 1.5 hours, washed

in PBS, and block stained for 1 hour in 3% v/v aqueous uranyl acetate. Samples were then washed again, dehydrated with graded alcohol, and embedded in Epon-Araldyte resin (Maynard Scientific). Ultrathin sections were cut on a Reichert ultramicrotome, counter-stained with 0.3% w/v lead citrate, and examined on a Philips EM420 electron microscope.

3.13 Assessment of PT Pore Opening by Confocal Imaging

Aliquots of 293T cells were grown on coverslips and transfected via the $CaPO_4$ method (Section 3.5.1). Coverslips were collected 9 to 10 hours after transfection and washed with HH buffer (10 mM Hepes, pH 7.2 diluted in 1x Hanks Balanced Salt Solution [HBSS; Giboco-BRL]) before staining with 1 μM calcein-AM (Molecular Probes, Eugene, OR) in the presence of 5 mM $CoCl_2$ at room temperature for 15 minutes. $CoCl_2$ was added to quench cytosolic staining so that mitochondrial fluorescence can be visualized as glowing bodies over a dark background (Bernardi *et al.*, 1999). Cells were washed four times and resuspended in HH buffer and imaged with an Olympus IX70 inverted confocal laser microscope equipped with Fluoview 2.0 software (Carson Group Inc., Markham, ON). A bandpass filter of 488 nm was used to capture the green calcein images, while Nomarski optics were used to obtain transmitted light images of the cells. To determine mitochondrial calcein fluorescence levels, individual cells were identified using Nomarski optics and total mitochondrial fluorescence per cell was measured digitally with Northern Eclipse software, version 5.0 (Empix Inc. Toronto, ON) yielding relative fluorescence units (RFU). Cells were then arbitrarily classified into low (0-40

000 RFU), intermediate (40 000 – 60 000 RFU), and high levels (> 60 000 RFU) of fluorescence.

3.14 Measurement of Mitochondrial $\Delta\psi m$ Suppression and ROS Production

Eight hours after transfection, changes in mitochondrial function were determined by incubating 1 x 10^6 293T cells, transiently transfected by the $CaPO_4$ method (Section 3.5.1), with either 1 μM JC-1, 40 nM $DiOC_6$, or 2 μM dihydroethidium (HE) (all from Molecular Probes) diluted in HBSS (Gibco-BRL) for 30 minutes at 37°C. Controls were performed in the presence or absence of 50 μM mCICCP or an excess of 30% v/v H_2O_2. For inhibition experiments, cyclosporin A or bongkrekic acid (a gift from Dr. J.A. Duine, Delft University, Delft, The Netherlands) were added two hours prior to transfection at the indicated concentrations. Aliquots were also stained with 1 μg/ml propidium iodide (PI) to assess cell death. Cells were scored using a FACScalibur flow cytometer (Becton-Dickinson) and data were analyzed with Cellquest software, version 3.1 (Becton-Dickinson). In all cases, samples were gated to exclude cellular debris.

4.0 Results

4.1 BNIP3 family members require the TM domain to induce cell death

Many BCL-2 pro-apoptotic proteins feature a carboxyl-terminal TM domain that is required for proper subcellular localization and dimerization (Adams and Cory, 1998; Minn *et al.*, 1998). Likewise, BNIP3 and NIX have a TM domain at residues 164 to 184 (Boyd *et al.*, 1994; Chen *et al.*, 1997; Chen *et al.*, 1999). It has been demonstrated that the TM domain of BNIP3 is required to induce nuclear morphology associated with apoptosis, as determined by Hoechst dye staining (Chen *et al.*, 1997). We confirmed this observation by an alternate assay. Briefly, constructs lacking the TM domain of BNIP3 (BNIP3ΔTM) or NIX (NIXΔTM) (Figure 9a) were co-expressed in 293T cells with a reporter plasmid encoding the β-galactosidase gene of *E. coli* and cell death was assessed by cellular morphology as described (Section 3.7). Deletion of the TM domain abolished the death promoting activities of both BNIP3 and NIX compared to full length BNIP3 and NIX, respectively (Figure 9b). Therefore, the TM domains of BNIP3 and NIX are required to induce cell death.

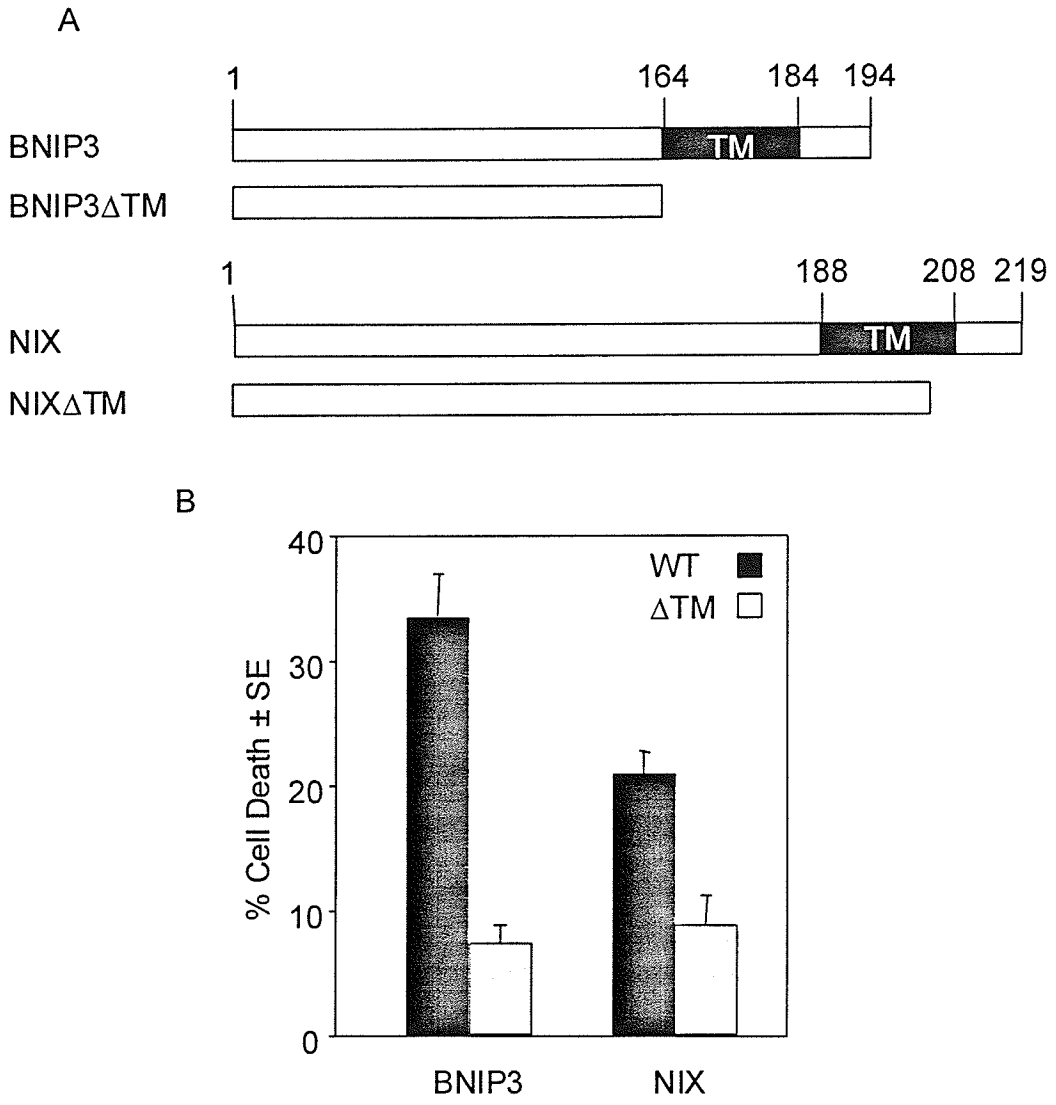

Figure 9: BNIP3 family members require the TM domain to induce cell death (A) Schematic representation of BNIP3 and NIX and their TM domain deletio mutants. (B) 293T cells were transiently co-transfected with the reporter plasmid pcDNA3-βgal and either wild type (WT) BNIP3-T7 or NIX-T7 (solid bars) or mutan (ΔTM) BNIP3ΔTM-T7 or NIXΔTM. Twenty-seven hours post transfection, cell were fixed, stained, and evaluated for dead cells as described in Section 3.7. The dat are representative of results obtained in two independent experiments.

4.2 BNIP3 induces cell death from mitochondrial and non-mitochondrial sites

Initial studies demonstrated that BNIP3 predominantly localized to the mitochondria and that this was mediated by the TM domain (Boyd *et al.*, 1994; Chen *et al.*, 1997). To determine if BNIP3 can induce cell death from alternate subcellular sites, cell death assays were repeated using BNIP3 substituted with heterologous TM domain sequences from BCL-2 and cytochrome b_5. BNIP3-BclTM was constructed by joining the cytoplasmic portion of BNIP3 (amino acids 1 to 163) to 21 residues of the BCL-2 TM domain, which has previously been shown to be sufficient to direct heterologous proteins to the outer mitochondrial membrane with the protein oriented towards the cytosol (Figure 10a) (Nguyen *et al.*, 1993; Janiak *et al.*, 1994). Similarly, residues 1 to 163 of BNIP3 were fused to 35 amino acids of rat hepatic cytochrome b_5, which is sufficient to target heterologous proteins to the cytoplasmic face of the endoplasmic reticulum (Figure 10a) (Mitoma and Ito, 1992; Zhu *et al.*, 1996). Localization of the chimeric proteins was confirmed by confocal imaging of fluorescently-labeled proteins as described in Section 3.6.1 (Figure 10b). As expected, wild type BNIP3 and BNIP3-BclTM localized to the mitochondria as determined by co-localization with the matrix protein, HSP60 (Figure 10b). In contrast, BNIP3-Cb5TM localized to sites that clearly did not overlap with mitochondrial HSP60 staining (Figure 10b).

To determine if these chimeric proteins were able to induce cell death as efficiently as BNIP3, the constructs were overexpressed in 293T and MCF-7 cells (Section 3.5.2) and cell death was determined as described (Section 3.7). Both BNIP3-BclTM and BNIP3-Cb5TM were equally able to induce cell death compared to wild type BNIP3 in MCF-7 cells (Figure 11). In 293T cells, however, the chimeric proteins were

still able to induce cell death, albeit BNIP3-Cb5TM induced cell death to a lesser extent. BNIP3ΔTM served a negative control, confirming Section 4.1.

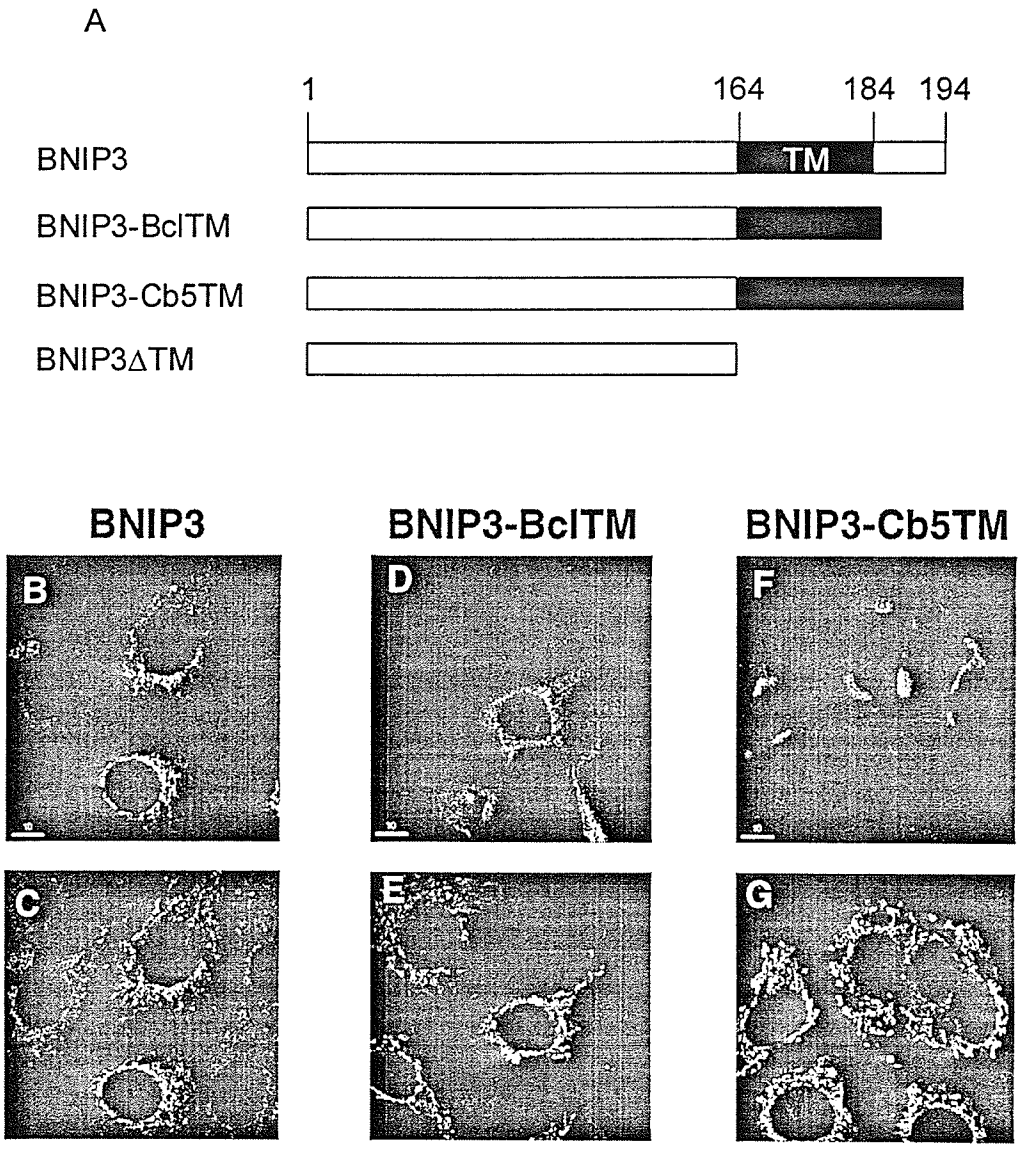

Figure 10: Localization of BNIP3 substituted with heterologous TM domains. (A) Schematic representation of BNIP3 fused with the TM domain sequences of BCL-2 and cytochrome b_5. (B) MCF-7 cells were transiently transfected with BNIP3, BNIP3-BclTM, or BNIP3-Cb5. Cells were co-stained with anti-BNIP3 and anti-HSP60 antibodies and then visualized with Cy3 and FITC-conjugated antibodies. The staining pattern for BNIP3 (B) and BNIP3-BclTM (D) resembles the punctate mitochondrial staining pattern characteristic of HSP60 in corresponding cells (C and E). BNIP3-Cb5TM shows a globular staining pattern (F) distinct from the distribution of HSP60 (G).

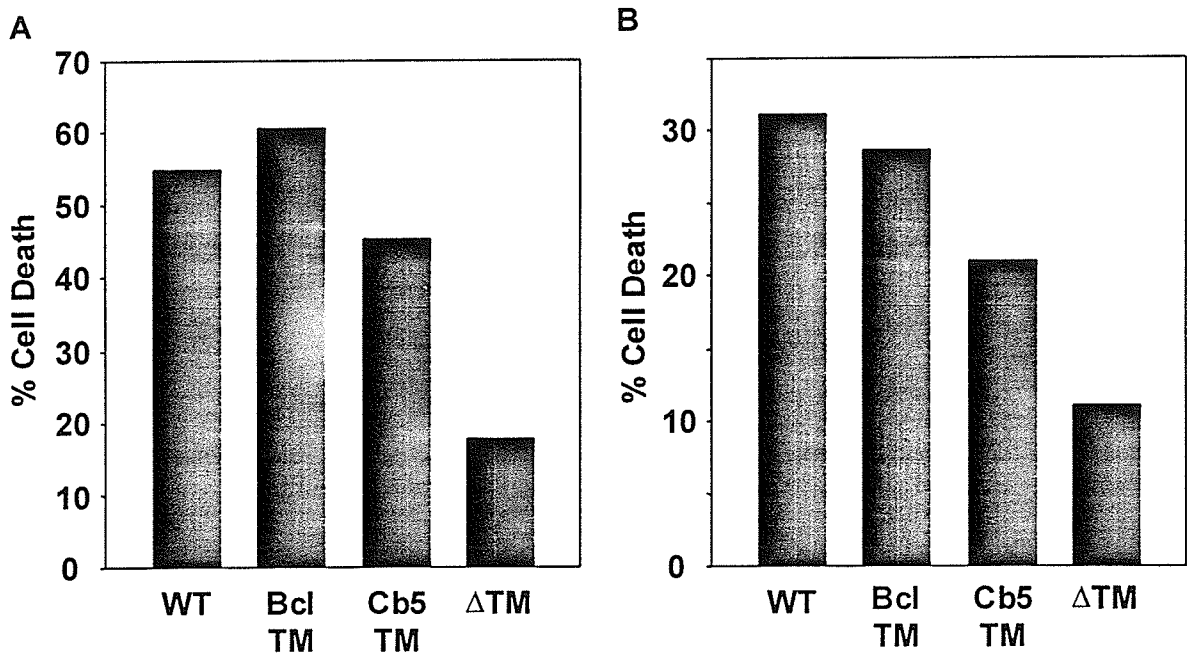

Figure 11: BNIP3 induces cell death from mitochondrial and non-mitochondrial sites. 293T (A) or MCF-7 (B) cells were transiently co-transfected with BNIP3 (WT), BNIP3-BclTM (BclTM), BNIP3-Cb5 (Cb5TM), or BNIP3ΔTM (ΔTM) and β-galactosidase reported plasmid. Twenty-seven hours post transfection, cells were fixed, stained, and evaluated for dead cells as described in Section 3.7. Results are representative of two independent experiments.

4.3 BNIP3-induced cell death is caspase-independent

BNIP3 was originally proposed to be a member of the 'BH3-only' subfamily of BCL-2 pro-apoptotic proteins. It is now known that the BH3-like domain is not required for the killing activity of BNIP3 (Ray *et al.*, 2000). However, this result did not rule out the possibility that BNIP3 induced cell death via caspase activation. To determine if BNIP3-induced cell death was mediated by caspases, we evaluated the effectiveness of the broad spectrum peptide caspase inhibitor Ac-zVAD-fmk and the baculovirus anti-apoptotic gene p35 in preventing BNIP3-induced cell death. Cells (293T) were transiently co-transfected with BNIP3 and a reporter plasmid encoding the β-galactosidase gene of *E. coli*, and subsequently treated with increasing concentrations of peptide inhibitor as described (Section 3.8). Cell death was assessed by cellular morphology (Section 3.7). BNIP3-induced cell death was unaffected by 100 μM Ac-zVAD-fmk, a concentration previously shown to effectively block caspase-mediated cell death (Li *et al.*, 1998; Desagher *et al.*, 1999). Furthermore, this concentration of inhibitor effectively suppressed cell death by greater than 50% in both tBID and caspase 9/Apaf-1 transfectants, both known to function via caspase activation (Figure 12a). The BNIP3 deletion mutant BNIP3ΔTM, which lacks the TM domain and has previously been shown to be incapable of mitochondrial localization and induction of cell death (Chen *et al.*, 1997; Chen *et al.*, 1999; Yasuda *et al.*, 1999 and Section 4.1), served as a negative control to verify that the observed cell death was specific in all cases. Increasing amounts of a vector encoding the known caspase inhibitor baculovirus p35 protein (Bump *et al.*, 1995; Xue and Horvitz, 1995) co-transfected with the other indicated vectors were similarly ineffective in abrogating BNIP3 cell death at concentrations of up

to 1.5 μg, well above the 0.5 μg p35 plasmid required to block caspase 9/Apaf-1 induced cell death (Figure 12b). These data provide indirect evidence for a lack of caspase involvement in BNIP3-induced cell death.

Caspase activity in lysates of transfected cells can be determined using a peptide containing a caspase specific cleavage site, which yields a colorgenic product. The caspase substrate Ac-DEVD-pNA was used to detect the activation of caspase 3-like proteases in 293T cells transiently transfected with BNIP3, tBID or the inactive mutant BNIP3ΔTM. Cells were harvested at 1, 12, 18, 24, and 36 hours post transfection then lysates prepared and incubated with the substrate. The colored product was detected at 405 nm with a spectrophotometer. All data were manipulated to be relative to lysates from untransfected cells, which were previously shown to be equivalent to mock transfected cells (unpublished observations) as decribed (Section 3.8). At all time points, lysates from cells transfected with BNIP3 or BNIP3ΔTM revealed only marginal increases in proteolytic activity. Furthermore, these activities were not inhibited by the caspase inhibitor of the same specificity, Ac-DEVD-fmk (Figure 13). In contrast, cells overexpressing tBID, a known activator of caspases, exhibited a 4-fold increase in substrate cleavage peaking at 12 hours and this was inhibited by treatment with 500 nM Ac-DEVD-fmk (Figure 13). The gradual decline in the DEVDase activity of tBID-transfected cells is likely due to high levels of tBID-induced cell death resulting in a decreased number of viable transfected cells relative to untransfected cells in the same population.

The lack of significant caspase activation was further confirmed in immunoblotting experiments. Experiments attempting to order the activation of caspases

have demonstrated that caspase 9 can proteolytically activate procaspases 3 and 7 (Slee *et al.*, 1999). Furthermore, poly-ADP ribosylating polymerase (PARP) is cleaved by active downstream caspases, such as caspase 3 and 7, and is commonly used as a marker for caspase activation (Schlegel *et al.*, 1996; Faleiro *et al.*, 1997; Zhang *et al.* 1999; Nguyen *et al.*, 2000). Whole cell lysates of BNIP3-expressing 293T cells were collected at 12, 24, 36, and 48 hours post-transfection and immunoblotted for the caspase substrate PARP and caspases 3, 7, and 9 (Section 3.6.2). There was little evidence of proteolytic processing of PARP (Figure 14d), and no processing of procaspase 3 (Figure 14a) in BNIP3 lysates. In contrast, efficient processing of PARP from 116 kD to 86 kD (Figure 14d), and procaspases 3, 7, and 9 (Figure 14a-c) were readily detected in lysates from BAX transfectants. No processing of procaspase 7 and 9 was observed in BNIP3 lysates up to 36 hours (Figure 14a and b).

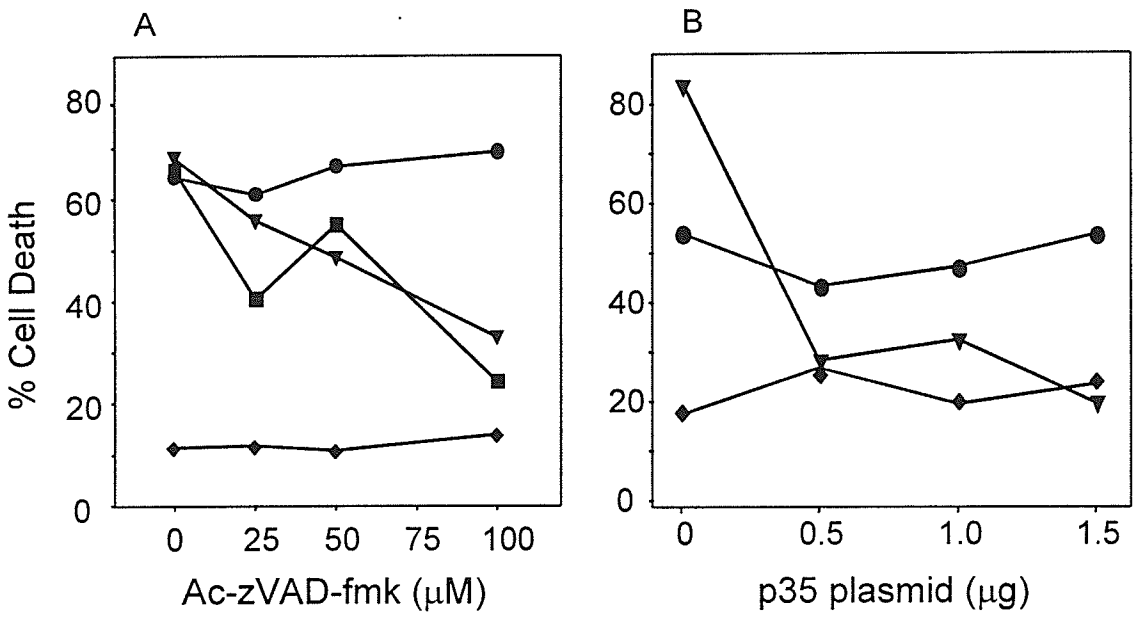

Figure 12: Broad spectrum caspase inhibitors Ac-zVAD-fmk and baculovirus p35 fail to inhibit BNIP3-induced cell death. (A) 293T cells were transiently co-transfected with the reporter plasmid, pcDNA3-βgal and either BNIP3-T7 (●) or inactive mutant BNIP3ΔTM-T7 (◆). Cells transfected with tBID-FLAG (■), or caspase 9-His_6 plus Apaf-1 (▼) served as positive controls. All groups were treated with increasing concentrations of Ac-zVAD-fmk. (B) In a parallel experiment, 293T cells were transfected as above with increasing concentrations of pcDNA1-p35. Twenty-seven hours post transfection, cells were fixed, stained, and evaluated for dead cells as described in Materials and Methods. The data are representative of results obtained in three independent experiments.

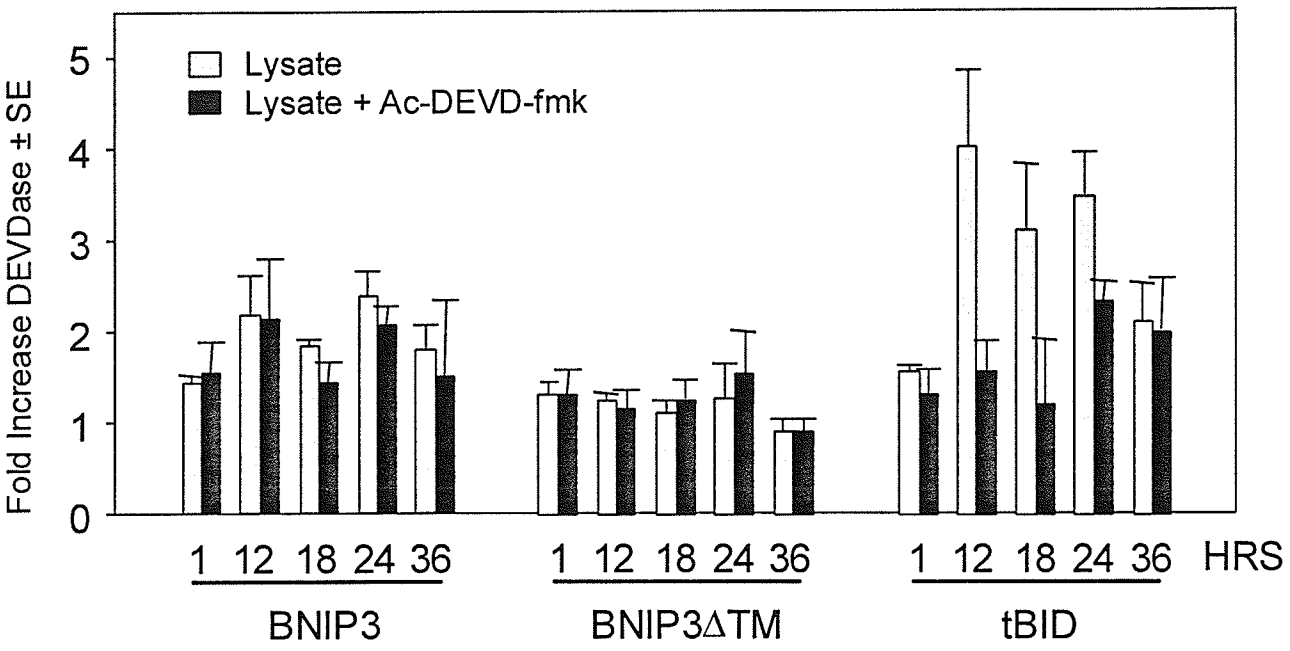

Figure 13: Overexpression of BNIP3 does not induce significant DEVDase activity. Lysates from 293T cells transfected with BNIP3-T7, BNIP3ΔTM-T7, or tBID-FLAG were harvested at 1, 12, 18, 24, and 36 hours and then incubated with the substrate DEVD-pNA in the presence (solid bars) or absence (shaded bars) of 500 nM of the inhibitor Ac-DEVD-fmk. Fold activation was determined as the ratio of cleavage activity observed in transfected cells to the cleavage activity of untransfected controls. Results are expressed as the mean ± standard error (SE) from at least three independent experiments.

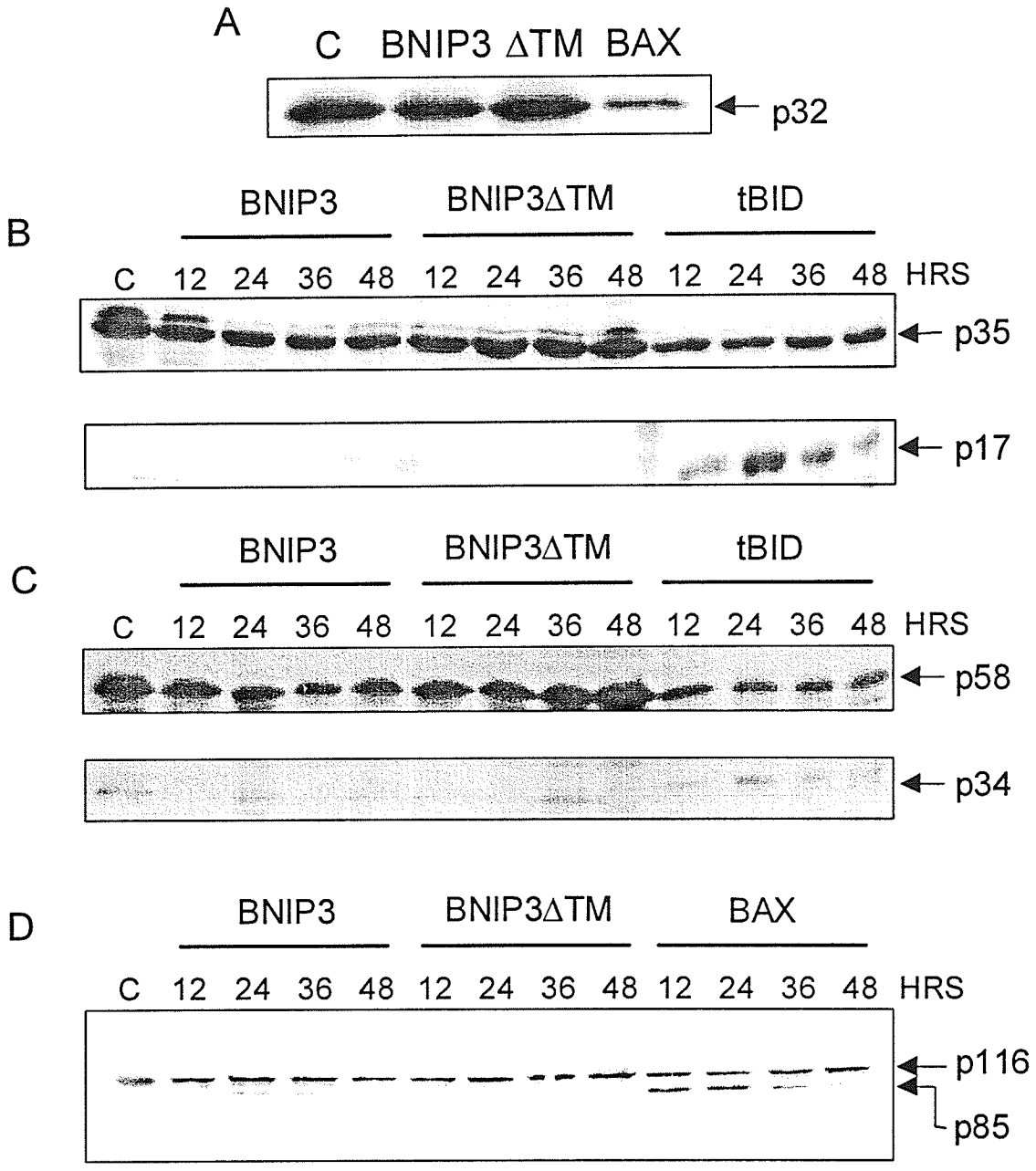

Figure 14: Overexpression of BNIP3 fails to activate procaspases and PARP cleavage. (A) Lysates from BNIP3-T7, BNIP3ΔTM-T7 (ΔTM), or BAX-transfected 293T cells were harvested 24 hours post-transfection and immunoblotted with mouse monoclonal anti-procaspase 3 antibody. The arrow indicates the unprocessed p32 band. Lysates from BNIP3-T7, BNIP3ΔTM-T7, BAX or tBID-transfected 293T cells were harvested at 12, 24, 36, and 48 hours post-transfection and immunoblotted with mouse monoclonal anti-procaspase 7 (B), anti-procaspase 9 (C), or anti-PARP (D) antibodies. Arrows indicate the unprocessed (larger) and processed (smaller) bands. Lane C, untransfected control.

4.4 Overexpression of BNIP3 does not induce significant cytochrome *c* release

Overexpression of BNIP3 has been shown to induce its integration into the mitochondrial outer membrane (Vande Velde *et al.*, 2000). We hypothesized that BNIP3 may function to initiate cell death by mitochondrial perturbation and subsequent release of cytochrome *c*, a critical cofactor for Apaf-1-mediated cell death (Liu *et al.*, 1996; Li *et al.*, 1997). We initially assessed cytochrome *c* release from the mitochondrial intermembrane space in transiently transfected cells via indirect immunofluorescence in which cytochrome *c* release was scored as the loss of a punctate staining pattern (Figure 15). BNIP3 and BNIP3ΔTM expressing cells were identified by immunostaining for the C-terminal T7-epitope tag (Section 3.6.1). In both cases, no significant cytochrome *c* release was observed in MCF-7 cells, and only a small amount was observed in 293T cells, even after 48 hours of expression (Figure 16). On the other hand, 71% of 293T and 91% of MCF-7 cells released cytochrome *c* 48 hours following transfection with tBID, while the level of cell death induced by overexpression of tBID and BNIP3 was equivalent (Figure 16). In tBID transfected cells, cytochrome c was released prior to apoptosis as determined by Hoechst dye staining (Figures 15 and 16).

We re-examined cytochrome *c* release via subcellular fractionation (Section 3.9) of transfected 293T cells harvested at 18, 24, and 36 hours post-transfection and subsequent immunoblotting of heavy membrane (HM) and cytosolic (S-100) fractions (Section 3.6.2). A significant increase in cytochrome *c* was observed in the S-100 fractions of tBID but not BNIP3 transfectants at 18 and 24 hours (Figure 17a). Loss of cell viability of tBID and BNIP3 transfectants was equivalent, as determined by trypan blue dye exclusion (Figure 17b). The decrease in cytochrome *c* levels in S-100 of tBID-

expressing cells at 36 hours was concomitant with extensive cell death. S-100 cytochrome *c* levels in BNIP3-transfected cells were similar to that of the inactive BNIP3ΔTM and control cells despite a five-fold difference in viability (Figure 17). A time course revealed that chromatin condensation following BNIP3 transfection preceded the release of cytochrome *c*, indicating that cytochrome *c* could not be responsible for the observed nuclear changes (Figure 15).

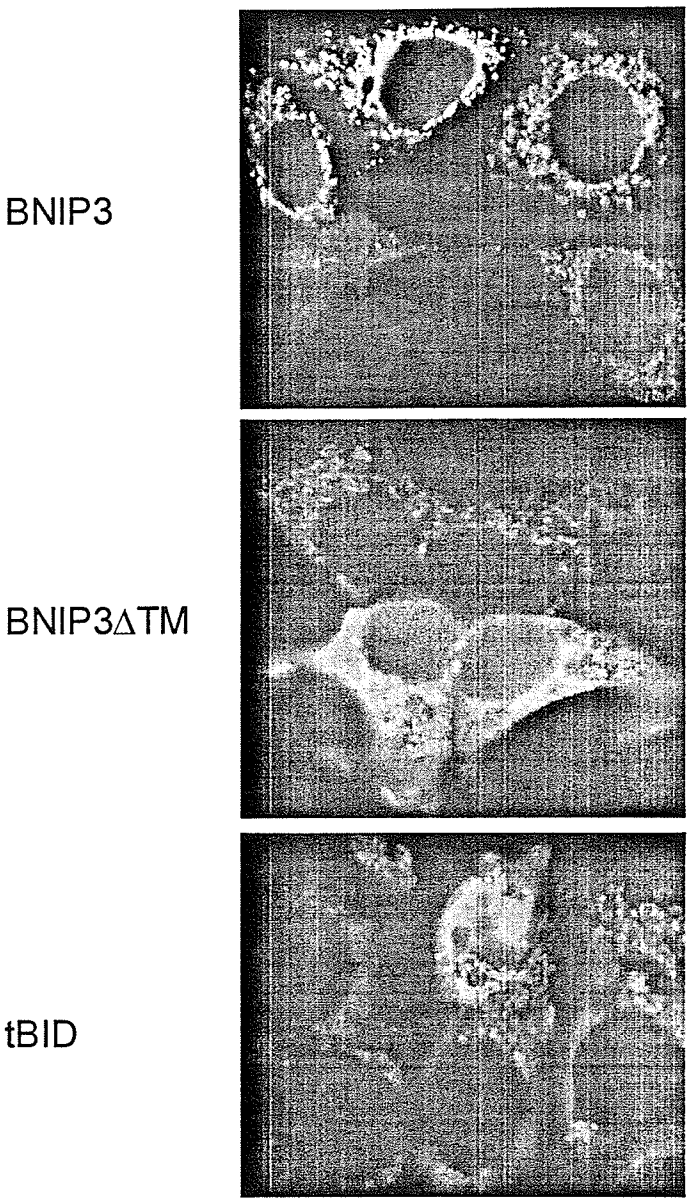

Figure 15: Overexpression of BNIP3 does not induce significant redistribution of cytochrome *c*. Twenty-four hours post-transfection, MCF-7 cells transiently transfected with BNIP3-T7, BNIP3ΔTM-T7, or tBID-FLAG were stained with Cy3-conjugated monoclonal anti-cytochrome *c* antibody and appropriate FITC-conjugated anti-epitope antibodies, and subsequently evaluated by fluorescent microscopy. Cytochrome *c* release was scored as the loss of punctate mitochondrial staining. Apoptotic cells were scored based on chromatin condensation following Hoechst dye staining.

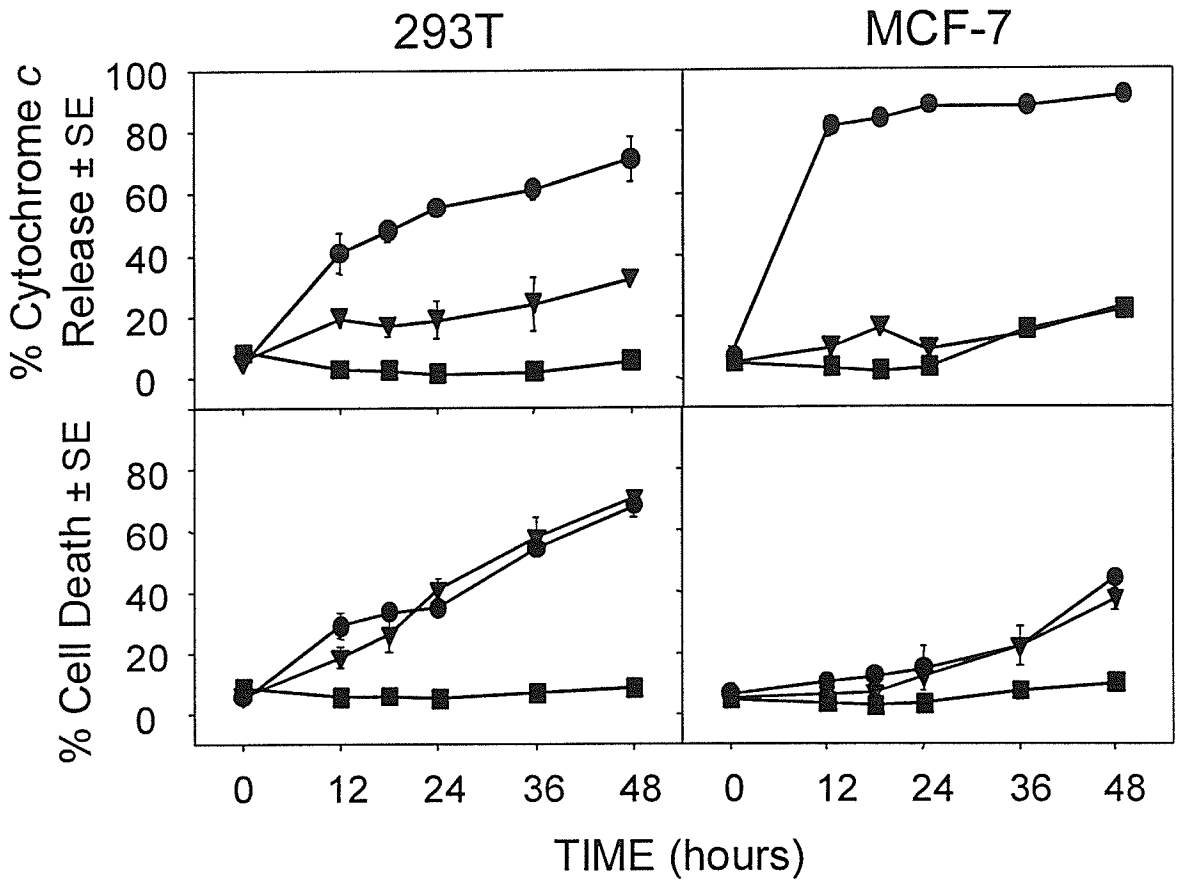

Figure 16: Overexpression of BNIP3 does not induce significant mitochondrial cytochrome *c* release. Cells transiently transfected with BNIP3-T7, BNIP3ΔTM-T7, or tBID-FLAG were stained with monoclonal anti-cytochrome *c* antibody and Cy3-labeled anti-mouse antibody then evaluated by fluorescent microscopy. Time course of cytochrome *c* release and apoptosis following BNIP3-T7 (▼), BNIP3ΔTM-T7 (■), or tBID-FLAG (●) transfection of 293T (left panels) and MCF-7 (right panels) cells is shown. Cytochrome *c* release was scored as the loss of cytoplasmic granular staining. Apoptotic cells were scored based on chromatin condensation following Hoechst dye staining. The data from three independent experiments are shown as the mean ± SE for each time point.

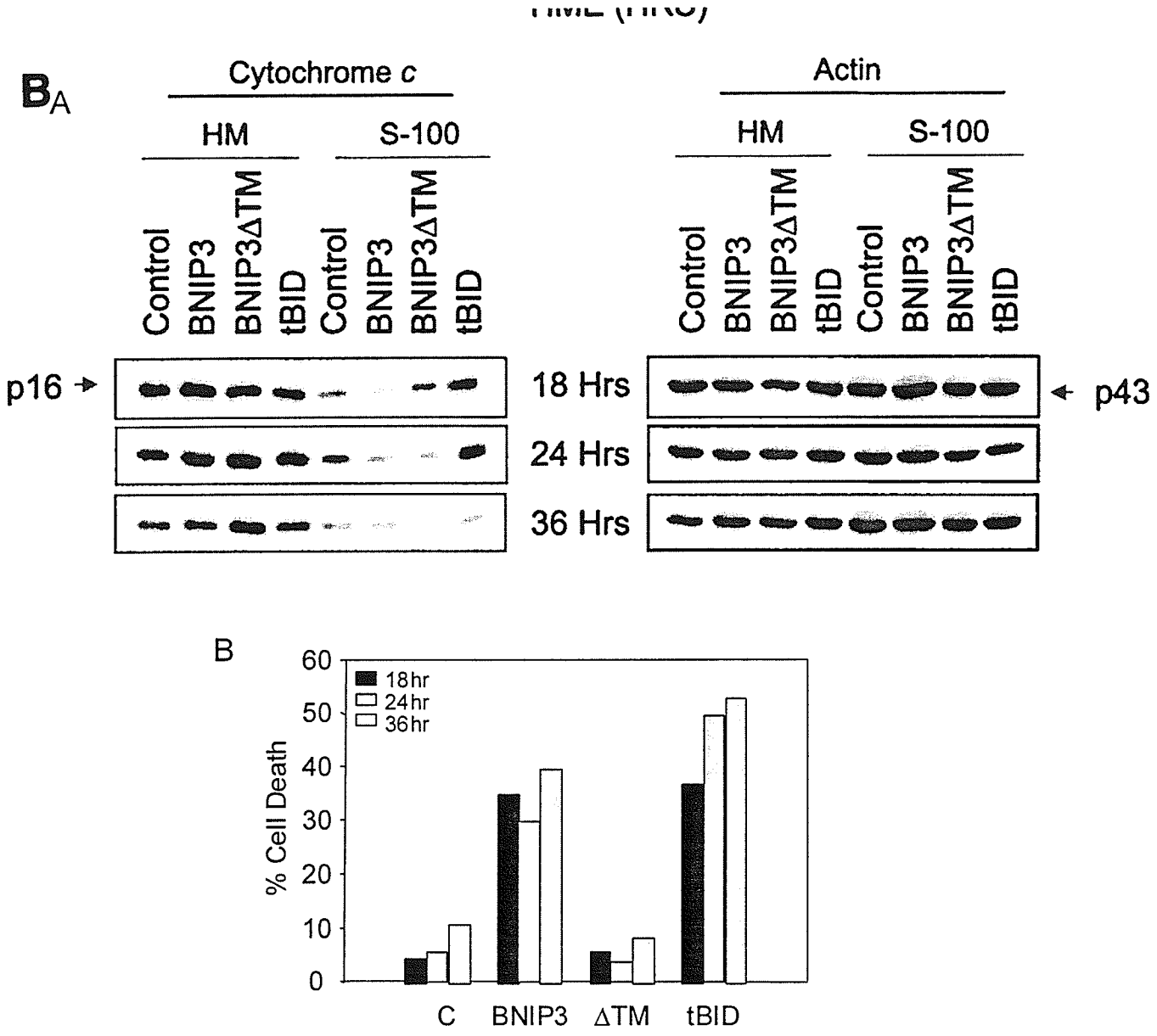

Figure 17: BNIP3 does not induce significant mitochondrial cytochrome *c* redistribution. Western blot analysis of the time course of release of cytochrome *c* from mitochondria-containing heavy membrane (HM) fractions to S-100 cytosol. 293T cells were transiently transfected with BNIP3-T7, BNIP3ΔTM-T7, or tBID-FLAG and harvested at 18, 24, and 36 hours post-transfection. Aliquots of 5 μg of HM and S-100 fractions were electrophoresed and immunoblotted with mouse anti-cytochrome *c* antibody (p16). The same filter was blotted with mouse anti-actin antibody (p43) to demonstrate equal loading. (B) Aliquots of cells used in panel A were stained with trypan blue. Failure to exclude trypan blue was used to determine cell death. Control (C), untransfected cells.

4.5 BNIP3 induces cell death in fibroblasts deficient in Apaf-1, caspase 9 or caspase 3

The previous experiments suggested that BNIP3 induced cell death without cytochrome *c* release or caspase activation. Therefore, we proceeded to examine the function of BNIP3 in cells genetically deficient in Apaf-1 or Apaf-1-activated caspases 9 and 3 (Zou *et al.*, 1997). Using the β-galactosidase cell death assay (Section 3.7), wild type, Apaf-$1^{-/-}$, caspase $9^{-/-}$, and caspase $3^{-/-}$ MEFs were transiently transfected with either BNIP3 or BNIP3ΔTM. Overexpression of BNIP3 induced cell death in approximately 50% of the transfected population in the wild type and all mutant MEF lines tested (Figure 18a). Expression of BNIP3ΔTM yielded results similar to mock transfected cells. In contrast, the mutant cells exhibited profound resistance to adriamycin-induced cell death (Figure R18b) confirming an earlier report (Hakem *et al.*, 1998). Immunoblot analysis of whole cell lysates demonstrated relatively equivalent expression of BNIP3 in all of the MEF cell lines (Figure 18c).

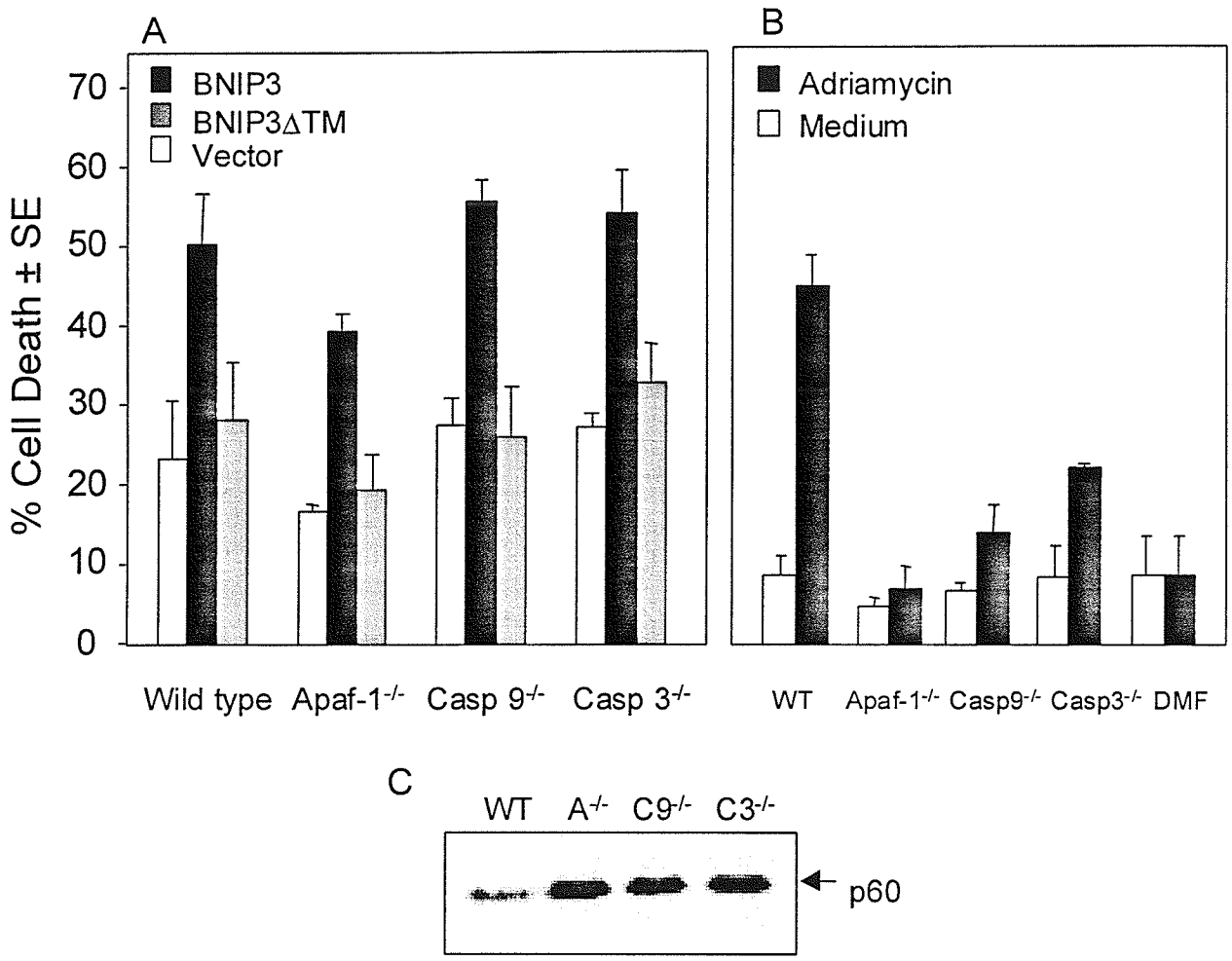

Figure 18: BNIP3-induced cell death in the absence of Apaf-1, caspase 9, or caspase 3. (A) Wild type, Apaf-$1^{-/-}$, caspase $9^{-/-}$ (Casp$9^{-/-}$), and caspase $3^{-/-}$ (Casp$3^{-/-}$) mouse embryo fibroblasts (MEFs) were transiently co-transfected with pcDNA3-βgal vector and either BNIP3-T7, BNIP3ΔTM-T7, or pcDNA3 and then scored for dead cells as described in Materials and Methods. Results are expressed as the mean ± SE from three independent experiments. (B) The same cell aliquots of wild-type (WT), Apaf-$1^{-/-}$, caspase-$9^{-/-}$, and caspase-$3^{-/-}$ MEFs used for the experiments described in panel A were transfected with pcDNA3-βgal and treated with medium or with 3 μg adriamycin per ml for 24 hours, and dead cells were enumerated in three experiments. *N,N*-Dimethyl formamide (DMF) was used to dilute adriamycin. (C) Lysates were collected from BNIP3-T7-transfected wild type (WT), Apaf-$1^{-/-}$ ($A^{-/-}$), caspase 9 ($C9^{-/-}$), and caspase 3 ($C3^{-/-}$) MEFs and immunoblotted with mouse anti-T7 antibody. Arrow indicates BNIP3 homodimer (p60).

4.6 Rapid loss of plasma membrane permeability in BNIP3-transfected cells

A morphological feature of cells undergoing apoptosis is the random redistribution of the inner leaflet phospholipid phosphatidylserine (PS) to the outer leaflet of the plasma membrane (Earnshaw *et al.*, 1999). Furthermore, apoptosis is characterized by the maintenance of an intact plasma membrane (McConkey, 1998). Plasma membrane integrity was determined as the ability of a cell to exclude propidium iodide (PI). A time course following BNIP3 transfection identified increased plasma membrane permeability as early as 2 hours post transfection and did not increase further over the following 12 hours (Figure 19a). Externalized PS can be detected via fluorescently-labeled annexin V, a calcium-dependent PS binding protein (Section 3.10) (Koopman *et al.*, 1994; Vermes *et al.*, 1995). Cells gated to determine annexin V binding as a measure of PS externalization in PI^- populations (intact plasma membrane) at 12 hours revealed no increase in annexin V staining of BNIP3-transfected in cells that excluded PI, in contrast to cells transfected with tBID, BAX or caspase 9/Apaf-1 (Figure 19b). BNIP3-expressing cells analysed at 18 and 24 hours similarly did not show any increase in annexin V staining in PI^- cells (Figure 19c). Thus, BNIP3 induces early permeability of the plasma membrane but not PS externalization.

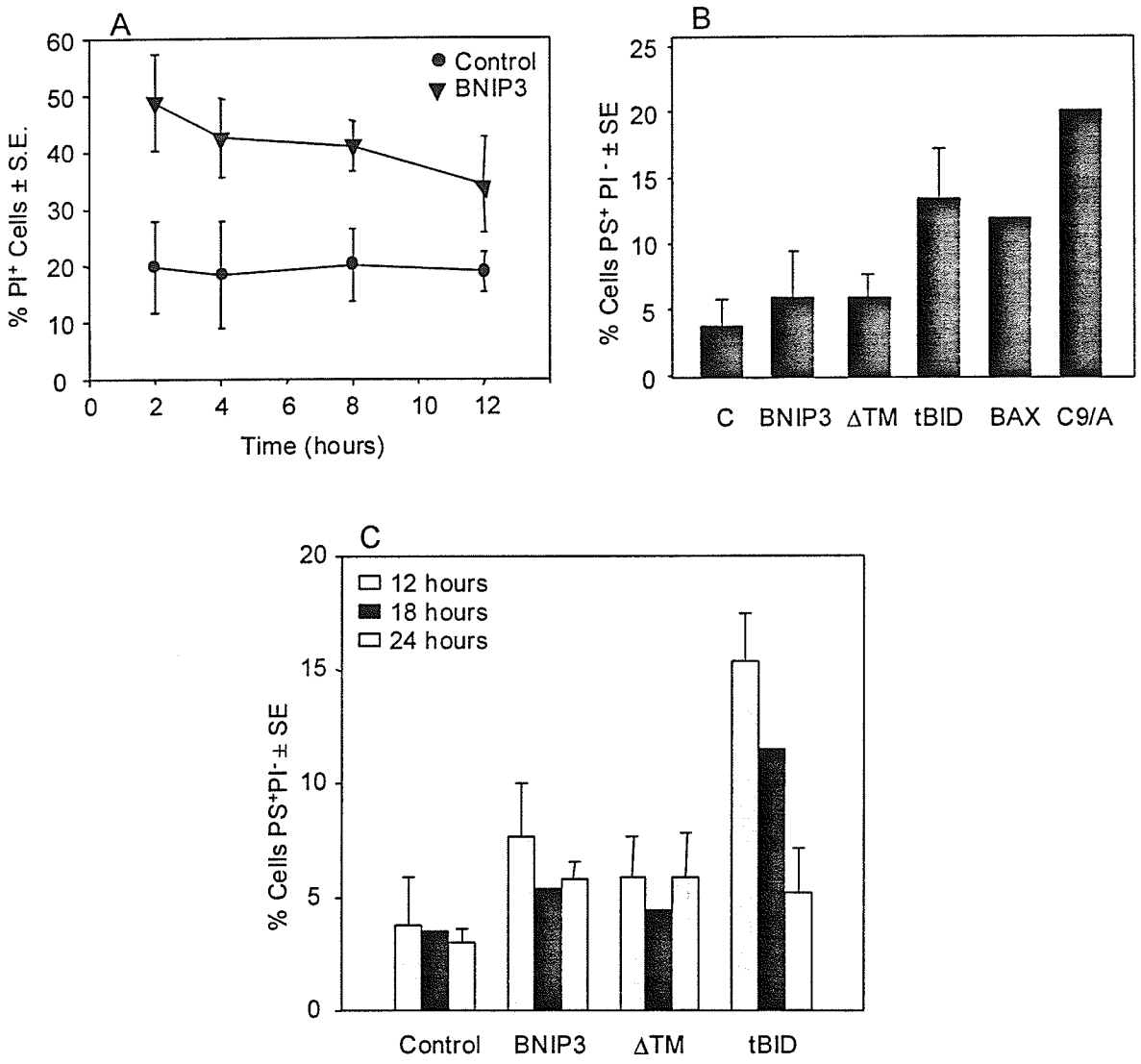

Figure 19: BNIP3 induces rapid plasma membrane permeability but not PS externalization. (A) Untransfected and BNIP3-T7-transfected 293T cells were harvested at 2, 4, 8, or12 hours post-transfection and stained with PI. PI^+ cells are expressed as the mean ± SE of three or four experiments for each time point. (B) Untransfected 293T cells (C) and 293T cells transfected with BNIP3-T7 (BNIP3), BNIP3ΔTM-T7 (ΔTM), tBID-FLAG (tBID), BAX or caspase 9/Apaf-1 (C9/A) were harvested at 12 hours post-transfection and were stained for annexin V and PI. Cells that were gated as PS^+ PI^- are expressed as the mean ± SE of three independent experiments. (C) Untransfected 293T cells (Control) and 293T cells transfected with BNIP3-T7 (BNIP3), BNIP3ΔTM-T7 (ΔTM), tBID-FLAG (tBID), were harvested at 12, 18, and 24 hours post-transfection and were stained for annexin V and PI. Cells that were gated as PS^+ PI^- are expressed as the mean ± SE of two independent experiments.

4.7 BNIP3 induces late DNA fragmentation that is independent of AIF translocation

DNA fragmentation and chromatin condensation are hallmarks of caspase-dependent, apoptotic cell death and have been consistently observed in BNIP3-transfected cells (Chen *et al.*, 1997; Chen *et al.*, 1999). Since we had demonstrated that plasma membrane was damaged early following BNIP3 expression (Section 4.6), we examined the relative rate at which DNA fragmentation occurred using the terminal deoxynucleotidyltransferase-mediated dUTP nicked end labeling (TUNEL) assay (Section 3.11.1). Cells were transfected with BNIP3 and assayed at 18, 24, and 36 hours post-transfection. BNIP3 transfectants showed increasing levels of TUNEL-positive cells over time, but no activity was detected until 18 to 24 hours and maximal levels were not reached until 36 hours, much slower than tBID-induced DNA damage where maximum damage was observed at 18 hours (Figure 20a). This contrasts with the initiation of plasma membrane damage by BNIP3 at 8 hours and its completion by 18 hours. In addition, we consistently observed only two or three TUNEL-positive foci in BNIP3 expressing cells, while tBID transfected cells exhibited much more extensive nuclear fragmentation with six to ten TUNEL-positive foci per cell (Figure 20b). DNA fragmentation could only be partially inhibited with 50 μM Ac-zVAD-fmk in BNIP3 transfectants but was nearly completely inhibited in tBID-expressing cells (Figure 20c). No effect was observed in parallel populations treated with 50 μM Ac-FA-fmk (Figure 20c).

Apoptotic DNA damage can also be detected via electrophoresis and appears as a series of bands (or rungs) commonly referred to as a DNA ladder (reviewed in Nagata,

2000). We confirmed the DNA fragmentation observed by TUNEL staining via electrophoresis on agarose gels stained with ethidium bromide as described (Section 3.11.2). An oligonucleosomal ladder was easily detected in tBID transfectants at 18, 24, and 36 hours, while little DNA degradation and ladder formation was observed in BNIP3 transfectants even at 36 hours (Figure 21). In both assays, cells transfected with the mutant BNIP3ΔTM did not have evident DNA damage, similar to untransfected controls (Figure 20 and 21). Chromatin condensation, determined via Hoechst dye staining (Section 3.6.1) had been previously observed (Figure 15)

Since wild-type BNIP3-induced chromatin condensation and DNA fragmentation were not completely blocked by treatment with Ac-zVAD-fmk, we hypothesized that AIF may also mediate BNIP3-induced DNA damage. AIF is a mitochondrial flavoprotein which, in response to an apoptotic stimulus, translocates to the nucleus to induce chromatin condensation and high molecular weight DNA fragmentation (Susin *et al.* 1999). Immunofluorescence analysis (Section 3.6.1) of BNIP3-transfected 293T cells at 18, 24, and 36 hours post-transfection found no AIF nuclear translocation, despite increases in the proportion of apoptotic cells observed by Hoechst dye staining (Figure 22a). Cells treated with staurosporine served as a positive control for AIF nuclear translocation (as verified by Dr. E. Daugas and Dr. G. Kroemer, INSERM, France). The data were confirmed in parallel samples where HM fractions were immunoblotted for AIF (Section 3.6.2). No difference in the level of mitochondrially-localized AIF protein was observed between BNIP3-transfectants and control untransfected or BNIP3ΔTM transfected cells (Figure 22b).

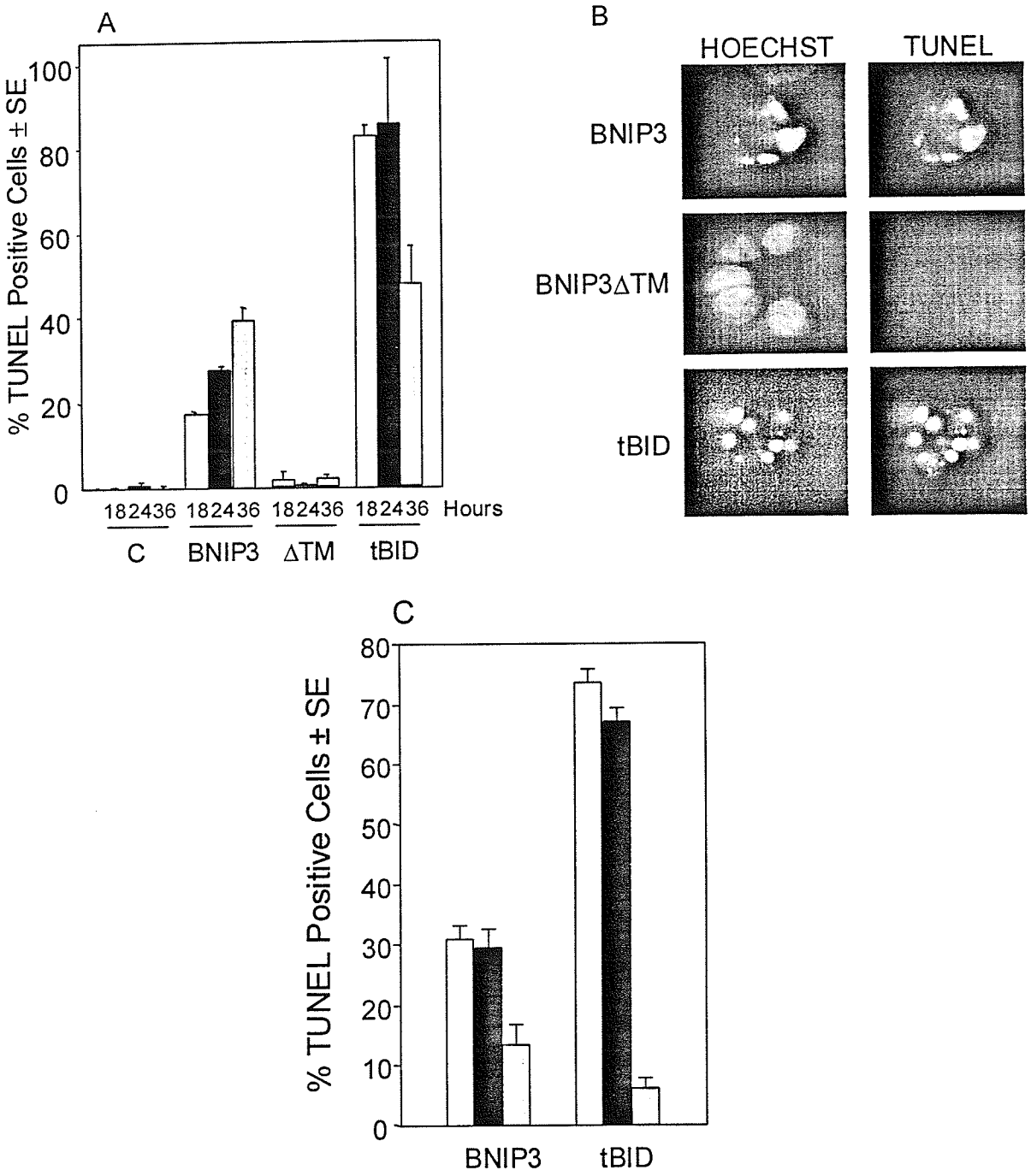

Figure 20: BNIP3-induced cell death is characterized by late DNA fragmentation. (A) Quantification of TUNEL-positive 293T cells transiently transfected with BNIP3-T7, BNIP3ΔTM-T7 (ΔTM), or tBID-FLAG and stained at 18, 24, and 36 hours. Values for BNIP3- and tBID-transfected cells were significantly higher than those observed for controls (C) at all time points ($P<0.01$). (B) Illustration of transfected cells as in panel A harvested 24 hours post-transfection and stained with the TUNEL reagent (right) or Hoechst dye (left). (C) Cells were transfected as in panel A in the absence (solid bars) or presence of 50 μM Ac-zVAD-fmk (grey bars) or 50 μM Ac-FA-fmk (white bars). Cells were TUNEL stained 24 hours post-transfection, and the percent positive was scored by fluorescent microscopy. Results are expressed as the mean ± SE from at least three independent experiments.

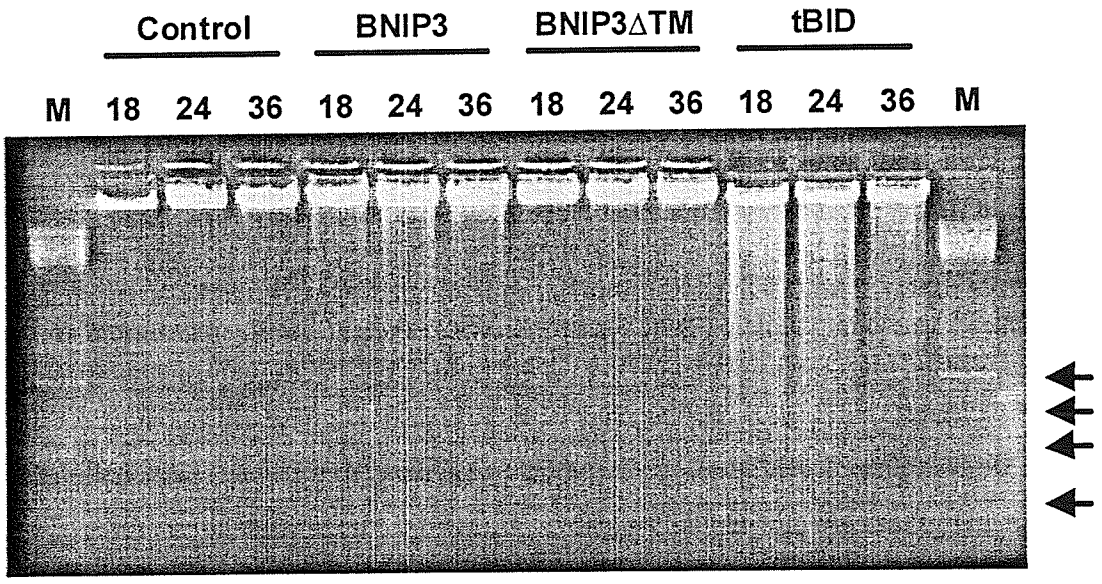

Figure 21: Overexpression of BNIP3 does not induce significant oligonucleosoma DNA laddering. Genomic DNA was extracted from 293T cells transientl transfected with BNIP3-T7, BNIP3ΔTM-T7, or tBID-FLAG at 18, 24, and 36 hour post-transfection. An aliquot of 10 μg DNA was electrophoresed on a 1.5% w/ agarose gel containing 1 μg ethidium bromide per ml. Result shown is representativ of three independent experiments. Arrows indicate oligonucleosomal fragments. M marker.

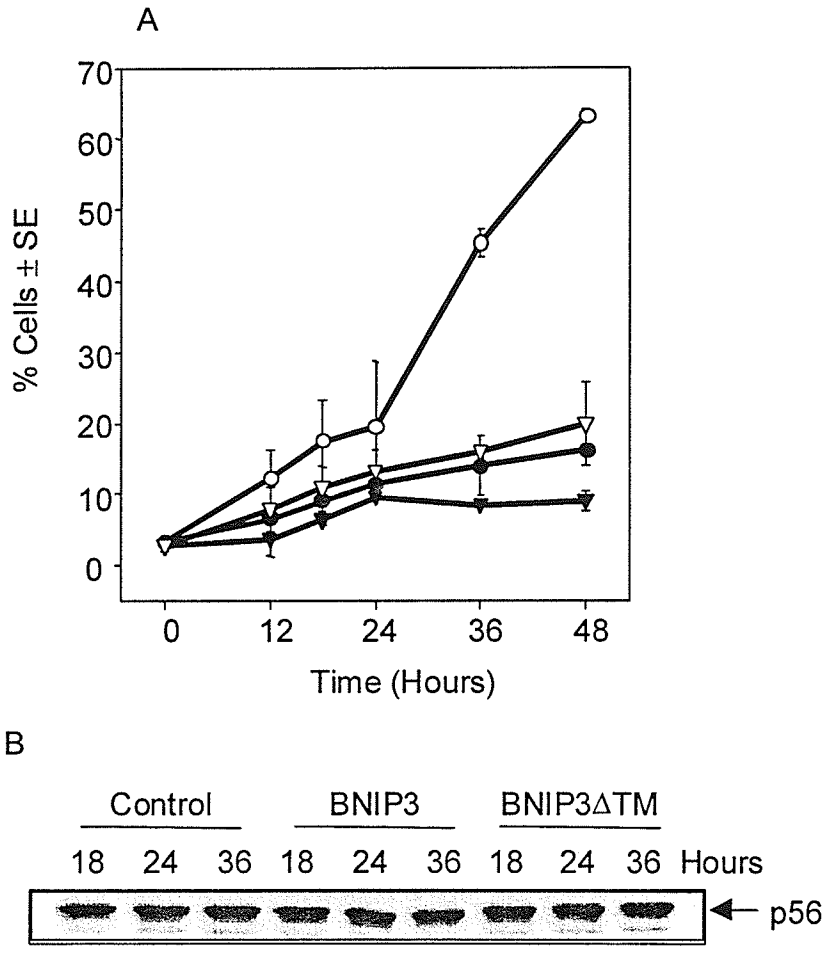

Figure 22: Overexpression of BNIP3 does not induce translocation of AIF. (A) Quantification of AIF nuclear translocation (closed symbols) and chromatin condensation (open symbols) in 293T cells transiently transfected with BNIP3-T7 (circles) or BNIP3ΔTM-T7 (triangles) and stained with Cy3-conjugated mouse anti-AIF antibody and Hoechst dye at 12, 18, 24, 36 and 48 hours post-transfection. Results are expressed as the mean ± SE from at least three independent experiments. (B) Heavy membrane fractions isolated from untransfected 293T cells (Control) and cells transiently transfected with BNIP3-T7 (BNIP3) or BNIP3ΔTM-T7 (BNIP3ΔTM) were harvested 18, 24, and 36 hours post-transfection and immunoblotted with mouse monoclonal anti-AIF antibody. The arrow indicates the p56 band of AIF.

4.8 BNIP3-expressing cells have ultrastructural features of necrosis

To determine the fine ultrastructural features of cells following BNIP3 expression, we performed transmission electron microscopy of 293T cells 24 hours post-transfection as described (Section 3.12; Performed by Ms. Eileen MacMillan-Ward, Manitoba Institute of Cell Biology). These experiments revealed a nuclear phenotype of lightly dispersed foci of chromatin condensation and heterochromatin (Figure 23b) rather than the globular condensation typical of apoptosis (Wyllie *et al.*, 1980). During a detailed examination of cellular organelles, we detected many rounded mitochondria in which the internal cisternae had been destroyed, while the inner and outer membranes of the mitochondria appeared to be intact in most cells (Figure 23c). The mitochondria did not appear to be undergoing gross swelling. Surprisingly, BNIP3-transfectants were characterized by extensive cytoplasmic vacuolation and dense bodies. High power examination of these structures revealed a heterogeneous mixture of electron-lucent and electron-dense regions, many of which appear to be vacuoles and autophagosomes (Figure 23 d and e) and some of the autophagic vacuoles contained whorls of membranous material (Figure 23f) that have been observed during autophagic cell death (Xue *et al.*, 1999).

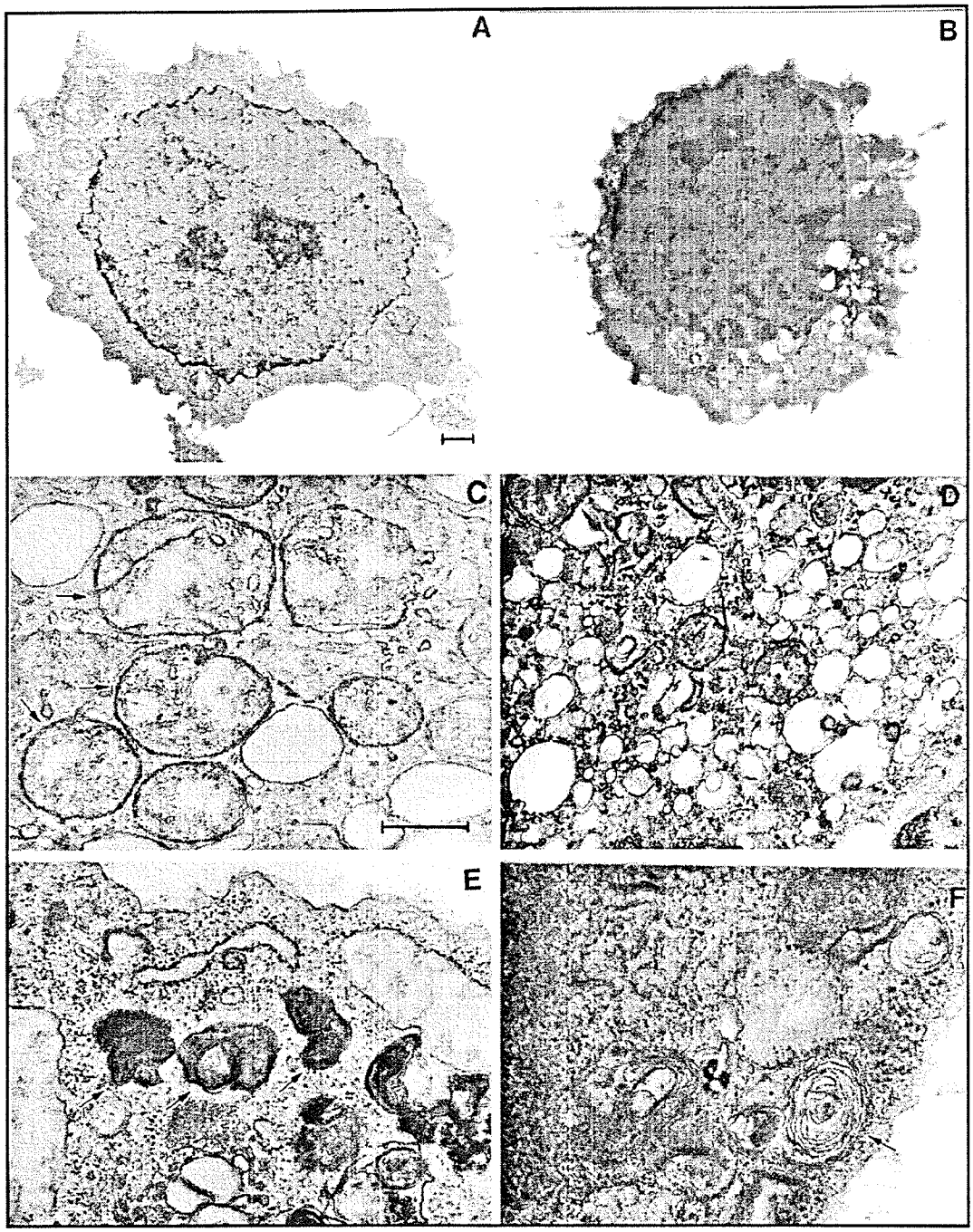

Figure 23: BNIP3 induces ultrastructural changes of necrosis. Normal 293T cells (A) and BNIP3-expressing 293T cells (B to F) were examined 24 hours post-transfection by transmission electron microscopy. Nuclei of BNIP3-expressing cells exhibited dispersed foci of chromatin condensation and heterochromatin (B) compared to control cells (A). High power magnifications of BNIP3 transfectants showed rounded mitochondria with disrupted internal structures (arrows) (C), extensive cytoplasmic vacuolation (D), autophagosomes (arrows) (E), and autophagic vacuoles containing membranous whorls (F). (A and B), bar = 1 μm; (C to F), bar = 0.5 μm. (Performed by Ms. Eileen MacMillan-Ward, Manitoba Institute of Cell Biology.)

4.9 BNIP3-induces mitochondrial PT pore opening, loss of $\Delta\Psi m$, and increased ROS production

BNIP3 is a mitochondrial outer membrane protein and electron micrographs of BNIP3-transfected cells featured disturbances in mitochondrial structure. Therefore, we hypothesized that BNIP3 may directly induce mitochondrial dysfunction. Opening of the mitochondrial PT pore often accompanies both apoptotic and necrotic cell death with the consequent loss of transmembrane potential ($\Delta\psi m$) and respiratory inhibition with ROS production (reviewed in Kroemer *et al.*, 1998). The status of the PT pore can be determined with the membrane-permeating fluorescent probe calcein-AM, which freely enters mitochondria but cannot exit except through an open PT pore following processing by cellular esterases. Using $CoCl_2$ quenching of cytosolic fluorescence as described by Bernardi *et al.* (1999), the release of calcein from mitochondria was analyzed by confocal laser microscopy as described (Section 3.13). Following BNIP3 transfection, 293T cells lose mitochondrial calcein staining as early as 8 hours post-transfection (Figure 24a), indicating opening of the PT pore. Quantitative image analysis was used to determine the relative fluorescence units (RFU) per cell, as outlined with Nomarski optics. Cells were arbitrarily classified into three levels of calcein staining, low (0 – 40 000 RFU), intermediate (40 000 – 60 000 RFU), and high (> 60 000 RFU). It was observed that BNIP3-transfectants could be primarily classified as calcein-low (Figure 24b), as illustrated in representative micrographs (Figure 24a). In contrast, BNIP3ΔTM-transfected and untransfected cells did not show any significant preferences for calcein staining state.

To determine if BNIP3-expressing cells also decrease their transmembrane potential, we used the cell-permeable lipophilic dye JC-1. Increased ROS production was assessed using dihydroethidium (HE), which is oxidized to ethidium in the presence of ROS. Cells were stained and analyzed 24 hours post-transfection by flow cytometry using gates established from untransfected 293T cells (Figure 25a). ClCCP (50 μM), an uncoupler of the mitochondrial electron transport chain and thus collapses the transmembrane potential across the inner mitochondrial membrane, was used to determine maximal $\Delta\psi m$ loss (Figure 25b). Cells that shifted down below a threshold established from untreated cells were scored as JC-1^{LO}. Likewise, hydrogen peroxide (30% v/v H_2O_2) was used to establish maximum production of ROS and HE^{HI} cells were defined as those which shifted analogously to H_2O_2 treatment (Figure 25c). Dead cells were identified by uptake of propidium iodide (PI). BNIP3 was almost as efficient as tBID at suppressing $\Delta\psi m$, increasing ROS generation, and inducing cell death (Figure 26 a to c). In contrast, there were no significant differences between untransfected cells and cells expressing the inactive mutant BNIP3ΔTM. BNIP3-induced $\Delta\psi m$ loss and ROS production were identified as early as 2 hours post transfection and did not increase further during 12 hours of analysis (Figure 27), indicating that the mitochondrial dysfunction was maximal and occurred as early as plasma membrane permeability and cell death as illustrated in Figure 19a.

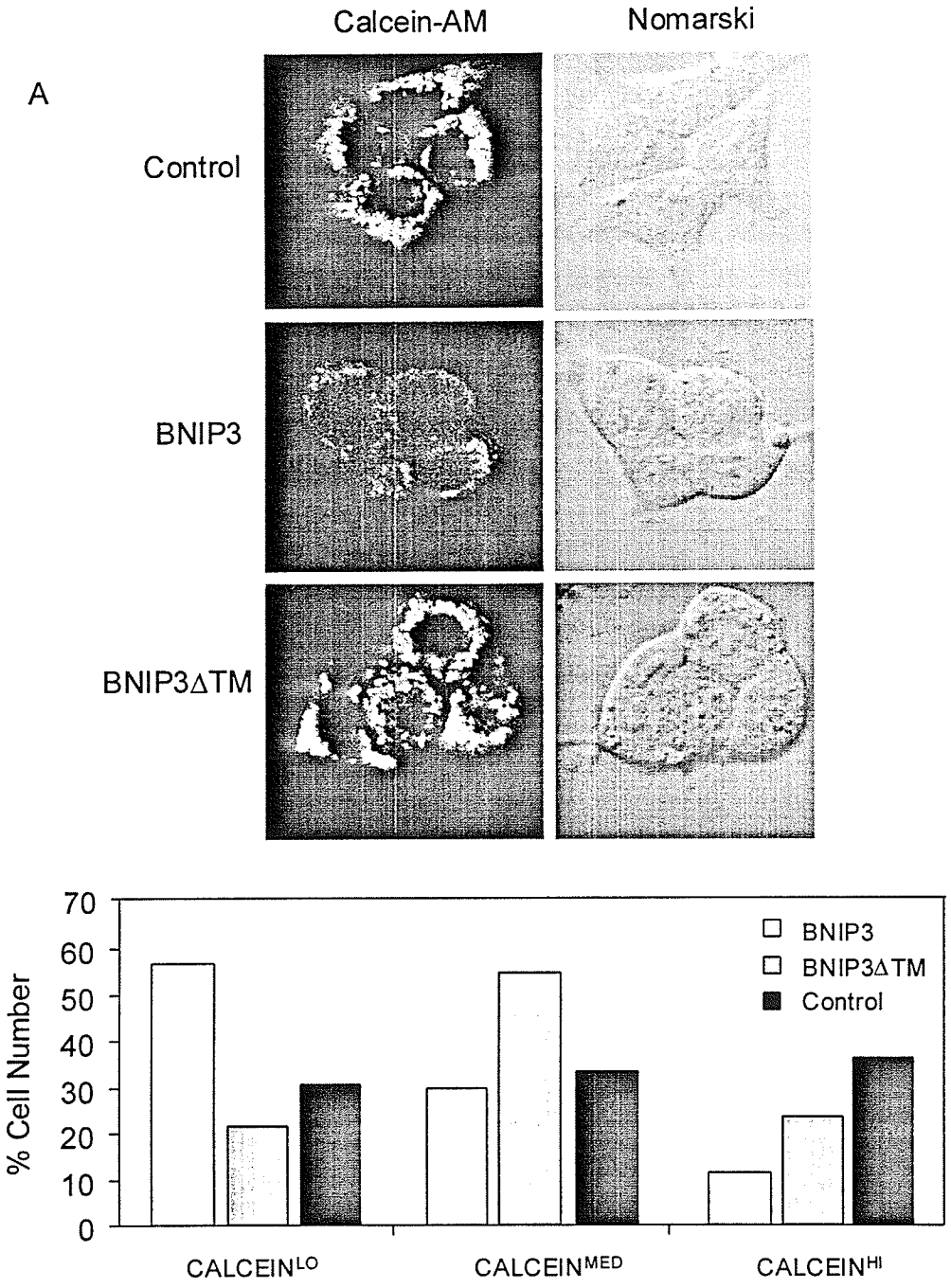

Figure 24: BNIP3-induced cell death is characterized by opening of the PT pore. (A) Untransfected (Control), BNIP3-T7 (BNIP3)- and BNIP3ΔTM-T7 (BNIP3ΔTM)-transfected 293T cells were harvested 24 hours after transfection and incubated with calcein-AM in the presence of $CoCl_2$ to quench cytoplasmic fluorescence. Cells were visualized by confocal laser microscopy (left) and Nomarski optics (right). (B) Quantitation of calcein fluorescence of cells transfected as described in panel A. The percentages of cells measured as low ($CALCEIN^{LO}$; 0 – 40 000 RFU), intermediate ($CALCEIN^{MED}$; 40 000 – 60 000 RFU) or high ($CALCEIN^{HI}$; > 60 000 RFU) total fluorescence units per cell are shown. The experiment was repeated with similar results. By chi analysis, $P<0.001$ for the comparison of control versus BNIP3, and BNIP3 ΔTM versus BNIP3.

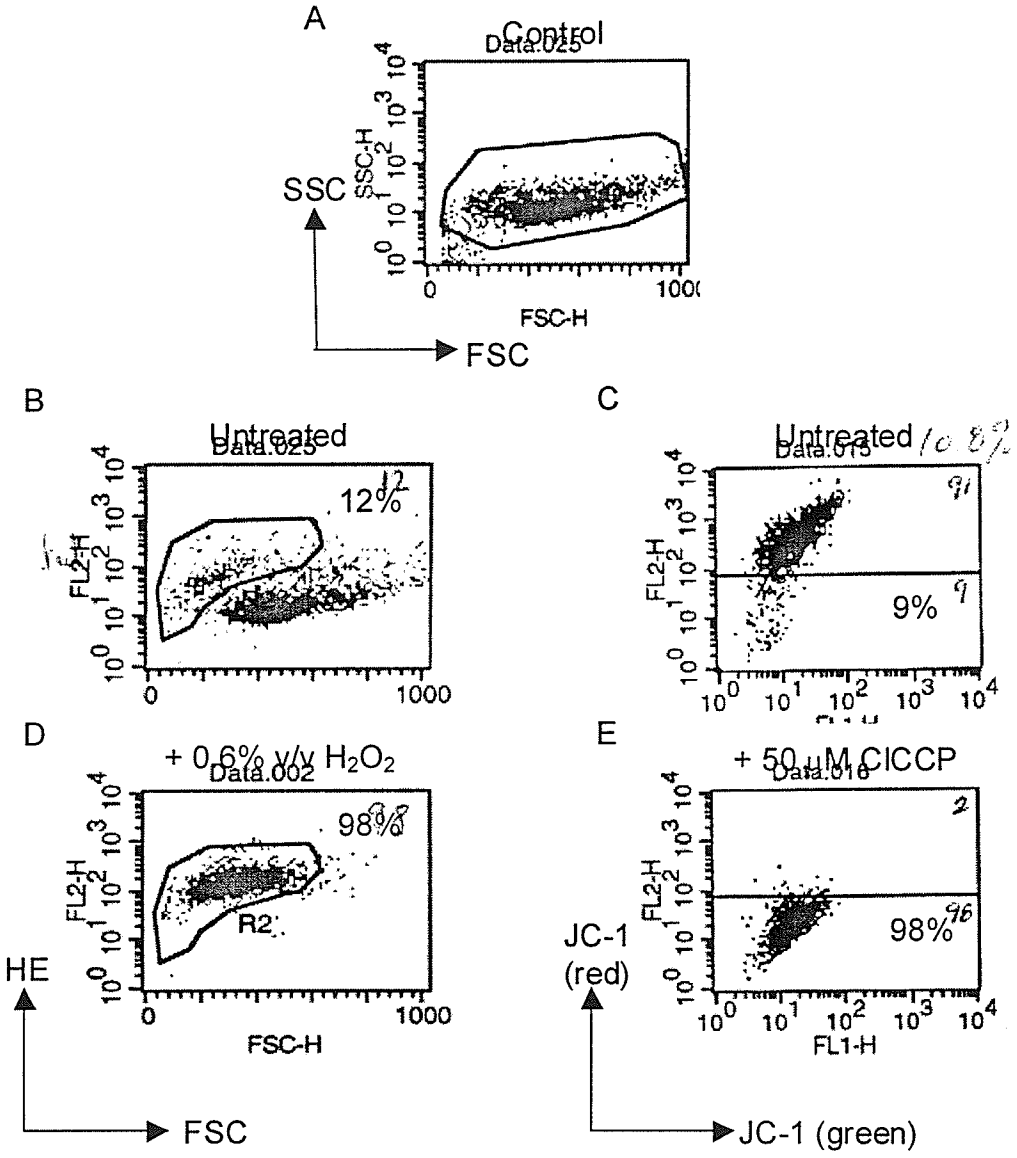

Figure 25: Establishment of flow cytometry parameters. (A) Representative flow cyometry histogram of untransfected (control) cells gated to exclude cellular debris using forward angle (FSC) and side angle (SSC) scatter. To establish a positive control for enhanced ROS production, gated populations of untransfected cells were stained with dihydroethidium (HE) in the absence (B) or presence (D) of 0.6% v/v H_2O_2. Migration into the region defined as R2 is indicative of increased ROS production. Similarly, to establish a positive control for suppression of mitochondrial transmembrane potential ($\Delta\psi m$), cells were stained with JC-1 in the absence (C) or presence (E) of 50 µM ClCCP. A loss of red JC-1 fluorescence is indicative of $\Delta\psi m$ loss.

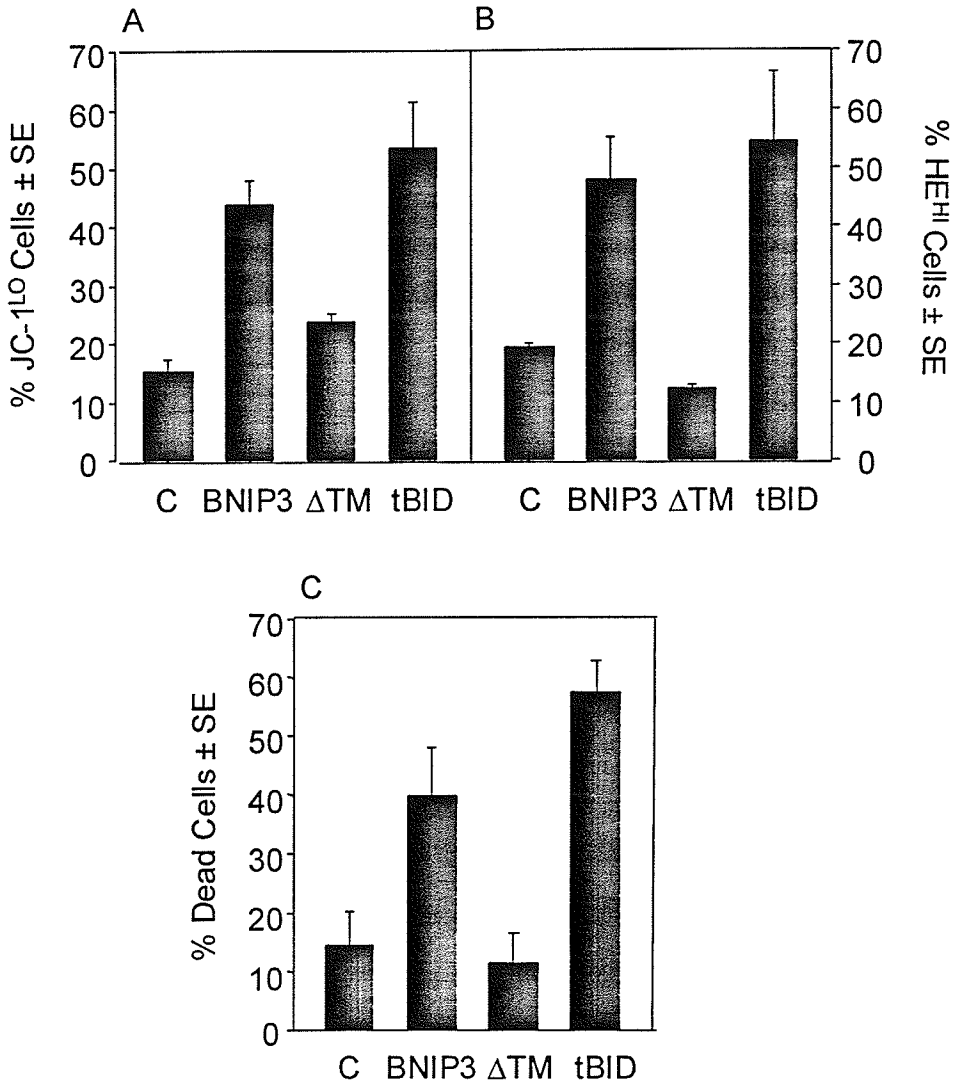

Figure 26: BNIP3-induced cell death is characterized by suppression of $\Delta\psi m$ and increased ROS production. (A) Untransfected (C) and BNIP3-T7 (BNIP3)-, BNIP3ΔTM-T7 (ΔTM)-, or tBID-FLAG (tBID)-transfected 293T cells were harvested at 24 hours, stained with JC-1, and analyzed by flow cytometry as a measure of $\Delta\psi m$. JC-1^{LO} cells were defined as cells that were gated within the same range as those treated with 50 μM ClCCP (~98%) as shown in Figure 25e. BNIP3- and tBID- but not BNIP3ΔTM-transfected cells were significantly suppressed compared to controls ($P<0.01$). (B) Cells treated as in panel A were stained with dihydroethidium (HE) to measure ROS production. HE ^{HI} cells were defined as cells that were gated within the same range as those treated with 30% v/v H_2O_2 for 15 minutes (~98%) as shown in Figure 25d. Levels in BNIP3- and tBID-expressing cells were significantly increased compared to untreated controls or BNIP3ΔTM transfectants ($P<0.03$). (C) Samples from the control and each of the transfections described in panel A were stained with trypan blue to determine cell death. BNIP3-and tBID-transfected cells were significantly increased compared to untreated controls or BNIP3ΔTM transfectants ($P<0.01$). Results are expressed as the mean ± SE from at least three independent experiments.

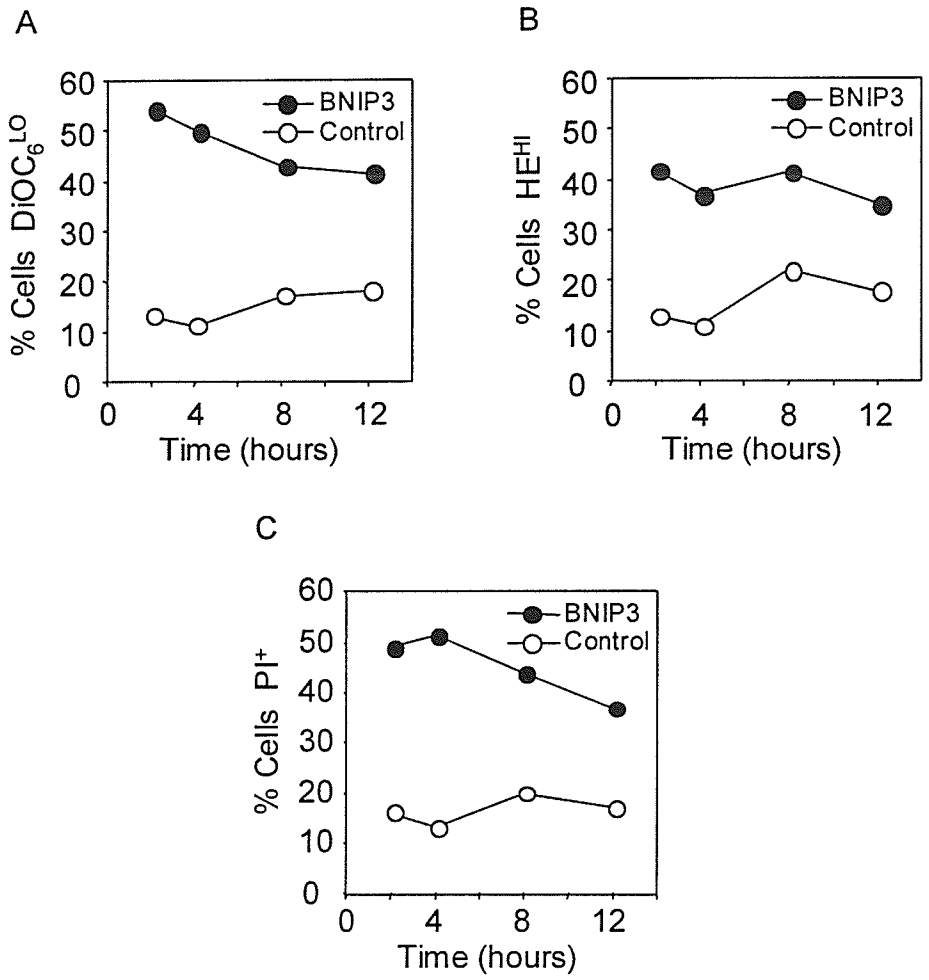

Figure 27: BNIP3-induced Δψm suppression, ROS production, and cell death occurs as early as two hours. (A) Untransfected (Control) and BNIP3-T7 (BNIP3)-transfected 293T cells were harvested at 2, 4, 6, and 8 hours post-transfection, stained with $DiOC_6$, and analyzed by flow cytometry as a measure of Δψm. $DiOC_6^{LO}$ cells were defined as cells that were gated within the same range as those treated with 50 μM ClCCP (~98%) as shown in Figure 25e. BNIP3-transfected cells showed a loss of Δψm as early as 2 hours post-transfection compared to controls. (B) Cells treated as in panel A were stained with dihydroethidium (HE) to measure ROS production. HE^{HI} cells were defined as cells that were gated within the same range as those treated with 30% v/v H_2O_2 for 15 minutes (~98%) as shown in Figure 25d. Levels in BNIP3-expressing cells were increased compared to untransfected cells (Control). (C) Samples from untransfected (Control) and BNIP3-transfected cells described in panel A were stained with propidium iodide (PI) to evaluate cell death. Data are representative of three independent experiments.

4.10 Inhibition of PT pore opening prevents mitochondrial dysfunction and cell death

To confirm that the loss of $\Delta\psi m$, increase in ROS production and ensuing cell death were the result of opening of the PT pore, we next examined the effect of PT pore inhibitors on BNIP3-induced cell death and mitochondrial deregulation using the potentiometric fluorescent probe, $DiOC_6$ in combination with HE (Section 3.14). ClCCP and H_2O_2 served as positive controls as described in Section 4.9. As noted earlier, the PT pore is a multi-protein complex located at the contact sites of the inner and outer mitochondrial membranes. Opening of the PT pore can be inhibited by cyclosporin A, which interacts with cyclophilin D, or bongkrekic acid, which binds to the ANT. Both cyclophilin D and ANT have been demonstrated to be components of the PT pore (Kroemer *et al.*, 1998). Cyclosporin A has some activity against calcineurin (Bernadi *et al.*, 1999), therefore we also employed a more specific inhibitor, bongkrekic acid. Previous studies have shown that 50 μM cyclosporin A or 100 μM bongkrekic acid is sufficient to inhibit $\Delta\psi m$ suppression (Bernardi *et al.*, 1999). Flow cytometry parameters were established by treatment of untransfected cells with 50 μM ClCCP and 30% v/v H_2O_2 as described for Figure 25. BNIP3-expressing cells showed ~50% $DiOC_6^{LO}$ and HE^{HI} cells as detected in the upper left quadrant of Figure 28a compared to untreated and untransfected controls, consistent with previous experiments with JC-1 (Figure 26). Cells were treated with cyclosporin A or bongkrekic acid for two hours and washed prior to transfection, a procedure that did not affect BNIP3 expression in the 293T cells (Figure 28b). Treatment of BNIP3-transfectants with either cyclosporin A or bongkrekic acid revealed a dose-dependent partial inhibition of $\Delta\psi m$ suppression and ROS generation

(Figure 29a and b). Cell death, as measured by uptake of PI, was similarly inhibited (Figure 29c). Maximum suppression was about 50% of untreated BNIP3-transfected cells.

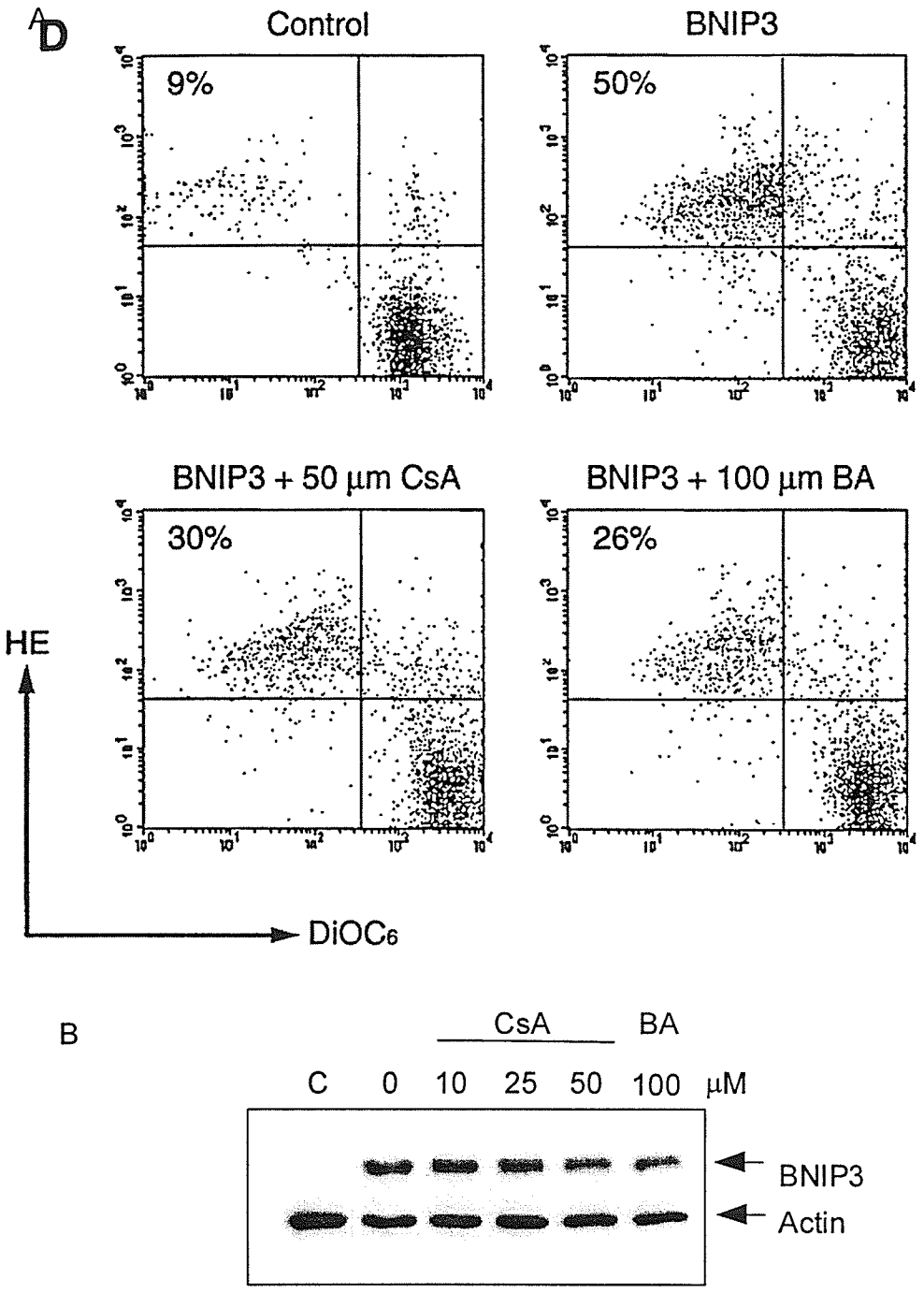

Figure 28: Inhibition of BNIP3-induced mitochondrial dysfunction and cell death by PT pore inhibitors. (A) Flow cyometric histograms of HE and $DiOC_6$ staining of BNIP3-T7-transfected cells treated with 50 μM cyclosporin A (CsA) or 100 μM bongkrekic acid (BA). Values indicate percentage of cells that are $DiOC_6^{LO}$ and HE^{HI}. (B) Western blot of BNIP3-transfected cells treated with 10, 25, and 50 μM CsA and 100 μM BA using anti-T7 epitope antibody. Anti-actin antibody was used as a loading control. Lane C, untransfected cells.

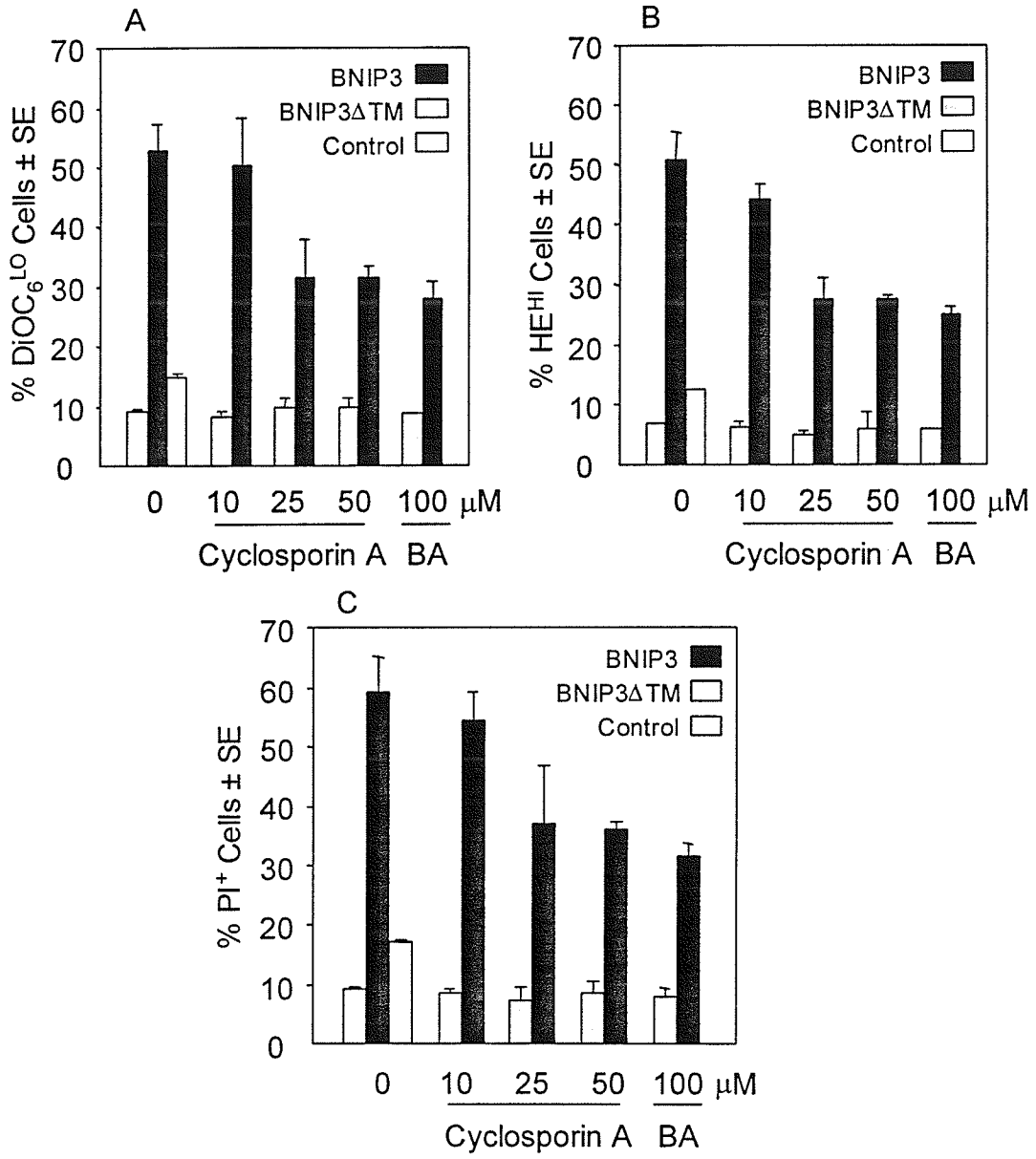

Figure 29: Inhibition of BNIP3-induced mitochondrial dysfunction and cell death by PT pore inhibitors. Untransfected (control) and BNIP3-T7 (BNIP3)-transfected 293T cells harvested 8 hours post-transfection were treated with increasing doses of cyclosporin A or 100 μM bongkrekic acid (BA), and stained with $DiOC_6$ (A), HE (B), or PI (C) and analyzed as described in Figure 26. BNIP3ΔTM-T7-transfected 293T cells were used as a negative transfection control. Results are expressed as the mean ± SE of at least three independent experiments. Low $DiOC_6$ levels in BNIP3-expressing cells was significantly inhibited when treated with 25 μM ($P<0.05$) and 50 μM ($P<0.02$) cyclosporin A and 100 μM bongkrekic acid ($P<0.02$) compared to untreated BNIP3 cells. Increase in HE fluorescence was inhibited at 25 μM ($P<0.03$) and 50 μM ($P<0.02$) cyclosporin A, and 100 μM bongkrekic acid ($P<0.02$). Cell death was significantly suppressed at 50 μM cyclosporin A ($P<0.02$) and 100 μM bongkrekic acid ($P<0.02$).

4.11 Overexpression of BCL-2 prevents BNIP3-induced cell death

Multiple reports have demonstrated that BCL-2 can inhibit PT pore opening, $\Delta\psi_{m}$ suppression, and ROS production (reviewed in Vander Heiden and Thompson, 1999; Harris and Thompson, 2000). Furthermore, overexpression of BCL-2 can also inhibit caspase-independent cell death (Okuno *et al.*, 1998). BNIP3 physically interacts with BCL-2 and BCL-X_L (Boyd *et al.*, 1994; Chen *et al.*, 1997; Ray *et al.*, 2000). Furthermore, overexpression of BCL-2 and BCL-X_L can partly suppress BNIP3-induced cell death, although this is overcome at high BNIP3 expression levels (Chen *et al.*, 1997; Chen *et al.*, 1999). We next examined the effect of BCL-2 on BNIP3-induced cell death in cells stably transfected with BCL-2 using PI staining as described (Section 3.14). In BNIP3-transfectants, plasma membrane damage, and thus cell death, was reduced to that of inactive BNIP3ΔTM in BCL-2-expressing cells (Figure 30a). Transfection efficiencies in both cell lines were relatively equivalent (Figure 30b).

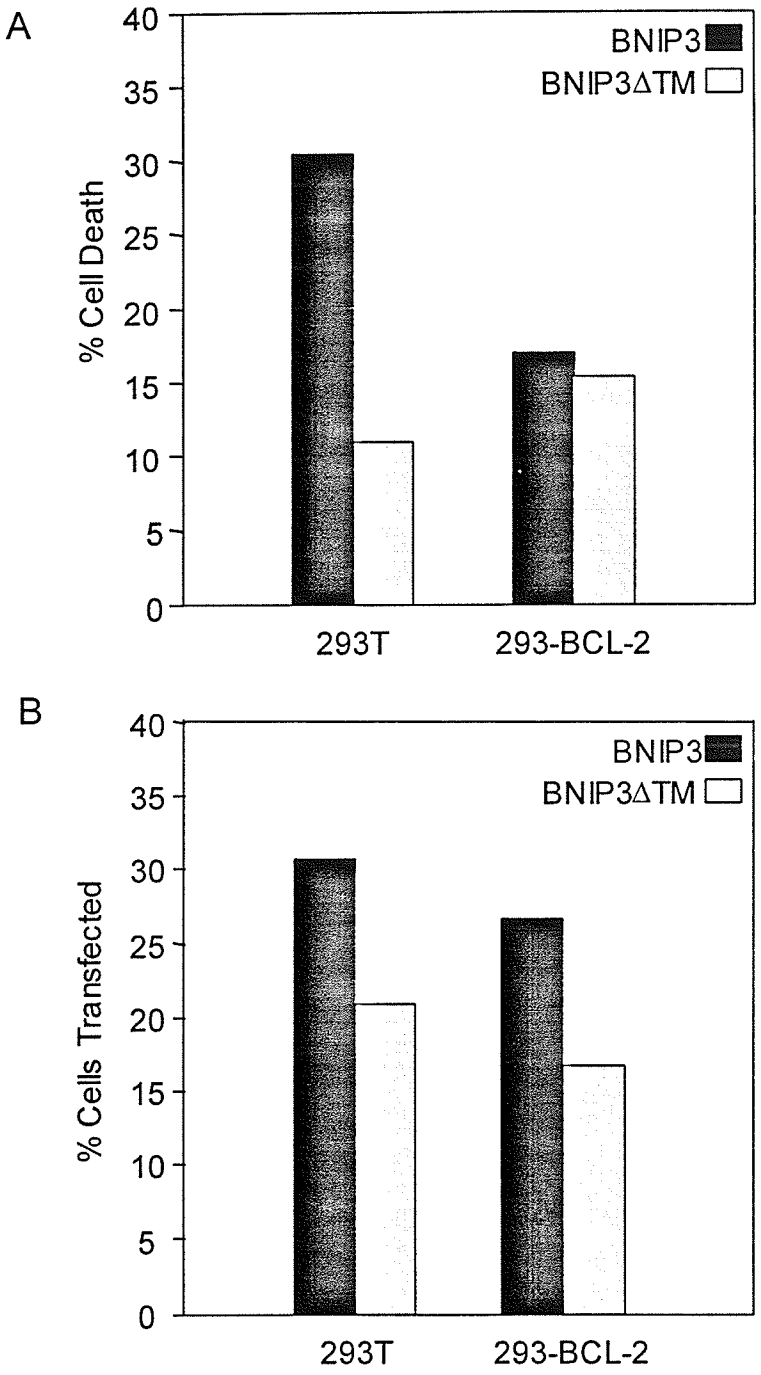

Figure 30: Inhibition of BNIP3-induced cell death by BCL-2 overexpression. (A) BNIP3-induced cell death (solid bars) in 293T cells and 293 cells overexpressing BCL-2 (293-BCL-2) compared to the inactive BNIP3ΔTM mutant (open bars). Eight hours following BNIP3 transfection, cells were stained with PI and evaluated by flow cytometry. The percent dead cells were calculated as the proportion of cells that were PI positive. (B) Equivalent transfection efficiency was obtained in both cell lines, as detected by immunostaining with mouse monoclonal anti-T7 antibody. Results are representative of two independent experiments.

5.0 Summary

In summary, the work described in this thesis identifies the mechanism of BNIP3-induced cell death. Overexpression of BNIP3 induces early and significant suppression of mitochondrial transmembrane potential and enhanced production of reactive oxygen species. These events are likely due to the opening of the permeability transition pore as a result of BNIP3 integration into the outer mitochondrial membrane (Vande Velde *et al.*, 2000). Furthermore, biochemical analysis revealed that there is no significant activation of primary apoptotic effectors, specifically caspases 3, 7, and 9. In addition, BNIP3-induced cell death occurred independent of cytochrome *c* and Apaf-1, both of which are critical components of caspase-mediated apoptosis. The early mitochondrial dysfunction observed in BNIP3-transfectants results in morphological features uncharacteristic of apoptosis. Furthermore, ultrastructural analysis of these cells reveal there is limited evidence of apoptotic cell death. Rather, BNIP3-expressing cells feature extensive cytoplasmic vacuolation, early loss of plasma membrane integrity, and destruction of mitochondrial cristae. Interestingly, failure to localize to the mitochondria, as in the case of the BNIP3ΔTM mutant, does not induce any significant mitochondrial dysfunction or cell death compared to control untransfected cells. However, targeting of BNIP3 to mitochondrial and non-mitochondrial sites, as in the case of the BNIP3-BclTM and BNIP3-Cb5TM mutants, respectively, was sufficient to induce cell death. This data suggests that the anchoring of the cytosolic portion of BNIP3 to intracellular membranes is sufficient to activate the mechanism of BNIP3-induced cell death, which manifests as necrotic-like cell death.

6.0 Discussion

6.1 BNIP3 requires anchoring to an intracellular membrane to induce cell death

Endogenous BNIP3 protein is abundant in viable murine and human skeletal muscle as a loosely associated protein that is not integrated into the mitochondrial membrane (Vande Velde *et al.*, 2000). However, when overexpressed, BNIP3 integrates into mitochondrial membrane through the carboxyl-terminal transmembrane domain (amino acids 164-184) with the protein oriented with its amino-terminus in the cytosol and is cytotoxic (Vande Velde *et al.*, 2000). Protein integration of BAX into the outer mitochondrial membrane has also been observed in FL5.12 cells in response to growth factor withdrawal and is regulated by its amino-terminus (Goping *et al.*, 1998). The regulatory mechanism that maintains endogenous BNIP3 in an inactive, non-integrated state, and the activating event which induces BNIP3 protein integration and cell death are unknown. At least two non-mutually exclusive mechanisms are possible: (i) endogenous BNIP3 assumes a conformation that prevents integration of the TM domain until it is altered by some post translational modification, or (ii) endogenous BNIP3 interacts with a regulatory protein that maintains it in an unintegrated form at the surface of the mitochondria until it dissociates. Since overexpression induces cell death, BNIP3 is able to overcome this inhibition in high concentrations, suggesting that the regulatory mechanism is saturable. Translocation from the cytoplasm to the mitochondria during induction of apoptosis has been reported for several members of the BCL-2 pro-apoptotic family including BID (Li *et al.*, 1998; Luo *et al.*, 1998), BAX (Goping *et al.*, 1998), BAK (Griffiths *et al.*, 1999), BAD (Zha *et al.*, 1996; Datta *et al.*, 1997), and BIM (Puthalakath *et al.*, 1999). These molecules can be regulated by phosphorylation, oligomerization, or

proteolytic cleavage (Gross *et al.*, 1999). In the absence of an apoptotic stimulus, BAD is phosphorylated by Akt (Zha *et al.*, 1996) and by mitochondrion-anchored protein kinase A (Harada *et al.*, 1999) and sequestered in the cytoplasm by 14-3-3 protein (Zha *et al.*, 1996). BAX, BAK, and BIM are held inactive in the cytoplasm and are translocated to the mitochondria after a cell death signal. Further regulation is suspected for BAX, as both unknown regulatory sequences in the amino-terminus and its TM domain have been implicated in regulating protein integration into the mitochondrial membrane following a death stimulus (Goping *et al.*, 1998; Suzuki *et al.*, 2000). Similarly, BID is cleaved by caspase 8 following Fas ligation, resulting in mitochondrial translocation (Li *et al.*, 1998; Luo *et al.*, 1998). Whether endogenous BNIP3 integration into the mitochondrial membrane is regulated by a post-translational mechanism similar to these proteins remains to be determined.

The carboxyl-terminal TM domain is essential for proper subcellular localization, membrane association, and function of several BCL-2 family members. For example, BCL-2 lacking its TM domain is no longer able to inhibit apoptosis and does not localize to its normal subcellular locations, including the mitochondria, ER, and nucleus (Minn *et al.*, 1998). Similarly, the TM domain of BAX mediates its localization and integration into the outer mitochondrial membrane in response to an apoptotic stimulus (Goping *et al.*, 1998). BNIP3 and its homologues also contain a carboxyl-terminal TM domain that is required for localization to the mitochondria and its death-promoting activity (Chen *et al.*, 1997; Chen *et al.*, 1999). Removal of the TM domain sequence produces a cytosolic and non-toxic protein (Chen *et al.*, 1997; Chen *et al.*, 1999; Imazu *et al.*, 1999; Ohi *et al.*, 1999; Cizeau *et al.*, 2000) that serves as a valuable negative control for cell death induced

by BNIP3 overexpression. However, the substitution of heterologous TM domain sequences restored its death-promoting activity (Ray *et al.*, 2000). Specifically, BNIP3 targeted to the mitochondria via the TM domain of BCL-2 induced cell death as efficiently as wild type BNIP3. As well, BNIP3 directed to a non-mitochondrial site via the TM domain of cytochrome b_5 was slightly less efficient, but still able to induce cell death. Therefore, the cytosolic portion of BNIP3 may contain all the necessary elements required to induce cell death and must be localized to an intracellular membrane to exert its function. This conclusion is dependent on an essential experimental control that is lacking in this thesis. Specifically, it is possible that simply overexpressing a mitochondria-targeted protein causes enough membrane instability to induce cell death. Therefore, in order to be sure that the observed cytotoxicity is specific to BNIP3 overexpression, it is necessary to repeat these experiments and verify that overexpression of an unrelated protein fused to a mitochondrial TM domain sequence does not induce cell death.

There has been substantially less work done on the involvement of the ER in cell death compared to the mitochondria. However, the ER stores intracellular calcium and its specific release can trigger apoptosis (Shibasaki and McKeon, 1995). Furthermore, there appears to be an intricate relationship between the anti-apoptotic protein BCL-2 and Ca^{++}. Specifically, BCL-2 can decrease the amount of Ca^{++} available for release from the ER, as well as accelerate the uptake of Ca^{++} into the ER (Kuo *et al.*, 1998; Foyouzi-Youssefi *et al.*, 2000). Although the ER is the major cellular store of calcium, mitochondria also contribute to maintenance of calcium homeostasis by absorbing cellular calcium (Ichas and Mazat, 1998). Intriguingly, mitochondrial response to

intracellular calcium levels is a contributing factor to the decision between apoptosis and necrosis and is mediated by the PT pore (Ichas and Mazat, 1998; Kruman and Mattson, 1999). In addition, mitochondrial calcium homeostasis can be regulated by BCL-2 (Zhu *et al.*, 1999). The pathway(s) governing mitochondrial and ER communication regarding intracellular calcium is unknown. It is possible that cytochrome b_5-directed BNIP3 induces cell death by deregulating calcium homeostasis, which in turn impacts mitochondrial calcium homeostasis and the PT pore. However, the possibility remains that mitochondrial-targeted BNIP3 directly disrupts mitochondrial calcium levels and induces cell death. It remains to be determined if expression of the BNIP3 mutants containing heterologous TM domain sequences inflict mitochondrial dysfunction similar to wild type BNIP3.

6.2 BNIP3 induces cell death independently of cytochrome *c* release

The mitochondrial membrane integration of many pro-apoptotic BCL-2 family members induces mitochondrial dysfunction, which plays an important role in the cell death pathway. One of the key events in apoptosis is the release of cytochrome *c*, which functions with dATP as a co-factor for Apaf-1 activation of the caspase cascade (Green and Reed, 1998). There are currently three proposed models to explain the mechanism of cytochrome *c* release: (i) PT pore-induced mitochondrial swelling and subsequent outer membrane rupture (Vander Heiden *et al.*, 1997); (ii) cytochrome *c* exit from the mitochondria through the PT pore (Shimizu *et al.*, 1999); and (iii) an undefined cytochrome *c*-specific channel in the mitochondrial outer membrane (Kluck *et al.*, 1999). In one model, the PT pore is hypothesized to serve as a conduit for cytochrome *c* release

into the cytoplasm. This is supported by experiments that show a direct interaction between BAX and components of the PT pore, including ANT (Marzo *et al.*, 1998) and VDAC (Narita *et al.*, 1998; Shimizu *et al.*, 2000b), and evidence that BAX may open the pore sufficiently to allow cytochrome *c* release (Shimizu *et al.*, 1999). In contrast to BAX, BNIP3 does not induce cytochrome *c* release despite evidence of early PT pore opening. Therefore, a model in which opening of the PT pore is sufficient to release cytochrome *c* is not supported by our data. BAX must have other effects on mitochondrial membrane proteins to account for the difference with BNIP3. Specifically, BAX oligomerizes in the outer mitochondrial membrane of apoptotic cells (Antonsson *et al.*, 2001). While BNIP3 is known to exist as a dimer, no higher order oligomers have been identified for BNIP3. In addition, BAX can directly interact with VDAC (Narita *et al.*, 1998; Shimizu *et al.*, 2000b). BAX-VDAC complexes exhibit a higher conductance than pores formed by either protein alone (Shimizu *et al.*, 2000b). It is unknown if BNIP3 interacts with mitochondrial pore proteins such as ANT and VDAC or whether it is capable of forming a pore itself. Furthermore, it remains to be determined if BNIP3 can form higher order structures analogous to BAX (Antonsson *et al.*, 2000). As well, BAX is able to form ion-specific channels via its α5/α6 region (Schlesinger *et al.*, 1997; Schendel *et al.*, 1998). It is unknown if BNIP3 has a similar pore-forming ability.

Although BNIP3 kills without cytochrome *c* release, it has been observed that the BNIP3 homologue, NIX/BNIP3L/BNIP3α/B5 recombinant protein induces cytochrome *c* release from isolated mitochondria (Imazu *et al.*, 1999). The reason for this difference with BNIP3 is not known, however, there are clear structural differences between the proteins that may account for this effect. Specifically, there are two regions in the amino-

terminus of NIX that are distinct from BNIP3 (Chen *et al.*, 1999). Furthermore, the observations made by Imazu *et al.* (1999) were based on an *in vitro* assay. It remains to be confirmed that overexpression of NIX induces similar effects *in vivo*. In mammalian cells, BNIP3 did not induce cytochrome *c* release from the mitochondria, as determined by both immunofluorescence and immunoblotting methods.

6.3 BNIP3-induced cell death is caspase- and Apaf-1-independent

The absence of mitochondrial cytochrome *c* release does not exclude the activation of a caspase-dependent apoptotic pathway. For example, two different death pathways have been described in Fas-induced apoptosis, one of which leads to direct activation of caspase 3 through receptor activated caspase 8 and does not require cytochrome *c*; and a second that requires mitochondrial release of cytochrome *c* to activate caspase 3 and apoptosis (Scaffidi *et al.*, 1998). BNIP3, on the other hand, requires neither Apaf-1/cytochrome *c* nor the downstream caspases, as BNIP3-induced cell death was unaffected by broad-spectrum caspase inhibitors and was fully functional in MEF cell lines deficient in Apaf-1, caspase 9, or caspase 3. Thus, BNIP3-induced cell death is primarily caspase-independent. Induction of caspase-independent cell death has been increasingly observed, and examples include the adenoviral protein E4ORF4 (Lavoie *et al.*, 1998), and cellular proteins PML (Quignon *et al.*, 1998), anti-CD2 (Deas *et al.*, 1998), oncogenic Ras (Chi *et al.*, 1999), FADD (Kawahara *et al.*, 1998) and granzyme A (Beresford *et al.*, 1999). Furthermore, BAX and BAK are able to induce cell death, as opposed to the nuclear changes of apoptosis, in the presence of the general caspase inhibitor Ac-zVAD-fmk (Xiang *et al.*, 1996; McCarthy *et al.*, 1997). In addition,

it has recently been shown that MEF cells deficient in Apaf-1 undergo caspase-independent cell death in response to staurosporine, cisplatinum, and UV irradiation (Miyazaki *et al.*, 2001).

6.4 The PT pore: apoptosis versus necrosis, cause or consequence

Opening of the PT pore, loss of $\Delta\psi m$, and increased ROS production are important contributors to cellular destruction (Zamzami *et al.*, 1995) and are events in both apoptosis and necrosis (Kroemer *et al.*, 1998; Crompton, 1999). However, the sequence of these events in the apoptotic pathway remains controversial. Specifically, Zamzami *et al.* (1995) have demonstrated that ROS are generated only after dissipation of $\Delta\psi m$ following dexamethasone treatment of splenic T cells. However, the loss of mitochondrial membrane potential and ROS production can be both an inducer and a consequence of PT pore opening depending on the death signal (reviewed in Zoratti and Szabo, 1995; Kroemer *et al.*, 1997; Crompton, 1999). It is also controversial whether PT pore opening is a cause or consequence of apoptotic cell death. Inhibition of the PT pore prevents cell death and nuclear changes characteristic of apoptosis, suggesting that the PT pore is the critical, initiating event of apoptosis (Castedo *et al.*, 1996; Marchetti *et al.*, 1996; Zamzami *et al.*, 1996). However, PT pore opening has also been observed as a late event, secondary to initial caspase activation, suggesting that it functions as an amplification step to propagate the apoptotic signal (Bossy-Wetzel *et al.*, 1998; Marzo *et al.*, 1998a; Finucane *et al.*, 1999). In necrotic cell death, PT pore opening is considered to be an early, pivotal event. During a necrotic insult, cyclosporin A can prevent PT pore opening and cell death (Kroemer *et al.*, 1998). Thus, apoptosis and necrosis may be

differentiated based on the late or early opening of the PT pore, respectively (Kroemer *et al.*, 1998). In addition, if caspase activation is delayed or absent, necrosis may occur before the apoptotic program can be implemented. This type of phenomenon has been previously observed. Overexpression of BAX or BAK in the presence of Ac-zVAD-fmk, to inhibit caspase activation, results in caspase-independent cell death with similar features to those observed in BNIP3-expressing cells (Xiang *et al.*, 1996; McCarthy *et al.*, 1997). BNIP3 does not induce caspase activation possibly due to ROS-mediated inhibition of caspase activity. Furthermore, overexpression of BNIP3 induces early, sustained PT pore opening with $\Delta\psi m$ suppression and ROS production. Therefore, the mitochondrial events in BNIP3-expressing cells are closely related to necrotic cell death. Furthermore, these events occur concurrently with plasma membrane permeabilization, a feature of necrosis. As well, the PT pore-specific inhibitors, cyclosporin A and bongkrekic acid, block both BNIP3-induced mitochondrial changes and cell death. Thus, PT pore opening is a pivotal event for BNIP3-induced cell death and thus fits with a more necrotic type of cell death. This is summarized in Figure 31. Although PT pore opening is a key mechanism that mediates BNIP3-induced cell death, the specific mitochondrial proteins that are targeted remain to be identified. However, BAX has been found to interact directly with components of the PT pore and directly modulate PT pore opening (Marzo *et al.*, 1998; Narita *et al.*, 1998). Therefore, BNIP3 may directly induce PT pore opening via analogous interactions with one or more components of the PT pore. Alternatively, BNIP3 may interact with or modulate the function of some unknown factor that itself directly regulates the state of the PT pore. Due to the observed cell death activity of cytochrome b_5-targetted BNIP3 (BNIP3-CybTM), BNIP3-mediated disruption

of Ca^{++} homeostasis is a possible mechanism as the intracellular Ca^{++} level is a known modulator of PT pore opening (Bernardi, 1999; Crompton, 1999). It is equally possible that BNIP3 targets an unrelated protein that suppresses transmembrane potential and enhances ROS production, events which themselves are sufficient to induce secondary PT pore opening.

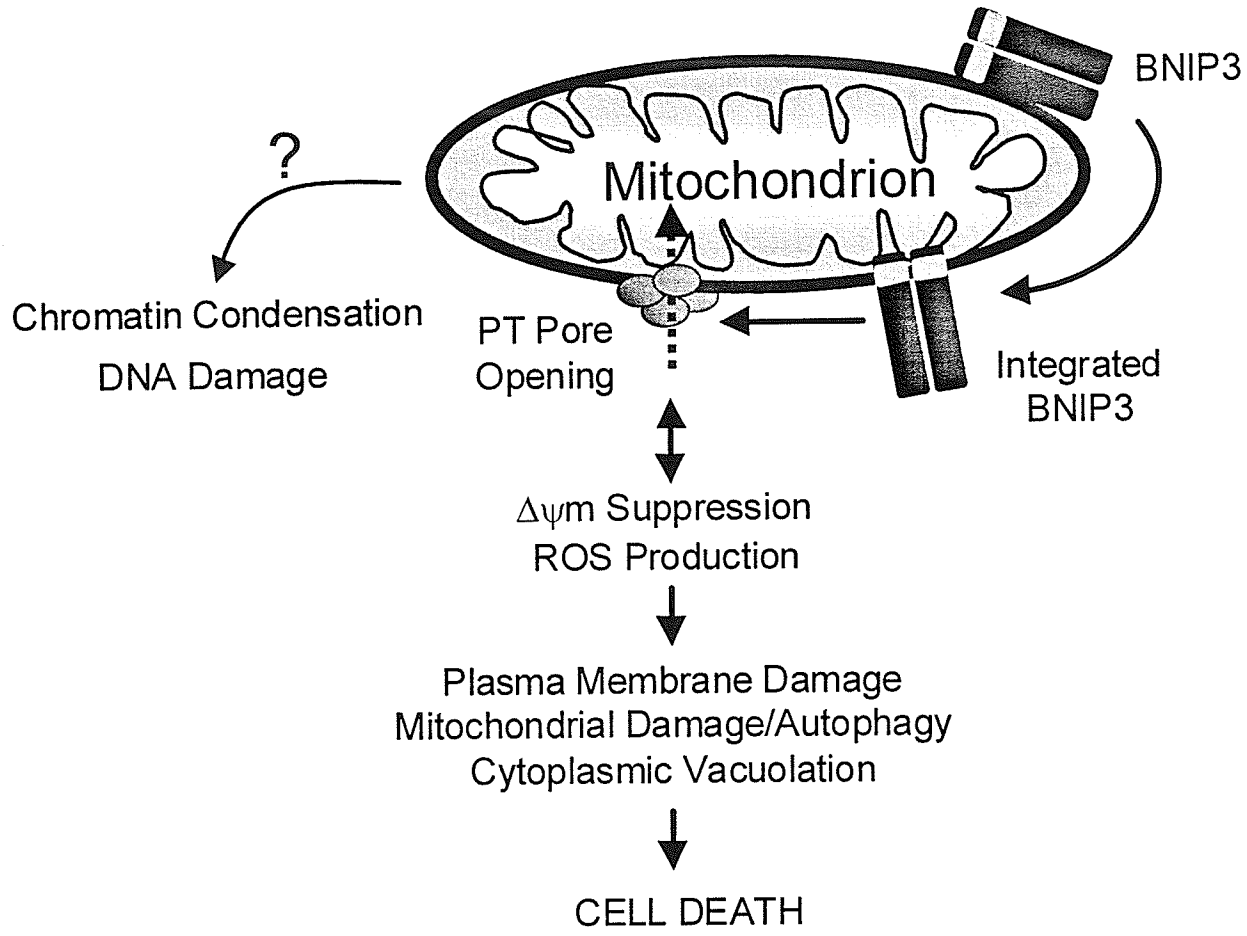

Figure 31: Model of BNIP3-induced cell death. Overexpression permits integration of BNIP3 into the outer mitochondrial membrane through its TM domain. BNIP3 then initiates permeability transition pore opening and $\Delta\psi m$ suppression with increased ROS production in an undefined sequence, leading to cell death. Late DNA fragmentation and chromatin condensation are also induced as a consequence of BNIP3 integration, via an unidentified pathway.

6.5 BNIP3 induces necrotic-like cell death

Although cell death may be caspase-independent, DNA fragmentation and chromatin condensation following most apoptotic signals requires downstream caspases (Earnshaw *et al.*, 1999). Nuclei in BNIP3 transfectants exhibit DNA fragmentation and focal chromatin condensation, although these nuclear changes are preceded by loss of plasma membrane integrity and thus the cells are likely already committed to die. Nevertheless, it is unclear how the nuclear changes are mediated, as there is only minimal DEVDase activation, even at the late time points. Furthermore, DNA fragmentation is only partially inhibited by Ac-zVAD-fmk. Immunofluorescence and immunoblotting of subcellular fractions exclude the participation of AIF, a caspase-independent mediator (Susin *et al.*, 1999), as it was not translocated from the mitochondria to the nucleus in BNIP3-transfected cells. Ultrastructural analysis of BNIP3-transfected cells revealed that the nuclei have a peculiar mottled appearance, with dispersed foci of chromatin condensation rather than the global large-scale condensation normally observed in caspase-dependent apoptosis. Although we have not definitively determined how BNIP3 induces DNA strand breaks, it appears that the mechanism is not mediated by one of the known apoptotic pathways. However, ROS is a known inducer of DNA strand breaks and DNA base damage (Bai *et al.*, 1999). Therefore, the ROS produced as a consequence of BNIP3-mediated events may be sufficient to induce the DNA damage observed in BNIP3-expressing cells. It is also possible that non-caspase proteases mediate the nuclear damage observed following overexpression of BNIP3. In the cell, a large pool of catabolic enzymes, including endonucleases, exists within the lysosome.

During some forms of cell death, the contents of the lysosome may be spilled into the cytosol (Bursch, 2001). Furthermore, autophagosomes are associated with lysosomal degradation (Bursch, 2001). Interestingly, autophagosomes are a major feature of BNIP3-expressing cells. Therefore, the nuclear damage observed in BNIP3-transfected cells may be due to an endonuclease derived from the autophagosome/lysosome compartment. Caspase-independent nuclear damage and cell death has also been observed in cells treated with the tryptase, granzyme A (Beresford *et al.*, 1999). Subsequent studies determined that the rapid degradation of nuclear histones by granzyme A may be responsible for the observed DNA damage (Zhang *et al.*, 2001).

BNIP3 transfectants exhibit an early loss in plasma membrane integrity and this precedes the appearance of DNA fragmentation detected by TUNEL. In contrast, cells expressing tBID, BAX and caspase 9/Apaf-1 showed both the expected apoptotic phenotype of an intact plasma membrane and PS externalization ($PS^{+}PI^{-}$) as well as some cells with early plasma membrane disruption. This observation suggests that the primary cause of BNIP3-induced cell death is the loss of membrane integrity, which would be more typical of a necrotic type of cell death. Interestingly, some species of oxygen radicals can inflict membrane damage via lipid peroxidation (Bai *et al.*, 1999). Therefore, the plasma membrane damage observed in BNIP3-induced cell death may be due to the enhanced ROS production induced by overexpression of BNIP3. Electron micrograph analysis of BNIP3-transfected cells supports the interpretation that BNIP3 induces necrotic-like cell death. The morphological changes show extensive cytoplasmic vacuolation and mitochondrial deformation with limited evidence of apoptotic nuclear damage. Similar vacuole formation has been observed in caspase-independent forms of

cell death including anti-CD2 treated cells (Deas *et al.*, 1998), neuronal cells subjected to nerve growth factor (NGF) withdrawal (Xue *et al.*, 1999), and Ac-zVAD-fmk-treated BAX and BAK transfectants (Xiang *et al.*, 1996; McCarthy *et al.*, 1997). BNIP3-expressing cells contain a heterogeneous population of electron-dense and electron-lucent vacuoles, some of which appear to be autophagic and are very similar to the structures recently observed in sympathetic neurons after NGF-withdrawal (Xue *et al.*, 1999). In this study, autophagic degeneration and vacuole formation were blocked by treatment with an autophagy inhibitor, 3-methyladenine, but not the caspase inhibitor Ac-zVAD-fmk, and may be similar to BNIP3-induced cell death. Furthermore, the appearance of autophagic vacuoles suggests that degradative enzymes may be released from the lysosome during the uncontrolled autophagy. Lysosomal proteases as mediators of cell death have been implicated in several systems (reviewed in Bursch, 2001). It is possible that this pool of proteases mediate the cellular and nuclear damage observed in BNIP3-expressing cells. BNIP3-mediated cell death also resembles the caspase- and Apaf-1-independent cell death in the interdigital spaces of mouse limb buds, including mottled nuclei and cytoplasmic vacuolation (Chautan *et al.*, 1999). A morphologically similar form of caspase-independent cell death, referred to as autophagic cell death, has been reported in the slime mold *Dictyostelium,* which was also inhibited by cyclosporin A (Cornillon *et al.*, 1994; Olie *et al.*, 1998). Even more intriguing is the observation of a similar type of cell death in *C. elegans* (Hall *et al.*, 1997).

6.6 Model of cell death induced by endogenous BNIP3 and its potential regulation

Based on the observed function of BNIP3 as a mediator of cell death resembling necrosis when overexpressed, it is reasonable to postulate that some forms of necrotic cell death may be mediated by endogenous BNIP3. Low oxygen conditions (hypoxia) are known to induce both apoptosis and necrosis (Bursch, 2001). Recently, increased endogenous BNIP3 mRNA and protein expression have been observed in CHO-K1 and HeLa cell lines as well as neonatal rat cardiomyocytes grown in hypoxic conditions (Bruick, 2000; Guo *et al.*, 2001). Upregulation of BNIP3 and NIX expression correlated with increased cell death in cells grown in hypoxic condition (Bruick, 2000; Guo *et al.*, 2001). Furthermore, expression analysis of nine BCL-2 family members revealed that hypoxia specifically upregulated BNIP3 and NIX (Bruick, 2000) suggesting a unique role for BNIP3-related proteins as mediators of hypoxic cell death. The role for BNIP3 in hypoxic cell death is strengthened by the identification of two hypoxia response elements (HRE) in the BNIP3 promoter (Bruick, 2000). HREs are binding sites for the highly oxygen-sensitive heterodimeric transcription factor, Hypoxia Inducible Factor-1 (HIF-1). One of the subunits of HIF-1, HIF-1α, contains an oxygen-dependent degradation domain that is rapidly degraded via the ubiquitin-proteasome pathway in the presence of low oxygen conditions (Salcedo and Caro, 1997; Huang *et al.*, 1998a; Kallio *et al.*, 1999). However, in hypoxic conditions, HIF-1α is stabilized and associates with its partner HIF-1β/ARNT to produce a transcription factor (Semenza, 2000). Target genes of HIF-1 include genes involved in glucose metabolism, erythropoiesis, and vascular development (Semenza, 2000). Furthermore, HIF-1-induced expression of target genes is primarily

geared towards cell survival (Semenza, 2000). However, the recent identification of functional HREs in the BNIP3 promoter strongly implicates BNIP3 in hypoxic cell death. However, in the study by Bruick (2000), there is a significant delay between mRNA expression and protein expression. Examination of the literature suggests a potential self-amplification mechanism for BNIP3. Specifically, BNIP3 induces increased ROS production. Interestingly, HIF-1α is regulated by intracellular levels of ROS. Therefore, removal of the proposed post-translational regulatory mechanism that permits integration of BNIP3 into the outer mitochondrial membrane results in significant ROS production. The increased levels of intracellular ROS contributes to an altered cellular redox status and provides the necessary environment for HIF-1α stabilization. The HIF-1 complex would then proceed to transcriptionally upregulate BNIP3 mRNA that would generate more protein and induce more ROS production, perpetuating a feed-forward self-amplification loop. The simultaneous expression of HIF-1-dependent survival/adaptation genes that permit a cell to partially adapt to hypoxia may account for the delay between BNIP3 upregulation and cell death observed by Bruick (2000).

It has recently been determined that the oxygen sensing mechanisms involved in stabilization of HIF-1α does not depend on the ROS generated by deregulation of the ETC (Srinivas *et al.*, 2001). Specifically, H_2O_2 was ruled out as a mediator in HIF-1 activation. However, there are still other possible oxygen-derived free radicals that could serve as viable candidates for HIF-1α stabilization. Interestingly, dihydroethidium (HE), the reagent used to detect ROS production in BNIP3-expressing cells, is primarily reactive with superoxide anion (Cai and Jones, 1998). Therefore, although the oxygen radical species generated in BNIP3-induced cell death are not defined, it is still possible

that BNIP3-induced ROS production is appropriate to induce HIF-1 activation. Further work using inhibitors specific to a subset of oxygen radicals could prove useful in determining the viability of this model. Intriguingly, an orthologue of HIF-1 has recently been identified in *C. elegans* (Jiang *et al.*, 2000). However, the deletion of the *hif-1* gene revealed that *hif-1* is required for *C. elegans*' adaptation to hypoxia (Jiang *et al.*, 2000). A hypoxia adaptation mechanism has been observed in mammalian cells and is presumably linked to HIF-1-mediated upregulation of glycolytic enzymes as a shift in cellular metabolic state was observed (Seagroves *et al.*, 2001). In addition, hypoxic conditions did not affect the viability of wild type nematodes despite the known existence of a *C. elegans* orthologue of BNIP3, ceBNIP3 (Yasuda *et al.*, 1998a; Cizeau *et al.*, 2000). However, BNIP3-induced cell death in mammalian cells is mitochondria-dependent/mediated, and therefore, this possible contradiction may be due to the fact that there is currently no evidence of a mitochondria-dependent/mediated cell death pathway in *C. elegans*. In humans, BNIP3 may play an important a role in disease models featuring hypoxic stress, such as ischemia, cardiac infarct, and solid tumor growth.

6.7 Future studies

Although the basic mechanism of BNIP3-induced cell death has been delineated, little is known about the physiological function of BNIP3. There are two approaches available to identifying the physiological role of endogenous proteins, including germline deletion of the gene and antisense technology. In both cases, removal of the gene product should effectively yield invaluable data about the endogenous role of BNIP3. The structure of the gene encoding BNIP3 is currently being determined (D. Dubik, A.H.

Greenberg, and J.M. Penninger, unpublished observations). Using the completed gene structure, appropriate targeting vectors can be constructed to generate mice deficient in BNIP3. Careful evaluation of *bnip3*$^{-/-}$ mice will undoubtedly uncover the role of BNIP3 in development and cellular homeostasis. Development of antisense probes specific for BNIP3 would also be helpful. As well, experimental systems of necrotic cell death, especially hypoxia, should yield valuable insight into the role of BNIP3 in disease models such as ischemia, cardiac infarct, and the development of large solid tumors. Development of antisense technology to prevent BNIP3-induced cell death in disease models may also provide valuable therapeutic avenues.

Significant strides have been made in understanding the relationship between mitochondrial physiology and cell death. Yeast have served as a valuable tool in these studies due to their ease of manipulation and ability to grow in both respiratory/aerobic and fermentative/anaerobic conditions (Harris *et al.*, 2000). Using yeast, a blueprint for cell death induced by BAX has recently been identified. Specifically, BAX requires oxidative phosphorylation to efficiently induce cell death in yeast (Harris *et al.*, 2000). In contrast to the yeast two hybrid system, in which the vectors are targeted to the nucleus to facilitate transcriptional activation of the reporter gene(s), these studies utilized full length BAX targeted to the mitochondria via its own TM domain, thus placing BAX in its "natural environment". If full length BNIP3 is similarly cytotoxic to yeast, it would be useful to explore expression of BNIP3 in a variety of yeast strains, each with specific mutations, under both aerobic and anaerobic conditions to determine the impact of BNIP3 on mitochondrial physiology. Specifically, it is possible that BNIP3 mediates a disruption of normal mitochondrial reactions so as to disturb cellular energy levels and

thus favor necrosis. As well, overexpression of BAX has been previously shown to trigger PT pore opening and caspase-independent cell death in the presence of caspase inhibitors (Xiang *et al.*, 1996). Here, PT pore opening is suspected to be regulated by protein-protein interactions as BAX can directly interact with ANT and VDAC (Marzo *et al.*, 1998; Narita *et al.*, 1998; Shimizu *et al.*, 2000b). These direct interactions may be facilitated by BAX protein integration into the outer mitochondrial membrane upon receiving a death stimulus (Goping *et al.*, 1998). BNIP3 overexpression induces PT pore opening and protein integration. Therefore, it is worthwhile to explore the possibility of direct interactions between BNIP3 and components of the PT pore. Such interactions could ultimately influence normal mitochondrial physiology and energy production/homeostasis.

The only truly biochemical definition of necrosis is significant ATP depletion (Nicotera and Leist, 1997; Tsujimoto, 1997; McConkey, 1998). The work described classifies BNIP3-induced cell death as necrotic-like based on morphological criteria and an apparent lack of apoptotic biochemical and morphological criteria. Note that although BNIP3-induced mitochondrial deregulation is early and likely indicative of necrosis, there is a significant amount of controversial data yet to be sorted out due to the apparent sharing of early PT pore opening by both apoptotic and necrotic cell death pathways. In any case, it would be useful to define the energy status of BNIP3-expressing cells. As well, this type of study in combination with previously suggested experiments, may provide additional information into the biochemical pathway invoked in BNIP3-induced cell death. In addition, an attempt to delineate the sequence of mitochondrial events,

including PT pore opening, ROS production, and $\Delta\psi m$ suppression in relation to one another, using specific pharmacological compounds may also prove useful.

Autophagy is a poorly understood mechanism in mammalian cells. The observation that BNIP3-expressing cells contain numerous autophagic vacuoles/autophagosomes suggests that BNIP3 may play a role in autophagic cell death. Similar autophagosome structures have been observed in sympathetic neurons deprived of nerve growth factor (Xue *et al.*, 1999). As well, there is some indication that PT pore opening influences autophagy (Bursch, 2001). Therefore, studies exploring BNIP3 expression in the presence of inhibitors of autophagy and PT pore opening, such as 3-methyladenine and cyclosporin A, respectively, may partly elucidate a much sought after mechanism for cellular removal by autophagy.

BNIP3 is a toxic protein and therefore must be regulated. Endogenous BNIP3 is held inactive as a non-integrated protein loosely associated with the mitochondrial membrane. The regulatory step(s) governing protein integration is/are unknown. As mentioned previously, there are at least two non-mutually exclusive mechanisms possible. First, endogenous BNIP3 may assume a conformation that is incompatible with protein integration. Protein conformation may be altered by some post translational modification that permits BNIP3 integration via the TM domain. Detailed analysis of possible post-translational modifications, including phosphorylation, myristolation, and glycosylation, may yield important regulatory information. Determination of the three-dimensional structure of BNIP3 may also be beneficial and perhaps even yield additional information about protein function. Second, endogenous BNIP3 may interact with a regulatory protein that maintains BNIP3 in an unintegrated form at the surface of the

mitochondria. Dissociation of the regulatory protein may permit integration of BNIP3. A possible interacting, regulatory protein could be identified via the yeast two hybrid system coupled with co-immunoprecipitation studies in mammalian cells.

6.8 Conclusion

In conclusion, BNIP3 overexpression initiates a necrotic-like cell death pathway. BNIP3-induced cell death requires early PT pore opening and is independent of caspases, Apaf-1, and cytochrome c release. Mitochondrial dysfunction and loss of plasma membrane integrity are early events in BNIP3-induced cell death. Other features of BNIP3-expressing cells include extensive cytoplasmic vacuolation, the appearance of autophagosomes, and disruption of normal mitochondrial architecture. The classification of BNIP3-induced cell death as necrotic-like (instead of necrotic) is largely due to a lack of formal evidence demonstrating a loss of cellular ATP, the only known event that is characteristic of necrosis, in BNIP3-expressing cells. However, the observation that necrotic-like cell death is induced by a protein, which is encoded by a gene, suggests that not all programmed cell death is apoptosis. Rather, programmed cell death can be apoptotic or necrotic in nature provided that it accomplishes a physiological function. Therefore, BNIP3 represents a new class of mitochondrial proteins involved in a necrotic-like cell death pathway.

7.0 References

Abdel-Rahman, W.M., I.B. Georgiades, L.J. Curtis, M.J. Arends, and A.H. Wyllie. 1999. Role of BAX mutations in mismatch repair-deficient colorectal carcinogenesis. *Oncogene* **18**:2139-2142.

Adams, J.M., and S. Cory. 1998. The Bcl-2 protein family: arbiters of cell survival. *Science* **281**:1322-1326.

Aita, V.M. X.H. Liang, V.V. Murty, D.L. Pincus, W. Yu, E. Cayanis, S. Kalachikov, T.C. Gilliam, and B. Levine. 1999. Cloning and genomic organization of beclin1, a candidate tumor suppressor gene on chromosome 17q21. *Genomics* **59**:59-65.

Alimonti, J.B., L. Shi, P.K. Baijal, and A.H. Greenberg. 2001. Granzyme B induces BID-mediated cytochrome c release and mitochondrial permeability transition. *J. Biol. Chem.* **276**:6974-6982.

Alnemri, E.S., D.J. Livingston, D.W. Nicholson, G. Salvesen, N.A. Thornberry, W.W. Wong, and J. Yuan. 1996. Human ICE/CED-3 protease nomenclature. *Cell* **87**:171.

Antonsson, B., S. Montessuit, B. Sanchez, and J.-C. Martinou. 2001. Bax is present as a high molecular weight oligomer/complex in the mitochondrial membrane of apoptotic cells. *J. Biol. Chem.* **276**:11615-11623.

Antonsson, B., S. Montessuit, S. Lauper, R. Eskes, and J.-C. Martinou. 2000. Bax oligomerization is required for channel-forming activity in liposomes and to trigger cytochrome *c* release from mitochondria. *Biochem. J.* **345**:271-278.

Antonsson, B., F. Conti, A. Ciavatta, S. Montessuit, S. Lewis, I. Martinou, L. Bernasconi, A. Bernard, J.-J. Mermod, G. Mazzei, K. Maundrell, F. Gambale, R. Sadoul, and J.-C. Martinou. 1997. Inhibition of Bax channel-forming activity by Bcl-2. *Science* **277**:370-372.

Aravind, L., V.M. Dixit, and E.V. Koonin. 2001. Apoptotic molecular machinery: vastly increased complexity in vertebrates revealed by genome comparisons. *Science* **291**:1279-1284.

Ashkenazi, A., and V.M. Dixit. 1998. Death receptors: signaling and m odulation. *Science* **281**:1305-1308.

Bai, J., A.M. Rodriquez, J.A. Melendez, and A.I. Cederbaum. 1999. Overexpression of catalase in cytosolic or mitochondrial compartment protects HepG2 cells against oxidative injury. *J. Biol. Chem.* **274**:26217-26224.

Baker, S.J., and E.P. Reddy. 1998. Modulation of life and death by the TNF receptor superfamily. *Oncogene* **17**:3261-3270.

Bakhshi, A., J.P. Jensen, P. Goldman, J.J. Wright, O.W. McBride, A.L. Epstein, and S.J. Korsmeyer. 1985. Cloning the chromosomal breakpoint of t(14;18) human lymphomas: clustering around J_H on chromosome 14 and near a transcriptional unit on 18. *Cell* **41**:889-906.

Barry, M., J.A. Heibein, M.J. Pinkoski, S.F. Lee, R.W. Moyer, D.R. Green, and R.C. Bleackley. Granzyme B short-circuits the need for caspase 8 activity during granule-mediated cytotoxic T-lymphocyte killing by directly cleaving Bid. *Mol. Cell. Biol.* **20**:3781-3794.

Beere, H.M., B.B. Wolf, K. Cain, D.D. Mosser, A. Mahboubi, T. Kuwana, P. Tailor, R.I. Morimoto, G.M. Cohen, and D.R. Green. 2000. Heat-shock protein 70 inhibits apoptosis by preventing recruitment of procaspase-9 to the Apaf-1 apoptosome. *Nature Cell Biol.* **2**:469-475.

Beresford, P.J., Z. Xia, A.H. Greenberg, and J. Lieberman. 1999. Granzyme A loading induces rapid cytolysis and a novel form of DNA damage independently of caspase activation. *Immunity* **10**:585-594.

Bernardi, P. 1999. Mitochondrial transport of cations: channels, exchangers and permeability transition. *Physiol. Rev.* **79**:1127-1155.

Bernardi, P., L. Scorrano, R. Colonna, V. Petronilli, and F. Di Lisa. 1999. Mitochondria and cell death: mechanistic aspects and methodological issues. *Eur. J. Biochem.* **264**:687-701.

Bertin, J., W.J. Nir, C.M. Fischer, O.V. Taylor, P.R. Errada, J.R. Grant, J.J. Keilty, M.L. Gosselin, K.E. Robinson, G.H. Wong, M.A. Glucksmann, and P.S. DiStefano. 1999. Human CARD4 protein is a novel CED-4/Apaf-1 cell death family member that activates NF-kappaB. *J. Biol. Chem.* **274**:12955-12958.

Beutner, G., A. Ruck, B. Riede, and D. Brdiczka. 1998. Complexes between porin, hexokinase, mitochondrial creatine kinase and adenylate translocator display properties of the permeability transition pore. Implication for regulation of permeability transition by the kinases. *Biochim. Biophys. Acta* **1368**:7-18.

Blanchard, H., L. Kodandapani, P.R. Mittl, S. Di Marco, J.F. Krebs, J.C. Wu, K.J. Tomaselli, and M.G. Grutter. 1999. The three-dimensional structure of caspase-8: an initiator enzyme in apoptosis. *Structure Fold Des.* **15**:1125-1133.

Blume-Jensen, P., R. Janknecht, and T. Hunter. 1998. The kit receptor promotes cell survival via activation of PI 3-kinase and subsequent Akt-mediated phosphorylation of Bad on Ser136. *Curr. Biol.* **8**:779-782.

Borner, C. 1996. Diminished cell prolifeation associated with the death-protective activity of BCL-2. *J. Biol. Chem.* **271**:12695-12698.

Borner, C., I. Martinou, C. Mattmann, M. Irmler, E. Schaerer, J.C. Martinou, and J. Tschopp. 1994. The protein BCL-2α does not require membrane attachment, but two conserved domains to suppress apoptosis. *J. Biol. Chem.* **126**:1059-1068.

Bossy-Wetzel, E., D.D. Newmeyer, and D.R. Green. 1998. Mitochondrial cytochrome *c* release in apoptosis occurs upstream of DEVD-specific caspase activation and independently of mitochondrial transmembrane depolarization. *EMBO J.* **17**:37-49.

Boveris, A., and B. Chance. 1973. The mitochondrial generation of hydrogen peroxide: general properties and effect of hyperbaric oxygen. *Biochem. J.* **134**:707-716.

Boyd, J.M., S. Malstrom, T. Subramanian, L.K. Venkatesh, U. Schaeper, B. Elangovan, C. D'Sa-Eipper, and G. Chinnadurai. 1994. Adenovirus E1B 19 kDa and Bcl-2 proteins interact with a common set of cellular proteins. *Cell* **79**:341-351.

Brancolini, C., D. Lazarevic, and C. Schneider. 1997. Dismantling cell-cell contacts during apoptosis is coupled to a caspase-dependent proteolytic cleavage of β-catenin. *J. Cell. Biol.* **139**:759-771.

Brancolini, C., M. Benedetti, and C. Schneider. 1995. Microfilament reorganization during apoptosis: the role of Gas2, a possible substrate for ICE-like proteases. *EMBO J.* **14**:5179-5190.

Branden, C., and J. Tooze. 1991. Introduction to protein structure. Garland Publishing Inc. New York, New York.

Bratton, S.B., G. Walker, S.M. Srinivasula, X.-M. Sun, M. Butterworth, E.S. Alnemri, and G.M. Cohen. 2001. Recruitment, activation and retention of caspases-9 and –3 by Apaf-1 apoptosome and associated XIAP complexes. *EMBO J.* **20**:998-1009.

Brimmell, M., R. Mendiola, J. Mangion, and G. Packham. 1998. BAX frameshift mutations in cell lines derived from human haemopoietic malignancies are associated with resistance to apoptosis and microsatellite instability. *Oncogene* **16**:1803-1812.

Bruick, R.K. 2000. Expression of the gene encoding the proapoptotic Nip3 protein is induced by hypoxia. *Proc. Natl. Acad. Sci. USA* **97**:9082-9087.

Bump, N.J., M. Hackett, M. Hugunin, S. Seshagiri, K. Brady, P. Chen, C. Ferenz, S. Franklin, R. Ghayur, P. Li, P. Licari, J. Mankovich, L. Shi, A.H. Greenberg, L.K. Miller, and W.W. Wong. 1995. Inhibition of ICE family proteases by baculovirus antiapoptotic protein p35. *Science* **269**:1885-1888.

Burkitt, M.J., and P. Wardman. 2001. Cytochrome *c* is a potent catalyst of dichlorofluorescin oxidation: implications for the role of reactive oxygen species in apoptosis. *Biochem. Biophys. Res. Commun.* **282**:329-333.

Bursch, W. 2001. The autophagosomal-lysosomal compartment in programmed cell death. *Cell Death Differ.* **8**:569-581.

Cai, J., and D.P. Jones. 1998. Superoxide in apoptosis: mitochondrial generation triggered by cytochrome *c* loss. *J. Biol. Chem.*, **273**:11401-11404.

Cain, K., S.B. Bratton, C. Langlais, G. Walker, D.G. Brown, X.-M. Sun, and G.M. Cohen. 2000. Apaf-1 oligomerizes into biologically active ~700-kDa and inactive ~1.4-Mda apoptosome complexes. *J. Biol. Chem.* **275**:6067-6070.

Castedo, M., T. Hirsch, S.A. Susin, N. Zamzami, P. Marchetti, A. Macho, and G. Kroemer. 1996. Sequential acquisition of mitochondrial and plasma membrane alterations during early lymphocyte apoptosis. *J. Immunol.* **157**:512-521.

Cecconi, F., G. Alvarex-Bolado, B.I. Meyer, K.A. Roth, and P. Gruss. 1998. Apaf1 (CED-4 homolog) regulates programmed cell death in mammalian development. *Cell* **94**:727-737.

Chai, J. C. Du, J.-W. Wu, S. Kyin, X. Wang, and Y. Shi. 2000. Structural and biochemical basis of apoptotic activation by Smac/DIABLO. *Nature* **406**:855-862.

Chandler, J.M., G.M. Cohen, and M. MacFarlane. 1998. Different subcellular distribution of caspase-3 and caspase-7 following Fas-induced apoptosis in mouse liver. *J. Biol. Chem.* **273**:10815-10818.

Chang, B.S., A.J. Minn, S.W. Muchmore, S.W. Fesik, and C.B. Thompson. 1997. Identification of a novel regulatory domain in Bcl-X_L and Bcl-2. *EMBO J.* **16**:968-977.

Chau, B.N., E.H. Cheng, D.A. Kerr, and J.M. Hardwick. 2000. Aven, a novel inhibitor of caspase activation, binds Bcl-x_L and Apaf-1. *Mol. Cell* **6**:31-40.

Chaudhary, D., K. O'Rourke, A.M. Chinnaiyan, and V.M. Dixit. 1998. The death inhibitory molecules CED-9 and CED-4L use a common mechanism to inhibit the CED-3 death protease. *J. Biol. Chem.* **273**:17708-17712.

Chautan, D., S. Rosen, J.C. Reed, S. Kharbanda, and K.C. Anderson. 2001. APAF-1/cytochrome-C independent and SMAC-dependent induction of apoptosis in multiple myeloma (MM) cells. *J. Biol. Chem.* [epub ahead of print].

Chautan, M., G. Chazal, F. Cecconi, P. Gruss, and P. Golstein. 1999. Interdigital cell death can occur through a necrotic and caspase-independent pathway. *Curr. Biol.* **9**:967-970.

Chen, P., and J.M. Abrams. 2000. *Drosophila* apoptosis and Bcl-2 genes: outliers fly in. *J. Cell Biol.* **148**:625-627.

Chen, F., B.M. Hersh, B. Conradt, Z. Zhou, D. Riemer, Y. Gruenbaum, and H.R. Horvitz. 2000. Translocation of *C. elegans* CED-4 to nuclear membranes during programmed cell death. *Science* **287**:1485-1489.

Chen, G., J. Cizeau, C. Vande Velde, J.H. Park, G. Bozek, J. Bolton, L. Shi, D. Dubik, and A. Greenberg. 1999. Nix and Nip3 form a subfamily of pro-apoptotic mitochondrial proteins. *J. Biol. Chem.* **274**:7-10.

Chen, G., R. Ray, D. Dubik, L.F. Shi, J. Cizeau, R.C. Bleackley, S. Saxena, R.D. Gietz, and A.H. Greenberg. 1997. The E1B 19K Bcl-2-binding protein Nip3 is a dimeric mitochondrial protein that activates apoptosis. *J. Exp. Med.* **186**:1975-1983.

Cheng, E.H., D.G. Kirsch, R.J. Clem, R. Ravi, M.B. Kastan, A. Bedi, K. Ueno, and J.M Hardwick. 1997. Conversion of Bcl-2 to a Bax-like death effector by caspases. *Science* **278**:1966-1968.

Cheng, E.H., B. Levine, L.H. Boise, and C.B. Thompson. 1996. Bax-independent inhibition of apoptosis by Bcl-x_L. *Nature* **379**:554-556.

Chi, S., C. Kitanaka, K. Noguchi, T. Mochizuki, Y. Nagashima, M. Shirouzu, H. Fujita, M. Yoshida, W. Chen, A. Asai, M. Himeno, S. Yokoyama, and Y. Kuchino. 1999. Oncogenic Ras triggers cell suicide through the activation of a caspase-independent cell death program in human cancer cells. *Oncogene* **18**:2281-2290.

Chinnaiyan, A.M., K. O'Rourke, B.R. Lane, and V.M. Dixit. 1997. Interaction of CED-4 with CED-3 and CED-9: a molecular framework for cell death. *Science* **275**:1122-1126.

Chittenden, T., C. Flemington, A.B. Houghton, R.G. Ebb, G.J. Gallo, B. Elangovan, G. Chinnadurai, and R.J. Lutz. 1995. A conserved domain in Bak, distinct from BH1 and BH2, mediates cell death and protein binding functions. *EMBO J.* **14**:5589-5596.

Chou, J.J., H. Li, G.S. Salvesen, J. Yuan, and G. Wagner. 1999. Solution structure of BID, an intracellular amplifier of apoptotic signaling. *Cell* **96**:615-624.

Chou, J.J., H. Matsuo, H. Duan, and G. Wagner. 1998. Solution structure of the RAIDD CARD and model for CARD/CARD interaction in caspase-2 and caspase-9 recruitment. *Cell* **94**:171-180.

Chu, Z.-L., F. Pio, Z. Xie, K. Welsh, M. Krajewska, S. Krajewski, A. Godzik, and J.C. Reed. 2001. A novel enhancer of the Apaf1 apoptosome involved in cytochrome *c*-dependent caspase activation and apoptosis. *J. Biol. Chem.* **276**:9239-9245.

Chung, S., T.L. Gumienny, M.O. Hengartner, and M. Driscoll. 2000. A common set of engulfment genes mediates removal of both apoptotic and necrotic cell corpses in *C. elegans*. *Nat. Cell Biol.* **2**:931-937.

Cizeau, J., R. Ray, G. Chen, R.D. Gietz, and A.H. Greenberg. 2000. The *C. elegans* orthologue ceBNIP3 interacts with CED-9 and CED-3 but kills through a BH3- and caspase-independent mechanism. *Oncogene* **19**:5453-5463.

Clarke, P.G.H. 1990. Developmental cell death: morphological diversity and multiple mechanisms. *Anat. Embryol.* **181**:195-213.

Cleary, M.L., and J. Sklar. 1985. Nucleotide sequence of a t(14;18) chromosomal breakpoint in follicular lymphoma and demonstration of a breakpoint cluster region near a transcriptionally active locus on chromosome 18. *Proc. Natl. Acad. Sci. USA* **82**:7439-7443.

Cleary, M.L., S.D. Smith, and J. Sklar. 1986. Cloning and structural analysis of cDNAs for *bcl-2*/immunoglobulin transcript resulting from the t(14;18) translocation. *Cell* **47**:19-28.

Clem, R.J., E.H. Cheng, C.L. Karp, D.G. Kirsch, K. Ueno, A. Takahashi, M.B. Kastan, D.E. Griffin, W.C. Earnshaw, M.A. Veliuona, and J.M. Hardmick. 1998. Modulation of cell death by Bcl-X_L through caspase interaction. *Proc. Natl. Acad. Sci. USA* **95**:554-559.

Cohen, G.M. 1997. Caspases: the executioners of apoptosis. *Biochem. J.* **326**:1-16.

Condorelli, F., P. Salomoni, S. Cotteret, V. Cesi, S.M. Srinivasula, E.S. Alnemri, and B. Calabretta. 2001. Caspase cleavage enhances the apoptosis-inducing effects of BAD. *Mol. Cell. Biol.* **21**:3025-3036.

Conradt, B., and H.R. Horvitz. 1998. The *C. elegans* protein EGL-1 is required for programmed cell death and interacts with the Bcl-2-like protein CED-9. *Cell* **93**:519-529.

Conus, S., T. Rosse, and C. Borner. 2000. Failure of Bcl-2 family members to interact with Apaf-1 in normal and apoptotic cells. *Cell Death Differ.* 7:947-954.

Conus, S., T. Kaufmann, I. Fellay, I. Otter, T. Rosse, and C. Borner. 2000a. Bcl-2 is a monomeric protein: prevention of homodimerization by structural constraints. *EMBO J.* **19**:534-1544.

Cornillon, S., C. Foa, J. Davoust, N. Buonavista, J.D. Gross, and P. Golstein. 1994. Programmed cell death in *Dictyostelium*. *J. Cell Sci.* **10**:2691-2704.

Costantini, P., A.-S. Belzacq, H.L.A. Vieira, N. Larochette, M.A. de Pablo, N. Zamzami, S.A. Susin, C. Brenner, and G. Kroemer. 2000. Oxidation of a critical thiol residue of the adenine nucleotide translocator enforces Bcl-2-independent permeability transition pore opening and apoptosis. *Oncogene* **19**:307-314.

Crompton, M. 2000. Bax, Bid and the permeabilization of the mitochondrial outer membrane in apoptosis. *Curr. Opin. Cell Biol.* **12**:414-419.

Crompton, M. 1999. The mitochondrial permeability transition pore and its role in cell death. *Biochem. J.* **341**:233-249.

Cryns, V., and J. Yuan. 1998. Proteases to die for. *Genes Dev.* **12**:1551-1570.

Cyrns, V.L., L. Bergeron, H. Zhu, H. Li, and J. Yuan. 1996. Specific cleavage of α-fodrin during Fas- and tumor necrosis factor-induced apoptosis is mediated by an

interleukin-1β-converting enzyme/Ced-3 protease distinct from the poly(ADP-ribose) polymerase protease. *J. Biol. Chem.* **271**:31277-31282.

Datta, S.R., H. Dudek, X. Tao, S. Masters, H.A. Fu, Y. Gotoh, and M.E. Greenberg. 1997. Akt phosphorylation of BAD couples survival signals to the cell-intrinsic death machinery. *Cell* **91**:231-241.

Daugas, E., S.A. Susin, N. Zamzami, K.F. Ferri, T. Irinopoulou, N. Larochette, M.C. Prevost, B. Leber, D. Andrews, J. Penninger, and G. Kroemer. 2000. Mitochondrio-nuclear translocation of AIF in apoptosis and necrosis. *FASEB J.* **14**:729-739.

Deas, O., C. Dumont, M. MacFarlane, C. Rouleau, F. Hebib, F. Harper, F. Hirsch, G.M. Charpentier, G.M. Cohen, and A. Senik. 1998. Caspse-independent cell death induced by anti-CD2 or staurosporine in activated human peripheral T lymphocytes. *J. Immunol.* **161**:3375-3383.

Degli Esposti, M., E. Hatzinisiriou, H. McLennan, and S. Ralph. 1999. Bcl-2 and mitochondrial oxygen radicals: new approaches with reactive oxygen species-sensitive proves. *J. Biol. Chem.* **274**:29831-29837.

del Peso, L., V.M. Gonzalez, and G. Nunez. 1998. *Caenorhabditis elegans* EGL-1 disrupts the interaction of CED-9 with CED-4 and promotes CED-3 activation. *J. Biol. Chem.* **273**:33495-33500.

del Peso, L., M. Gonzalez-Garcia, C. Page, R. Herrera, and G. Nunez. 1997. Interleukin-3-induced phosphorylation of BAD through the protein kinase Akt. *Science* **278**:687-689.

Denecker, G., D. Vercammen, W. Declercq, and P. Vandenabeele. 2001. Apoptotic and necrotic cell death induced by death domain receptors. *Cell. Mol. Life Sci.* **58**:356-370.

Desagher, S., A. Osen-Sand, A. Nichols, R. Eskes, S. Montessuit, S. Lauper, K. Maundrell, B. Antonsson, and J.C. Martinou. 1999. Bid-induced conformational change of Bax is responsible for mitochondrial cytochrome *c* release during apoptosis. *J. Cell Biol.* **144**:891-901.

Deveraux, Q.L., and J.C. Reed. 1999. IAP family proteins- suppressors of apoptosis. *Genes Dev.* **13**:239-252.

Deveraux, Q.L., E. Leo, H.R. Stennicke, K. Welsh, G.S. Salvesen, and J.C. Reed. 1999. Cleavage of human inhibitor of apoptosis protein XIAP results in fragments with distinct specificities for caspases. *EMBO J.* **18**:5242-5251.

Deveraux, Q.L., N. Roy, H.R. Stennicke, T. Van Arsdale, Q. Zhou, M. Srinivasula, E.S. Alnemri, G.S. Salvesen, and J.C. Reed. 1998. IAPs block apoptotic events induced by caspase-8 and cytochrome *c* by direct inhibition of distinct caspases. *EMBO J.* **15**:2685-2689.

Deveraux, Q.L., R. Takahashi, G.S. Salvesen, and J.C. Reed. 1997. X-linked IAP is a direct inhibitor of cell death proteases. *Nature* **388**:300-303.

D'Herde, K., B. De Preset, S. Mussche, P.schotte, R. Beyaert, R. Van Coster, and F. Roels. 2000. Ultrastructural localization of cytochrome *c* in apoptosis demonstrates mitochondrial heterogeneity. *Cell Death Differ.* **7**:331-337.

Doran, E., and P.A. Halestrap. 2000. Cytochrome *c* release from isolated rat liver mitochondria can occur independently of outer-membrane rupture; possible role of contact sites. *Biochem. J.* **348**:343-350.

Droin, N., M. Beauchemin, E. Solary, and R. Bertrand. 2000. Identification of a caspase-2 isoform that behaves as an endogenous inhibitor of the caspase cascade. *Cancer Res.* **60**:7039-7047.

Du, C., M. Fang, Y. Li, L. Li, and X. Wang. 2000. Smac, a mitochondrial protein that promotes cytochrome *c*-independent caspase activation by eliminating IAP inhibition. *Cell* **102**:33-42.

Dumont, A., S.P. Hehner, T.G. Hofmann, M. Ueffing, W. Droge, and M.L. Schmitz. 1999. Hydrogen peroxide-induced apoptosis is CD95-independent, requires the release of mitochondria-derived oxygen species and the activation of NF-κB. *Oncogene* **18**:747-757.

Earnshaw, W.C., L.M. Martins, and S.H. Kaufmann. 1999. Mammalian caspases: structure, activation, substrates, and functions during apoptosis. *Annu. Rev. Biochem.* **68**:383-424.

Eberstadt, M., B. Huang, Z. Chen, R.P. Meadows, S.-C. Ng, L. Zheng. M.J. Lenardo, and S.W. Fesik. 1998. NMR structure and mutagenesis of the FADD (Mort1) death-effector domain. *Nature* **392**:941-945.

Eguchi, Y., A. Srinivasan, K.J. Tomaselli, S. Shimizu, Y. Tsujimoto. 1999. ATP-dependent steps in apoptotic signal transduction. *Cancer Res.* **59**:2174-2181.

Ekert, P., J. Silke, C. Hawkins, A. Verhagen, and D. Vaux. 2001. Diablo promotes apoptosis by removing miha/xiap from processed caspase 9. *J. Cell Biol.* **152**:483-490.

Elkins, P., A. Bunker, W.A. Cramer, and C.V. Stauffacher. 1997. A mechanism for toxin insertion into membranes is suggested by the crystal structure of the channel-forming domain of colicin E1. *Structure* **5**:443-458.

Enari, M., H. Sakahira, H. Yokoyama, K. Okawa, A. Iwamatsu, and S. Nagata. 1998. A caspase-activated DNase that degrades DNA during apoptosis. *Nature* **391**:43-50.

Erhardt, P., K.J. Tomaselli, and G.M. Cooper. 1997. Identification of the MDM2 oncoprotein as a substrate for CPP32-like apoptotic proteases. *J. Biol. Chem.* **272**:15049-15052.

Fadok, V.A., D.L. Bratton, D.M. Rose, A. Pearson, R.A. Ezekowitz, and P.M. Henson. 2000. A receptor for phosphatidylserine-specific clearance of apoptotic cells. *Nature* **405**:85-90.

Faleiro, L., and Y. Lazebnik. 2000. Caspases disrupt the nuclear-cytoplasmic barrier. *J. Cell Biol.* **151**:951-959.

Faleiro, L., R. Kobayashi, H. Fearnhead, and Y. Lazebnik. 1997. Multiple species of CPP32 and Mch2 are the major active caspases present in apoptotic cells. *EMBO J.* **16**:2271-2281.

Ferri, K.F., and G. Kroemer. 2001. Mitochondria – the suicide organelles. *BioEssays* **23**:111-115.

Ferri, K.F, E. Jacotot, J. Blanco, J.A. Este, N. Zamzami, S.A. Susin, Z. Xie, G. Brothers, J.C. Reed, J.M. Penninger, and G. Kroemer. 2000. Apoptosis control in syncytia induced by the HIV type 1-envelope glycoprotein complex: role of mitochondria and caspases. *J. Exp. Med.* **192**:1081-1092.

Finucane, D.M., E. Bossy-Wetzel, N.J. Waterhouse, T.G. Cotter, and D.R. Green. 1999. Bax-induced caspase activation and apoptosis via cytochrome *c* release from mitochondria is inhibitable by Bcl-x_L. *J. Biol. Chem.* **274**:2225-2233.

Fisher, A.J., W. dela Cruz, S.J. Zoog, C.L. Schneider, and P.D. Friesen. 1999. Crystal structure of baculovirus P35: role of a novel reactive site loop in apoptotic caspase inhibition. *EMBO J.* **18**:2031-2039.

Formigli, L., L. Papucci, A. Tani, N. Schiavone, A. Tempestini, G.E. Orlandini, S. Capaccioli, and S.Z. Orlandini. 2000. Aponecrosis: morphological and biochemical exploration of a syncretic process of cell death sharing apoptosis and necrosis. *J. Cell. Physiol.* **182**:41-49.

Foyouzi-Youssefi, R., S. Arnaudeau, C. Borner, W.L. Kelley, J. Tschopp, D.P. Lew, N. Demaurex, and K.-H. Krause. 2000. Bcl-2 decreases the free Ca^{2+} concentratioin within the endoplasmic reticulum. *Proc. Natl. Acad. Sci. USA* **97**:5723-5728

Frey, T.G., and C.A. Mannella. 2000. The internal structure of mitochondria. *Trends Biochem. Sci.* **25**:319-324.

Fujita, N., and T. Tsuruo. 1998. Involvement of Bcl-2 cleavage in the acceleration of VP-16-induced U937 cell apoptosis. *Biochem. Biophys. Res. Commun.* **246**:484-488.

Fujita, N., A. Nagahashi, K. Nagashima, S. Rokudai, and T. Tsuruo. 1998. Acceleration of apoptotic cell death after the cleavage of Bcl-X_L protein by caspse-3-like proteases. *Oncogene* **17**:1295-1304.

Fulda, S., E. Meyer, C. Friesen, S.A. Susin, G. Kroemer, and K.-M. Debatin. 2001. Cell type specific involvement of death receptor and mitochondrial pathways in drug-induced apoptosis. *Oncogene* **20**:1063-1075.

Furlong, I.J., C. Lopez Mediavilla, R. Ascaso, A. Lopez Rivas, and M.K.L. Collins. 1998. Induction of apoptosis by valinomycin: mitochondrial permeability transition causes intracellular acidification. *Cell Death Differ.* **5**:214-221.

Geddes, B.J., L. Wang, W.-J. Huang, M. Lavellee, G.A. Manji, M. Brown, M. Jurman, J. Cao, J. Morgenstern, S. Merriam, M.A. Glucksmann, P.S. DiStefano, and J. Bertin. 2001. Human CARD12 is a novel CED4/Apaf-1 family member that induces apoptosis. *Biochem. Biophys. Res. Commun.* **284**:77-82.

Gervais, F.G., N.A. Thornberry, S.C. Ruffolo, D.W. Nicholson, and S. Roy. 1998. Caspases cleave focal adhesion kinase during apoptosis to generate a FRNK-like polypeptide. *J. Biol. Chem.* **273**:17102-17108.

Gobeil, S., C.C. Boucher, D. Nadeau, and G.G. Poirier. 2001. Characterization of the necrotic cleavage of poly(ADP-ribose) polymerase (PARP-1): implication of lysosomal proteases. *Cell Death Differ.* **8**:588-594.

Goping, I.S., A. Gross, J.N. Lavoie, M. Nguyen, R. Jemmerson, K. Roth, S.J. Korsmeyer, and G.C. Shore. 1998. Regulated targeting of BAX to mitochondria. *J. Cell Biol.* **143**:207-215.

Grandgirard, D. E. Struder, L. Monney, T. Belser, I. Fellay, C. Borner, and M.R. Michel. 1998. Alphaviruses induce apoptosis in Bcl-2-overexpressing cells: evidence for a caspase mediated, proteolytic inactivation of Bcl-2. *EMBO J.* **17**:1268-1278.

Green, D.R., and J.C. Reed. 1998. Mitochondria and apoptosis. *Science* **281**:1309-1312.

Greenhalf, W., C. Stephan, and B. Chaudhuri. 1996. Role of mitochondria and C-terminal membrane anchor of Bcl-2 in Bax induced growth arrest and mortality in *Saccharomyces cerevisiae*. *FEBS Lett.* **380**:169-175.

Griffiths, G.J., L. Dubrez, C.P. Morgan, N.A. Jones, J. Whitehouse, B.M. Corfe, C. Dive, and J.A. Hickman. 1999. Cell damage-induced conformational changes of the pro-apoptotic protein Bak *in vivo* precede the onset of apoptosis. *J. Cell Biol.* **144**:903-914.

Gross, A., K. Pilcher, E. Blachly-Dyson, E. Basso, J. Jockel, M.C. Bassick, S.J. Korsmeyer, and M. Forte. 2000. Biochemical and genetic analysis of the mitochondrial response of yeast to BAX and BCL-X_L. *Mol. Cell. Biol.* **20**:3125-3136.

Gross, A., J.M. McDonnell, and S.J. Korsmeyer. 1999. BCL-2 family members and the mitochondria in apoptosis. *Genes Dev.* **13**:1899-1911.

Gross, A., X.M. Yin, K. Wang, M.C. Wei, J. Jockel, C. Milliman, H. Erdjument-Bromage, P. Tempst, and S.J. Korsmeyer. 1999a. Caspase cleaved BID targets

mitochondria and is required for cytochrome *c* release, while BCL-X_L prevents this release but not tumor necrosis factor-R1/Fas death. *J. Biol. Chem.* **274**:1156-1163.

Gross, A., J. Jockel, M.C. Wei, and S.J. Korsmeyer. 1998. Enforced dimerization of BAX results in its translocation, mitochondrial dysfunction, and apoptosis. *EMBO J.* **17**:3878-3885.

Ha, H.C., and S.H. Snyder. 1999. Poly(ADP-ribose) polymerase is a mediator of necrotic cell death by ATP depletion. *Proc. Natl. Acad. Sci. USA* **96**:13978-13982.

Hacki, J., L. Egger, L. Monney, S. Conus, T. Rosse, I. Fellay, and C. Borner. 2000. Apoptotic crosstalk between the endoplasmic reticulum and mitochondria controlled by Bcl-2. *Oncogene* **19**:2286-2295.

Hakem, R., A. Hakem, G.S. Duncan, J.T. Henderson, M. Woo, M.S. Soengas, A. Elia, J.L. De la Pompa, D. Kagi, W. Khoo, J. Potter, R. Yoshida, S.A. Kaufman, S.W. Lowe, J.M. Penninger, and T.W. Mak. 1998. Differential requirement for caspase 9 in apoptotic pathways *in vivo*. *Cell* **94**:339-352.

Halder, S., N. Jena, and C.M. Croce. 1995. Inactivation of Bcl-2 by phosphorylation. *Proc. Natl. Acad. Sci USA* **92**:4507-4511.

Hall, D., G. Gu, J. Garcia-Anoveras, L. Gong, M. Chalife, and M. Driscoll. 1997. Neurology of degenerative cell death in *Caenorhabditis elegans*. *J. Neurosci.* **17**:1033-1045.

Hampton, M.B., and S. Orrenius. 1997. Dual regulation of caspase activity by hydrogen peroxide: implications for apoptosis. *FEBS Lett.* **414**:552-556.

Hanada, M., C. Aime-Sempe, T. Sato, and J.C. Reed. 1995. Structure-function analysis of Bcl-2 protein. Identification of conserved domains important for homodimerization with Bcl-2 and heterodimerization with Bax. *J. Biol. Chem.* **270**:11962-11969.

Harada, H. B. Becknell, M. Wilm, M. Mann, L.J.S. Huang, S.S. Taylor, J.D. Scott, and S.J. Korsmeyer. 1999. Phosphorylation and inactivation of BAD by mitochondria-anchored protein kinase A. *Mol. Cell* **3**:413-422.

Harris, M.H., and C.B. Thompson. 2000. The role of the Bcl-2 family in the regulation of outer mitochondrial membrane permeability. *Cell Death Differ.* **7**:1182-1191.

Harris, M.H., M.G. Vander Heiden, S.J. Kron, and C.B. Thompson. 2000. Role of oxidative phosphorylation in Bax toxicity. *Mol. Cell. Biol.* **20**:3590-3596.

Hengartner, M.O. 2001. Apoptosis: corralling the corpses. *Cell* **104**:325-328.

Hengartner, M.O., and H.R. Horvitz. 1994. *C. elegans* cell survival gene *ced-9* encodes a functional homolog of the mammalian proto-oncogene *bcl-2*. *Cell* **76**:665-676.

Hengartner, M.O., R. Ellis, and H.R. Horvitz. 1992. *C. elegans* gene *ced-9* protects cells from programmed cell death. *Nature* **356**:494-499.

Hildeman, D.A., T. Mitchell, T.K. Teague, P. Henson, B.J. Day, J. Kappler, and P.C. Marrack. 1999. Reactive oxygen species regulate activation-induced T cell apoptosis. *Immunity* **10**:735-744.

Hirsch, T., P. Marchetti, S.A. Susin, B. Dallaporta, N. Zamzami, I. Marzo, M. Geuskens, and G. Kroemer. 1997. The apoptosis-necrosis paradox: apoptogenic proteases activated after mitochondrial permeability transition determine the mode of cell death. *Oncogene* **15**:1573-1581.

Hlaing, T., R.-F. Guo, K.A. Dilley, J.M. Loussia, T.A. Morrish, M.M. Shi, C. Vincenz, and P.A. Ward. 2001. Molecular cloning and characterization of DEFCAP-L and -S, two isoforms of a novel member of the mammalian Ced-4 family of apoptosis proteins. *J. Biol. Chem.* **276**:9230-9238.

Hockenbery, D.M., Z.N. Oltvai, X.M. Yin, C.L. Milliman, and S.J. Korsmeyer. 1993. Bcl-2 functions in an antioxidant pathway to prevent apoptosis. *Cell* **75**:241-251.

Horvitz, H.R. 1999. Genetic control of programmed cell death in the nematode *Caenorhabditis elegans*. *Cancer Res.* **59**:1701s-1706s.

Hu, Y., M.A. Benedict, L. Ding, and G. Nunez. 1999. Role of cytochrome *c* and dATP/ATP hydrolysis in Apaf-1-mediated caspase-9 activation and apoptosis. *EMBO J.* **18**:3586-3595.

Hu, Y., L. Ding, D.M. Spencer, and G. Nunez. 1998. WD-40 repeat region regulates Apaf-1 self-association and procaspase-9 activation. *J. Biol. Chem.* **275**:33489-33494.

Huang, Y., N.H. Shin, Y. Sun, and K.K. Wang. 2001. Molecular cloning and characterization of a novel caspase-3 variant that attenuates apoptosis induced by proteasome inhibition. *Biochem. Biophys. Res. Commun.* **283**:762-769.

Huang, D.C.S., J.M. Adams, and S. Cory. 1998. The conserved N-terminal BH4 domain of Bcl-2 homologues is essential for inhibition of apoptosis and interaction with CED-4. *EMBO J.* **17**:1029-1039.

Huang, L.E., J. Gu, M. Schau, and H.F. Bunn. 1998a. Regulation of hypoxia-inducible factor 1α is mediated by an O_2-dependent degradation domain via the ubiquitin-proteasome pathway. *Proc. Natl. Acad. Sci. USA* **95**:7987-7992.

Huang, B., Eberstadt, M., E.T. Olejniczak, R.P. Meadows, and S.W. Fesik. 1996. NMR structure and mutagenesis of the Fas (APO-1.CD95) death domain. *Nature* **384**:638-641.

Hunter, J.J., B.L. Bond, and T.G. Parslow. 1996. Functional dissection of the human Bcl-2 protein: sequence requirements for inhibition of apoptosis. *Mol. Cell Biol.* **16**:877-883.

Ichas, F., and J.-P. Mazat. 1998. From calcium signaling to cell death: two conformations for the mitochondrial permeability transition pore. Switching from low- to high-conductance state. *Biochim. Biophys. Acta.* **1366**:33-50.

Imazu T., S. Shimizu, S. Tagami, M. Matsushima, Y. Nakamura, T. Miki, A. Okuyama, and Y. Tsujimoto. 1999. Bcl-2/E1B 19 kDa-interacting protein 3-like (Bnip3L) interacts with Bcl-2/Bcl-x_L and induces apoptosis by altering mitochondrial membrane permeability. *Oncogene* **18**:4523-4529.

Ink, B., M. Zornig, B. Baum, N. Hajibagheri, C. James, T. Chittenden, and G. Evan. 1997. Human Bak induces cell death in *Schizosaccharomyces pombe* with morphological changes similar to those with apoptosis in mammalian cells. *Mol. Cell. Biol.* **17**:2468-2474.

Inohara, N., and G. Nunez. 2000. Genes with homology to mammalian apoptosis regulators identified in zebrafish. *Cell Death Differ.* **7**:509-510.

Inohara, N., T. Koseki, Y. Hu, C. Yee, S. Chen, R. Carrio, J. Merino, D. Liu, J. Ni, and G. Nunez. 1999. Nod1, an Apaf-1-like activator of caspase-9 and nuclear factor-kappaB. *J. Biol. Chem.* **274**:14560-14567.

Ionov, Y., H. Yamamoto, S. Krajewski, J.C. Reed, and M. Perucho. 2000. Mutational inactivation of the proapoptotic gene BAX confers selective advantage during tumor clonal evolution. *Proc. Natl. Acad. Sci. USA* **97**:10872-10877.

Ito, T., X. Deng, B. Carr, and W.S. May. 1997. Bcl-2 phosphorylation required for anti-apoptosis function. *J. Biol. Chem.* **272**:11671-11673.

Jabs, T. 1999. Reactive oxygen intermediates as mediators of programmed cell death in plants and animals. *Biochem. Pharmacol.* **57**:231-245.

Jacobson, M.D. 1996. Reactive oxygen species and programmed cell death. *Trends Biochem. Sci.* **21**:83-86.

James, C., S. Gschmeissner, A. Fraser, and G.I. Evan. 1997. CED-4 induces chromatin condensation in *Schizosaccharomyces pombe* and is inhibited by direct physical association with CED-9. *Curr. Biol.* **7**:246-252.

Janiak, F., B. Leber, and D.W. Andrews. 1994. Assembly of Bcl-2 into microsomal and outer mitochondrial membranes. *J. Biol. Chem.* **269**:9842-9849.

Janicke, R.U., P.A. Walker, X.Y. Lin, and A.G. Porter. 1996. Specific cleavage of the retinoblastoma protein by an ICE-like protease in apoptosis. *EMBO J.* **15**:6969-6978.

Jiang, H., R. Guo, and J.A. Powell-Coffman. 2001. The *Caenorhabditis elegans hif-1* gene encodes a bHLH-PAS protein that is required for adaptation to hypoxia. *Proc. Natl. Acad. Sci. USA* **98**:7916-7921.

Jiang, X., and X. Wang. 2000. Cytochrome *c* promotes caspase-9 activation by inducing nucleotide binding to Apaf-1. *J. Biol. Chem.* **275**:31199-31203.

Johnson. D.E., B.R. Gastman, F. Wieckowski, G.Q. Wang, A. Amoscato, S.M Delach, and H. Rabinowich. 2000. Inhibitor of apoptosis protein hILP undergoes caspase-mediated cleavage during T lymphocyte apoptosis. *Cancer Res.* **60**:1818-1823.

Joza, N., S.A. Susin, E. Daugas, W.L. Stanford, S.K. Cho, C.Y.J. Li, T. Sasaki, A.J. Elia, H.-Y.M. Cheng, L. Ravagnan, K.F. Ferri, N. Zamzami, A. Wakeham, R. Hakem, H. Yosida, Y.-Y. Kong, T.W. Mak, J.C. Zuniga-Pflucker, G. Kroemer, and J.M. Penninger. 2001. Essential role of mitochondrial apoptosis-inducing factor in programmed cell death. *Nature* **410**:549-554.

Jurgensmeier, J.M., S. Krajewski, R.C. Armstrong, G.M. Wilson, T. Oltersdorf, L.C. Fritz, J.C. Reed, and S. Ottilie. 1997. Bax- and Bak-induced cell death in the fission yeast *Schizosaccharomyces pombe*. *Mol. Biol. Cell* **8**:325-339.

Kallio, P.J., W.J. Wilson, S. O'Brien, Y. Makino, and L. Poellinger. 1999. Regulation of the hypoxia-inducible factor 1α by the ubiquitin proteasome pathway. *J. Biol. Chem.* **274**:6519-6525.

Kamada, S., H. Kusano, H. Fujita, M. Ohtsu, R.C. Koya, N. Kuzumaki, and Y. Tsujimoto. 1998. A cloning method for caspase substrates that uses the yeast two-hybrid system: cloning of the antiapoptotic gene gelsolin. *Proc. Natl. Acad. Sci. USA* **95**:8532-8537.

Kane, D.J., T.A. Sarafian, R. Anton, H. Hahn, E.B. Gralla, J.S. Valentine, T. Ord, and D.E. Bredesen. 1993. Bcl-2 inhibition of neural death: decreased generation of reactive oxygen species. *Science* **262**:1274-1277.

Kataoka, T., N. Holler, O. Micheau, F. Martinon, A. Tinel, K. Hofmann, and J. Tschopp. 2001. Bcl-rambo, a novel Bcl-2 homologue that induces apoptosis via its unique C-terminal extension. *J. Biol. Chem.* **276**:19548-19554.

Kawahara, A., Y. Ohsawa, H. Matsumara, Y. Uchiyama, and S. Nagata. 1998. Caspase-independent cell killing by Fas-associated protein with death domain. *J. Cell Biol.* **143**:1353-1360.

Kayalar, C., T. Ord. M.P. Testa, L.-T. Zhong, and D.E. Bredesen. 1996. Cleavage of actin by interleukin 1β-converting enzyme to reverse DNase I inhibition. *Proc. Natl. Acad. Sci. USA* **93**:2234-2238.

Kelekar, A., and C.B. Thompson. 1998. Bcl-2 family proteins: the role of the BH3 domain in apoptosis. *Trends Cell Biol.* **8**:324-330.

Kerr, J.F.R., A.H. Wyllie, and A.R. Currie. 1972. Apoptosis: a basic biological phenomenon with wide-ranging implications in tissue kinetics. *Br. J. Cancer* **26**:239-257.

Khaled, A.R., K. Kim, R. Hofmeister, K. Muegge, and S.K. Durum. 1999. Withdrawal of IL-7 induces Bax translocation from cytosol to mitochondria through a rise in intracellular pH. *Proc. Natl. Acad. Sci. USA* **96**:14476-14481.

Kirsch, D.G., A. Doseff, B. N. Chau. D.-S. Lim, N.C. de Souza-Pinto, R. Hansford, M.B. Kastan, Y.A. Lazebnik, and J.M. Hardwick. 1999. Caspase-3-dependent cleavage of Bcl-2 promotes release of cytochrome *c*. *J. Biol. Chem.* **274**:21155-21161.

Kitanaka, C., and Y. Kuchino. 1999. Caspase-independent programmed cell death with necrotic morphology. *Cell Death Differ.* **6**:508-515.

Kluck, R.M., M. Degli Esposti, G. Perkins, C. Renken, T. Kuwana, E. Bossy-Wetzel, M. Goldberg, T. Allen, M.J. Barber, D.R. Green, and D.D. Newmeyer. 1999. The pro-apoptotic proteins, Bid and Bax, cause a limited permeabilization of the mitochondrial outer membrane that is enhanced by cytosol. *J. Cell Biol.* **147**:809-822.

Kluck, R.M., E. Bossy-Wetzel, D.R. Green, and D.D. Newmeyer. 1997. The release of cytochrome *c* from mitochondria: a primary site for Bcl-2 regulation of apoptosis. *Science* **275**:1132-1136.

Koopman, G., C.P. Reutelingsperger, G.A. Kuijten, R.M. Keehnen, S.T. Pals, and M.H. van Oers. 1994. Annexin V for flow cytometric detection of phosphatidylserine expression on B cells undergoing apoptosis. *Blood* **84**:1415-1420.

Korsmeyer, S. J., M.C. Wei, M. Saito, S. Weiler, K.J. Oh, and P.H Schlesinger. 2000. Pro-apoptotic cascade activates BID, which oligomerizes BAK or BAX into pores that result in the release of cytochrome *c*. *Cell Death Differ.* **7**:1166-1173.

Kothakota, S., T. Azuma, C. Reinhard, A. Klippel, J. Tang, K. Chu, T.J. McGarry, M.W. Kirschner, K. Koths, D.J. Kwiatkowski, and L.T. Williams. 1997. Caspase-3-generated fragment of gelsolin: effector of morphological change in apoptosis. *Science* **278**:294-298.

Kou, T.H., H.-R. Choi Kim, L. Zhu, Y. Yu, H.-M. Lin, and W. Tsang. 1998. Modulation of endoplasmic reticulum calcium pump by Bcl-2. *Oncogene* **17**:1903-1910.

Krajewski, S., M. Krajewska, L.M. Ellerby, K. Welsh, Z. Xie, Q.L. Deveraux, G.S. Salvesen, D.E. Bredesen, R.E. Rosenthal, G. Fiskum, and J.C. Reed. 1999. Release of caspase-9 from mitochondria during neuronal apoptosis and cerebral ischemia. *Proc. Natl. Acad. Sci. USA* **96**:5752-5757.

Krajewski, S., S. Tanaka, S. Takayama, M.J. Schibler, W. Fenton, and J.C. Reed. 1993. Investigation of the subcellular distribution of the bcl-2 oncoprotein: residence in the nuclear envelope, endoplasmic reticulum, and outer mitochondrial membranes. *Cancer Res.* **53**:4701-4714.

Kroemer, G., B. Dallaporta, and M. Resche-Rigon. 1998. The mitochondrial death/life regulator in apoptosis and necrosis. *Annu. Rev. Physiol.* **60**:619-642.

Kroemer, G., N. Zamzami, and S.A. Susin. 1997. Mitochondrial control of apoptosis. *Immunol. Today* **18**:44-51.

Kruman, I., and M.P. Mattson. 1999. Pivotal role of mitochondrial calcium uptake in neural cell apoptosis and necrosis. *J. Neurochem.* **72**:529-540.

Kruman, I., Q. Guo, and M.P. Mattson. 1998. Calcium and reactive oxygen species mediate staurosporine-induced mitochondrial dysfunction and apoptosis in PC12 cells. *J. Neurosci. Res.* **51**:293-308.

Kumar, S., and P.A. Colussi. 1999. Prodomains – adaptors – oligomerization: the pursuit of caspase activation in apoptosis. *Trends Biochem. Sci.* **24**:1-4.

Lauber, K., H.A. Appel, S.F. Schlosser, M. Gregor, K. Schulze-Osthoff, and S. Wesselborg. 2001. The adapter protein Apaf-1 is proteolytically processed during apoptosis. *J. Biol. Chem.* [epub ahead of print].

Lavoie, J.N., M. Nguyen, R.C. Marcellus, P.E. Branton, and G.C. Shore. 1998. E4orf4, a novel adenovirus death factor that induces p53-independent apoptosis by a pathway that is not inhibited by zVAD-fmk. *J Cell Biol.* **140**:637-645.

Lazebnik, Y.A., A. Takahashi, R.D. Moir, R.D. Goldman, G.G. Poirier, S.H. Kaufmann, and W.C. Earnshaw. 1995. Studies of the lamin proteinase reveal multiple parallel biochemical pathways during apoptotic execution. *Proc. Natl. Acad. Sci. USA* **94**:13642-13647.

Lee, S.T., K.P., Hoeflich, G.W. Wasfy, J.R. Woodgett, B. Leber, D.W. Andrews, D.W. Hedley, and L.Z. Penn. 1999. Bcl-2 targeted to the endoplasmic reticulum can inhibit apoptosis induced by Myc but not etoposide in Rat-1 fibroblasts. *Oncogene* **18**:3520-3528.

Lehninger, A.L., D.L. Nelson, and M.M. Cox. 1993. Principle of Biochemistry, second edition. Worth Publishers: New York, NY, USA, pages 553-554.

Leist, M. B. Single, A.F. Castoldi, S. Kuhnle, and P. Nicotera. 1997. Intracellular adenosine triphosphate (ATP) concentrations: a switch in the decision between apoptosis and necrosis. *J. Exp. Med.* **185**:1481-1486.

Lemasters, J.J. 1999. Necrapoptosis and the mitochondrial permeability transition: shared pathways to necrosis and apoptosis. *Am. J. Physiol.* **276**:G1-G6.

Lemasters, J.J., T. Qian, S.P. Elmore, L.C. Trost, Y. Nishimura, B. Herman, C.A. Bradham, D.A. Brenner, A.L. Nieminen. 1998. Confocal microscopy of the mitochondrial permeability transition in necrotic cell killing, apoptosis and autophagy. *Biofactors* **8**:283-285.

Lemasters, J.J., A.-L., Nieminen, T. Qian, L.C. Trost, S.P. Elmore, Y. Nishimura, R.A. Crowe, W.E. Cascio, C.A. Bradham, D.A. Brenner, and B. Herman. 1998a. The

mitochondrial permeability transition in cell death: a common mechanism in necrosis, apoptosis, and autophagy. *Biochim. Biophys. Acta* **1366**:177-196.

Li, H., H. Zhu, C.J. Xu, and J. Yuan. 1998. Cleavage of BID by caspase 8 mediates the mitochondrial damage in the Fas pathway of apoptosis. *Cell* **94**:491-501.

Li, P., D. Nijhawan, I. Budihardjo, S.M. Srinivasula, M. Ahmad, E.S. Alnemri, and X. Wang. 1997. Cytochrome *c* and dATP-dependent formation of Apaf-1/Caspase-9 complex initiates an apoptotic protease cascade. *Cell* **91**:479-489.

Liang, X.H., S. Jackson, M. Seaman, K. Brown, B. Kempkes, H. Hibshoosh, and B. Levine. 1999. Induction of autophagy and inhibition of tumorigenesis by *beclin1*. *Nature* **402**:672-676.

Lieberthal, W., V. Triaca, J.S. Koh, P.J. Pagano, and J.S. Levine. 1998. Role of superoxide in apoptosis induced by growth factor withdrawal. *Am. J. Physiol.* **275**:F691-F702.

Liest, M., B. single, A.F. Castoldi, S. Kuhnle, and P. Nicotera. 1997. Intracellular adenosine triphosphate (ATP) concentration: a switch in the decision between apoptosis and necrosis. *J. Exp. Med.* **185**:1481-1486.

Liu, X., P. Li, P. Widlak, H. Zou, X. Luo, W.T. Garrard, and X. Wang. 1998. The 40-kDa subunit of DNA fragmentation factor induces DNA fragmentation and chromatin condensation during apoptosis. *Proc. Natl. Acad. Sci. USA*. **95**:8461-8466.

Liu, X., H. Zou, C. Slaughter, and X. Wang. 1997. DFF, a heterodimeric protein that functions downstream of caspase-3 to trigger DNA fragmentation during apoptosis. *Cell* **89**:175-184.

Liu, X., C.N. Kim, J. Yang, R. Jemmerson, and X. Wang. 1996. Induction of apoptotic program in cell-free extracts: requirement for dATP and cytochrome *c*. *Cell* **86**:147-157.

London, E. 1992. Diphtheria toxin: membrane interaction and membrane translocation. *Biochim. Biophys. Acta* **1113**:25-51.

Lorenzo, H.K., S.A. Susin, J. Penninger, and G. Kroemer. 1999. Apoptosis inducing factor (AIF): a phylogenetically old, caspase-independent effector of cell death. *Cell Death Differ.* **6**:516-524.

Luo, X., I. Budihardjo, H. Zou, C. Slaughter, and X. Wang. 1998. Bid, a Bcl2 interacting protein, mediates cytochrome *c* release from mitochondria in response to activation of cell surface death receptors. *Cell* **94**:481-490.

Marchetti, P., M. Castedo, S.A. Susin, N. Zamzami, T. Hirsch, A. Macho, A. Haeffner, F. Hirsch, M .Geuskens, and G. Kroemer. 1996. Mitochondrial permeability transition is a central coordinating event of apoptosis. *J. Exp. Med.* **184**:1155-1160.

Martins, S.J., G.A. O'Brien, W.K. Nishioka, A.J. McGahon, A. Mahboubi, T.C. Saido, and D. R. Green. 1995. Proteolysis of fodrin (non-erythroid spectrin) during apoptosis. *J. Biol. Chem.* **270**:6425-6428.

Marzo, I., C. Brenner, N. Zamzami, J.M. Juergensmeier, S.A. Susin, H.L.A. Vieira, M.C. Prevost, Z.H. Xie, S. Matsuyama, J.C. Reed, and G. Kroemer. 1998. Bax and adenine nucleotide translocator cooperate in the mitochondrial control of apoptosis. *Science* **281**:2027-2031.

Marzo, I. C. Brenner, N. Zamzami, S.A. Susin, G. Beutner, D. Brdiczka, R. Remy, Z.H. Xie, J.C. Reed, and G. Kroemer. 1998a. The permeability transition pore complex: a target for apoptosis regulation by caspases and Bcl-2-related proteins. *J. Exp. Med.* **187**:1261-1271.

Mashima, T., M. Naito, K. Noguchi, D.K. Miller, D.W. Nicholson, and T. Tsuruo. 1997. Actin cleavage by CPP-32/apopain during the development of apoptosis. *Oncogene* **14**:1007-1012.

Matsumura, H., Y. Shimizu, Y. Ohsawa, A. Kawahara, Y. Uchiyama, and S. Nagata. 2000. Necrotic death pathway in Fas receptor signaling. *J. Cell Biol.* **151**:1247-1255.

Matsushima, M., T. Fujiwara, E. Takahashi, T. Minaguchi, Y. Eguchi, Y. Tsujimoto, K. Suzumori, and Y. Nakamura. 1998. Isolation, mapping, and functional analysis of a novel human cDNA (BNIP3L) encoding a proteins homologous to human NIP3. *Genes Chrom. Cancer* **21**:230-235.

Matsuyama, S., and J.C. Reed. 2000. Mitochondria-dependent apoptosis and cellular pH regulation. *Cell Death Differ.* **7**:1155-1165.

Matsuyama, S., J. Llopis, Q.L. Deveraux, R.Y. Tsien, and J.C. Reed. 2000. Changes in intramitochondrial and cytosolic pH: early events that modulate caspase activation during apoptosis. *Nat. Cell Biol.* **2**:318-325.

Matsuyama, S., Q. Xu, J. Velours, and J.C. Reed. 1998. The mitochondrial F_0F_1-ATPase proton pump is required for function of the proapoptotic protein Bax in yeast and mammalian cells. *Mol. Cell* **1**:327-336.

McCarthy, N.J., M.K.B. Whyte, C.S. Gilbert, and G.I. Evan. 1997. Inhibition of Ced-3/ICE-related proteases does no prevent cell death induced by oncogenes, DNA damage, or the Bcl-2 homologue Bak. *J. Cell Biol.* **136**:215-227.

McConkey, D.J. 1998. Biochemical determinants of apoptosis and necrosis. *Toxicol. Lett.* **99**:157-168.

McDonnell, J.M., D. Fushman, C.L. Milliman, S.J. Korsmeyer, and D. Cowburn. 1999. Solution structure of the proapoptotic molecule BID: a structural basis for apoptotic agonists and antagonists. *Cell* **96**:625-634.

Metzstein, M.M., G.M. Stanfield, and H.R. Horvitz. 1998. Genetics of programmed cell death in *C. elegans*: past, present and future. *Trends Genet.* **14**:410-416.

Minn, A.J., C.S. Kettlum, H. Laing, A. Kelekar, M.G. Vander Heiden, B.S. Chang, S.W. Fesik, M. Fill, and C.B. Thompson. 1999. Bcl-x_L regulates apoptosis by heterodimerization-dependent and -independent mechanisms. *EMBO J.* **18**:632-643.

Minn, A.J., R.E. Swain, A. Ma, and C.B. Thompson. 1998. Recent progress on the regulation of apoptosis by Bcl-2 family members. *Adv. Immunol.* **70**:245-279.

Minn, A.J., P. Velez, S.L. Schendel, H. Liang, S.W. Muchmore, S.W. Fesik, M. Fill, and C.B. Thompson. 1997. Bcl-x_L forms an ion channel in synthetic lipid membranes. *Nature* **285**:353-357.

Minn, A.J., L.H. Boise, and C.B. Thompson. 1996. Bcl-x_S antagonizes the protective effects of Bcl-x_L. *J. Biol. Chem.* **271**:6306-6312.

Mitoma, J., and A. Ito. 1992. The carboxy-terminal 10 amino acid residues of cytochrome b5 are necessary for its targeting to the endoplasmic reticulum. *EMBO J.* **11**:4197-4203.

Mittl, P.R. S. Di Marco, J.F. Krebs, X. Bai, D.S. Karanewsky, J.P. Priestle, K.J. Tomaselli, M.G. Grutter. 1997. Structure of recombinant human CPP32 in complex with the tetrapeptide acetyl-Asp-Val-Ala-Asp fluoromethyl ketone. *J. Biol. Chem.* **272**:29238-29242.

Miura, M., H. Zhu, R. Rotello, E.A. Hartwieg, and J. Yuan. 1993. Induction of apoptosis in fibroblasts by IL-1β-converting enzyme, a mammalian homolog of the *C. elegans* cell death gene *ced-3*. *Cell* **75**:653-660.

Miyazaki, K., H. Yoshida, M. Sasaki, H. Hara, G, Kimura, T.W. Mak, and K. Nomoto. 2001. Caspase-independent cell death and mitochondrial disruptions observed in the Apaf1-deficient cells. *J. Biochem.* **129**:963-969.

Mizushima, N., T. Noda, T. Yoshimori, T. Tanaka, T. Ishii, M.D. George, D.J. Klionski, M. Ohsumi, and Y. Ohsumi. 1998. A protein conjugation system essential for autophagy. *Nature* **395**:395-398.

Montal, M., and P. Mueller. 1972. Formation of bimolecular membranes from lipid monolayers and a study of their electrical properties. *Proc. Natl. Acad. Sci. USA* **69**:3561-3566.

Muchmore, S.W., M. Sattler, H. Laing, R.P. Meadows, J.E. Harlan, H.S. Yoon, D. Nettesheim, B.S. Chang, C.B. Thompson, S.L. Wong, S.L. Ng, and S.W. Fesik. 1996. X-ray and NMR structure of human Bcl-x_L, an inhibitor of programmed cell death. *Nature* **381**:335-341.

Nagata, S. 2000. Apoptotic DNA fragmentation. *Exp. Cell Res.* **256**:12-18.

Nakagawa, T., H. Zhu, N. Morishima, E. Li, J. Xu, B.A. Yankner, and J. Yuan. 2000. Caspase-12 mediates endoplasmic-reticulum-specific apoptosis and cytotoxicity by amyloid-β. *Nature* **403**:98-103.

Narita, M., S. Shimizu, T. Ito, T. Chittenden, R.J. Lutz, H. Matsuda, and Y. Tsujimoto. 1998. Bax interacts with the permeability transition pore to induce permeability transition and cytochrome *c* release in isolated mitochondria. *Proc. Natl. Acad. Sci. USA* **95**:14681-14686.

Newmeyer, D.D., E. Bossy-Wetzel, R.M. Kluck, B.B. Wolf, H.M. Beere, and D.R. Green. 2000. Bcl-x_L does not inhibit the function of Apaf-1. *Cell Death Differ.* 7:402-407.

Ng, F.W., M. Nguyen, T. Kwan, P.E. Branton, D.W. Nicholson, J.A. Cromlish, and G.C. Shore. 1997. p28 Bap31, a Bcl-2/Bcl-X_L- and procaaspase-8-associated protein in the endoplasmic reticulum. *J. Cell Biol.* **139**:327-338.

Nguyen, M., D.G. Breckenridge, A. Ducret, and G.C. Shore. 2000. Caspase-resistant BAP31 inhibits fas-mediated apoptotic membrane fragmentation and release of cytochrome c from mitochondria. *Mol. Cell. Biol.* **20**:6731-6740.

Nguyen, M., D.G. Millar, V.W. Yong, S.J. Korsmeyer, and G.C. Shore. 1993. Targeting of Bcl-2 to the mitochondrial outer membrane by a COOH-terminal signal anchor sequence. *J. Biol. Chem.* **268**:25265-25268.

Nicotera, P., and M. Leist. 1997. Energy supply and the shape of death in neurons and lymphoid cells. *Cell Death Differ.* **4**:435-442.

Nunez, G., M.A. Benedict, Y. Hu, and N. Inohara. 1998. Caspases: the proteases of the apoptotic pathway. *Oncogene* **17**:3237-3245.

Oda, E., R. Ohki, H. Murasawa, J. Nemoto, T. Shibue, T. Yamashita, T. Tokino, T. Taniguchi, and N. Tanaka. 2000. Noxa, a BH3-only member of the Bcl-2 family and candidate mediator of p53-induced apoptosis. *Science* **288**:1053-1058.

Ogura, Y., N. Inohara, A. Benito, F.F. Chen, S. Yamaoka, and G. Nunez. 2001. Nod2, a Nod1/Apaf-1 family member that is restricted to monocytes and activates NF(kappa)B. *J. Biol. Chem.* **276**:4812-4818.

Ohi, N., A. Tokunaga, H. Tsunoda, K. Nakano, K. Haraguchi, K. Oda, N. Motoyama, and T. Nakajima. 1999. A novel adenovirus E1B19K-binding protein B5 inhibits apoptosis induced by Nip3 by forming a heterodimer through the C-terminal hydrophobic region. *Cell Death Differ.* **6**:314-325.

Okuno, S., S. Shimizu, T. Ito, M. Nomura, E. Hamada, Y. Tsujimoto, and H. Matsuda. 1998. Bcl-2 prevents caspase-independent cell death. *J. Biol. Chem.* **273**:34272-34277.

Olie, R.A., F. Durrieu, S. Cornillon, J. Loughran, J. Gross, W.C. Earnshaw, and P.C. Golstein. 1998. Apparent caspase independence of programmed cell death in *Dictyostelium*. *Curr. Biol.* **8**:955-958.

Oltvai, Z.N., C.L. Milliman, and S.J. Korsmeyer. 1993. Bcl-2 heterodimerizes in vivo with a conserved homolog, Bax, that accelerates programmed cell death. *Cell* **74**:609-619.

Orth, K., A.M. Chinnaiyan, M. Garg, C.J. Froelich, and V.M. Dixit. 1996. The CED-3/ICE-like protease Mch2 is activated during apoptosis and cleaves the death substrate lamin A. *J. Biol. Chem.* **271**:16443-16446.

Pastorino, J.G., M. Tafani, R.J. Rothman, A. Marcineviciute, J.B. Hoek, and J.L. Farber. 1999. Functional consequences of the sustained or transient activation by Bax of the mitochondrial permeability transition pore. *J. Biol. Chem.* **274**:31734-31739.

Pastorino, J.G., S.-T. Chen, M. Tafani, J.W. Snyder, and J.L Farber. 1998. The overexpression of Bax produces cell death upon induction of the mitochondrial permeability transition. *J. Biol. Chem.* **271**:7770-7775.

Patterson, S.D., C.S. Spahr, E. Daugas, S.A. Susin, T. Irinopoulou, C. Koehler, and G. Kroemer. 2000. Mass spectrometric identification of proteins released from mitochondria undergoing permeability transition. *Cell Death Differ.* **7**:137-144.

Pear, W.S., G.P. Nolan, M.L. Scott, and D. Baltimore. 1995. Production of high-titer helper-free retroviruses by transient transfection. *Proc. Natl. Acad. Sci. USA* **90**:8392-8396.

Petronilli, V., D. Penzo, L. Scorrano, P. Bernardi, and F. Di Lisa. 2001. The mitochondrial permeability transition, release of cytochrome *c* and cell death: correlation with the duration of pore openings *in situ*. *J. Biol. Chem.* **276**:12030-12034.

Poommipanit, P.B., B. Chen, and Z.N. Oltvai. 1999. Interleukin-3 induces the phosphorylation of a distinct fraction of bcl-2. *J. Biol. Chem.* **274**:1033-1039.

Priault, M., N. Camougrand, B. Chaudhuri, J. Schaeffer, and S. Manon. 1999. Comparison of the effects of *bax*-expression in yeast under fermentative and respiratory conditions: investigation of the role of adenine nucleotides carrier and cytochrome *c*. *FEBS Lett.* **456**:232-238.

Purring-Koch, C., and G. McLendon. 2000. Cytochrome *c* binding to Apaf-1: the effects of dATP and ionic strength. *Proc. Natl. Acad. Sci. USA* **97**:11928-11931.

Puthalakath, H., D.C.S. Huang, L.A. O'Reilly, S.M. King, and A. Strasser. 1999. The proapoptotic activity of the Bcl-2 family member Bim is regulated by interaction with the dynein motor complex. *Mol. Cell.* **3**:287-296.

Quignon, F., F. De Bels, M. Koken, J. Feunteun, J.-C. Ameisen, and H. de The. 1998. PML induces a novel caspase-independent death process. *Nat. Genet.* **20**:259-265.

Raff, M.C. 1992. Social controls on cell survival and cell death. *Nature* **356**:397-400.

Ranger, A.M., B.A. Malynn, and S.J. Korsmeyer. 2001. Mouse models of cell death. *Nat. Genetics* **28**:113-118.

Rao, L., D. Perez, and E. White. 1996. Lamin proteolysis facilitates nuclear events during apoptosis. *J. Cell Biol.* **135**:1441-1455.

Ray, R. 2000. Structure-function analysis of a mitochondrial cell death protein, Bcl-2/E1B 19K interacting protein 3 (BNip3). Ph.D. thesis, University of Manitoba, Manitoba, Canada.

Ray, R., G. Chen, C. Vande Velde, J. Cizeau, R.D. Gietz, J.C. Reed, and A.H. Greenberg. 1999. BNIP3 heterodimerizes with Bcl-2/Bcl-X_L and induces cell death independent of the BH3 domain at both mitochondrial and non-mitochondrial sites. *J. Biol. Chem.* **275**:1439-1448.

Ray, C.A., R.A. Black, S.R. Kronheim, T.A. Greenstreet, P.R. Sleath, G.S. Salvesen, and D.J. Pickup. 1992. Viral inhibition of inflammation: cowpox virus encodes an inhibitor of the interleukin-1 beta converting enzyme. *Cell* **69**:597-604.

Reed, J.C. 1997. Double identity for proteins of the Bcl-2 family. *Nature* **387**: 73-776.

Reed, J.C. 1997b. Cytochrome *c*: can't live with it – can't live without it. *Cell* **91**: 559-562.

Roberts, D.L., W. Merrison, M. MacFarlane, and G.M. Cohen. 2001. The inhibitor of apoptosis protein-binding domain of Smac is not essential for its proapoptotic activity. *J. Cell Biol.* **153**:221-227.

Rogers, S., R. Wells, and M. Rechsteiner. 1986. Amino acid sequences common to rapidly degraded proteins: the PEST hypothesis. *Science* **234**:364-368.

Roy, N., Q.L. Deveraux, R. Takahashi, G.S. Salvesen, and J.C. Reed. 1997. The c-IAP-1 and c-IAP-2 proteins are direct inhibitors of specific caspases. *EMBO J.* **16**:6914-6925.

Sahara, S., M. Aoto, Y. Eguchi, N. Imamoto, Y. Yoneda, and Y. Tsujimoto. 1999. Acinus is a caspase-3-activated protein required for apoptotic chromatin condensation. *Nature* **401**:168-173.

Sakahira, H., M. Enari, S. Nagata. 1998. Cleavage of CAD inhibitor in CAD activation and DNA degradation during apoptosis. *Nature* **391**:96-99.

Salcedo, S., and J. Caro. 1997. Hypoxia-inducible factor 1α (HIF-1α) protein is rapidly degraded by the ubiquitin-proteasome system under normoxic conditions: its stabilization by hypoxia depends on redox-induced changes. *J. Biol. Chem.* **272**:22642-22647.

Saleh, A., S.M. Srinivasula, L. Balkir, P.D. Robbins, and E.S. Alnemri. 2000. Negative regulation of the Apaf-1 apoptosome by Hsp70. *Nature Cell Biol.* **2**:476-483.

Salvesen, G.S., and V.M. Dixit. 1999. Caspase activation: the induced-proximity model. *Proc. Natl. Acad. Sci. USA* **96**:10964-10967.

Samali, A., H. Nordgren, B. Zhivotovsky, E. Peterson, and S. Orrenius. 1999. A comparative study of apoptosis and necrosis in HepG2 cells: oxidant-induced caspase-inactivation leads to necrosis. *Biochem. Biophys. Res. Commun.* **255**:6-11.

Sambrook, J., E.F. Fritch, and T. Maniatis. 1989. Molecular cloning: a laboratory manual. Second Edition. Cold Spring Harbour Laboratory Press. Cold Spring Harbour, New York.

Sattler, M., H. Liang, D. Nettesheim, R.P. Meadows, J.E. Harlan, M. Eberstadt, H.S. Yoon, S.B. Shukar, B.S. Chang, A.J. Minn, C.B. Thompson, and S.W. Fesik. 1997. Structure of Bcl-x_L-Bak peptide complex: recognition between regulators of apoptosis. *Science* **275**:983-986.

Scaffidi, C., I. Schmitz, J. Zha, S.J. Korsmeyer, P.H. Krammer, and M.E. Peter. 1999. Differential modulation of apoptosis sensitivity in CD95 type I and type II cells. *J. Biol. Chem.* **274**:22532-22538.

Scaffidi, C., S. Fulda, A. Srinivasan, C. Friesen, F. Li, K.J. Tomaselli, K.M. Debatin, P.H. Krammer, and M.E. Peter. 1998. Two CD95 (APO-1/Fas) signaling pathways. *EMBO J.* **17**:1675-1687.

Schendel, S.L., R.Asimov, K.Pawlowski, A. Godzik, B.L. Kagan, and J.C. Reed. 1999. Ion channel activity of the BH3 only Bcl-2 family member, BID. *J. Biol. Chem.* **274**:21932-21936.

Schendel, S.L., M. Montal, and J.C. Reed. 1998. Bcl-2 family proteins as ion-channels. *Cell Death Differ.* **5**:372-380.

Schendel, S.L., Z. Xie, M.O. Montal, S. Matsuyama, M. Montal, and J.C. Reed. 1997. Channel formation by anti-apoptotic protien Bcl-2. *Proc. Natl. Acad. Sci. USA* **93**:5113-5118.

Schlegel, J., I. Peters, S. Orrenius, D.K. Miller, N.A. Thornberry, T.T. Yamin, and D.W. Nicholson. 1996. CPP32/apopain is a key interleukin 1 beta converting enzyme-like protease involved in Fas-mediated apoptosis. *J. Biol. Chem.* **271**:1841-1844.

Schlegel, R.A., and P. Williamson. 2001. Phosphatidylserine, a death knell. *Cell Death Differ.* **8**:551-563.

Schlesinger, P.H., A. Gross, X.-M. Yin, K. Yamamoto, M. Saito, G. Waksman, and S.J. Korsmeyer. 1997. Comparison of the ion channel characteristics of proapoptotic BAX and antiapoptotic BCL-2. *Proc. Natl. Acad. Sci. USA* **94**:11357-11362.

Seagroves, T.N., H.E. Ryan, H. Lu, B.G. Wouters, M. Knapp, P. Thibault, K. Laderoute, and R.S. Johnson. 2001. Transcription factor HIF-1 is a necessary mediator of the pasteur effect in mammalian cells. *Mol. Cell. Biol.* **21**:3436-3444.

Semenza, G.L. 2000. HIF-1 and human disease: one highly involved factor. *Genes Dev.* **14**:1983-1991.

Seol, D.-W., and T.R. Billiar. 1999. A caspase-9 variant missing the catalytic site is an endogenous inhibitor of apoptosis. *J. Biol. Chem.* **274**:2072-2076.

Shaham, S. 1998. Identification of multiple *Caenorhabditis elegans* caspases and their potential roles in proteolytic cascades. *J. Biol. Chem.* **273**:35109-35117.

Shi, L., G. Chen, G. MacDonald, L. Bergeron, H. Li, M. Miura, R.J. Rotello, D.K. Miller, P. Li, T. Seshadri, J. Yuan, and A.H. Greenberg. 1996. Activation of an interleukin 1 converting enzyme-dependent apoptosis pathway by granzyme B. *Proc. Natl. Acad. Sci. USA* **93**:11002-11007.

Shi, L., R.P. Kraut, R. Aebersold, and A.H. Greenberg. 1992. A natural killer cell granule protein that induces DNA fragmentation and apoptosis. *J. Exp. Med.* **175**:553-566.

Shibasaki, F., and F. McKeon. 1995. Calcineurin functions in Ca(2+)-activated cell death in mammalian cells. *J. Cell Biol.* **131**:735-743.

Shibasaki, F., E. Kondo, T. Akagi, and F. McKeon. 1997. Suppression of signaling through transcription factor NF-AT by interactions between calcineurin and Bcl-2. *Nature* **386**:728-731.

Shimizu, S., and Y. Tsujimoto. 2000. Proapoptotic BH3-only Bcl-2 family members induce cytochrome *c* release, but no mitochondrial membrane potential loss, and do not directly modulate voltage-dependent anion channel activity. *Proc. Natl. Acad. Sci. USA* **97**:577-582.

Shimizu, S., A. Konishi, T. Kodama, and Y. Tsujimoto. 2000a. BH4 domain of antiapoptotic Bcl-2 family members closes voltage-dependent anion channel and inhibits apoptotic mitochondrial changes and cell death. *Proc. Natl. Acad. Sci. USA* **97**:3100-3105.

Shimizu, S., T. Ide, T. Yanagida, and Y. Tsujimoto. 2000b. Electrophysiological study of a novel large pore formed by Bax and the voltage-dependent anion channel that is permeable to cytochrome *c*. *J. Biol. Chem.* **275**:12321-12325.

Shimizu, S., M. Narita, and Y. Tsujimoto. 1999. Bcl-2 family proteins regulate the release of apoptogenic cytochrome *c* by the mitochondrial channel VDAC. *Nature* **399**:483-487.

Shimizu, S., Y. Eguchi, W. Kamike, Y. Funahashi, A. Mignon, V. Lacronique, H. Matsuda, and Y. Tsujimoto. 1998. Bcl-2 prevents apoptotic mitochondrial dysfunction by regulating proton flux. *Proc. Natl. Acad. Sci. USA* **95**:1455-1459.

Simonian, P.L., D.A.M. Grillot, R. Merino, and G. Nunez. 1996. Bax can antagonize Bcl-x_L during etoposide and cisplatin-induced cell death independently of its heterodimerization with Bcl-x_L. *J. Biol. Chem.* **271**:22764-22772.

Slee, E.A., C. Adrain, and S.J. Martin. 2001. Executioner caspase-3, -6, and -7 perform distinct, non-redundant roles during the demolition phase of apoptosis. *J. Biol. Chem.* **276**:7320-7326.

Slee, E.A., M.T. Harte, R.M. Kluck, B.B. wolf, C.A. Casiano, D.D. Newmeyer, H.-G. Wang, J.C. Reed, D.W. Nicholson, E.S. Alnemri, D.R. Green, and S.J.Martin. 1999. Ordering the cytochrome *c*-initiated caspase cascade: hierarchical activation of caspases-2, -3, -6, -7, -8, and –10 in a caspase-9-dependent manner. *J. Cell. Biol.* **144**:281-292.

Slee, E.A., H. ZHU, S.C. Chow, M. MacFarlane, D.W. Nicholson, and G.M. Cohen. 1996. Benzyloxycarbonyl-Val-Ala-Asp (OMe) fluoromethylketone (Z-VAD.FMK) inhibits apoptosis by blocking the processing of CPP32. *Biochem. J.* **315**:21–24.

Srinivas, V., I. Leshchinsky, N. Sang, M.P. King, A. Minchencko, and J. Caro. 2001. Oxygen sensing and HIF-1 activation does not require an active mitochondrial respiratory chain electron-transfer pathway. *J. Biol. Chem.* **276**:21995-21998.

Srinivasula, S.M., M. Ahmad, T. Fernandes-Alnemri, and E.S. Alnemri. 1998. Autoactivation of procaspase-9 by Apaf-1-mediated oligomerization. *Mol. Cell* **1**:949-957.

Srivastava, R.K., Q.S. Mi, J.M. Hardwick, and D.L. Longo. 1999. Deletion of the loop region of Bcl-2 completely blocks paclitaxel-induced apoptosis. *Proc. Natl. Acad. Sci. USA* **96**:3775-3780.

Steinman, H.M. 1995. The Bcl-2 oncoprotein functions as a pro-oxidant. *J. Biol. Chem.* **270**:3487-3490.

Stennicke, H.R., and G.S. Salvesen. 2000. Caspases – controlling intracellular signals by protease zymogen activation. *Biochem. Biophys. Acta.* **1477**:299-306.

Stennicke, H.R., Q.L. Deveraux, E.W. Humke, J.C. Reed, V.M. Dixit, and G.S. Salvesen. 1999. Caspase-9 can be activated without proteolytic processing. *J. Biol. Chem.* **274**:8359-8362.

Stennicke, H.R., and G.S. Salvesen. 1997. Biochemical characteristics of caspases-3, -6, -7, and -8. *J. Biol. Chem.* **272**:25719-25723.

Stroh, C., and K. Schulze-Osthoff. 1998. Death by a thousand cuts: an ever increasing list of caspase substrates. *Cell Death Differ.* **5**:997-1000.

Sulston, J.E., E. Schierenberg, J.G. White, and J.N. Thomson. 1983. The embryonic cell lineage of the nematode *Caenorhabditis elegans*. *Dev. Biol.* **100**:64-119.

Susin, S.A., N. Larochette, M. Geuskens, and G. Kroemer. 2000. Purification of mitochondria for apoptosis assays. *Methods Enzymol.* **322**:205-208.

Susin, S.A., H.K. Lorenzo, N. Zamzami, I. Marzo, B.E. Snow, G.M. Brothers, J. Mangion, E. Jacotot, P. Constantini, M. Loeffler, N. Larochette, D.R. Goodlett, R. Aebersold, D.P. Siderovski, J.M. Penninger, and G. Kroemer. 1999. Molecular characterization of mitochondrial apoptosis-inducing factor. *Nature* **397**:441-446.

Susin, S.A., H.K. Lorenzo, N. Zamzami, I. Marzo, C. Brenner, N. Larochette, M.-C. Prevost, P.M. Alzari, and G. Kroemer. 1999a. Mitochondrial release of caspase-2 and –9 during the apoptotic process. *J. Exp. Med.* **189**:381-393.

Sutton, V.R., J.E. Davis, M. Cancilla, R.W. Johnstone, A.A. Ruefli, K. Sedelies, K.A. Browne, and J.A. Trapani. 2000. Initiation of apoptosis by granzyme B requires direct cleavage of bid, but not direct granzyme B-mediated caspase activation. *J. Exp. Med.* **192**:1403-1414.

Suzuki, Y., Y. Nakabayashi, K. Nakata, J.C. Reed, and R. Takahashi. 2001. XIAP inhibits caspase-3 and -7 in distinct modes. *J. Biol. Chem.* [epub ahead of print].

Suzuki, M., R.J. Youle, and N. Tjandra. 2000. Structure of Bax: coregulation of dimer formation and intracellular localization. *Cell* **103**:645-654.

Takahashi, A., E.S. Alnemri, Y.A. Lazebnik, T. Fernandes-Alnemri, G. Litwack, R.D. Moir, R.D. Goldman, G.G. Poirier, S.H. Kaufmann, and W.C. Earnshaw. 1996. Cleavage of lamin A by Mch2α but not CPP32: multiple interleukin 1β-converting enzyme-related proteases with distinct substrate recognition properties are active in apoptosis. *Proc. Natl. Acad. Sci. USA* **93**:8395-8400.

Takeyama, N., N. Matsuo, and T. Tanaka. 1993. Oxidative damage to mitochondria is mediated by the Ca(2+)-dependent inner-membrane permeability transition. *J. Biochem.* **294**:719-725.

Tan, S., Y. Sagara, Y. Liu, P. Maher, and D. Schubert. 1998. The regulation of reactive oxygen species production during programmed cell death. *J. Cell Biol.* **141**:1423-1432.

Tao, W., C. Kurschner, and J.I. Morgan. 1998. Bcl-X_L and Bad potentiate the death suppressing activities of Bcl-X_L, Bcl-2, and A1 in yeast. *J. Biol. Chem.* **273**:23704-23708.

Tao, W., C. Kurschner, and J.I. Morgan. 1997. Modulation of cell death in yeast by the Bcl-2 family of proteins. *J. Biol. Chem.* **272**:15547-15552.

Thompson, C.B. 1995. Apoptosis in the pathogenesis and treatment of disease. *Science* **267**:1456-1462.

Thornberry, N.A., and Y. Lazebnik. 1998. Caspases: enemies within. *Science* **281**:1312-1316.

Thornberry, N.A., T.A. Ranon, E.P. Pieterson, D.M. Rasper, T. Timkey, M. Garcia-Calvo, V.M. Houtzager, P.A. Nordstrom, S. Roy, J.P. Vaillancourt, K.T. Chapman, and D.W. Nicholson. 1997. A combinatorial approach defines specificities of members of the caspase family and granzyme B - functional relationships established for key mediators of apoptosis. *J. Biol. Chem.* **272**:17907-17911.

Tsujimoto, Y. 1997. Apoptosis and necrosis: intracellular ATP level as a determinant for cell death modes. *Cell Death Differ.* **4**:429-434.

Tsujimoto, Y., J. Cossman, E. Jaffe, and C. Croce. 1985. Involvement of the bcl-2 gene in human follicular lymphoma. *Science* **228**:1440-1443.

Turrens, J.F. 1997. Superoxide production by the mitochondrial respiratory chain. *Bioscience Reports* **17**:3-8.

Vanags, D.M., M.I. Porn-Ares, S. Coppola, D.H. Burgess, and S. Orrenius. 1996. Protease involvement in fodrin cleavage and phosphatidylserine exposure in apoptosis. *J. Biol. Chem.* **271**:31075-31085.

Van de Craen, M., G. Van Loo, S. Pype, W. Van Criekinge, I. Van den brande, F. Molemans, W. Fiers, W. Declercq, and P. Vandenabeele. 1998. Identification of a new caspase homologue: caspase-14. *Cell Death Differ.* **5**:838-846.

Vander Heiden, M.G., N.S. Chandel, X.X. Li, P.T. Schumacker, M. Colombini, and C.B. Thompson. 2000. Outer mitochondrial membrane permeability can regulate coupled respiration and cell survival. *Proc. Natl. Acad. Sci. USA* **97**:4666-4671.

Vander Heiden, M.G., and C.B. Thompson. 1999. Bcl-2 proteins: regulators of apoptosis or of mitochondrial homeostasis? *Nat. Cell Biol.* **1**:E209-E216.

Vander Heiden, M.G., N.S. Chandel, P.T. Schumacher, and C.B. Thompson. 1999a. Bcl-x_L prevents cell death following growth factor withdrawal by facilitating mitochondrial ATP/ADP exchange *Mol. Cell* **3**:159-167.

Vander Heiden, M.G., N.S. Chandel, E.K. Williamson, P.T. Schumacker, and C.B. Thompson. 1997. Bcl-x_L regulates the membrane potential and volume homeostasis of mitochondria. *Cell* **91**:627-637.

Vande Velde C., J. Cizeau, D. Dubik, J. Alimonti, T. Brown, S. Israels, R. Hakem, and A.H. Greenberg. 2000. BNIP3 and genetic control of necrosis-like cell death through the mitochondrial permeability transition pore. *Mol. Cell Biol.* **20**:5454-5468.

Vaux, D.L., G. Haecker, and A. Strasser. 1994. An evolutionary perspective on apoptosis. *Cell* **76**:777-779.

Vaux, D.L., I.L. Weissman, and S.K. Kim. 1992. Prevention of programmed cell death in *Caenorhabditis elegans* by human *bcl-2*. *Science* **258**:1955-1957.

Vercammen, D., R. Beyaert, G. Denecker, V. Goosens, G. Van Loo, W. Declercq, J. Grooten, W. Fiers, and P. Vandenabeele. 1998. Inhibition of caspases increases the sensitivity of L929 cells to necrosis mediated by tumor necrosis facotr

Verhagen, A.M., P.G. Ekert, M. Pakusch, J. Silke, L.M. Connolly, G.E. Reid, R.L. Moritz, R.J. Simpson, and D.L. Vaux. 2000. Identification of DIABLO, a mammalian protein that promotes apoptosis by binding to and antagonizing IAP proteins. *Cell* **102**:43-53.

Vermes, I., C. Haanen, H. Steffens-Nakken, and C. Reutelingsperger. 1995. A novel assay for apoptosis. Flow cytometric detection of phosphatidylserine expression on early apoptotic cells using fluorescein labeled Annexin V. *J. Immunol. Methods* **184**:39-51.

Vernooy, S.Y., J. Copeland, N. Ghaboosi, E.E. Griffin, S.J. Yoo, and B.A. Hay. 2000. Cell death regulation in *Drosophila*: conservation of mechanism and unique insights. *J. Cell Biol.* **150**:F69-F75.

Vieira, H.L.A., D. Haouzi, C. El Hamel, E. Jacotot, A.-S. Belzacq, C. Brenner, and G. Kroemer. 2000. Permeabilization of the mitochondrial inner membrane during apoptosis: impact of the adenine nucleotide translocator. *Cell Death Differ.* 7:1146-1154.

Voehringer, D.W., D.L. Hirschberg, J. Xiao, Q. Lu, M. Roederer, C.B. Lock, L.A. Herzenberg, and L.A. Herzenberg. 2000. Gene microarray identification of redox and mitochondrial elements that control resistance and sensitivity to apoptosis. *Proc. Natl. Acad. Sci. USA* **97**:2680-2685.

Von Ahsen, O., N.J. Waterhouse, T. Kuwana, D.D. Newmeyer, and D.R. Green. 2000. The 'harmless' release of cytochrome *c*. *Cell Death Differ.* 7:1192-1199.

Von Ahsen, O., C. Renken, G. Perkins, R.M. Kluck, E. Bossy-Wetzel, and D.D. Newmeyer. 2000a. Preservation of mitochondrial structure and function after Bid- or Bax-mediated cytochrome *c* release. *J. Cell Biol.* **150**:1027-1036.

von Harsdorf, R., P.-F. Li, and R. Dietz. 1999. Signaling pathways in reactive oxygen species-induced cardiomyocyte apoptosis. *Circulation* **99**:2934-2941.

Walker, N.P.C., R.V. Talanian, K.D. Brady, L.C. Dang, N.J. Bump, C.R. Ferenz, S. Franklin, T. Ghayur, M.C. Hackett, L.D. Hammill, L. Herzog, M. Hugunin, M. Houy,

J.A. Mankovich, L. McGuiness, E. Orlewicz, M. Paskind, C.A. Pratt, P. Reis, A. Summani, M. Terranova, J.P. Welch, L. Xiong, A. Moller, D.E. Tracey, R. Kamen, and W.W. Wong. 1994. Crystal structure of the cysteine protease interleukin-1β-converting enzyme: a (p20/p10)2 homodimer. *Cell* **78**:343-352.

Wang, S., Z. Wang, L. Boise, P.Dent, and S. Grant. 1999. Loss of the Bcl-2 phosphorylation loop domain increases resistance of human leukemia cells (U937) to paclitaxel-mediated mitochondrial dysfunction and apoptosis. *Biochem. Biophys. Res. Commun.* **259**:67-72.

Wang, K.K.W., R. Posmantur, R. Nath, K. McGinnis, M. Whitton, R.V. Talanian, S.B. Glantz, and J.S. Morrow. 1998. Simultaneous degradation of αII- and βII-spectrin by caspase 3 (CPP32) in apoptotic cells. *J. Biol. Chem.* **273**:22490-22497.

Wang, H.-G., U.R. Rapp, and J.C. Reed. 1996. Bcl-2 targets the protein kinase Raf-1 to mitochondria. *Cell* **87**:629-638.

Watt, W., K.A. Koeplinger, A.M. Mildner, R.L. Heinrikson, A.G. Tomasselli, and K.D. Watenpaugh. 1999. The atomic-resolution structure of human caspase-8, a key activator of apoptosis. *Structure Fold Des.* **15**:1135-1143.

Wei, M.C., W.-X. Zong, E.H.-Y. Cheng, T. Lindsten, V. Panoutsakopoulou, A.J. Ross, K.A. Roth, G.R. MacGregor, C.B. Thompson, and S.J. Korsmeyer. 2001. Proapoptotic BAX and BAK: a requisite gateway to mitochondrial dysfunction and death. *Science* **292**:727-730.

Wei, Y., T. Fox, S.P. Chambers, J. Sintchak, J.T. Coll, J.M. Golec, L. Swenson, K.P. Wilson, and P.S. Charifson. 2000. The structures of caspases-1, -3, -7 and -8 reveal the basis for substrate and inhibitor selectivity. *Chem. Biol.* 7:423-432.

Wei, M.C., T. Lindsten, V.K. Mootha, S. Weiler, A. Gross, M. Ashiya, C.B. Thompson, and S.J. Korsmeyer. 2000a. tBID, a membrane targeted death ligand, oligomerizes BAK to release cytochrome *c*. *Genes Dev.* **14**:2060-2071.

Wen, L.-P., J.A. Fahrni, S. Troie, J.-L. Guan, K. Orth, and G.D. Rosen. 1997. Cleavage of focal adhesion kinase by caspases during apoptosis. *J. Biol. Chem.* **272**:26056-26061.

Wilson, K.P., J.-A.F. Black, J.A. Thomson, E.E. Kim, J.P. Griffith, M.A. Navia, M.A. Murcko, S.P. Chambers, R.A. Aldape, S.A. Raybuck, and D.J. Livingston. 1994. Structure and mechanism of interleukin-1β-converting enzyme. *Nature* **370**:270-275.

Wolf, B.B., and D.R. Green. 1999. Suicidal tendencies: apoptotic cell death by caspase family proteinases. *J. Biol. Chem.* **274**:20049-20052.

Wolf, B.B., M. Schuler, F. Echeverri, and D.R. Green. 1999. Caspase-3 is the primary activator of apoptotic DNA fragmentation via DNA fragmentation factor-45/inhibitor of caspase-activated DNase inactivation. *J. Biol. Chem.* **274**:30651-30656.

Wu, D., H.D. Wallen, and G. Nunez. 1997. Interaction and regulation of subcellular localization of CED-4 by CED-9. *Science* **275**:1126-1129.

Wyllie, A.H., F.F.R. Kerr, and A.R. Currie. 1980. Cell death: the significance of apoptosis. *Int. Rev. Cytol.* **68**:251-305.

Xiang, J.L., D.T. Chao, and S.J. Korsmeyer. 1996. BAX-mediated cell death may not require interleukin 1beta-converting enzyme-like proteases. *Proc. Natl. Acad. Sci. USA* **93**:14559-14563.

Xue, L.Z., G.C. Fletcher, and A.M. Tolkovsky. 1999. Autophagy is activated by apoptotic signalling in sympathetic neurons: an alternative mechanism of death execution. *Mol. Cell Neurosci.* **14**:180-198.

Xue, D., and H.R. Horvitz. 1995. Inhibition of the *Caenorhabditis elegans* cell death protease CED-3 by a CED-3 cleavage site in baculovirus p35 protein. *Nature* **377**:248-251.

Yang, E., and S.J. Korsmeyer. 1996. Molecular thanatopsis: a discourse on the BCL-2 family and cell death. *Blood* **88**:386-401.

Yang, X., H.Y. Chang, and D. Baltimore. 1998. Essential role of CED-4 oligomerization in CED-3 activation and apoptosis. *Science* **281**:1355-1357.

Yang, J., X. Liu, K. Bhalla, C.N. Kim, A.M. Ibrado, J. Cai, T.I Peng, D.P. Jones, and X. Wang. 1997. Prevention of apoptosis by Bcl-2: release of cytochrome *c* from mitochondria blocked. *Science* **275**:1129-1132.

Yasuda, M., J.W. Han, C.A. Dionne, J.M. Boyd, and G. Chinnadurai. 1999. BNIP3α: A human homolog of mitochondrial proapoptotic protein BNIP3. *Cancer Res.* **59**:533-537.

Yasuda, M., P. Theodorakis, T. Subramanian, and G. Chinnadurai. 1998. Adenovirus E1B-19K/BCL-2 interacting protein BNIP3 contains a BH3 domain and a mitochondrial targeting sequence. *J. Biol. Chem.* **273**:12415-12421.

Yasuda, M., C. D'Sa-Eipper, X. Gong, and G. Chinnadurai. 1998a. Regulation of apoptosis by a *Caenorhabditis elegans* BNIP3 homolog. *Oncogene* **17**:2525-2530.

Yin, C., C.M. Knudson, S.J. Korsmeyer, and T. Van Dyke. 1997. Bax suppresses tumorigenesis and stimulates apoptosis *in vivo*. *Nature* **385**:637-640.

Yin, X.M., Z.N. Oltvai, and S.J. Korsmeyer. 1994. BH1 and BH2 domains of Bcl-2 are required for inhibition of apoptosis and heterodimerization with Bax. *Nature* **369**:321-323.

Yoshida, H., Y.-Y. Kong, R. Yoshida, A.J. Elia, A. Hakem, R. Hakem, J.M. Penninger, and T.W. Mak. 1998. Apaf1 is required for mitochondrial pathways of apoptosis and brain development. *Cell* **94**:739-750.

Yuan, J., S. Shaham, S. Ledoux, H. Ellis, and H.R. Horvitz. 1993. The *C. elegans* cell death gene *ced-3* encodes a protein similar to mammalian interleukin-1β-converting enzyme. *Cell* **75**:641-652.

Zakeri, Z., W. Bursch, M. Tenniswood, and R.A. Lockshin. 1995. Cell death: programmed, apoptosis, necrosis, or other? *Cell Death Differ.* **2**:87-96.

Zamzami, N., C. Brenner, I. Marzo, S.A. Susin, and G. Kroemer. 1998. Subcellular and submitochondrial mode of action of Bcl-2-like oncoproteins. *Oncogene* **16**:2265-2282.

Zamzami, N., S.A. Susin, P. Marchetti, T. Hirsch, I. Gomex-Monterrey, M. Castedo, and G. Kroemer. 1996. Mitochondrial control of nuclear apoptosis. *J. Exp. Med.* **183**:1533-1544.

Zamzami, N., P. Marchetti, M. Castedo, D. Decaudin, A. Macho, T. Hirsch, S.A. Susin, P.X. Petit, B. Mignotte, and G. Kroemer. 1995. Sequential reduction of mitochondrial transmembrane potential and generation of reactive oxygen species in early programmed cell death. *J. Exp. Med.* **182**:367-377.

Zha, J., S. Weiler, K.J. Oh, M.C. Wei, and S.J. Korsmeyer. 2000. Posttranslational N-myristoylation of BID as a molecular switch for targeting mitochondria and apoptosis. *Science* **290**:1761-1765.

Zha, H., and J.C. Reed. 1997. Heterodimerization-independent functions of cell death regulatory proteins Bax and Bcl-2 in yeast and mammalian cells. *J. Biol. Chem.* **272**:31482-31489.

Zha. J.P., H. Harada, E. Yang, J. Jockel, and S.J. Korsmeyer. 1996. Serine phosphorylation of death agonist BAD in response to survival factor results in binding to 14-3-3 not BCL-X_L. *Cell* **87**:619-628.

Zha, H., H.A. Fisk, M.P. Yaffe, N. Mahajan, B. Herman, and J.C. Reed. 1996a. Structure-function comparisons of the proapoptotic protein Bax in yeast and mammalian cells. *Mol. Cell. Biol.* **16**:6494-6508.

Zhang, D., M.S. Pasternack, P.J. Beresford, L. Wagner, A.H. Greenberg, and J. Lieberman. 2001. Induction of rapid histone degradation by the cytotoxic T lymphocyte protease Granzyme A. *J. Biol. Chem.* **276**:3683-3690.

Zhang, J., M.C. Reedy, Y.A. Hannun, and L.M. Obeid. 1999. Inhibition of caspases inhibits the release of apoptotic bodies: Bcl-2 inhibits the initiation of formation of apoptotic bodies in chemotherapeutic agent-induced apoptosis. *J. Cell Biol.* **145**:99-108.

Zhang, Y., O. Marcillat, C. Giulivi, L. Ernster, and K.J.A. Davies. 1990. The oxidative inactivation of mitochondrial electron transport chain components and ATPase. *J. Biol. Chem.* **265**:16330-16336.

Zhivotovsky, B., A. Samali, A. Gahm, and S. Orrenius. 1999. Caspases: their intracellular localization and translocation during apoptosis. *Cell Death Differ.* **6**:644-651.

Zhou, Q., S. Snipas, K. Orth, M. Muzio, V.M. Dixit, and G.S. Salvesen. 1997. Target protease specificity of the viral serpin CrmA: analysis of five caspases. *J. Biol. Chem.* **272**:7797-7800.

Zhu, L., S. Ling, X.-D. Yu, L.K. Venkatesh, T. Subramanian, and G. Chinnadurai. 1999. Modulation of mitochondrial Ca^{2+} homeostasis by Bcl-2. *J. Biol. Chem.* **274**:33267-33273.

Zhu, W., A. Cowie, G.W. Wasfy, L.Z. Penn, B. Leber, and D.W. Andrews. 1996. Bcl-2 mutants with restricted subcellular location reveal spatially distinct pathways for apoptosis in different cell types. *EMBO J.* **15**:4130-4141.

Zoog, S.J., J. Bertin, and P.D. Friesen. 1999. Caspase inhibition by baculovirus P35 requires interaction between the reactive site loop and the β-sheet core. *J. Biol. Chem.* **274**:25995-26002.

Zoratti, M., and I. Szabo. 1995. The mitochondrial permeability transition. *Biochem. Biophys. Acta* **1241**:139-176.

Zou, H., Y. Li, X. Liu, and X. Wang. 1999. An APAF-1-cytochrome *c* multimeric complex is a functional apoptosome that activates procaspase-9. *J. Biol. Chem.* **274**:11549-11556.

Zou, H., W.J. Henzel, X. Liu, A. Lutschg, and X. Wang. 1997. Apaf-1, a human protein homologous to *C. elegans* CED-4, participates in cytochrome *c*-dependent activation of caspase-3. *Cell* **90**:405-413.